Investigating the role of macrophages in pulmonary arterial hypertension using the *MacLow* mouse model

Amira Abdulmajid Zawia

Summary

Macrophages are proposed to play an important regulatory role in the pathogenesis of pulmonary arterial hypertension (PAH), as excessive infiltration is detected around vascular lesions in patients and animal models of the disease. The exact 'causal' role for macrophages, and whether their presence or absence is required for the vascular remodelling seen in PAH remains unclear. Using a novel inducible macrophage depletion model (*MacLow* mouse) I aimed to determine the role of macrophages in the pulmonary arterial remodeling associated with PAH.

Macrophage depletion was induced in *MacLow* mice by administration of doxycycline, where macrophage- specific induction of the cytotoxic diphtheria toxin A chain (DTA) is driven by the CD68 promoter. Male but not female *MacLow* mice developed a spontaneous PAH phenotype compared to controls following six week doxycycline treatment, this was associated with increased right ventricular hypertrophy and pulmonary vascular remodelling.

Immunohistochemical analysis of diseased lungs demonstrated dominancy of the CD206+ macrophages suggesting that M2- like macrophage population may drive this PAH phenotype. Differentiation towards M2 phenotype has been also observed *in vitro* using primary cells obtained from *MacLow* mice. Furthermore, by tracing the origin of the effector macrophages responsible for the development of *MacLow*- induced PAH using different chimeric mice, it seems that the major contributor cells originate within the lung tissue and that male bone marrow cells were not sufficient to induce disease in female recipient. Finally, culturing of bone marrow-derived macrophages and alveolar macrophages showed unique characteristic differences in term of their polarization, expression of DTA and expression of leukotriene B4 following stimulation with doxycycline. The data suggested that alveolar macrophage might be resistant to the doxycycline-induced depletion which may lead to activation of the alveolar macrophages following loss of the interstitial subtype.

In conclusion, loss of CD68+ macrophages in *MacLow* mice led to the development of PAH spontaneously in male and not female mice, and the pathogenesis might involve activation of alveolar macrophages. Also these data further highlight the gender imbalance in PAH and add immune cells to this paradigm.

Acknowledgements

Author's declaration

I declare that the work presented within this thesis is my own work and has not been previously submitted for any other degree.

Table of Contents

List of figures

List of Tables

Abbreviations

%	percent
5-HT	5- hydroxytryptamine
5-LO	5-lipoxygenase
ADMA	asymmetric dimethyl arginine
ALK-1	activin receptor like kinase 1
AM	alveolar macrophage
APCs	antigen presenting cells
BALF	broncho-alveolar lavage fluid
BM	bone marrow
BMDM	bone marrow-derived macrophages
BMPR-2	bone morphogenic protein receptor type 2
BMPs	bone- morphogenic proteins
BMT	bone marrow transplant
BSA	bovine serum albumin
cAMP	cyclic adenosine monophosphate
CAV	caveolin
CCL	chemokine (c-c motif) ligand
CTEPH	chronic thromboembolic pulmonary hypertension
DMSO	di-methyl sulfoxide
Dox	doxycycline
DTA	diphtheria toxin- A
E2	oestrogen
ECM	extracellular matrix
ECs	endothelial cells
EGF	epidermal growth factor

ENG	endoglin
eNOs	endothelial nitric oxide synthase
GM-CSF	granulocyte macrophage colony stimulating factor
HBSS	Hank's buffered salt solution
HDACs	histone deacetylases
HIF	hypoxia induced factor
HIV	human immunodeficiency virus
HO-1	heme- oxygenase
ICC	immunocytochemistry
IF	immunofluorescence
ILs	interleukins
IM	interstitial macrophages
IPAH	idiopathic pulmonary hypertension
IVC	individually ventilated cage
KLF	Kruppel- like factor
LPS	lipopolysaccharide
LTA4H	leukotriene A4 hydrolase
LTB4	leukotriene B4
LVOT	left ventricle out-flow tract
MCP-1	monocyte chemoattractant protein 1
M-CSF	macrophage colony stimulating factor
MHC	major histocompatibility complex
MNC	mono-nuclear cells
mRNA	messenger RNA
NK	natural killer
NO	nitric oxide
OPG	osteoprotegerin

PAAT	pulmonary artery acceleration time
PAET	pulmonary artery ejection time
PAH	pulmonary arterial hypertension
PASMCs	pulmonary artery smooth muscle cells
PBMC	peripheral blood mononuclear cell
PBS	phosphate buffered saline
PCNA	proliferating cell nuclear antigen
PCR	polymerase chain reaction
PDGF	platelets derived growth factor
PGI	prostacyclin
PH	pulmonary hypertension
PIER	proteolytic induced epitope retrival
PVR	pulmonary vascular resistance
RIPA	radio-immunoprecipitation assay
RVESP	right ventricular end systolic pressure
SDF	stromal cell derived factor
SEM	standard error of the mean
SERT	serotonin transporter
siRNA	small (or short) interfering RNA
SMCs	smooth muscle cells
SPVDU	Sheffield pulmonary vascular disease unit
TBI	total body irradiation
TBS	Tris buffers saline
TGF-β	transforming growth factor β
TLR	toll- like receptor
TNF	tumour necrosis factor
TRAIL	tumour necrosis factor related apoptosis- induced ligand

Treg	regulatory T cell
VEGF	vascular endothelial growth factor
VTI	velocity timed interval
v/v	volume to volume ratio
vWF	Von willebrand factor
w/v	weight to volume ratio
WBCs	white blood cells
WSPH	world symposium of pulmonary hypertension
Xg	multiplied by gravity
µl	microliter

1 General introduction

1.1 Pulmonary hypertension

Pulmonary Hypertension (PH) was first reported in 1891 by the German physician Dr Von Romberg, he described the pathology from patient autopsy as pulmonary vascular lesions with unknown etiology and referred to the case as 'pulmonary vascular sclerosis' (Romberg, 1891). After the introduction of the catheterization technique for measurement of pulmonary blood pressure in patients, PH is defined as an elevation of mean pulmonary artery blood pressure (mPAP) of ≥ 25 mmHg at rest, recorded by heart catheterization (Galiè et al., 2009, Galie et al., 2010, Hoeper et al., 2013a). According to the latest classification agreed by the WHO in the 5th world symposium of pulmonary hypertension (WSPH) PH can be classified into five main classes based on their causes and pathology which are: Pulmonary Arterial Hypertension, Pulmonary Hypertension due to left heart disease, Pulmonary Hypertension due to Lung disease and/ or hypoxia, chronic thromboembolic Pulmonary Hypertension (CTEPH) and PH with unclear multifactorial mechanisms (Simonneau et al., 2013).

1.2 Pulmonary arterial hypertension

1.2.1 Disease definition and classification

Pulmonary arterial hypertension (PAH) is a complex, rare syndrome characterized by the increased vascular resistance of the pulmonary artery due to narrowing of the vascular lumen. Haemodynamically, PAH is defined by mPAP of higher than 25mmHg in rest and above 30mmHg in exercise (Kiely et al., 2013) associated with a pulmonary vascular resistance of more than 3 Wood units and

the end-expiratory pulmonary artery wedge pressure of ≤ 15mmHg (Hoeper et al., 2013b).

The restricted blood flow within the pulmonary artery alongside with the elevated pulmonary pressure and the resistance will lead to the weakening of cardiac muscles and in most of the cases to right heart failure and death.

According to the classification of the 5th WSPH, group 1 PAH is further subdivided into idiopathic pulmonary arterial hypertension (IPAH), heritable PAH, drug and toxin-induced PAH and PAH associated with other conditions such as HIV infection, connective tissue disease, schistosomiasis and congenital heart diseases. In addition, there is also a persistent pulmonary hypertension of the new-born which classified under PAH category (Table 1.1) (Simonneau et al., 2013).

PAH has a prevalence range of 15-50 person / a million of the population (average age of 50 years), and the prevalence is higher in specific patients groups, notably (5-10%) in those with congenital heart diseases, (9%) in those with systemic sclerosis and (0.5%) in those with HIV (Kiely et al., 2013).

Gender bias has been also implicated in PAH. According to the REVEAL registry, the female to male ratio of having PAH is 4.3:1 and 4.1:1 of IPAH. Although the prevalence was higher in women, men showed higher mPAP and poorer prognosis compared to the women, who have higher survival rate (Badesch et al., 2010).

Table 1.1. An updated classification of Pulmonary Arterial Hypertension modified in the 5th WSPH in Nice, France 2013.

1. Pulmonary arterial hypertension

    1.1 Idiopathic PAH

    1.2 Heritable PAH

        1.2.1 BMPR2

        1.2.2 ALK-1, ENG, SMAD9, CAV1, KCNK3

        1.2.3 Unknown

    1.3 Drug and toxin-induced

    1.4 Associated with:

        1.4.1 Connective tissue disease

        1.4.2 HIV infection

        1.4.3 Portal hypertension

        1.4.4 Congenital heart diseases

        1.4.5 Schistosomiasis

1' Pulmonary veno-occlusive disease and/ or pulmonary capillary hemangiomatosis

1''. Persistent pulmonary hypertension of newborn (PPHN)

BMPR2 = bone morphogenic protein receptor type II, ALK-1 = activin receptor- like kinase 1, ENG = endoglin, CAV 1= caveolin-1, HIV= human immunodeficiency virus.

1.2.2 Pathobiology and pathophysiology of pulmonary arterial hypertension

It is still not completely clear how the disease initiates, however it has been hypothesized that an injury to the vessel wall of the distal pulmonary arteries (such as viral infection, shear stress, mechanical stretching, hypoxia, inflammation or another unknown insult) alongside with environmental and

genetic factors can trigger pathological changes (Galie et al., 2010). Several mechanisms including different pathways and molecules have been proposed to be involved in the pathogenicity of PAH, but again the full mechanism of the disease progression is still unclear.

The pathogenicity of PAH includes multifactorial, complex processes that cause vasoconstriction, vascular wall remodelling and thrombosis, these processes eventually lead to stiffening of the vasculature, narrowing of the lumen, increased vascular resistance, increased blood pressure, increased right ventricle workload and consequently heart failure. The following sections will introduce the main cellular and molecular pathways that have been shown to be involved in the development of PAH.

1.2.2.1 Genetic factors associated with pulmonary arterial hypertension

It is well recognised by now that the major heritable risk factor for the development of PAH is the altered bone morphogenetic protein receptor type 2 (BMPR2) signalling, via mutation in the *BMPR2* gene, a member of the growth factor receptor family of transforming growth factors-β (TGF-β) (Nichols et al., 1997, Deng et al., 2000, Simonneau et al., 2013). In the heritable/ familial subtype of PAH approximately 80% of the cases carry a germline mutation in *BMPR2* (Machado et al., 2009). However, the prevalence of PAH among the BMPR2 mutation carriers is less than 20%, and patients with IPAH can have a reduced expression of BMPR2 even though no mutations detected (Morrell et al., 2009, Machado et al., 2009, Pfarr et al., 2013, Pousada et al., 2014). This suggests that other environmental/ host factors are required (second hits) to fully establish the disease state.

The importance of environmental factors in addition to impaired BMPR2 signalling is also evidenced by data collected from BMPR2 deficient animal models. For examples, heterozygous BMPR2 mutant do not develop PH spontaneously while when exposed to inflammatory stress (Song et al., 2005) or serotonin (Long et al., 2006) the disease susceptibility increased. In addition, conditional ablation of BMPR2 in endothelial cells (ECs) (Hong et al., 2008) or overexpression of a dominant negative BMPR2 in smooth muscle cells (SMCs) (West et al., 2005) only 30% of mice showed evidences of increased right ventricular systolic pressure (RVSP). However, recent mouse model using heterozygous knock-in allele (*BMPR2*[+/ R899X]) bearing the R899X stop codon in exon 12 (a *bmpr*2 mutation associated with human PAH), the animals developed spontaneous increase in RVSP which was reversed by BMP9 treatment (Long et al., 2015).

Within the lung, BMPR2 is highly expressed on vascular endothelium of pulmonary arteries and to less extent in smooth muscle cells and fibroblast (Atkinson et al., 2002). In ECs, the response to BMPs is dependent on specific BMP ligand; as BMP4 and BMP6 activates proliferation, migration and tubular formation of ECs, the BMP9 on the other hand, act to inhibit ECs proliferation and promote monolayer integrity in cultured ECs (Long et al., 2015).

Reduction in BMPR2 signalling in ECs may compromise the endothelial barrier and consequently this makes the underlying SMCs exposed to mediators and growth factors stimulating proliferation.

Mutations in other genes such as Activin- Like receptor Kinase-1 (*ALK-1*), endoglin (*ENG*), Caveolin-1 (*CAV1*), potassium channel subfamily K member 3

(*KCNK3)* and *SMAD9* have been also discovered in families with PAH (Simonneau et al., 2013, Austin and Loyd, 2014).

1.2.2.2 Endothelial cell dysfunction in pulmonary arterial hypertension

The endothelium of the blood vessel is a thin layer of ECs forming an interface layer between the circulating blood and the rest of the vessel wall layers (figure 1.1). The endothelium function to control vessel haemostasis and tone, white blood cells infiltration and hormone trafficking. PAH featured by ECs apoptosis leading to intima disruption and leakage of different mediators to the underlying SMCs (Morrell et al., 2009). Dysfunction of ECs assimilates in the imbalanced production of vasodilators versus vasoconstrictors, SMC growth inhibitors versus growth stimulators and antithrombotic and thrombotic factors (Humbert et al., 2008).

The balance between vasodilators/ growth inhibitors such as nitric oxide (NO) and prostacyclin, and between vasoconstrictors/ co-mitogens such as endothelin-1 and thromboxane A2 is essential to maintain vascular tone. Patients with PAH have shown an elevated level of vasoconstrictors (endothelin) (Giaid et al., 1993) and a reduction in vasodilators (NO and prostacyclin) (Christman et al., 1992). In addition, increased Thromboxane A2 (also cause vasoconstriction, platelet activation and aggregation) have been detected in patient's samples (Christman et al., 1992).

Endothelin-1 (ET-1) is a key vasoconstrictor that work through ET_A and ET_B receptors. The ET_A receptor found on vascular SMCs while the ET_B found on SMCs and ECs (Seo et al., 1994). Normally, ET-1 level in plasma is low, however, in PAH patients the circulating level of ET-1 shown to be elevated and associated

with right arterial pressure and PVR (Giaid et al., 1993, Cacoub et al., 1997). Drugs that antagonise the effect of ET-1 such as Bosentan and Macitentan have been approved for clinical use in PAH and showed improved clinical outcomes (Rubin et al., 2002, Sitbon et al., 2003, Renshall et al., 2018).

NO is also important regulator of vascular tone that shown to be reduced in PAH. NO produced in ECs from L-arginine substrate by endothelial nitric oxide synthase (eNOS). Reduced NO level in PAH could result from either reduced expression of eNOs, NO inactivation by superoxide anion or eNOs inhibition (Takemoto et al., 2002, Xu et al., 2004). In addition, IPAH patients showed an increased level of the eNOs inhibitor, known as ADMA (asymmetric dimethylarginine) in the plasma and in pulmonary artery endothelium (Pullamsetti et al., 2005).

Furthermore, deficiency of prostacyclin (cardio-protective hormone), prostacyclin synthase and increased thromboxane are reported in PAH (Christman et al., 1992). In animal models, prostacyclin overexpression protect against hypoxia-induced PH (Geraci et al., 1999), while prostacyclin-receptor knock-out mice develop severe hypoxia- induced PH (Hoshikawa et al., 2001).

In addition, in IPAH patients, ECs have been shown to produce excess leptin (the 'satiety hormone' that controls hunger and feeling of satiety) (Huertas et al., 2012). the high leptin plasma level of IPAH patients has been correlated to the exaggerated immune responses and the insulin resistance which are also features of PH (Huertas et al., 2012).

Taken together, the ECs dysfunction seems to have an integral role in the structural changes that occur within the pulmonary vasculature.

1.2.2.3 Smooth muscle cell proliferation and migration in pulmonary arterial hypertension

SMCs is the principal cells composing the media layer of vessel wall (figure 1.1). The up-normal proliferation of SMCs is a crucial pathological element in PAH. Many pathways shown to be fundamental in PAH are also involved in the proliferation and migration processes of SMCs such as the serotonin (or 5-Hydroxytryptamine 5-HT) signalling pathways (Herve et al., 1995, MacLean et al., 2000, Eddahibi et al., 2001), prostacyclin pathway and the expression of osteoprotegerin (OPG) (Lawrie et al., 2008).

Serotonin is an important mediator that influences the pathogenicity of PH. It is synthesized by converting L-tryptophan to 5-hydroxy-L-tryptophan (5-HT) via the activity of tryptophan hydroxylase (TPH). It has been shown that some patients with IPAH can have a high plasma level of serotonin (Herve et al., 1995). Also, pulmonary arterial endothelial TPH1 expression is increased in PAH patients and the derived serotonin can have paracrine effect on the underlying pulmonary artery SMCs (Eddahibi et al., 2006) .Serotonin exert a constricting effect on SMCs via binding to the 5-HT receptor and a mitogenic effect that is mediated by the 5-HT transporter (5-HTT). There are three major subtype of 5-HT receptors; $5-HT_1$, $5-HT_2$ and $5-HT_3$ (van den Berg et al., 2004). The response of pulmonary artery to serotonin is mediated mainly by the 5-HT1B receptor (Macintyre et al., 1992, MacLean et al., 1996a, Rondelet et al., 2003). In experimental PH, the pulmonary arterial response to the 5-HT1B receptor are amplified and receptor antagonism or deletion reverse the PH (MacLean et al., 1996b, Keegan et al., 2001). Furthermore, the disruption of the 5-HTT gene in animal models resulted in less severe hypoxia-induced PH phenotype when compared to control (Eddahibi et

al., 2001), while the overexpression the 5-HTT gene led to a spontaneous increase in the right ventricle pressure and exaggerated hypoxia-induced PH in female mice (MacLean et al., 2004).

As described above, prostacyclin is an important cardioprotective hormone which has been found to be reduced in PAH (Christman et al., 1992). Prostacyclin is produced by the endothelium of blood vessel and when coupled to its receptor it induces the formation of the cyclic adenosine monophosphate (cAMP). In vascular SMCs, cAMP mediates relaxation and inhibits the proliferation of the cells, thus the therapeutic utility of prostacyclin to treat PAH has been worked on extensively (Ruan et al., 2010, Safdar, 2011, Mitchell et al., 2014, Pluchart et al., 2017).

OPG is a regulatory protein with a main function of regulating osteclastogenesis. However, OPG can also bind to the tumour necrosis factor related apoptosis-induced ligand (TRAIL) to inhibit TRAIL-induced apoptosis (Emery et al., 1998). OPG expression and release is mediated by serotonin, BMPs and interleukin-1 (IL-1) and shown to be highly expressed within pulmonary vascular lesions and in patient's serum of IPAH (Lawrie et al., 2008). In addition, stimulation of human pulmonary artery SMCs with OPG induce proliferation and migration, OPG mRNA found to be 2-fold higher in pulmonary artery SMCs from IPAH patients compared to control and that high serum level predict poor survival (Condliffe et al., 2012). So OPG could provide an effective biomarker and a therapeutic target (Lawrie et al., 2008, Condliffe et al., 2012). The expression of TRAIL was also found to be elevated in patients with IPAH, TRAIL was shown to stimulate remodelling of pulmonary vascular cells and its blockage prevented PAH development in an animal model (Hameed et al., 2012).

In conclusion, An impaired balance between proliferation and apoptosis favours proliferation, resulting in muscularisation or thickening of the pulmonary vessel wall which is a hallmark pathogenic feature in PAH (Rabinovitch, 2008).

1.2.2.4 The adventitia remodelling in pulmonary arterial hypertension

Although the ECs and SMCs have received much attention from vascular biologists, the adventitial layer has also been noted to have a role in the pathogenicity of PAH and the associated remodelling. Fibroblasts are the key cells in the connective tissue that form the adventitia layer of the vessel wall (figure 1.1), they produce the tropocollagen and the ground substances that fill the spaces between cells of connective tissue (Stenmark et al., 2011). Activation of fibroblasts in response to injury or stress results in fibroblast proliferation, migration, and differentiation. In response to hypoxia, fibroblasts have shown the capability of proliferation with high propensity and differentiation into myofibroblast which can then either accumulate in adventitia or migrate to the other layers of the vessel wall. Activated fibroblast are also involved in inducing inflammatory cell recruitment, increasing the release of the extracellular matrix (ECM), and production of angiogenic chemokines to support neovascular growth (Stenmark et al., 2005, Li et al., 2011). In addition, recent publications have described adventitial fibroblast population in chronic hypoxic models of PH that possess pro-inflammatory phenotype (defined by high expression of pro-inflammatory markers such as IL-1β, CCL-2, GM-CSF, IL-6, CXCL12 and CCL-5), this phenotype was suggested to be a result of the epigenetic modification brought by histone-modifying enzymes specifically class I histone deacetylase HDACs (Li et al., 2011).

1.2.2.5 Inflammation in pulmonary arterial hypertension

Inflammation is another key feature of the PAH pathology. Excessive recruitment of different inflammatory cells such as dendritic cells, B cells, T cells and macrophages has been detected in the vascular lesions in patients and in animal models of PAH (Frid et al., 2006, Savai et al., 2012). Stacher et al reported that most of the pulmonary vascular remodelling and haemodynamic parameters in PAH are correlated with infiltration of perivascular inflammatory cells and that persistent inflammatory processes contribute to pulmonary vascular diseases (Stacher et al., 2012). Moreover, other studies showed that BMPR2 mutation also correlates with advanced inflammatory pathology, suggesting that in experimental PH the immune alteration is a cause rather than a consequence of the disease since inflammation precedes vascular remodelling (Tamosiuniene et al., 2011, Rabinovitch et al., 2014).

In this research thesis, inflammation in PAH is the main aspect of interest and will be discussed in detail in following sections.

1.2.2.6 Other mediators and growth factors

As discussed above, excessive proliferation is a key pathogenic feature of PAH, and different growth factors shown to be involved. Platelet-derived growth factor (PDGF), vascular endothelial growth factor (VEGF) and epidermal growth factor (EGF) are of the major growth factors which have been linked to the exaggerated proliferation, migration and apoptosis-resistance of pulmonary vascular cells in PAH (Humbert et al., 1998, Eddahibi et al., 2000, Cohen et al., 2003).

PDGF is a peptide growth factor considered as a potent mitogen for the VSMCs as its deletion or disruption of its signalling cascade attenuates neo-intimal

formation and inhibits SMC proliferation and migration (Boucher et al., 2003, Caglayan et al., 2011). It has been shown to have a role in fibro-proliferative disorders including PAH (Humbert et al., 1998). Recent approaches using primary cell culture and experimental PH showed the effectiveness of PDGF receptor inhibitors (such as imatinib) in attenuating proliferation (Lanner et al., 2005, Schermuly et al., 2005, Perros et al., 2008). Clinical trial has also shown the effectiveness of imatinib in patients, however, severe adverse effects were reported that limited its applicability (Ghofrani et al., 2005, Ghofrani et al., 2010, Hoeper et al., 2013a)

VEGF is also a powerful angiogenic growth factor which is released at the site of injury by the platelets to promote wound healing and endothelial repair in combination with other platelets-derived mitogens such as PDGF. Platelets contents of VEGF has been found to be elevated in patients with severe PAH while the PDGF content do not change (Eddahibi et al., 2000). However, the exact mechanistic role of VEGF in the development of PAH remains unclear particularly since treating rodents with VEGF receptor blocker (SU5416 or SUGEN) in presence of a second hit such as chronic hypoxia causes angio-obliterative PAH and right heart failure (Taraseviciene-Stewart et al., 2001). Some researchers suggest that VEGF exert either angiogenic or antiangiogenic functions depending on the type of receptor, the ligand and the duration of ligand-receptor binding (Ferrara et al., 2003)

Finally, EGF and its receptor EGFR are also emerging as important players in PAH pathology. The inhibition of EGFR attenuates PAH in the monocrotaline rat model (Merklinger et al., 2005). Furthermore, clinically approved EGF inhibitors such as gefitinib (Cohen et al., 2003) and erlotinib (Cohen et al., 2005) are also

available to treat some type of cancers. Despite this information, therapeutic use of EGF inhibitors in experimental PAH still did not show any effectiveness in targeting the disease (Dahal et al., 2010).

Collectively, different cell types contribute to the progression of the pulmonary vascular remodelling associated with PAH including ECs, VSMCs, fibroblasts and inflammatory cells. The uncontrolled proliferation and migration lead to medial thickening, increased vascular resistance, increased right ventricular afterload and eventually right ventricular failure and death.

1.2.3 Treatment of pulmonary arterial hypertension

PAH is a multicomponent syndrome that involves different pathological pathways, treatments available tend only to improve the patient's symptoms and quality of life. However there is no cure for PAH, and in many cases, lung transplantation is the final option.

Currently used drugs aim to reduce the vascular resistance of the vessels via targeting the three major pathological causes of vasoconstriction; nitric oxide, prostacyclin and endothelin-1 (figure 1.1). Mainly, there are four groups of drugs used in PAH treatment:

- Prostacyclin and its analogues: epoprostenol, treprostinil, beraprost, iloprost and the oral drug selexipac.

- Phosphodiesterase-5 inhibitor: sildenafil, vardenafil and tadalafil.

- Endothelin receptor antagonist: bosentan, macitentan and ambrisentan.

- And guanylate cyclase stimulator: riociguat.

The effectiveness of the prescribed therapeutic regimen can be assessed by the '6-minute walk' test, where the distance walked in 6 minutes is measured.

Phosphodiesterase-5 inhibitors are important clinically used drugs that show effectiveness and improved clinical outcomes in PAH patients (Galiè et al., 2009). Phosphodiesterase-5 is the degrading enzymes that inactivate NO and shown to be elevated in PAH patient's lungs and heart (Corbin et al., 2005, Nagendran et al., 2007). Interestingly, sex may influence the effectiveness of phosphodiesterase-5 inhibitors as male showed better outcomes in the 6-minutes' walk test compared to female (Montani et al., 2009).

The endothelin system can be targeted effectively by blocking both endothelin receptors, Bosentan and Macitentan are both dual ET_A/ET_B receptor antagonists approved for clinical use in PAH and showed improved clinical outcomes (Rubin et al., 2002, Sitbon et al., 2003, Renshall et al., 2018)

In addition to the groups described above, blocking calcium influx into PASMCs provide a scope to promote vasodilation. Indeed, high-dose calcium channel blockers such as nifedipine and diltiazem can be only recommended for patients following a positive acute vasoreactivity test (Kiely et al., 2013).

It should be noted here that there is evidence in the literature to show that anti-inflammatory and immunosuppressive agents could improve PAH (Meloche et al., 2013). In addition, some of the currently used medications may have, to some extent, an immune-modulatory activity that participates in their efficiency (Cohen-Kaminsky et al., 2014). This indicates that novel drugs specifically targeting the immunological component of the disease could be considered.

Ongoing work on developing novel antibodies targeting different pathological pathways in PAH is underway such as the vasoactive intestinal peptides (VIP), Rho kinases, Apelin and anti-OPG antibody. In summary, the facts describe the severity of PAH as a life-shortening disease, patient's quality of life will change dramatically after diagnosis and the accelerated pathogenesis of the disease will make them (even in young age) incapable to finish the six-minute walking test. Therefore, it is urgent first to validate the available treatment options and try to use and deliver them properly, and secondly to investigate new therapeutic targets that aim to selectively inhibit the vascular remodelling.
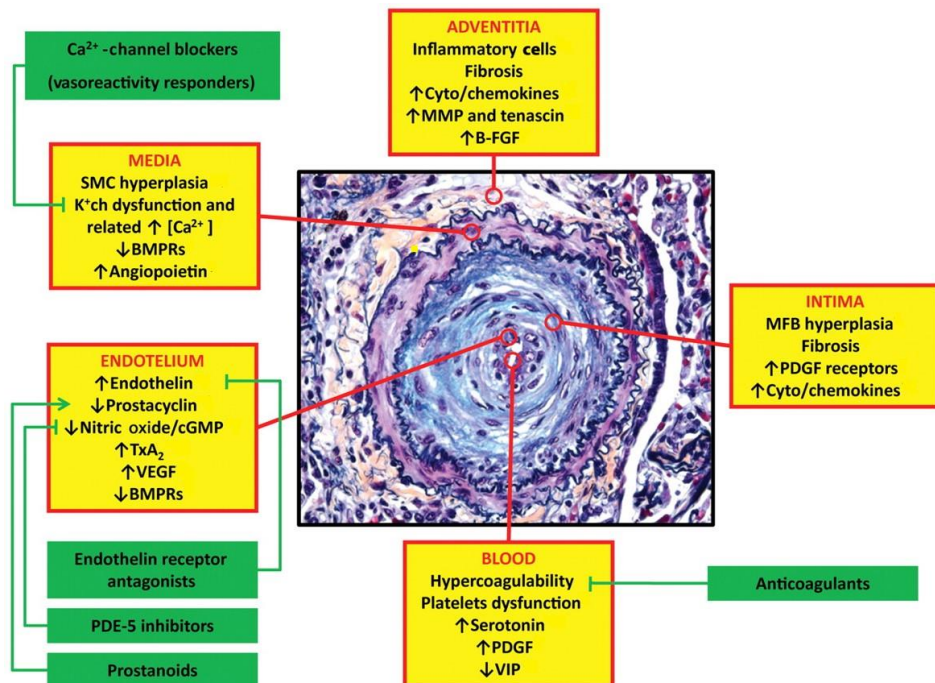
Figure 1.1- Pathobiology of the three layers of the vessel wall and the blood with the related therapy: Increased thickness of different layers of the vessel wall and severe reduction of the vascular lumen. Currently, available treatment aims to target the main pathological causes of vasoconstriction. Reused with permission from (Galie et al., 2010). MFB= myofibroblast, PDGF= platelet-derived growth factor, B-FGF= basic fibroblast growth factor, VIP= vasoactive intestinal peptide, TxA2= thromboxane A2, MMP= matrix-metalloprotienase, K^+ = potassium.

1.3 Inflammation in diseases

Inflammation is an aspect of the protective immune response of the body against any type of harmful stimuli, the reaction involves vasodilation, increased blood flow, the release of molecular mediators, release of extravascular fluids and the recruitment of immune cells (Ferrero-Miliani et al., 2007). Inflammation occurs to minimize cell injury, clear the dead cells and potentiate tissue repair.

Inflammation can be either acute or chronic. The acute inflammatory process is the quick, initial response of the body to harmful stimuli, it involves the increased movement of white blood cells from the blood into the site of injury. On the other hand, the chronic inflammation has a longer duration and can cause a progressive shift in the type of cells present at the site of inflammation and destruction of the tissue from the inflammatory process (Pullamsetti et al., 2011). Normally the inflammatory response is self-limiting, however, in many disorders, the inflammatory processes become continuous leading to chronic inflammation.

1.3.1 Role of inflammation in pulmonary arterial hypertension

As discussed above, impaired inflammation and altered immune responses are important aspects in the pathology of PAH. Excessive infiltration of inflammatory cells such as mast cells, dendritic cells (CD209$^+$), T cells (CD3$^+$), cytotoxic T cells (CD8$^+$), macrophages (CD68$^+$), macrophages/Monocytes (D14$^+$) and helper T cells (CD4$^+$) has been detected in the vascular lesion in clinical and experimental PAH (Frid et al., 2006, Savai et al., 2012, Stacher et al., 2012, Vergadi et al., 2011).

In addition, a vascular injury normally promotes an immune response in which natural killer cells (NK cells) and Tregs prevent the prolonged inflammation (Gill,

2010). Coordination between adaptive immunity (T and B lymphocyte) and innate immunity (NK cells and macrophages) is essential to suppress the reparative immune response when the danger has been eliminated. Treg cells regulate other T cells function as well as monocyte, macrophage, NK cells and B cells function. The altered Treg function has been observed in PAH patients (Tamosiuniene et al., 2011, Huertas et al., 2012). Also, congenital defects cause an absence of Treg cells in the athymic rat model led to massive inflammatory cell infiltration (B cells, mast cells and macrophages) into the lung after a vascular injury resembling the lesions seen in PAH patients, an effect which was prevented by Treg reconstitution (Tamosiuniene et al., 2011).

Furthermore, different inflammatory cytokines and chemokine such as interleukin-1β, IL-6, IL-8, MCP-1, CCL5/RANTES and TGF-B are shown to be elevated in PAH. Some of these cytokines mediate specific recruitment of leukocytes into the vascular compartment and are correlated with poor prognosis (Tuder et al., 2013). Evidence has been provided to show that pulmonary vascular cells, as well as inflammatory cells, are important source of local cytokines and chemokines, which lead to recruitment of different inflammatory cells and eventually cause pulmonary vascular remodelling (figure 1.2) (Pullamsetti et al., 2011).

Cytokines are multifunctional inflammatory mediators that can cause increased proliferation and contractility of vascular cells. IL-1 is pro-inflammatory cytokine secreted from macrophages, monocytes and vascular cells, the IL-1 level is found to be elevated in the patient's serum (Humbert et al., 1995) and the high level correlated to poor prognosis. It has been proposed that it has a role in mediating proliferative response in pulmonary vasculature's SMC and fibroblast (Steiner et

al., 2009). In the monocrotaline mouse model of PAH and in the IL-1 knockout mouse, the disease was attenuated following treatment with IL-1 receptor antagonist which emphasizes the implication of this cytokine in PAH pathology (Lawrie et al., 2011).

Furthermore, IL-6 is another important cytokine that has a role in the pathogenesis of PAH and shown to be elevated in patients serum (Humbert et al., 1995). In experimental PH, lung specific overexpression of IL-6 transgenic mice display spontaneous PH and exaggerated hypoxia-induced PH (Steiner et al., 2009), while IL-6 deficient mice showed resistance to hypoxia-induced PH (Hashimoto-Kataoka et al., 2015). Recombinant IL-6 can cause mild remodelling when given to rodents, and can further exaggerate the response in the presence of hypoxia (Golembeski et al., 2005). Furthermore, IL-6 can induce fibroblast growth factor-2 via KLF-5 transcription factor (Kruppel- like factor) and this may lead to pulmonary artery SMCs proliferation. In addition, blockage of IL-6 using receptor blocker prevents the hypoxia-induced PH and blocks the downstream IL-21 signalling, this was shown by suppression of IL-21 accumulation and the suppression of TH17 cell accumulation (TH17 is the source of IL-21) (Hashimoto-Kataoka et al., 2015). Thus IL-6 and the downstream IL-21 signalling could provide potential therapeutic for treating PAH.
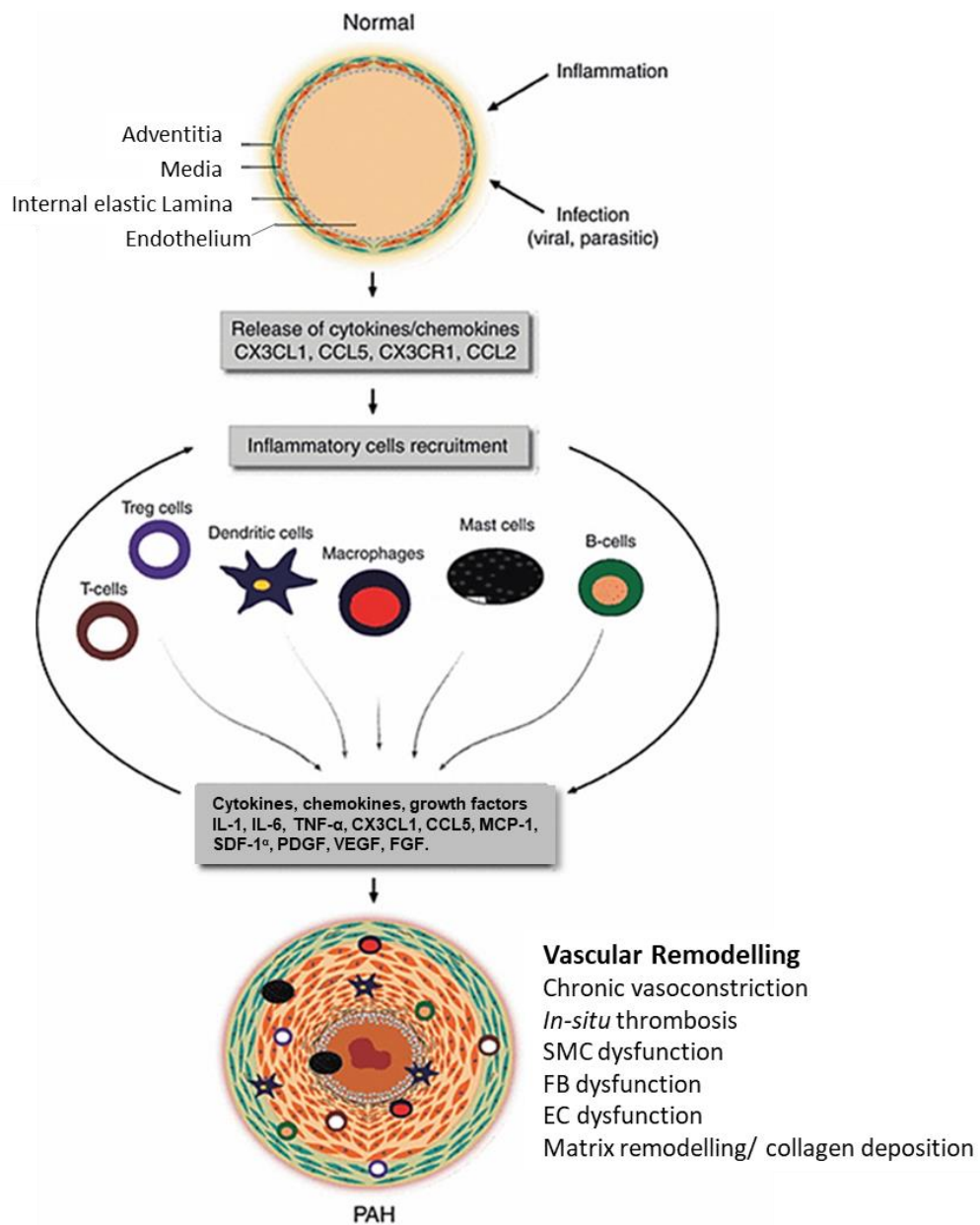
Figure 1.2- Schematic illustration of inflammation-mediated vascular remodelling: As a response to noxious stimuli (such as infection or inflammation), cells within pulmonary vasculature start to produce inflammatory mediators that attract the inflammatory cells (mast cell, B-cells, macrophages, T-cells, Treg-cells and Dendritic cells), these could further release inflammatory mediators and growth factors. These processes collectively may lead to vascular remodelling via collagen deposition, matrix remodelling, vascular cell proliferation/ migration and thrombosis. Reused with permission from (Pullamsetti et al., 2011).

Macrophages are another inflammatory cell that have had the attention of different research groups in attempts to understand the role of infiltrated macrophages to the pulmonary arterioles. Frid et al. (2006) have shown that the number of leukocyte/monocyte markers is increased by 50% in rat and bovine models of hypoxia-induced PH when compared to controls, and after tracing their origin they found that these cells are blood-borne cells (Frid et al., 2006). They suggested that the changes associated with hypoxia-induced PH such as the proliferation of adventitia, deposition of collagen and accumulation of smooth muscle-like cells (known as myofibroblast and express α- smooth muscle actin) are not only caused by the resident adventitial fibroblast, but also the recruited monocyte/ macrophage cells may directly contribute.

Macrophages are the cell of interest in this current work, thus the following section will include basic background related to monocyte and macrophage populations, focusing on macrophage function, subtype and their role in diseases which will lead onto my aims and hypotheses.

1.3.2 Monocytes

Monocytes are large, phagocytic white blood cells, which have an important role in the immune system and expansion of lymphocytes. Monocytes are generated from haematopoietic stem cells in the bone marrow and released into the circulation where then can either migrate to tissues to develop into macrophages (this cell lineage referred to as monocyte/macrophage) or stored in body tissue mainly the spleen, which acts as a reservoir for immature monocytes (Hettinger et al., 2013, Ziegler-Heitbrock et al., 2010b).

Although monocytes has been considered as the precursors for tissue macrophages and dendritic cells, some tissue macrophages and dendritic cells shown to be originated independently of monocytes (Geissmann et al., 2010).

In murine blood cells, monocytes can be distinguished from lymphocytes and granulocytes by their high expression of CD115 (M-CSF receptor) (Geissmann et al., 2008).

In human, monocytes were initially grouped into two subsets based on expression of the CD16 antigen; the CD14+CD16- and CD14+CD16+ monocyte subsets (Passlick et al., 1989). Later on, monocytes have been further segregated into three subsets according to the expression of the surface markers CD14 and CD16: CD14 $^{++}$ CD16 $^{-}$ [CD16^{-}] cells or the classical monocyte, CD14 $^{++}$ CD16^{+} [CD16^{+}] cells or the intermediate monocyte and CD14^{+}CD16^{++} the non-classical monocytes (Ziegler-Heitbrock et al., 2010a). In mice, monocytes can be similarly subdivided but with different markers: classical monocytes Ly6C^{++}CD43^{+}, intermediate monocytes Ly6C^{++}CD43^{++} and the non-classical monocytes Ly6C^{+}CD43^{++} (Ziegler-Heitbrock et al., 2010b, Wong et al., 2012).

Recent studies have advanced the knowledge regarding the three monocyte subsets. Apart from their gene expression, monocyte subpopulations reveals distinct functions, cytokine profiles and definite relationships. For instance, about 85% of all monocyte are classical monocytes and they have superior phagocytic properties, while the intermediate monocytes possess only 5% of total monocytes and their described functions include T-cell proliferation and stimulation and superior ROS production (Wong et al., 2012).

1.3.3 Macrophages

Following monocyte migration from the blood to the tissues, monocytes differentiate into dendritic cells or macrophages by aid of colony stimulation factors GM-CSF and M-CSF. Macrophages were first introduced in the 19th century by Elie Metchnikoff who described macrophages-phagocytic activity (Metchnikoff, 1893). Later on, this concept extended to include broader description of macrophages; macrophages described as phagocytic, antigen presenting cells (APC), mainly mononuclear (multinuclear in bone), which play different roles in innate and acquired immunity (Duffield et al., 2005). Macrophages shown to perform different functions including presenting the degraded protein to T-cells, tissue repair and reorganization. Also macrophages participate in lymphocyte activation and shown to have microbiocide activity (Epelman et al., 2014).

Macrophages named according to their anatomical location, for example: osteoclast in bones, Kupffer cell in the liver, alveolar macrophages in the lung and the microglia in the brain (Duffield et al., 2005, Gheryani et al., 2013).

Macrophages, as well as monocytes, neutrophils, dendritic cells and mast cells, express cell surface receptors such as the Toll-like receptors (TLRs) and scavenger receptors, these receptors specifically detect signals arising normally from non-healthy tissue or invading organisms and so-called 'professional phagocytic cells' (Murray and Wynn, 2011).

Macrophages can be distinguished from other cells by their expression of unique surface markers such as F4/80 and CD68 (table1.2). Moreover, whole genome analysis revealed further heterogeneity and overlapping within macrophages

population. Based on the gene expression profile, chemokine expression profile and response to different stimulus macrophage subsets were introduced.

Table 1.2. Examples of murine macrophages-surface markers that commonly used in research

Cell surface marker	Expression	Example reference
CD11b	All myeloid lineage	(Hettinger et al., 2013)
CD68	Most tissue macrophages	(Gheryani et al., 2013, Higashi-Kuwata et al., 2010)
CD86	Most tissue macrophages Suitable for M1 macrophages	(Talati et al., 2014)
CD204	Scavenger receptors Suitable for M2 macrophages	(Higashi-Kuwata et al., 2010, Talati et al., 2014)
CD206	Mannose receptor Suitable for M2 macrophages	(Moreno et al., 2014)
F4/80	Most tissue macrophages in the mouse. Predominantly expressed on eosinophils in human.	(Gheryani et al., 2013)
Ly6C+	Inflammatory monocytes	(Hettinger et al., 2013)
NHC II	Professional Antigen Presenting Cells. Suitable for M1 macrophages	(Talati et al., 2014, Moreno et al., 2014)

1.3.3.1   Macrophage subset

Classically activated macrophages (M1): This macrophage population stimulated by TLRs-ligand such as polysaccharide and interferon gamma (Mosser and Edwards, 2008). The M1 macrophages produce pro-inflammatory cytokines and reactive nitrogen and oxygen intermediates. The M1 macrophages mediate the defensive mechanisms against invading pathogens such as bacteria and viruses and possess some anti-tumour activity (Sica and Mantovani, 2012).

Commonly defined markers for M1 macrophages include inducible nitric oxide synthase, MHC class II, IL-12β and co-stimulatory molecules as CD86, which can be detected and quantified by immunostaining and PCR (Higashi-Kuwata et al., 2010, Moreno et al., 2014).

Alternatively activated macrophages (M2): This macrophage subset is the anti-inflammatory macrophages that are activated by IL-4 or IL-13 (Stein et al., 1992). The M2 macrophages participate in debris scavenging, regulate wound healing, have immune-regulatory functions and promote tumour progression (Jensen et al., 2009, Weisser et al., 2012, Gheryani et al., 2013). The M2 macrophages express mannose receptor CD206, arginase 1 (arg-1), IL-4 receptor α-chain amongst others (Moreno et al., 2014, Sica and Mantovani, 2012).

Biswas and Mantovani have described a functional macrophage subtype that shares some features with M2 cells such as the expression of mannose receptor, but differ in other properties such as chemokine expression repertoire when induced by different signals as IL-10 or molecules released from the immune complex. They refer to this subtype as M2-like macrophages (Biswas and Mantovani, 2010). Furthermore, in some instances, the literature shows a slightly

different classification scheme for macrophages: some research articles categorize them as [M1] classically activated, [M2] alternatively activated and the [regulatory] anti-inflammatory macrophages, where the major feature of the regulatory macrophages is their promotion of immunosuppression and high production of IL-10 and low IL-12 (Vergadi et al., 2011).

Different researchers use different types of cell marker to distinguish macrophages from other cells and/or macrophage subsets from each other. Moreover, expression of a combination of specific macrophage markers in a specific manner can be used to identify different macrophage subpopulation. For example, in a study by Moreno et al, a combination of CD11b$^+$CD45^{hi} was used for the identification of monocyte-derived macrophages, CD11b$^+$CD45^{lo} for microglia, CD206$^+$Arg$^+$Ym1$^+$ for M2 and Ly6c^{hi}MHCII$^+$CD86$^+$iNOS$^+$ for M1 macrophages. To do so they used either flow cytometry, RT-PCR or immunofluorescent labelling (Moreno et al., 2014). However, in a study by Talati et al another combination of cell markers were used to distinguish between lung macrophages using cell sorting and immunohistochemical staining. They used CD45$^+$ CD68^{low} CD11$^+$ Gr1$^-$ for interstitial macrophages, CD45$^+$ CD68^{hi} CD11c$^+$ F4/80$^+$ for alveolar macrophages, F4/80$^+$ MHCII$^+$ CD86$^+$ for M1 and f4/80$^+$ CD204$^+$ for M2 macrophages (Talati et al., 2014).

1.3.3.2 Macrophages in disease

In case of tissue injury or stress, the resident macrophages might be insufficient to control the damage, so the circulating monocytes recruit to the damaged organ or tissue and differentiate into macrophages. These newly recruited macrophages are pro-inflammatory and secrete inflammatory mediators

including IL-1, IL-12, IL-23, nitric oxide and TNF-α (Murray and Wynn, 2011). However, inflammatory macrophages can initially be beneficial since they clear the debris, but they could also cause collateral damage to the tissue because of the toxic activity of the oxygen and nitrogen species they produce (Fang, 2004). Thus, excessive release of these mediators must be controlled quickly or it becomes pathogenic and contributes to the progression of many diseases.

To protect tissue integrity macrophages undergo apoptosis or switch their phenotype to the anti-inflammatory M2 phenotype (Arnold et al., 2007). The presence of two macrophage subtypes and/or switching of macrophages between inflammatory and anti-inflammatory has a great impact on the progression of many chronic diseases such as cancer (Jensen et al., 2009), fibrosis (Duffield et al., 2005) and atherosclerosis (Martinet et al., 2007). Macrophages are versatile and possess various, and sometimes opposing functions. For example, in a skeletal muscle regeneration study, macrophage activation was traced using latex beads to label the monocytes in $CXCR1^{GFP/+}$ mice. The study showed that the recruited monocytes were only $CXCR1^{lo}/$ Ly-$6C^+$, but were also a pro-inflammatory and non-dividing. Later on, these cells switched within the muscle to become anti-inflammatory $CX3CR1^{hi}/Ly\text{-}6C^-$ cells, which then differentiate to $F4/80^{hi}$ macrophages (Arnold et al., 2007). In addition, *in vitro* experiments showed that the switch from pro-inflammatory to anti-inflammatory macrophages is induced by phagocytosis of tissue debris and releasing TGF-β1 (Arnold et al., 2007).

1.3.3.3 Macrophages in pulmonary arterial hypertension

In PAH, excessive infiltration of macrophages and high levels of IL-6 and IL-1 have been detected in patients (Frid et al., 2006). These findings suggest that macrophages may play a key role in the remodelling processes associated with PAH. However, their exact role remains unclear.

Vergadi has investigated the link between macrophage phenotype and hypoxia-induced PH, using a bi-transgenic mouse model where doxycycline induces lung-specific expression of heme-oxygenase-1 (HO-1). The study showed that HO-1 has a protective function via an immunomodulatory pathway since overexpression of HO-1 inhibited macrophage recruitment and alternative activation in response to hypoxia, this suggested that early macrophages recruitment and activation are essential for later development of hypoxia-induced PH (Vergadi et al., 2011). Furthermore, the temporal profile of broncho-alveolar lavage fluid (BALF) cell content showed that the number of monocyte/ macrophage reach the peak after two days of hypoxia and then dropping significantly in the control animal, while overexpression of HO-1 suppressed the accumulation of macrophages at all-time interval investigated (Vergadi et al., 2011).

Moreover, in the same study, analysis of BALF- isolated alveolar macrophages by PCR and immunofluorescent staining showed upregulation of M2 macrophage markers (such as Arg-1 and Fizz 1) in hypoxic mice, whereas no changes in M1 marker were detected. Overexpression of HO-1 suppressed the M2 alternatively activated marker in the transgenic animal. Their data strongly suggested that the M2 macrophage phenotype is the dominant polarized form of alveolar

macrophages in hypoxia-induced PH (Vergadi et al., 2011). Vergadi study presented a link between M2 macrophages and the development of PH, particularly since M2 macrophages have been shown to be involved in the pathogenesis of other diseases including lung disease (Lewis and Murdoch, 2005, Mosser and Edwards, 2008) but further work is required to investigate the underlying mechanism of action of these subsets.

In severe PAH, plexiform lesions (complex mass of vascular formation originated from the pulmonary artery) are common and have also shown to be rich in macrophages (Sakao et al., 2009, Jonigk et al., 2011, Vergadi et al., 2011), but again, the exact role of macrophages within these lesions is not yet known. In addition, plexiform lesion have been shown to contain high numbers of macrophages expressing leukotriene A4 hydrolase (LTA_4H) (Tian et al., 2013). LTA_4H is the biosynthesis enzyme of leukotriene B4 (LTB_4) and high levels of LTB_4 have been detected in PH patient's plasma (Tian et al., 2013). LTB_4 derived from macrophages has shown the ability to induce apoptosis in pulmonary artery ECs and cause proliferation of SMCs possibly by inhibition of endothelial Sphingosine-kinase/ endothelial nitric oxide synthase pathways (Tian et al., 2013).

In order to study the function of macrophages in different inflammatory based diseases, researchers aimed to deplete macrophages *in vivo* using different approaches to investigate macrophages distinct role in case of their absence.

1.3.3.4 Macrophage depletion models

Many methods have been utilised to deplete specific cells in order to investigate their functions. The oldest approaches involve the use of toxic chemicals such as

silica and asbestos (Kagan and Hartmann, 1984), however, many unwanted toxic effects hinder these approaches. Early genetic approaches such as the knockout of colony-stimulating factor-1 in mice (*op/op* mutant mice (Yoshida et al., 1990)), resulted in severe macrophage loss especially in bones (leading to congenital osteopetrosis), skeletal deformity, growth abnormality, poor fertility and weak immunity. These severe abnormalities shortened the lifespan of the animals and hindered further pathological studies (Stanley et al., 1997).

To improve specificity of cell depletion, recent models have been generated using gene targeting and genetic engineering technologies. Still, most of these models carry some level of toxicity or lacking of specificity. Some of these models are: liposome-mediated depletion (Vanrooijen and Sanders, 1994), transgenic FAS-induced apoptosis (Burnett et al., 2004), transgenic expression of the diphtheria toxin receptor (Duffield et al., 2005), pharmacological- initiation of cell death in atherosclerosis (Martinet et al., 2007) and the use of gadolinium chloride (GdCl3) (Singh et al., 2004).

Among the most commonly used approaches in research is the liposome-mediated depletion model. The model (also called macrophage suicide model) involves the use of liposome encapsulated drug dichloromethylene diphosphonate (CL2MDP) to cause macrophage death due to disturbances in cell metabolism following phagocytosis of the liposome (Vanrooijen and Sanders, 1994). This approach has managed to some extent to be specific to macrophages, however, it targets all the phagocytic cell including dendritic cells (Weisser et al., 2012). Also, some safety issues are still a concern since the 'bystander effect' was not controlled. The bystander effect becomes apparent when the macrophages died and their toxic content (lysosomal enzyme,

proteases and cytokines) are released, this may lead to an inflammatory response, lymphocyte recruitment and pH changes (Rogers et al., 2014).

The transgenic expression of the diphtheria toxin receptor is another commonly used approach for cell depletion in rodents. The ablation system adopted in this model relies on expression of human diphtheria toxin receptor (DTR; also known as human heparin binding-EGF) under the control of CD11b followed by diphtheria toxin (DT) administration (Duffield et al., 2005). The DT *in vitro* cleaves to DT-A and DT-B chains, DT-B chain binds to the heparin-binding EGF and internalize the A chain to the cell by endocytosis. DT-A chain causes the toxicity via inhibition of protein synthesis. Mice lack the hb-EGF binding receptor and thus are insensitive to DT (Duffield et al., 2005). This model showed effectiveness in deleting the CD11b cells, however, DT is a highly toxic molecule and any non-specific expression would be lethal (Rogers et al., 2014).

1.3.3.5 *MacLow* mouse model for macrophage depletion

To deplete a vital cell such as a macrophage, it is important to adopt a depletion model with the least side effects and to overcome the limitations associated with the common depletion models such as specificity, toxicity, longevity and complexity (described above). The *MacLow* model newly developed in Sheffield, is a macrophage ablation model, based on the cell specific induction of macrophage ablation in mice using doxycycline (Gheryani et al., 2013).

It has been shown that conditional cell elimination can be achieved when the expression of DTA gene is regulated by tetracycline responsive element in conjunction with using cell-specific promoter (Lee et al., 1998). In the *MacLow*

mouse model the CD68 promoter (macrophage-specific encoding gene) was used to selectively deplete macrophages *in vivo* (Gheryani et al., 2013).

The model demands generation of a double-transgenic mouse containing CD68-rtTA-eGFP and tetDTA transgenes which then treated with doxycycline to induce the expression of diphtheria toxin in CD68 positive cells. The first transgene expresses the reverses tetracycline transcriptional activator (rtTA) under the control of a CD68 promoter, in addition to IRES (internal ribosome entry site) and enhanced green fluorescence protein eGFP. The second transgene express diphtheria toxin A-chain (DTA) downstream of tetracycline responsive element TRE (figure 1.3).

Using the *MacLow* mouse model, up to a 40% reduction in macrophage number within the liver was achieved after 48h of doxycycline injection, whilst up to 50% reduction was achieved following continuous two weeks doxycycline treatment in diet (Gheryani et al., 2013). Moreover, extending the experimental duration to six weeks did not show any further reduction in macrophage number, but interestingly the remaining macrophage population in doxycycline-treated double transgenic animals were smaller and had reduced cytokine production in response to LPS (Gheryani et al., 2013).

The advantages of *MacLow* mouse model over other macrophage ablation model can be summarized as follow:

1- In contrast to other knockout methods, the double transgenic animals in this model were healthy and suitable for further pathological investigation.

2- No external diphtheria toxin is used, so no potential toxicity.

3- Unlike other models that use complex and expensive materials with a complex delivery system, *MacLow* model involves the use of doxycycline which is safe, readily available and easily administered reagent.

4- The macrophage specificity is a major benefit of this model, since only cell expressing CD68 were depleted.

In my previous work undertaken for completion of my MSc degree (Zawia, 2011) I utilized the *MacLow* mice to correlate macrophages and vascular remodelling in hypoxia-induced PAH. *MacLow* mice were fed either doxycycline containing diet or normal chow for 2 weeks to induce macrophage ablation, and then PAH was

induced by the insult of hypoxia (10% Oxygen) for another 2 weeks with continuous doxycycline administration (parallel groups were left in the normal air as controls). The findings showed that reducing the number of CD68+ macrophages did not protect against hypoxia-induced PAH, but it also showed an interesting trend (not significant) whereby an unexpected increase in the right ventricular end systolic pressure (RVESP) of the normoxic control group (specifically male mice) was seen after the loss of macrophages (figure 1.4).
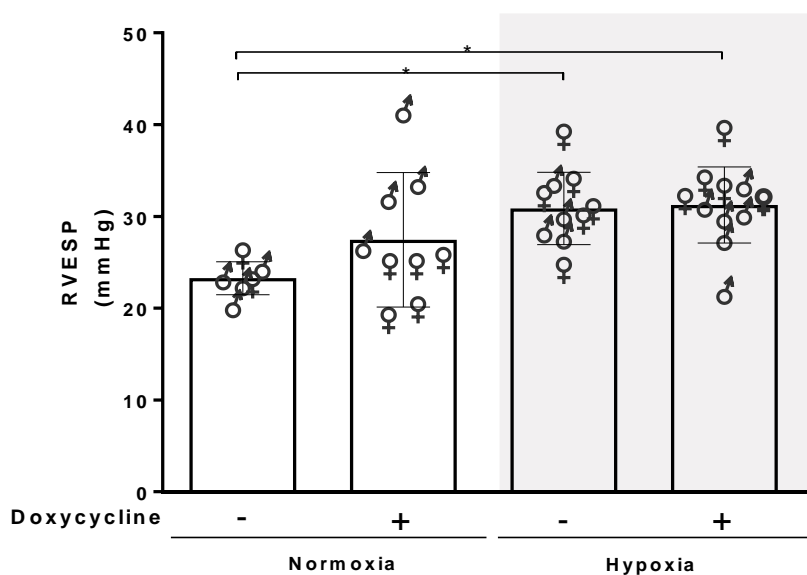
Figure 1.4- loss of CD68+ macrophages did not protect against hypoxia-induced PAH: the graph shows the right ventricle systolic pressure (mmHg) measured by closed chest cardiac pressure-volume catheterization. Error bars represent mean ±SD, * P< 0.05. modified from (Zawia, 2011)

For the current research, undertaken for completion of my PhD, I intended to pursue this work further and explore the modulatory mechanism of macrophages using the same *MacLow* animal model.

1.4   Hypothesis of the study

I hypothesized that macrophage depletion in *MacLow* mouse will reduce/ protect the mice from induced PAH.

1.5   Aim of the study

The main goal of this research was to determine the role of macrophages in the pulmonary arterial hypertension and whether they are required for the pulmonary vascular remodelling (and/ or reverse remodelling).

The objectives include:

- To confirm that loss of macrophages can cause sex- specific spontaneous PAH phenotype as suggested by my previous work.

- To trace the origin of lung macrophages during the disease and whether the majority of macrophage population are lung resident macrophages or blood- borne cells.

- To determine if a particular macrophage subset is dominant in the *MacLow-* induced PAH phenotype.

- To investigate whether *MacLow*-derived macrophages have unique characters compared to control macrophages.

2 Materials and methods

2.1 Animal work

2.1.1 Generation of the double transgenic mouse (*MacLow* mouse)

To generate the double transgenes CD68-rtTA- EGFP/ tetDTA (CDTD or the *MacLow* mouse) the heterozygous single transgenic mouse CD68-rtTA-EGFP (CD) was crossed with a homozygous tetDTA (TD) transgenic line (see section 1.3.3.5 for the generation of the single transgenes). The line was maintained by crossing the heterozygous (CDTD) with the homozygous tetDTA (TD) at the biological service unit of the University of Sheffield. Mice were kept in high health state facilities in a controlled environment with a 12 hour light/ dark cycle, and with free access to food and water *ad libidum*. All animal works were approved by both the University of Sheffield Ethicals committee and the UK Home office regulation (project licence number 40/3517 and 70/8910) under the Animal Scientific procedure act (1986).

The genotype of the double transgenic mice generated was assessed by using polymerase chain reaction PCR. For a rapid DNA extraction for genotyping, mouse ear clips were incubated in 150 µl of DNA extraction solution that consists of 300 µg/ml proteinase K (Proteinase K from Tritirachium album supplied by SIGMA) in Tail Lysis Buffer (see appendix II for recipe) at 55ºC overnight, then the reaction was heated up to 100 ºC for 12 minutes to inactivate the proteinase K in the extraction buffer. For the genotyping PCR, primer pairs used were the

CD68 GT F 5′-GACGTAAACGGCCACAAGTT-3′ and CD68 GT R 5′-TGCTCAGGTAGTGGTTGTCG-3′ primer pair to amplify the 526 bp fragment within the CD transgene. And TetDTA F_1 5′-TCGTACCACGGGACTAAACC- 3′ and TetDTA R_1 5′-ACTTGCTCCATCAACGGTTC -3′ primer pair to amplify the 299 bp fragment of the DTA transgenes. The PCR reaction mixture consisted of 9 µl master mix (containing 3 µl of the 5X Go Taq Flexi buffer with dye, 1.5 µl of the 10X dNTPs, 0.12 µl Promega GoTaq® G2 Flexi DNA polymerase and 3.48 µl millicurie water) 2 µl of each primer and 2 µl of the DNA sample to make a final volume of 15 µl. Samples containing a known DNA were used as a positive and a negative control, a no-template control that contains no DNA was used as a negative control as well.

The reaction was first heated to 94 ºC for 4 minutes, followed by 30 amplification cycle each consists of: denaturation at 94 ºC for 30 seconds, annealing at 57 ºC for 30 seconds and extension at 72 ºC for 30 seconds, finally the reaction preserved at 72 ºC for 10 minutes using MyCycler ™ Thermal Cycler, USA. Resulted products were then visualized using gel electrophoresis, the gel was made as 0.8% w/v agarose gel (Fisher BioReagent®) in 1X LTB buffer (see appendix II for recipe) containing 5 µl of 10 mg/ml ethidium bromide (SIGMA). The gel ran at 100 V for 30 minutes in 1X LTB buffer. A DNA marker (GeneRuler™ 1 Kb DNA ladder) containing a set of DNA fragments of known sizes was loaded alongside the sample to confirm the size of the DNA in test samples. The bands were visualized using BioDoc-it image system with the UV transilluminator UVP (figure 2.1). Mice shown to be a non-double transgenic (CD68 negative) were either kept to use as controls in some studies or culled if not required.
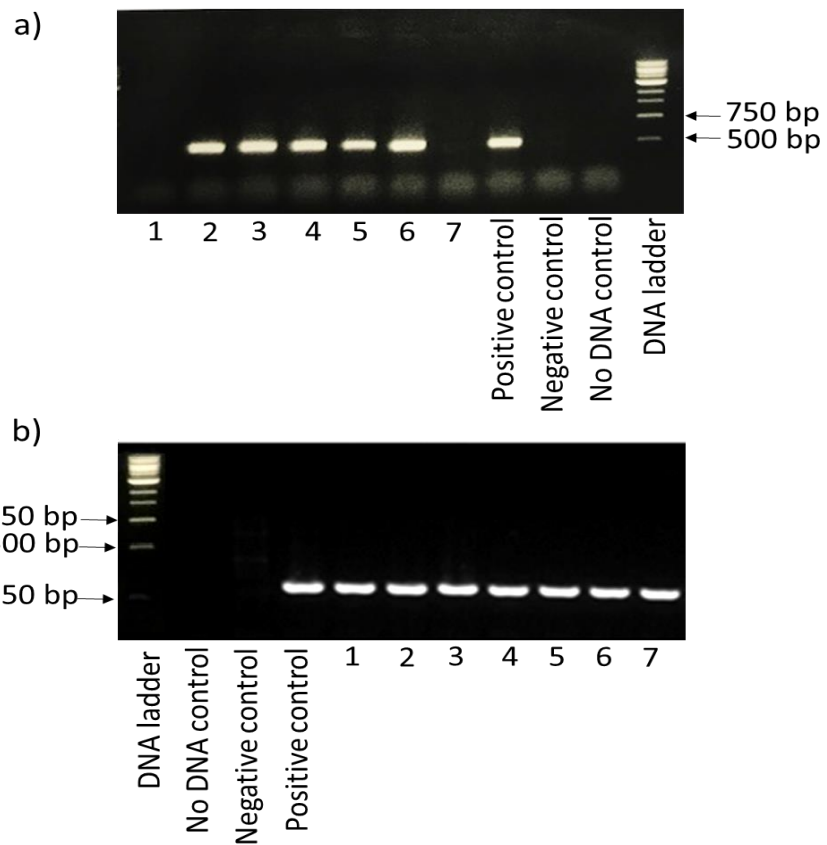
Figure 2.1- Generation of *MacLow* mouse: Representative images of agarose gel showing PCR amplification of DNA extracted from mouse ear clips for genotyping. An example of PCR gel that shows the positive samples for the CD68 genes (2, 3, 4, 5 and 6) appeared in 546bp bands (a). And an example of PCR gel that shows positive samples having the tetDTA genes appeared in 299bp bands (b).

2.1.2 Induction of macrophage ablation

To induce macrophage ablation in *MacLow* mice, animals were treated with doxycycline either orally (with food) or by intraperitoneal injection as stated in each study. In the doxycycline time- point study, a single intraperitoneal injection of doxycycline (doxycycline hyclate, 002R27, Sigma-Aldrich) in a dose of 80 mg/kg body weight was given to mice which then culled at different time points.

Doxycycline hyclate was dissolved in water for injection to make up an injection volume of about 200μl for each animal.

On other longer-term studies, doxycycline was given as doxycycline containing diet (contains 625 mg/kg, ENVIGO laboratories Inc, Madison, USA), where 5 grams of diet allocated to each mouse for each day. Doxycycline has poor stability in light and in water so the diet was replaced with fresh every 2-3 days to ensure the activity of the drug.

2.1.3 Bone marrow transplant procedure and generation of the chimeric mice

To generate the targeted chimeric mice, a donor inoculum was given to a pre-irradiated recipient mouse, the inoculum used contains hematopoietic stem cells harvested from the bone marrow of the donor mouse with known genotype. For the bone marrow transplant procedure (BMT) all mice were kept in individually ventilated caging (IVC) under the barrier area in the biological service unit in Hallamshire hospital, mice were fed standard chow and given acidified drinking water (see appendix II for recipe) one day before the transplant to minimized the risk of infection.

On the day of transplant, recipient mice were given a lethal single dose of whole-body irradiation equals to 10 Gy (1000 rad) using a CIS IBL 437 Cs-137 irradiator (BM0435/CA5869). The time of exposure was calculated using the dosing guide provided with the machine. Following the irradiation, mice were placed in 35 ºC incubator for 1 hour before receiving donor bone marrow cells.

Donor mice (aged 5-7 weeks) were euthanized by cervical dislocation. From each mouse, both legs were harvested intact in a clearly labelled petri dish on ice. It

was essential to maintain aseptic conditions during the whole procedure by spraying the mouse periodically with 70% ethanol. Under the fume hood, bones were cleaned up from fur and muscles as much as possible before placing them in cold media (RPMI- 1640 media 'phenol red-free' contains 10% v/v HI FBS). Epiphyses removed using sterile scissors and the bone marrow flushed with 26-27 G syringe contains 2 ml media, cells were passes through 40 µm cell strainer then centrifuged at 4 ºC 500 *Xg* for 5 minutes. Pellets re-suspended in Hank's buffered salt solution (HBSS) containing 10% v/v heat- inactivated fetal bovine serum (FBS) and counted with a haemocytometer using 1% v/v acetic acid to lyse the red blood cells. Cell suspension left on ice ready for tail vein injection, each mouse produces an average of 15-25 X10^6 cells/ ml.

For efficient and fluent tail vein injection procedure, recipient mice were sedated with subcutaneous injection of Hypnorm® solution and sent back to the incubator for few minutes before injection. Each mouse received between 5 and 6 x 10^6 cells in 100-200 µl cell suspension the left in the incubator to recover from sedation for 2-3 hours. Mice were closely monitored daily for the first two weeks for any sign of non-engraftment. This protocol was established and optimized according to the results of two pilot studies that I performed to enhance the survival rate (see chapter 4, section 4.3.1). Using this optimized protocol, we get a survival rate of 100% in our experiments and a successful engraftment of the donor bone marrow.

2.1.4 Echocardiography

To assess the changes in shape, size and functions of the heart following PAH induction echocardiography was performed, echocardiography is a non-invasive technique that uses the ultra-sound waves to produces a moving image of the

heart and the associated vessels (Singh and Goyal, 2007). The readings were taken at the baseline, midpoint and at the end of the study using the Vevo 770 system (Visual Sonics, Toronto, Canada) and the RMV 707B scan head. Mice were immediately weighed, then anaesthesia induced by 5 % v/v isoflurane, 2 L/ min oxygen. The anaesthetised mouse was then placed on the platform with a heating lamp directed to it to minimise heat loss, the mouse needs to be flat down with limbs secured well and with cushions on sides to prevent sliding. General anaesthesia was confirmed by loss of pedal reflex.

Biological parameters such as temperature, heart rate and respiratory rate were recorded constantly during the procedure with the accompanied Visual Sonic temperature control and ECG amplifier. Anaesthesia maintained by 0.5- 2 % v/v Isoflurane through oxygen using facemask and manipulated to keep the heart rate within the range of 450- 500 bpm as possible. The chest area was shaved properly and pre-heated ultrasound gel was applied before starting taking readings

The right ventricle cavity dimensions were taken from the right long axis view by M-Mode of the free wall, while left ventricle functions were assessed at 2 dimensions, the left long axis view and the short axis view by M-Mode at the level of papillary muscle. For the calculations of cardiac output Doppler pulse wave of the aortic valve from the right axis view and the left ventricle outflow tract diameter (LVOT diameter) from the left axis view were taken. The pulmonary artery flow measurements (pulmonary artery acceleration time PAAT, ejection time PAET and velocity timed interval VTI) were also recorded from the short axis view at the level of the pulmonary valve.

The analysis was performed using the Vevo 770, version 3.0; visual sonics software, measurements were taken offline when the cardiac cycle did not correspond with inspiration phase.

2.1.5 Cardiac catheterization

At the end stage studies and following echocardiography, left and right ventricular catheterisation was performed using a closed chest method. The technique involves insertion of a thin flexible tube called a catheter into the blood vessel and guided to the heart, despite its invasiveness it is required to definitively diagnose PAH as it gives important information about the dynamic inside the heart. Left and right ventricles were reached through the right internal carotid artery and the right external jugular vein respectively (figure 2.2), Isoflurane-induced anaesthesia was maintained throughout the procedure (0.5- 2 % v/v Isoflurane). First, to expose the jugular vein, a small incision was made in the neck to the right of the midline, then the tissue surrounding the vein were dissected carefully using fine curved forceps. The clear vein ligated with one suture distal to the heart and another loose suture proximal to the heart. Millar SPR-1030 1F catheter (Millar Instruments Inc, Houston, TX, USA) inserted through the vein by the aid of a bent 25G needle to help to pull up the vein and inserting the catheter simultaneously. After this stage, the loose proximal suture can be tied off slightly and the recording can be started using the PowerLab system version 7 (AD Instruments, Oxford, UK), the catheter advanced carefully until reaching the right ventricle. The right ventricle haemodynamic parameters are taken when normal and stable RV tracing established. The tracing recorded for about a minute to allow multiple data extraction points then the catheter pulled carefully and the vein tied properly.

Similar principles were applied to cannulate the right internal carotid artery for the measurements of left ventricle loop haemodynamic using Millar SPR-1035 1F catheter (Millar Instruments Inc, Houston, TX, USA). If the systemic pressure was needed, the catheter pulled out slightly from the left ventricle to the aorta and the aortic pressure recorded. Data recorded using the Lab Chart Pro software (version 7.0, AD instrument, Oxfordshire, UK).
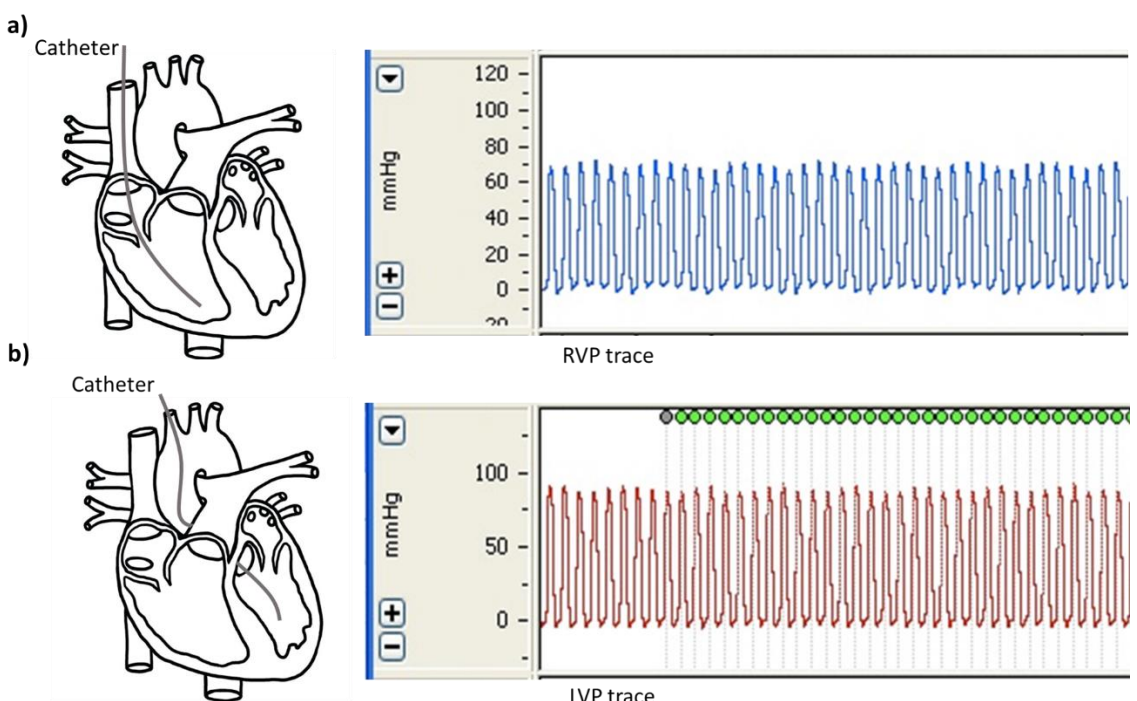
Figure 2.2- Ventricular pressure measurements: a) Diagram shows catheter inserted into right ventricle via jugular vein to record right ventricular pressure measurement (RVP) and a trace of the RVP. Y axis in mmHg. b) Diagram shows catheter inserted into left ventricle via right carotid artery to record left ventricular pressure measurement (LVP) and a trace of the LVP. Y axis in mmHg.

2.1.6 Blood collection and tissue harvesting

In the majority of the studies, blood collected from anaesthetized animals by cardiac puncture. Cardiac puncture is an effective technique to obtain a large volume of peripheral blood with a good quality from mice under deep terminal

anaesthesia. Animals were placed on their back on flat stage or preheated mat, blood collected directly from the heart using 20 G needle, preferably from the left ventricle where the needle inserted through the left side of the chest just down the sternum, the blood then is withdrawn slowly to prevent heart collapsing. 0.1–1 ml blood can be drawn up from the heart depending on mouse age and size and whether the heart was beating or not.

Cardiac puncture has not been used when lungs need to be lavaged for bronchial fluid collection, as heart and lungs must be undamaged and puncturing the heart may lead to leakage of blood into the peritoneal cavity. Therefore, blood was collected from the posterior vena cava, this was reached by cutting through the abdomen then the intestine and liver pushed gently to expose the vena cava where the blood can be withdrawn.

The collected blood was then used to isolate the peripheral blood mononuclear cells (PBMC) or for serum separation. To isolate the PBMC, blood collected in tubes containing sodium citrate (3.8 % w/v, approximately 130 µl is required for each ml of blood) and placed on ice to preserve the integrity. For serum isolation, blood collected in empty covered tubes and left to clot at room temperature.

After culling the mouse, a transverse incision was made below the diaphragm after peeling back chest skin, then by holding up the zyphoid process (the cartilaginous lower part of the sternum) a tiny hole was made in the diaphragm and the whole rib cage traced and removed carefully without piercing the lungs.

Saline-filled syringe injected into the right ventricle to wash off the remaining blood in the heart and lungs. To expose the trachea a midline incision at the neck was made then the heart and both lungs were harvested *en bloc,* the right lung

was tied off and snap freeze in either RNAlater ® (R0901- 500ML SIGMA) and/or liquid nitrogen. The left lung was perfusion- fixed with slowly injected 10% formalin at 20-22 cm height via the trachea, 2 inches polyethylene tube (PE-90 tubing from Becton Dickinson) fitted with 20G needle was used for lung perfusion. Heart and left lung then placed in formalin for 24 hours for fixing. Liver and spleen were also harvested in formalin containing tubes for 24 hours fixation.

Femur and tibia bones were collected with care in sterile petri-dish on ice for bone marrow cell harvesting, bones should stay intact as the cutting may compromise the sterility of bone marrow. Tissue kept in formalin for 24 hours then moved to sterile phosphate buffered saline (PBS) and stored in cold place to be processed for paraffin fixation and immune- staining.

2.1.7 Isolation of mouse mononuclear cells for flow cytometry analysis

In each experimental group, blood was pooled from the treated mice to make a volume of 3-5 ml of whole blood to perform density gradient isolation of mononuclear Cells (MNC). Blood diluted with equal volume of sterile PBS which then overlaid carefully into equal volume of density gradient medium Histopaque® 1077 (10771, Sigma- Aldrich). The preparation then centrifuged at 400 *Xg* for 30- 40 minutes at 18- 20 ºC with no brakes to not compromise the layers generated. The MNC layer will be the cloudy layer in the middle which can be transferred by sterile Pasteur to another fresh centrifuge tube for washing. To wash, 3 ml of PBS was added then the sample centrifuged at 500 *Xg* for 5 minutes at 18- 20 ºC, the supernatant discarded.

For flow cytometry analysis, MNCs were counted using haemocytometer and then spliced between two tubes each containing 1×10^6 cell, one tube was the unstained control tube and the other stained with anti-mouse CD115 (Alexa Fluor ® 488 anti-mouse CD115, BioLegend) according to manufacturer instructions (detailed in section 2.4.1).

2.1.8 Isolation of serum for biochemical analysis

After collecting the whole blood from each mouse in a cover tube, blood left to clot undisturbed at room temperature for at least 15 minutes, the clot was then removed by centrifuging the sample at 1000- 2000 rpm in a refrigerated centrifuge. Following centrifugation, the liquid component (serum) was transferred immediately into clean polypropylene tube using a Pasteur pipette and stored at -80 °C.

2.1.9 Harvesting bone marrow cells

After isolating the tibia and femur bones into a sterile petri dish, the bones were cleaned from fur and muscles in a sterile condition, then placed in DMEM (Dulbecco's Modified Eagle's Medium with glucose and L-glutamine, Lonza bioWhittaker®). Epiphyses removed using sterile scissors and forceps and the bone flushed with a 26G syringe filled with 5 ml DMEM to extrude bone marrow out to a petri dish. Cells were homogenized by plastic pipette or 26G syringe and counted using haemocytometer, then centrifuged at 300 *Xg* for 5 minutes. Pellets re-suspended in either culture medium for culturing or in freezing medium (containing 90% FCS, 10% dimethyl-sulfoxide DMSO) and frozen in cryovials at -80 ºC for storage.

2.1.10   Collection of broncho- alveolar lavage fluid

To collect the broncho- alveolar lavage fluid (BALF) from mice, the mice were culled by anaesthetic overdose (pentobarbital 100-150µl intraperitoneal injection). The neck and thoracic cage exposed using a fine scissor and the tissues surrounding the trachea were dissected, rib cages traced partially to expose the heart and lungs. With caution not to pierce the organs, a piece of thread passed underneath the trachea then 24G cannula inserted into the trachea in a distance about 2- 3 mm from its proximal end, the thread then tied off properly around the cannula after withdrawing the needle. After setting up the cannula 1 ml of cold normal saline injected slowly into lungs which confirmed by lung inflating, then the fluid collected back into the syringe resulting in lung shrinking. This wash repeated for 5 times to collect approximately 4 ml lavage fluid in 15 ml falcon tube on ice, tubes then centrifuged at 450 *Xg* for 5 minutes. The supernatant transferred to cryovials for freezing at -80 ºC, while the pellets re-suspended in either 100 µl cold media (RPMI medium 1640 contains 10% FBS, 100 IU/ ml penicillin and 100 IU/ ml streptomycin) for culturing and preparation of cytospin slides, or in cold PBS for flow cytometry analysis. The yield was then counted with a haemocytometer (EVOS XL Core, life technologies® haemocytometer).

To prepare a cytospin slide, an apparatus consists of a microscopic slide mounted with filter card and cytospin funnel into a metal holder was used. 100µl cell suspension was loaded into the funnel and centrifuged for 6 minutes at 250 *X*g using cytocentrifuge. The slide was then removed from the holder and left to dry for few seconds before fixation with few drops of methanol. To stain the cells, the slide was dipped into Eosin stain for few seconds, drained on a tissue then

stained with methylene blue for few seconds and finally washed with water. After air drying the slides mounted with DPX.

2.1.11   Assessment of right ventricular hypertrophy

Heart and left lung were perfusion fixed via the trachea at 20 cm using 10% formalin, the heart was dissected in a way that the atria, aorta, and the pericardial fat were all separated, and then the right ventricular free wall dissected from the left ventricle plus the septum and dried off. The right ventricular hypertrophy index (RVH index) was calculated by dividing the weight of the right ventricular (RV) over the weight of left ventricular free wall plus septum (LV+S).

2.2   Immunohistochemistry

2.2.1 Tissue preparation for immunohistochemical staining

Liver, lung and spleen were harvested and stored for paraffin fixation as in section (2.1.6). Each tissue was embedded and cut into 3-4 pieces according to the sample size, the pieces were then placed in the standard size plastic cassette for dehydration. Cassettes were transferred through ascending concentrations of ethanol (starting from 50% v/v, 70%, 90% and 100%v/v for 1 hour each) then moved to a mixture of 50:50 xylene: ethanol followed by two changes of 100% xylene for 1 hour each before placing in molten wax for overnight (60°C oven), these steps were performed either manually or by using LEICA TP 1020 wax tissue processor automated system.

For tissue embedding using paraffin wax, the LEICA EG 1150 (H) and (C) embedding stations were used as a working station. Using a proper size mould, each piece of tissue was placed on the flat side facing the bottom of the mould,

and then the warm wax used to fill the mould. Mould covered immediately with the labelled plastic lid and left to dry.

Embedded tissues were left to dry overnight before cutting the sections. On the day of sectioning, tissue blocks removed from their mould and placed on ice for 1 hour. A five micrometre thick sections were cut using Leica RM2135 microtome (Leica microsystems, Wetzlar, Germany). Sections floated out on 37ºC water inside water bath to flatten the sections then mounted on Polysine ᵀᴹ slides and left to dry on 40ºC oven overnight, at this stage the slides were ready for staining.

For the preparation of frozen lung sections, snap frozen lung tissue were sectioned using a cryostat (a -20 ºC freezer enclosing a microtome). Tissue was moulded using embedding compound (CRYO-M-BED, Bright) then frozen with aid of freezing spray (Cryospray 134A, Bright) onto the specialized metal grid or the specimen chuck that supplied with the cryostat (LEICA CM3050 S). 5µm thick sections were cut and transferred within 1 minute to a room temperature slide as the section melted onto the surface. The slides were stored in -20ºC freezer for future staining.

2.2.2 Immunohistochemical staining

2.2.2.1 Staining of tissue macrophages

Lung, liver and spleen paraffin sections were immuno-stained with: anti- F4/80 antibody as a pan-macrophage marker to estimate the level of ablation, and with anti-iNOS antibody and Anti-CD206 as M1 and M2 markers respectively. Lung paraffin sections were also stained with anti-IL-4 antibody to detect IL-4 expressing cells.

For the immunohistochemical staining a standard protocol was followed for all of the antibodies, the protocol started with dewaxing and re-hydration steps by immersing the slides in 100% v/v xylene for 10 minutes moving through graded alcohol to water (100% v/v xylene, 100% v/v ethanol, 100% v/v ethanol, 90% v/v ethanol, 70% v/v ethanol and 50% v/v ethanol for 1 minute each). 3% hydrogen peroxide was then used for 10 minutes to block endogenous peroxidases followed by rinsing with water.

For antigen retrieval, heat- mediated antigen retrieval (also known as heat-induced epitope retrieval HIER) was performed using 1:10 dilution of 10mM citrate buffer at PH6 for 20 minutes at 95ºC.

To improve antibody penetration, it was important (except for anti- F4/80 antibody) to use Triton X-100 on the slides for 10 minutes as a popular detergent used for this purpose.

To block any non- specific binding of the secondary antibody and to exclude the false positive staining, 1% w/v milk blocking buffer (MARVEL original dried skimmed milk, Premier foods Ltd, UK / from a supermarket) was used for 30 minutes before adding the primary antibody.

Excess milk drained out without washing and a primary antibody was added and left for overnight at 4ºC in a humidity chamber. Antibodies used were either: anti-F4/80 antibody (1:100 dilutions; Abcam, ab6640), anti-iNOS antibody (1:100 dilutions; Abcam, ab15323), anti-CD206 (1:100 dilution; R & D systems, AF2535) or anti-IL-4 (1:150 dilution; Biorbyt, orb360766). Antibodies were diluted to the appropriate concentration using PBS in final volume enough to cover the slides (100 µl/ slide). Slides were then washed with PBS for 3 times 5 minutes each before incubating with the appropriate secondary antibody for 30 minutes (see

Appendix III for the types and dilutions used) followed by 3 washes with PBS. Control sections were included for each antibody application to confirm the absence of false positive staining; these were either by carrying out the protocol without adding the primary antibody or without adding the secondary antibody.

The slides were incubated with Vectastain Elite ABC kit working reagent (Vector Laboratories) for 30 minutes, then washed further with PBS before incubation with DAB substrate (SIGMAFAST ™ 3,3'- Diamino-benzidine; SIGMA) for 3-8 minutes and rinsing quickly with water.

Finally, the slides were counterstained by Carazzi's Haematoxylin for 1 minute then washed in water and dehydrated back through the graded alcohols (50% v/v ethanol, 70% v/v ethanol, 90% v/v ethanol, 100% v/v ethanol, 100% v/v ethanol) to 100% v/v xylene for 1 minute each. The slides were mounted with DPX and left to dry overnight. Histological images were visualized using Zeiss multi-slides scanning microscope (Imager.Z2, CarlZeiss limited) using Axiocam 506 colour camera. Slides were scanned sequentially using X20 magnification objective lens and saved to be analysed with the accompanying software.

2.2.2.2 Staining of pulmonary blood vessels

To assess the vascular remodelling, lung sections were stained against alpha-smooth muscle actin as a marker for smooth muscle, with Alcian blue Elastin Van Gieson (ABEVG) to assess the percentage of muscularised pulmonary arterioles, and with Von Willebrand to assess the state of endothelial cells.

The same standard protocol detailed above was followed to stain the blood vessels in the lung sections. The protocol started with dewaxing and re-hydration steps by immersing the slides in 100% v/v xylene for 10 minutes moving through

graded alcohol to water (100% v/v xylene, 100% v/v ethanol, 100% v/v ethanol, 90% v/v ethanol, 70% v/v ethanol and 50% v/v ethanol for 1 minute each). Then, 3% hydrogen peroxide was used for 10 minutes to block endogenous peroxidases followed by rinsing with water.

Antigen retrieval step was used in case of the vWF staining only, no- heat antigen retrieval was utilized. The no-heat method (also called proteolytic induced epitope retrieval (PIER)) depends on the enzyme digestion where 0.1% trypsin in TBS was used for 10 min at 37 ºC.

To block any non- specific binding of the secondary antibody 1% w/v milk blocking buffer (MARVEL original dried skimmed milk, Premier foods Ltd, UK / from a supermarket) was used for 30 minutes before adding the primary antibody.

Excess milk drained out without washing and the primary antibody added. The primary antibodies used to stain the blood vessels were: alpha- smooth muscle actin (1:150 dilution; Dako Mouse monoclonal anti-human- α- SMA antibody, M0851) and with vWF (1:300 dilution; Dako rabbit anti-human vWF, A0082). The primary antibody was left for 1 hour at room temperature in a humidity chamber. The antibodies were diluted to the appropriate concentration using PBS in sufficient final volume to cover the slides (100 µl/ slide). Slides were washed with PBS for 3 times 5 minutes each before incubating with the secondary antibody for 30 minutes (see appendix II for the types and dilutions used) followed by 3 washes with PBS. Control sections were also included for each antibody application to confirm the absence of false positive staining.

The slides were then incubated with Vectastain Elite ABC kit working reagent (Vector Laboratories) for 30 minutes and washed further with PBS before

incubation with DAB substrate (SIGMAFAST ™ 3,3'- Diamino-benzidine; SIGMA) for 3-8 minutes and rinsing quickly with water.

Finally, the slides were counterstained by Carazzi's Haematoxylin for 1 minute then washed in water and dehydrated back through the graded alcohols (50% v/v ethanol, 70% v/v ethanol, 90% v/v ethanol, 100% v/v ethanol, 100% v/v ethanol) to 100% v/v xylene for 1 minute each. The slides were mounted with DPX and left to dry overnight.

For Alcian blue Elastin Van Gieson (ABEVG) staining, slides were dewaxed and re-hydrated as above, then oxidized with 0.25% w/v potassium permanganate for 3 minutes. Sections were rinsed with water for 3 minutes and then bleached with oxalic acid for another 3 minutes and washed again. The slides then stained with Carazzi's haematoxylin for 2 minutes to stain the nuclei before been differentiated in 1% acid alcohol for few seconds. Hot running tap water used to wash the slides for 5 minutes then stained with Alcian blue stain (1% in 3% acetic acid, PH 2.5) for 5 minutes. Slides were rinsed in water first then rinsed with 95% industrial methylated spirits (IMS) before they transferred to the Miller Elastin stain for 30 minutes. The slides then rinsed and differentiated in 95% IMS followed by a brief rinse in water before the Curti's modified Van Gieson was added for 6 minutes. Finally, after rinsing the slides with water they were dehydrated back through the graded alcohols 70% v/v ethanol, 100% v/v ethanol and 100% v/v xylene then mounted with DPX (see Appendix III for more information about the antibodies used and preparation of buffers).

Histological images were visualized using Zeiss multi-slides scanning microscope (Imager.Z2, CarlZeiss limited) using Axiocam 506 colour camera.

Slides were scanned sequentially using X20 magnification objective lens and saved to be analysed with the accompanying software.

2.2.3 Immunohistochemical analysis

To determine the level of macrophage ablation, the number of the remaining macrophages within the tissues was calculated by counting positively stained cells for the anti-F4/80 antibody (pan-macrophage marker), anti-CD206 (M2 marker) and anti- iNOS (M1 marker) remained within the liver, lung and spleen of treated mice. Six fields of view with a high density of stained cells were recorded under X20 objective. The average number of macrophages per field of view was normalized to the average of the control group.

2.2.4 Analysis of vessel wall remodelling

To determine the effect macrophage ablation had on the pulmonary arteries, two parameters were measured to quantify and assess the degree of remodelling within these vessels. The first includes calculating the ratio of the media to the cross-sectional area (media/ CSA) of the whole vessel in sections stained with α-smooth muscle actin staining (identifying vascular smooth muscle cells). The second parameter assess the degree of muscularisation in sections stained with Miller Elastin stain (ABEVG), this was performed by classifying the vessels to muscularised (has double elastic lamina) and non- muscularised (one thin elastic lamina layer), then expressed as a percentage of muscularised vessels to total pulmonary vessels.

For both of the parameters, around 50-100 vessel were scored in each mouse, and the vessels were divided according to their size into 3 categories: small or

distal pulmonary arteries with an outer diameter of less than 50µm, medium pulmonary arteries with a diameter between 50-100 µm and large pulmonary arteries having an external diameter more than 100µm.

Analysis performed using Zeiss multi-slides scanning microscope accompanied ZEN software.

2.2.5 Immunofluorescence staining

For the Immunofluorescence detection of SMA in the formalin- fixed, paraffin-embedded lung tissue, The slides were de-waxed and re-hydrated by immersing in 100% v/v xylene for 10 minutes moving through graded alcohol to water (100% v/v xylene, 100% v/v ethanol, 100% v/v ethanol, 90% v/v ethanol and 70% v/v ethanol for 1 minute each). 3% v/v hydrogen peroxide were then used for 10 minutes to block endogenous peroxidases followed by rinsing with water.

To block the non-specific binding of the antibody, the slides were incubated in blocking solution (5% v/v goat serum, 1% w/v BSA in BPS-T (0.05% v/v tween 20 in PBS)) for 1 hour at room temperature. Excess blocking solution was drained out without washing and the primary added (1:150 from Dako Mouse monoclonal anti-human- α- SMA antibody) and left for overnight at 4 ºC in a humidity chamber. The antibody was diluted to the appropriate concentration using the blocking solution in sufficient final volume to cover the slides (100µl/ slide). Slides were then washed with PBS-T for 5 times 5 minutes each before incubating with the secondary antibody. The secondary antibody used was goat anti- mouse Alexa 555 at 1:200 dilution in PBS. The slides incubated in the secondary antibody for 1 hour at the room temperature in dark then washed with PBS-T and mounted with Vectashield® with DAPI mounting media (by Vector laboratories). Slides

were sealed with nail polish and kept in dark. Negative control slides that incubated with either no primary antibody, no secondary antibody or none of them were also included.

To examine the co-distribution of macrophages in smooth muscle cells in one paraffin section, the double immunofluorescence staining was carried out using two primary antibodies (anti-F4/80 for macrophages and anti-SMA for smooth muscle cells) raised in different species in a mixture. The same protocol described above was performed using primary antibodies mixture that contains anti-F4/80 (rat monoclonal; Abcam, ab6640) at 1:100 dilutions with anti- SMA (mouse monoclonal; Dako, M0851) at 1:150 dilution in PBS-T. The secondary antibodies mixture solution used contains (Goat anti- rat Alexa 488 and Goat anti-mouse Alexa 555) at 1:200 dilution each.

To examine the proliferation capacity of macrophages in frozen lung section, the double immunofluorescence staining was carried out using the two primary antibodies (anti-F4/80 for macrophages and PCNA for proliferating cells) raised in different species in a mixture. For double immunofluorescence staining of frozen lung section, the slides were fixed with ice- cold acetone for 10 minutes then washed with PBS-T for 3 times for 5 minutes each. To block the non-specific binding, the slides incubated in blocking buffer (1% w/v BSA, 5% v/v goat serum in PBS-T) for 1 hour at room temperature. Excess blocking solution was drained out without washing and the primary antibodies mixture that contains rat monoclonal anti-F4/80 (Abcam, ab6640) at 1:150 dilution with the monoclonal mouse anti-PCNA (Dako; M0876) at 1:125 dilution was added and left for overnight at 4ºC in a humidity chamber. The antibody was diluted to the appropriate concentration using the blocking solution in sufficient final volume to

cover the slides (100µl/ slide). Slides were washed with PBS-T for 5 times 5 minutes each before incubating with the secondary antibody. The secondary antibodies used were the goat anti-mouse Alexa 555 and goat anti-rat Alexa 488 in a mixture at 1:200 dilution in PBS. The slides were incubated in the secondary antibodies solution for 1 hour at the room temperature in dark then washed with PBS-T and mounted with Vectashield® with DAPI mounting media (by Vector laboratories). Slides were sealed with nail polish and kept in dark. Negative control slides that were incubated with either no primary antibodies, no secondary antibodies or none of them were also included.

2.2.6 Immunofluorescence analysis

Immunofluorescence images were visualized using Zeiss multi-slides scanning microscope (Imager.Z2, CarlZeiss limited) using the MRm camera and the appropriate filter for each fluorophore. Slides were scanned using X20 magnification objective lens and saved to be analysed with the accompanying software.

2.3   Culturing of mouse primary cells

2.3.1 Culturing of bone marrow- derived macrophages

Frozen or fresh bone marrow- derived macrophages (BMDMs) were thawed or suspended in DMEM culture medium containing 100IU/ml Penicillin/ Streptomycin antibiotics, 10% FBS, 20ng/ml M-CSF (gibco® by life technologies), cells were then incubated in a humidified incubator with 5% CO2 at 37ºC, after 3 days of growing the media discarded and the cells washed with PBS before adding a fresh media. At day 7 mature BMDM were obtained and they were ready

for splitting as required (figure 2.3). As macrophages adhere strongly to the flask, room-temperature trypsin was used to incubate the cells twice at 37ºC (5 minutes each) before scrapping them gently of the flask. Formation of the mature BMDM was evaluated using flow cytometry analysis and fluorophore-conjugated antibodies to detect cells expressing F4/80 and CD68.

To study cells polarization and differentiation, cells were seeded at 2 $X10^5$ /ml and on the following day they stimulated with either LPS (100 ng/ml; cell- signal®) with IFNγ (50ng/ml; R&D system) for M1 activation, IL-4 (10 ng/ml; R&D system) for M2 activation, or doxycycline (1µg/ml, 5µg/ml, 10µg/ml and 40µg/ml). After 48 hours cell phenotype was investigated using flow cytometry.

For the viability assay, cells were seeded in 96-well plate at a density of 20,000 cells per well. The viability assay performed at the zero time then the cells treated with a fixed dose of doxycycline and their viability assessed again at the different time point (see section 2.7)

For immunocytochemical staining, cells were seeded in 6 well plate at 0.5 $X10^6$ cell/ well before stimulating with doxycycline (see section 2.5.2).

The morphological investigation was performed using approximately 8 $X10^6$ cell in each well of 6- well plate and then differentiated into the different macrophage populations as described above. Images were taken by EVOS XL Core, life technologies® haemocytometer, with 20X magnification. Conditioned media was also collected from each cell type generated and stored at -80ºC freezer for future work.

2.3.2 Culturing of alveolar macrophages

Fresh cells from BALF were cultured using warm RPMI media (contains 10% FBS, 100 IU/ml Penicillin/ Streptomycin) after passing through a 35µl cell strainer. Collected cells were confirmed to be mainly alveolar macrophages (AMs) using flow cytometry analysis (figure 2.4).

About 0.5 X10^6 cell/ml were placed per well into 6 well plate, then allowed to adhere inside the incubator for 2 hours. Cells were stimulated with either LPS/ INFγ, IL-4 or doxycycline as above. After 48 hours, cell phenotype and their polarization following stimulation were investigated using flow cytometry and immunocytochemistry.

For the viability assay, cells were seeded in 96-well plate at a density of 20,000 cells per well. The viability assay performed at the zero time then the cells treated with a fixed dose of doxycycline and their viability assessed again at the different time point (see section 2.6).
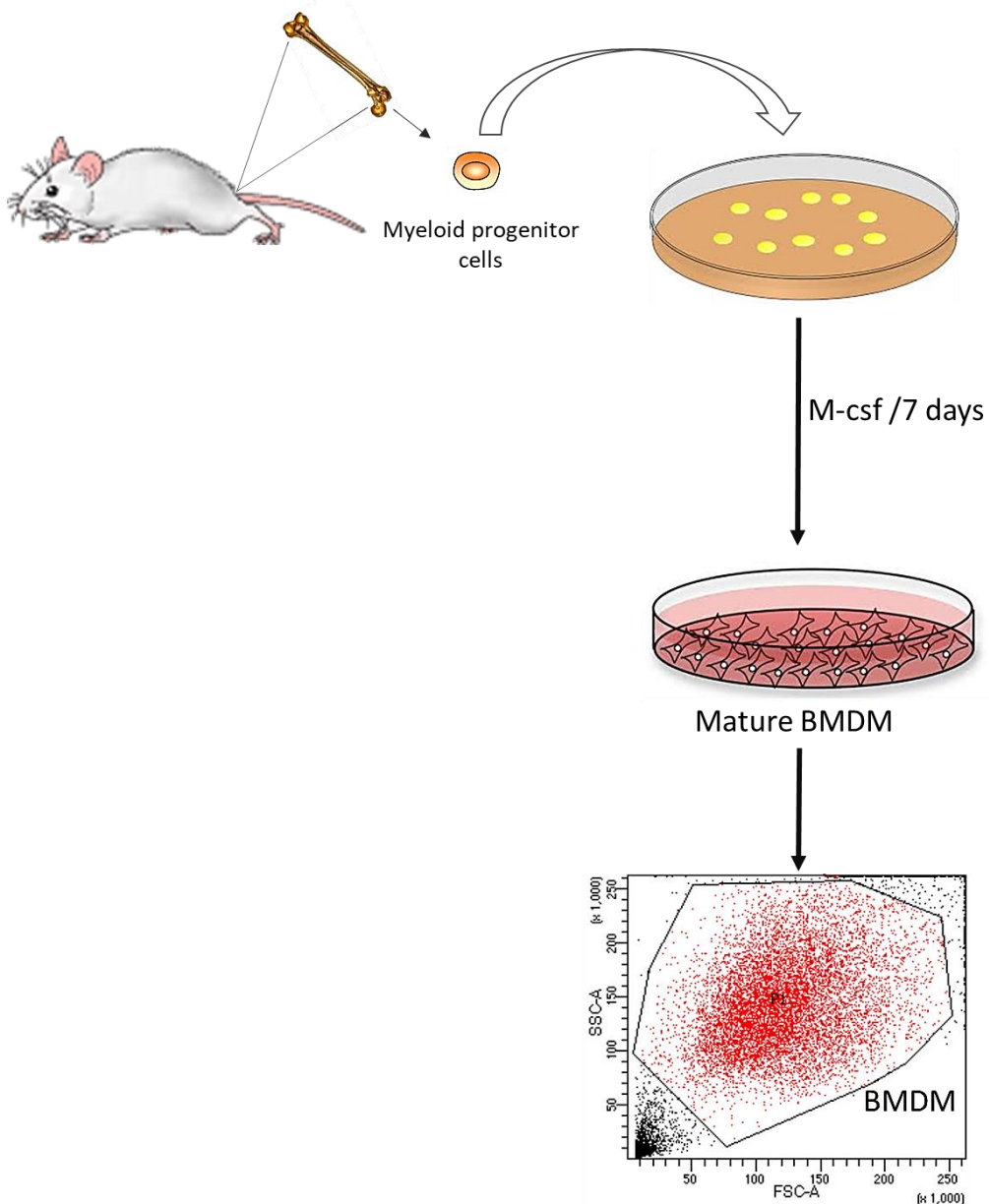
Figure 2.3- Culturing of bone marrow-derived macrophages: Diagram describes, in brief, the process of collecting and culturing of mouse bone marrow cells. Myeloid progenitor cells harvested from the bone then cultured in M-CSF containing media for 7 days to differentiate to mature bone marrow-derived macrophages (BMDM), mature BMDM formation confirmed by flow cytometry.

For immunocytochemical staining, cells were seeded in 6 well plate at 0.5 X10^6 cell/ well before stimulating with doxycycline (see section 2.5.2).

The morphological investigation was performed using approximately 8 $X10^6$ cell in each well of 6- well plate and then differentiated into the different macrophage populations as described above. Images were taken by EVOS XL Core, life technologies® haemocytometer, with 20X magnification.

Conditioned media was also collected from each cell type generated and stored at -80°C freezer for future work.
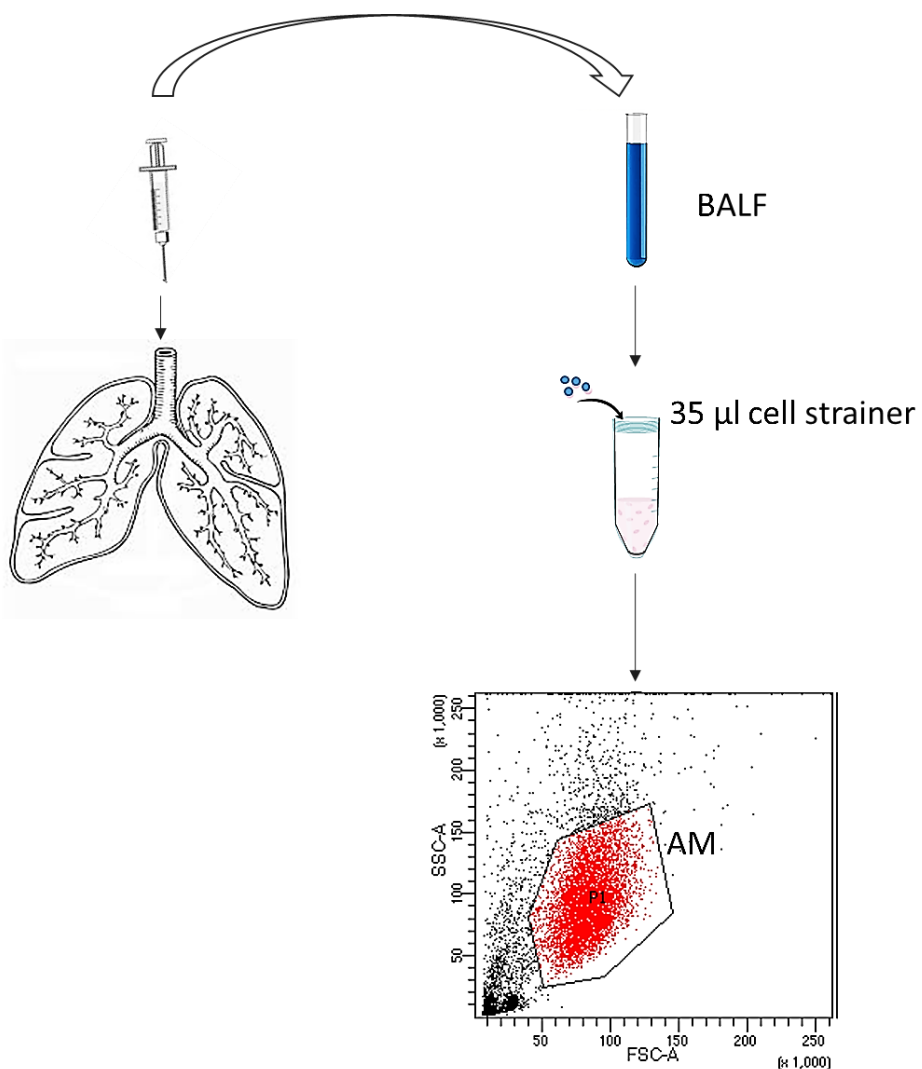
Figure 2.4- Culturing of Alveolar macrophages: a diagram describes, in brief, the process of collecting and culturing of alveolar macrophages. Broncho-alveolar lavage fluid (BALF) collected from mouse lung and passed through a cell strainer, cells confirmed to be alveolar macrophages by flow cytometry.

2.4 Flow cytometry analysis

2.4.1 Flow cytometry analysis of mouse blood

For flow cytometry analysis of the mouse blood, MNCs were spliced between two tubes (1 x 10^6 cell each), one tube was left unstained as a control while the other was stained with anti-mouse CD115 (Alexa Fluor ® 488 anti-mouse CD115, 0.5mg/ml, BioLegend). 2µl of the antibody was used for each 1 million cell, incubated on ice in the dark for 20- 40 minutes. Following incubation, both tubes were washed twice with 2ml washing buffer (PBS) and centrifuged at 500*Xg* for 5 minutes. Pellets were re-suspended in 300µl PBS and kept on ice until the time of flow cytometry analysis. BD LSR II flow cytometer was used (BD Biosciences, Pharmingen) for flow cytometry. Blood monocyte was identified on the basis of their size and granularity using the forward and side light scatter plot. For each sample, a minimum of 10,000 events was recorded, and the data analysed with FlowJo software version 10.2.

2.4.2 Flow cytometry analysis of mouse primary cells

For flow cytometry analysis of mouse BMDM and BALF, cells were collected by detaching from the flask using warm trypsin and scrapping as previously described. Cells then washed with PBS and stained with the antibodies. The antibodies used were: APC anti-mouse F4/80. FITC anti-mouse CD68, PE anti-mouse CD206 (MMR) and the Pacific Blue™ anti-mouse all from Biolegend®, (more information about the antibodies used in appendix IV). Negative unstained controls or the proper isotypes were run in parallel to each antibody. 1µl of each antibody was used for each 1 million cell, incubated on ice in dark for 20-40 minutes. Following incubation, both tubes washed twice with 2ml washing buffer

(PBS) and centrifuged at 500Xg for 5 minutes. Pellets were re-suspended in 300µl PBS and kept on ice until the time of flow cytometry analysis. BD LSR II flow cytometer was used (BD Biosciences, Pharmingen). For each sample, a minimum of 10,000 events was recorded, and the data analysed with FlowJo software version 10.2.

2.5 Immunocytochemistry

2.5.1 Cells preparation for immunocytochemistry

In a sterile tissue culture hood, glass coverslips (18mm X 18mm, Zeiss) were sterilized by dipping in 70% v/v ethanol, slips were left to dry out then placed in sterile 6 well plates. 2 ml cell suspension (mature BMDM or fresh BAL cells) containing 0.2 – 0.4 X 10^6 cells were added over each coverslip in the plate, then placed in the incubator for 24 hours before been stimulated according to the experiment design.

2.5.2 Immunocytochemical/ immunofluorescence staining

Culture medium from each well was aspirated and the cells gently rinsed twice with PBS at room temperature. For the immunofluorescence staining, general protocol was adopted. In brief, cells were fixed by incubation in 4% v/v paraformaldehyde in PBS for 10 minutes then rinsed three times with PBS. To permeabilize the cells, cells were incubated for 15 minutes in 0.1% v/v Triton X-100 in PBS at room temperature. Again cells were washed gently three times with PBS. Cells were then incubated in blocking buffer (1% BSA in PBS contains 0.1% v/v tween 20) for 1 hour before adding the primary antibody.

The primary antibody used was the anti-5 lipoxygenase antibody (Abcam, ab39347) in a dilution of 1:100 in the blocking buffer, the final volume should be should be sufficient to cover the whole coverslip (minimum of 500µl per well). Cells incubated with the primary antibody overnight at 4°C in dark then washed three times with PBS. The secondary antibody was diluted in the blocking buffer away from light to the appropriate concentration (1:200 of Goat anti- rabbit IgG Alexa Fluor® 555, Abcam), cells were incubated with the secondary antibody for 1 hour in dark at room temperature.

To confirm the absence of autofluorescence and the non-specific binding, a parallel protocol was carried out without adding the primary antibody or without adding the secondary antibodies to the cells as negative controls.

Cells were rinsed thoroughly with PBS three times/ 5 minutes each away from light. Enough microscope slides were labelled and one drop of mounting medium (Vectashield with DAPI) was added to each slide, then each coverslip was carefully mounted on the slide with the cell- side face down and left to dry for few minutes. Nail polish was used to seal the edges of the coverslips to the slides and the slides visualized using the fluorescence channel with the appropriate filters of the Zeiss multi-scanning microscope. Analysis was performed using FiJi image processor software (ImageJ 1.51; USA).

2.6 Cell viability assay

To examine the effect of doxycycline on cell death *in vitro*, cell viability analysis was performed using the ApoTox-Glo™ Triplex assay kit (Promega, Madison, USA). This assay is a three in one technique that allows assessment of viability, cytotoxicity and caspase activation (a hallmark of apoptosis) in a single assay,

also to determine the mechanism of cell death. The kit includes three substrates; a viability substrate (glycyl-phenyl-alanyl-aminofluorocoumarin; GF-AFC) which is a cell-permeable peptide that cleaved by the live- cell protease when entering the intact cell and generates fluorescent signals correlate to the number the living cells. A cytotoxicity substrate (bis-alanylalanyl-phenylalanyl-rhodamine 110; bis-AAF-R110) which is a cell-impermeable peptide that cleaved by the dead-cell protease and generates fluorescent signals correlate to a number of cells that lost their cell membrane.

Both of the fluorogenic products (AFC and R110) can be detected simultaneously as they have different excitation and emission spectra thus both of the substrates can be added at the same time. And the caspase -3/7 luminogenic substrate, which added lastly to the cells as it leads to cell lysis, caspase cleavage and generation of a glow-type luminescent signal from the luciferase, this signal is proportional to the caspase activity.

In this experiment, mature BMDM or BAL cells derived from *MacLow* and control mice were tested. The aim was to detect the cell viability, cytotoxicity and the probable apoptosis (caspase activity) following doxycycline treatment at the different time point to compare between the MacLow vs control derived cells and BMDM vs AM in term of effect of doxycycline as an inducer of cell death. The cells were seeded in a 96-well plate at a density of 20,000 cell per well with the appropriate media for a 100µl final volume. The viability assay performed at day zero following the manufacturer protocol. In brief, at the first part of the assay 20µl of the reagent mixture contains the viability and cytotoxicity substrates was added to each well, then mixed by orbital shaker (500rpm for 30 seconds) followed by 30 minutes incubation at 37ºC. The fluorescence measured at an

excitation wavelength of 400nm and an emission of 505nm for the viability and 485 nm excitation/ 520 nm emission for the cytotoxicity. On the second part, 100µl of the Caspase-Glo® 3/7 reagent added to each well, then mixed at 500rpm for 30 seconds followed by 30 minutes incubation at 37ºC, then the luminescence measured.

Following the zero time viability assay, doxycycline was added at a concentration of 5 µg/ml, and the assay performed again after 2,4,5 and 7 days. The fluorescence/ luminescence was measured by the advanced spectral scanning multimode reader, the Varioskan Flash (Thermo Scientific).

2.7 Dot blot technique for detection of protein expression

Dot blot technique is used for detecting and identifying the expression of Diphtheria Toxin A protein (DTA) in cell lysate after inducing its synthesis with doxycycline (figure 2.5). The technique is different from western blot in that the protein samples are not separated electrophoretically but instead spotted directly onto the membrane. For the preparation of cell lysate, BMDM or BAL cells derived from *MacLow* mice were stimulated with 5 µg/ml doxycycline or left with no stimulation for 48 hours. The cells were washed with ice-cold PBS then lysed using 1:100 protease and phosphatase inhibitor cocktail in RIPA lysing buffer (see appendix V for recipe), the flask left on ice for 20 minutes before storing in the -80ºC freezer. The lysed cell were then scrapped from the flask and transferred to Eppendorf tube for further analytical experiments.

For the dot blot experiment, a nitrocellulose membrane (Amersham™ protran ™ 0.45µm NC) was prepared by drawing a grid using a pencil to identify the samples region, then a narrow- mouth pipette tip was used to spot 2µl of each sample onto

the centre of the grid. The membrane left to dry for few minutes then soaked in the blocking buffer (30% Odyssey® blocking buffer; LI-COR® diluted in PBS) to block the none specific sites for 1 hour in a rocker. With no washing, the membrane incubated in 1:2000 of the primary antibody (anti- DTA antibody; Abcam, ab8308) diluted in 30% blocking buffer for 1 hour. The membranes were washed 3 times using the washing solution (0.05% v/v Tween 20 in PBS) for 5 minutes each before incubating with the secondary antibody (1:10000 of Goat anti-mouse; Dyssey®) diluted in 30% blocking buffer for 1 hour in a rocker. Finally, the membranes were washed 3 times for 5 minutes each using the washing solution then visualized by the LI-COR ® reader using the proper channels.
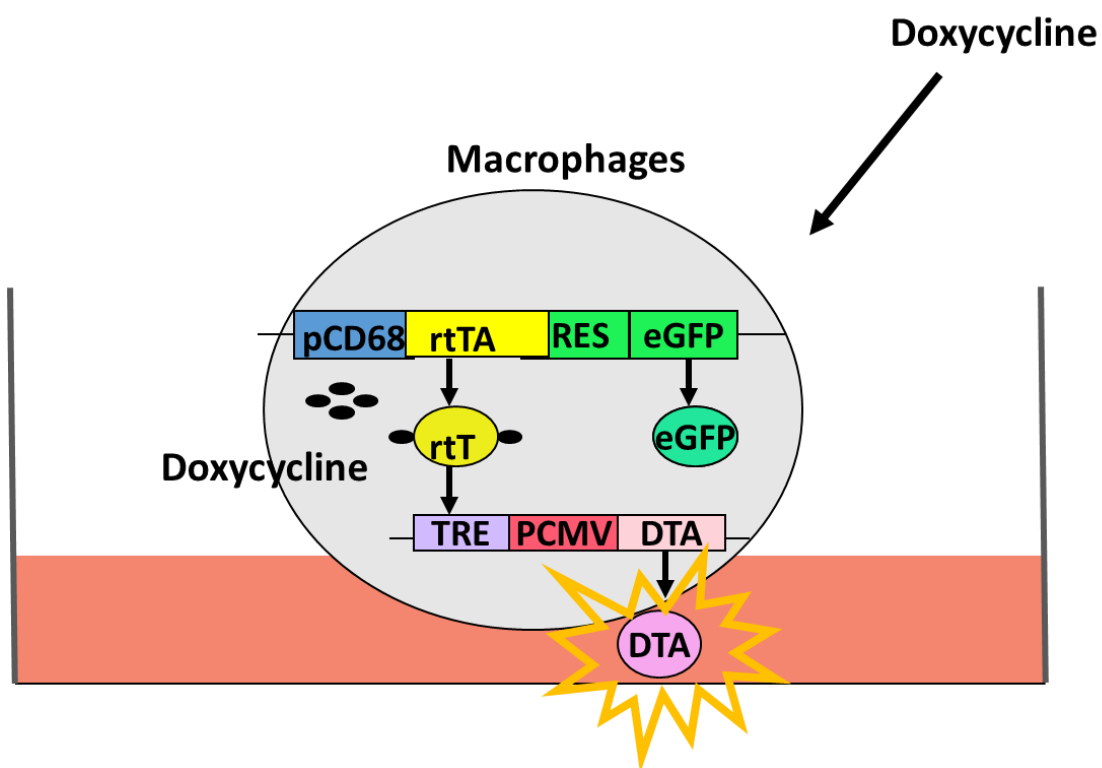
Figure 2.5- Expression of Diphtheria toxin A DTA: a diagram describes the rationale of DTA expression in culture. Doxycycline induces the expression of DTA under control of a CD68 promoter. The resulted DTA was detected using the dot blot technique.

2.8   Statistical analysis

All statistics were performed using GraphPad prism version 7.2 (GraphPad software, SanDiego, California USA). Statistical comparison between the different groups was established by the use of one- way analysis of variance (ANOVA) followed by Bonferroni post- hoc analysis. When comparing between groups that have two or more independent variables, the two-way ANOVA was used. Unpaired *t-test* was used when comparing only two independent groups. Values are presented as mean ± SEM, and differences of $P < 0.05$ values were taken as significant.

3 Impact of CD68+ cell depletion on the development of pulmonary arterial hypertension

3.1 Introduction

Inflammation in PAH has been an area of great interest in experimental research during the last decade. The presence of different inflammatory cells such as mast cells, lymphocytes, dendritic cells and macrophages around the vascular lesions point towards their contribution in disease pathology, however, their definitive role is still unclear. It is important to understand the different immune pathways associated with PAH to support the argument about the utility of designed immune-therapy for patients with PAH.

A study by Savai and colleagues showed in an elegant way that the CD68+ macrophages were significantly higher in lungs of IPAH subjects compared to donor's lungs, they also showed that these cells accumulated in large numbers in the adventitial layer of small, medium and large pulmonary arteries of IPAH lungs. Furthermore, they showed that by blocking the recruitment of the inflammatory cells (including CD68+ macrophages) they could attenuate the PH phenotype in monocrotaline rat model (Savai et al., 2012).

In my research, I am using the *MacLow* mouse model for specific macrophage ablation to investigate the role of macrophages in PAH. The *MacLow* mouse

model utilizes the tet-on system to switch on the expression of DTA in the CD68 positive cell following doxycycline treatment leading to 50% loss of tissue macrophages (Gheryani et al., 2013, Rumney et al., 2017).

This chapter will address the first objective of this research, which is to investigate whether loss of macrophages can actually cause a spontaneous PAH phenotype in *MacLow* mice as suggested by my previous findings (refer to figure 1.4). First, a doxycycline time- point study was conducted to determine the duration of action of doxycycline as a gene inducer and the level of ablation caused by a single dose of doxycycline was determined. Then, a longer- term macrophage depletion study (*MacLow*- induced PAH study) was conducted to determine the effect of long-term depletion on the development of PAH. The depletion of M1 and M2 subsets after doxycycline treatment was also investigated.

3.2 Material and methods

3.2.1 Doxycycline time- point study design

Sixteen age- and sex- matched adult *MacLow* mice were used in this study, animals were divided into four groups of four (two males and two females). In addition, single transgenic tetDTA mice were also used as controls in each group. All animals were injected with a single intraperitoneal injection of doxycycline (80 mg/kg body weight) and then a single group was sacrificed at zero, 24 hours, 72 hours and 7 days after injection (figure 3.1-a).

3.2.2 *MacLow*- induced pulmonary arterial hypertension study design

Four groups of mice (two male groups and two female groups) were used in this study. A male and a female group (n= 8 per group) 12- 14 week age *MacLow* mice were used as treatment groups, parallel groups of age and sex- matched single transgenic mice were used as control groups. All the groups were treated with doxycycline in the diet for six weeks, mice were maintained in a normal environment with a 12 hour light/ dark cycle, normal air (21% oxygen) and normal humidity. Doxycycline was given in a dose of 80 mg/kg body weight in doxycycline containing diet (contains 625 mg/kg doxycycline) (figure 3.5-a).

Mice were weighed weekly for first 3 weeks, then on every other day for the remaining 3 weeks, the echocardiographic analysis was performed to monitor the disease development at the 3 weeks midpoint, disease progression assessed at the endpoint using echocardiography, closed chest cardiac and lung immunostaining.

3.2.3 Echocardiography and cardiac catheterization

Following six weeks of doxycycline treatment, non- invasive assessment of the disease was performed using echocardiography under anaesthesia as described in section 2.1.4. Then the closed chest cardiac catheterization was used to take the pressure- volume measurements from both sides of the heart as described in section 2.1.5.

3.2.4 Histological analysis

Tissues were harvested, fixed, processed, and stained according to the standard laboratory procedure described in sections 2.1.6 and 2.2.

3.2.5 Statistical analysis

All statistics were performed using GraphPad Prism version 7.2 (GraphPad software, SanDiego, California USA). Statistical comparison between the different groups was established by the use of one- way analysis of variance (ANOVA) followed by Bonferroni post- hoc analysis. Two- way ANOVA was used when comparing groups with two or more variables. Values are presented as mean ± SEM, and differences of $P< 0.05$ values were taken as significant.

3.3 Results

3.3.1 Doxycycline time-point study

To assess the duration of action of doxycycline as a gene inducer and determine the level of macrophage depletion caused after one dose of doxycycline, a single intraperitoneal injection (i.p) of doxycycline was administered to *MacLow* and control groups. Total tissue macrophages, as well as M1 and M2 macrophages subsets and blood monocytes, were assessed at zero, 1, 3 and 7 days following the injection.

3.3.1.1 Reduction of F4/80 + macrophages within different tissues following doxycycline injection

To determine the level of macrophage ablation, the number of macrophages remaining following doxycycline injection was calculated by counting cells stained

positively for the anti-F4/80 antibody (pan-macrophage marker) in the liver, lung and spleen of injected mice. In the *MacLow* mouse model the targeted cells are CD68 positive macrophages, however, no difference was observed previously in term of macrophage quantification between the use of anti-F4/80 and anti-CD68 antibodies (Gheryani et al., 2013, Rumney et al., 2017), thus anti-F4/80 was chosen as the staining protocol as it was more reliable. Six fields of view with a high density of stained cells were quantified under X20 objective. The average number of macrophages at each time point was normalized to the day zero count.

The results showed that single i.p injection of doxycycline caused an approximate 30-40% reduction in the total number of F4/80+ macrophages within the lung, liver and spleen of *MacLow* mice, however the reduction was not significant. The percentage of reduction of F4/80 positive macrophages within the liver showed a significant decrease at day 3 in *MacLow* group compared to day zero (figure 3.1). The pattern of reduction was similar between the three tissues investigated (lung, liver and spleen) where the reduction of macrophages occurs within the first 3 days following the injection, then the number rises again to baseline levels. The control mice showed no clear pattern in their macrophage count over the 7 days. It was recommended to increase the power of the study (by increasing the number of mice in each group) to get clear statistical analysis, However, this was hindered by ethical restrains as the i.p injections of doxycycline were causing pain and distress to the mice.

a)

b)
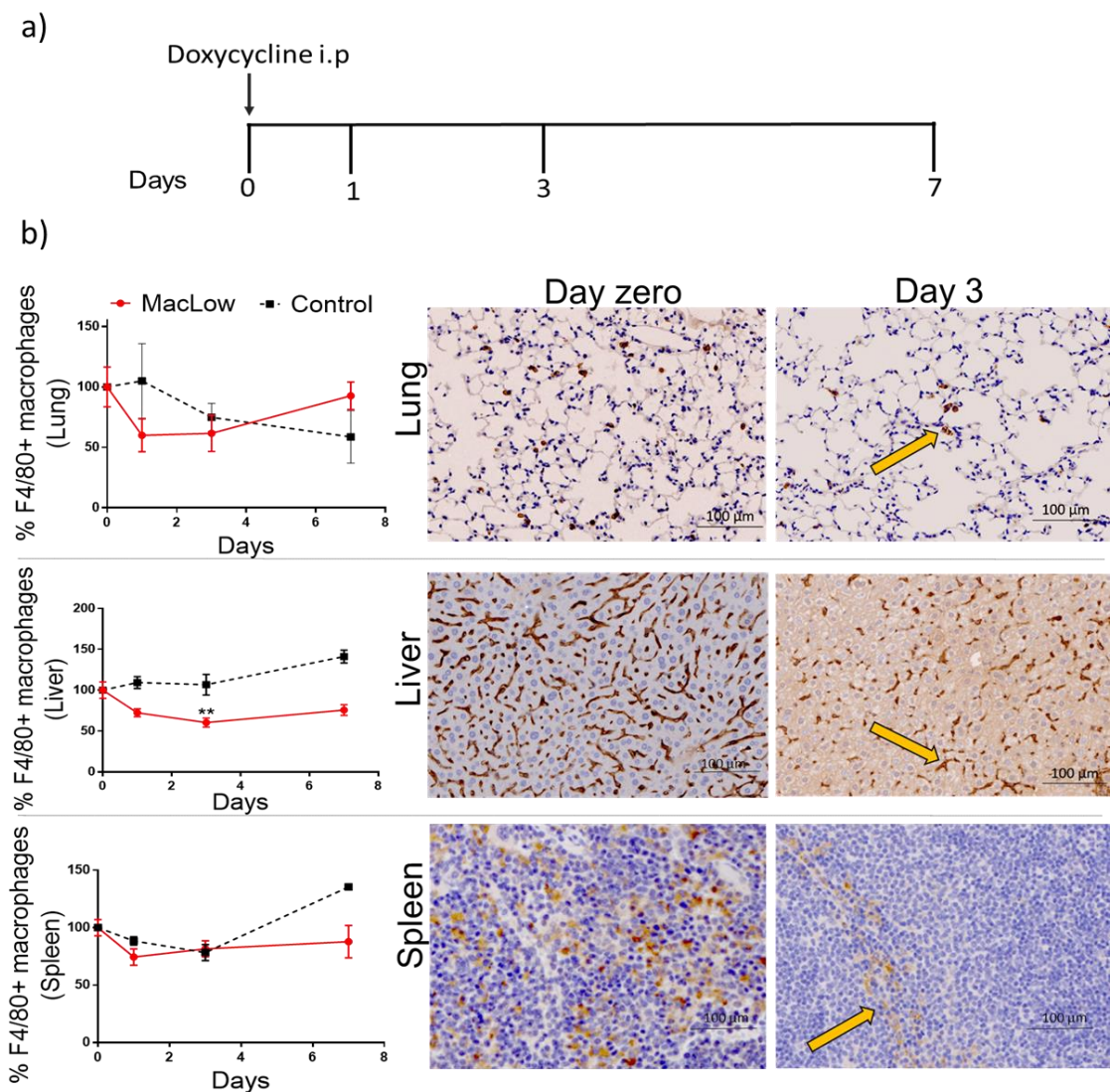
Figure 3.1- Macrophage quantification after a single dose of doxycycline: a) Schematic of the study design of doxycycline time- point study displaying the different time-points selected for macrophage quantification following a doxycycline i.p injection (80 mg/kg body weight). b) Graphs with the corresponding representative histological images show the difference in number of macrophages (arrow-head) over time within lung, liver and spleen normalised to day zero time. Tissues stained with anti- F4/80 antibody (stained brown). Scale bar = 100µm. n= 4/ *MacLow* group, n= 3/ control group. **P<0.005 using the two-way ANOVA.

3.3.1.2 Reduction of M1 and M2 macrophages within different tissues following doxycycline injection

To further investigate whether the *MacLow* model has a dominant effect on one macrophage subset over another, two cell markers were used to quantify the cells remaining within the tissues after doxycycline injection. For the M2 subset (alternatively activated macrophages) antiCD206 antibody was used, while anti-iNOS antibody was used to identify and count the M1 subset (classically activated macrophages).

The analysis of positively stained cells for both antibodies showed no significant differences in any of the time point compared to zero time. However, the doxycycline injection shown to cause 20-30% reduction in cell count within the first 3 days in both subsets in all tissues investigated, but again the reduction was not significant (figures 3.2 and 3.3). This suggests that the induced ablation of macrophages with doxycycline might affect both M1 and M2 subsets. There was an unexplainable increase in a number of CD206 + macrophages within the livers of the *MacLow* mice after 1 day of the injection.
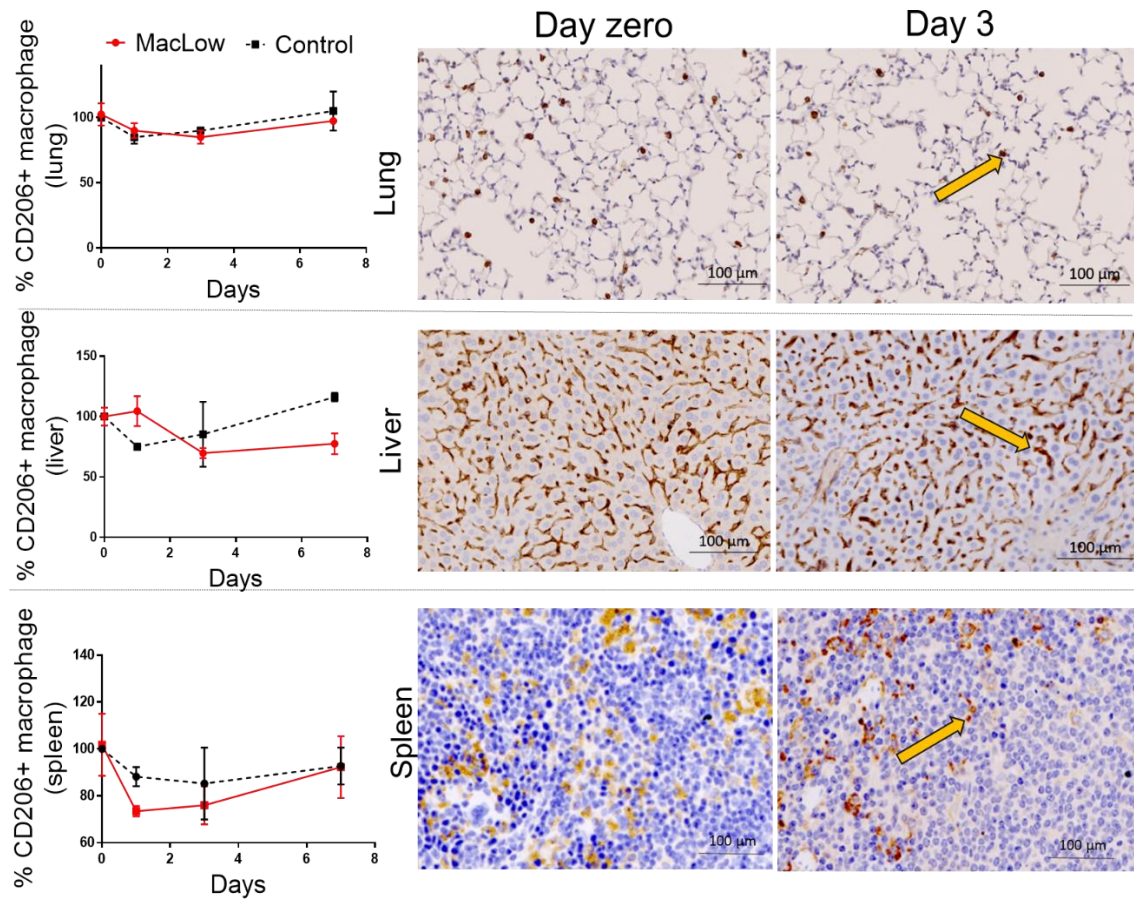
Figure 3.2- M2 macrophage quantification after a single dose of doxycycline: Graphs with the corresponding representative histological images show the difference in a number of CD206+ macrophages (arrow-head) over time within lung, liver and spleen normalised to day zero time. Tissues stained with anti- CD206 antibody (stained brown). Scale bar = 100µm. n= 4/ *MacLow* group, n= 3/ control group. Data analysed with two-way ANOVA.
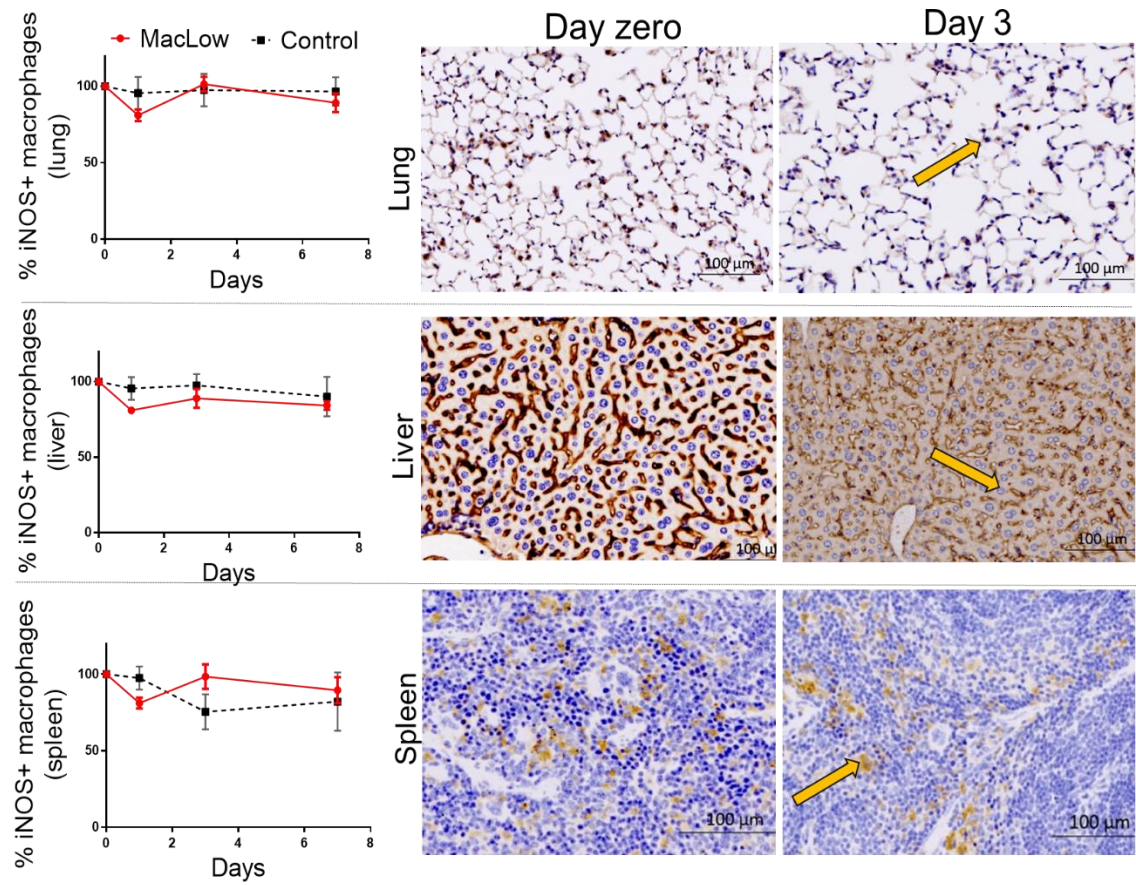
Figure 3.3- M1 macrophage quantification after a single dose of doxycycline: Graphs with the corresponding representative histological images displaying the change in numbers of iNOS+ macrophages (arrow-head) over time within lung, liver and spleen normalised to day zero time. Tissues stained with anti- iNOS antibody (stained brown). Scale bar = 100μm. n= 4/ *MacLow* group, n= 3/ control group. Data analysed with two-way ANOVA.

3.3.1.3 Reduction in blood monocyte following doxycycline injection

To determine if the number of circulating monocytes changed over the time course and if their numbers were affected by the alteration in macrophage number. Flow-cytometry using anti- CD115 antibody (to detect murine monocytes) was performed. Blood was pooled from all mice (n=4) in each group of *MacLow* mice into one sample, then peripheral blood mononuclear cells isolated and stained with Alexa Fluor® 488 anti-mouse CD115 (refer to sections 2.1.7 and 2.4). Because the minimum amount of blood required to isolate blood monocyte is 3-4 ml, no data were acquired from the control groups at any time point.

Interestingly, the data shows that the number of circulating monocyte was massively depleted within the first three days of the injection, with a peak at 24 hours (more than 50% reduction) then the level increased continuously to above the baseline count (figure 3.4). The pattern of reduction was consistent with that of tissue macrophages. However, none of these data was statistically analysed as the samples had to be pooled.

a)

b)
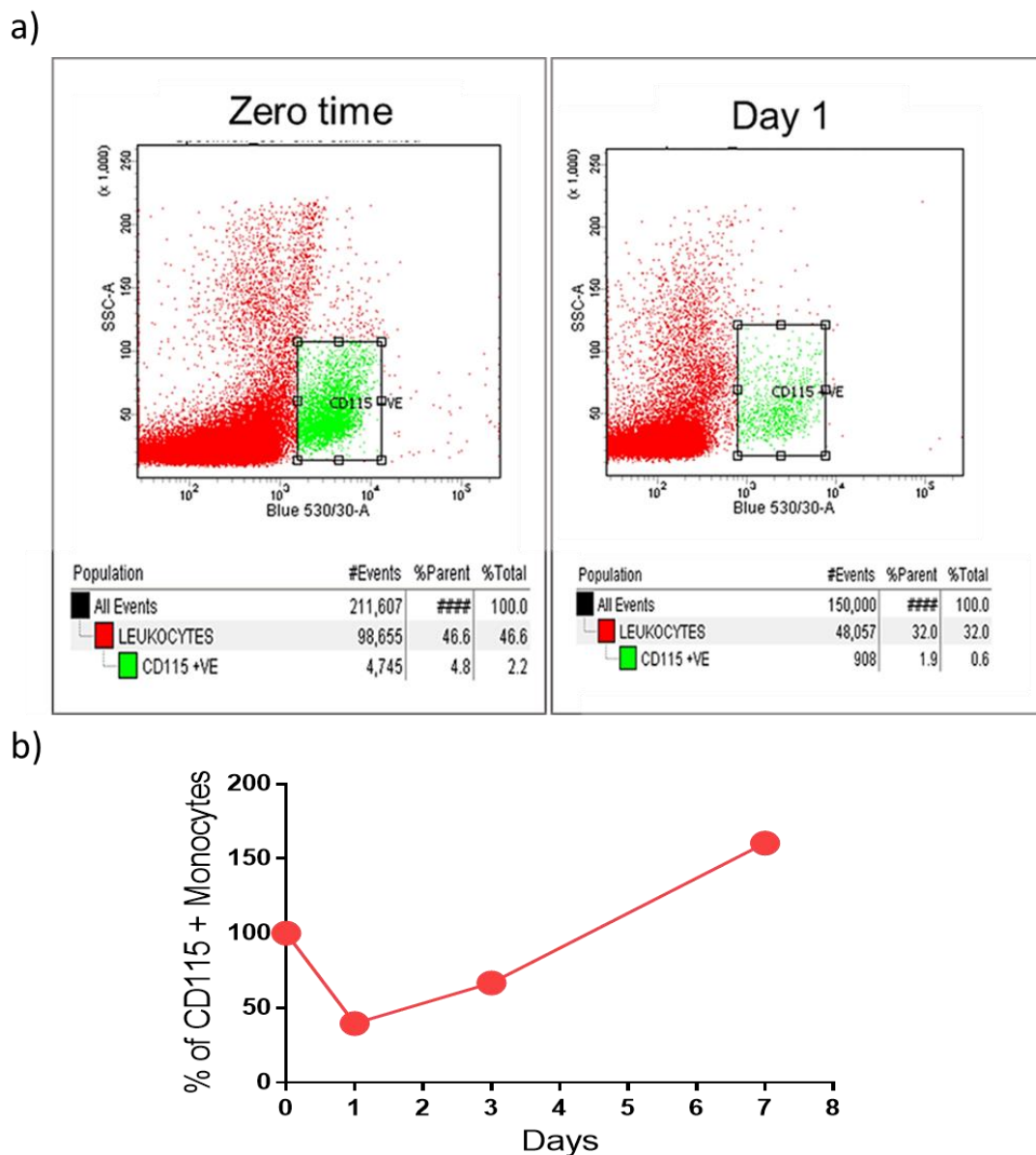
Figure 3.4- Flow cytometric analysis of the circulating monocyte after a single dose of doxycycline: a) representative examples of the flow cytometric plot of peripheral blood mononuclear cells stained with Alexa Fluor ® 488 anti-mouse CD115. The plot shows approximately 4.8% of the total parent cells at zero time are CD115 positive (left plot) whereas this drops to 1.9 % after 24 hours of doxycycline injection (right plot). b) A graph showing the pattern of reduction of monocyte count in the blood of MacLow mice over the period of 7 days after the doxycycline injection. Each point represents the result from a pooled blood sample from the *MacLow* group. n=4.

3.3.2 *MacLow-* induced pulmonary arterial hypertension

To determine the effect of long-term loss of macrophages (specifically lung macrophages) in *MacLow* mice, mice were treated with doxycycline for six weeks with no other insult, and then the development of the PAH phenotype was assessed.

3.3.2.1 Confirmation of macrophage depletion in *MacLow* mice

To confirm depletion of macrophages in the *MacLow* model, the number of macrophages within the livers was calculated. 5 μm paraffin-embedded liver sections were stained with anti-F4/80 antibody, and then macrophages were counted as previously described (sections 2.2.2 and 2.2.3). The results showed a significant reduction (approximately 35- 40%) in the total macrophage numbers in male and female *MacLow* groups compared to the corresponding controls (figure 3.5). although the expected level of depletion is 50 % reduction (Gheryani et al., 2013, Zawia, 2011), the obtained level of macrophage reduction was still acceptable and statistically significant. In addition, the data showed no difference between males and females in term of their loss of macrophages after the six weeks doxycycline treatment.

3.3.2.2 Assessment of PAH in *MacLow* mice

3.3.2.2.1 Haemodynamic evaluation

Following doxycycline treatment, disease progression was first assessed by the different haemodynamic parameters (gathered from the heart catheterization and echocardiography) as well as the right ventricle hypertrophy value (Fulton index). Interestingly, male *MacLow* mice but not female displayed a spontaneous disease phenotype after doxycycline administration with a significant increase in

their right ventricular end- systolic pressure (RVESP) compared with the controls

(66.1 mmHg vs 24.5 mmHg respectively) (figure 3.6-a). This effect was also seen

in most of the other haemodynamic parameters measured from the right side of

the heart such as the contractility assessment (dp/dt max) and the arterial

elastance (Ea) (see appendix I), with no effect on the measurements from the

left-side of the heart especially the left ventricular end- systolic pressure (LVESP)

(figure 3.6-b). No change was detected in the left ventricle internal diameter

(LVID) nor the cardiac index between the groups (figure 3.6- d,e).

To investigate whether this increase in pressure has led to right ventricular

hypertrophy (RVH), the RVH index was calculated. RVH value represents a

hallmark of right ventricular hypertrophy and was assessed on the basis of the

ratio of RV free wall weight to the left ventricle free wall weight plus septum. The

results show a significant increase in the RVH value of male *MacLow* mice

compared to the control group (figure 3.6-f). No weight changes between the

different groups were noted.

a)

b)

c)
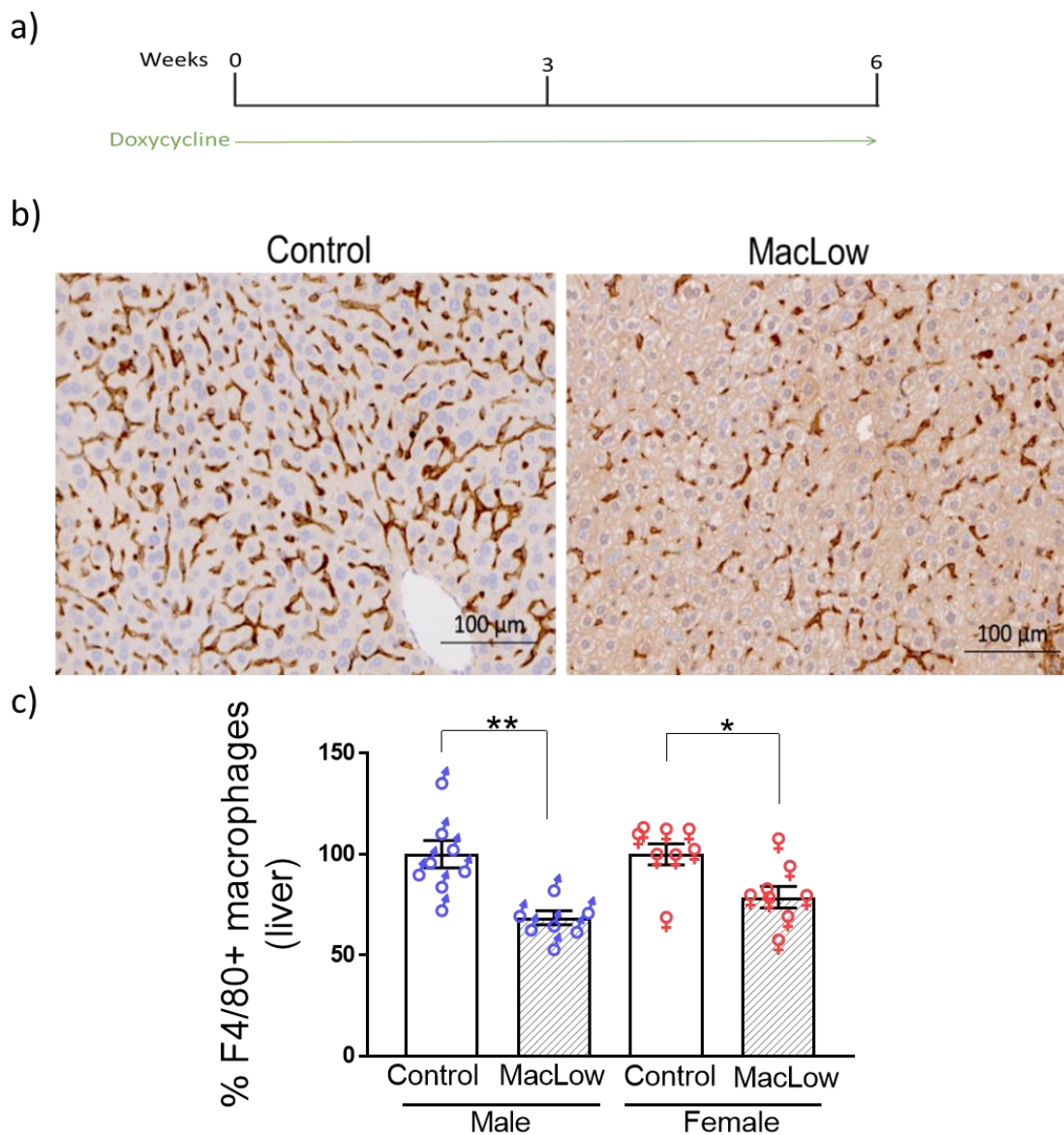
Figure 3.5- Confirming macrophages depletion in the liver after doxycycline treatment:
a) Experimental time-line; *MacLow* and control mice treated with doxycycline on diet for six weeks, the disease was monitored at week 3 by echocardiography and assessed at the end-point by echocardiography and cardiac catheterization. b) Quantification of the number of macrophages remaining within the liver after six weeks treatment with doxycycline. Positively stained cells (stained brown) were counted in 6 fields of view at X20 magnification. c) Representative histological image of liver sections stained with anti-F4/80 antibody. Data analysed using a one- way ANOVA with Bonferroni post hoc test. Error bars represent mean ±SEM, n= 7- 8/ group. *P <0.05, **P< 0.01. (♂) males, (♀) females.
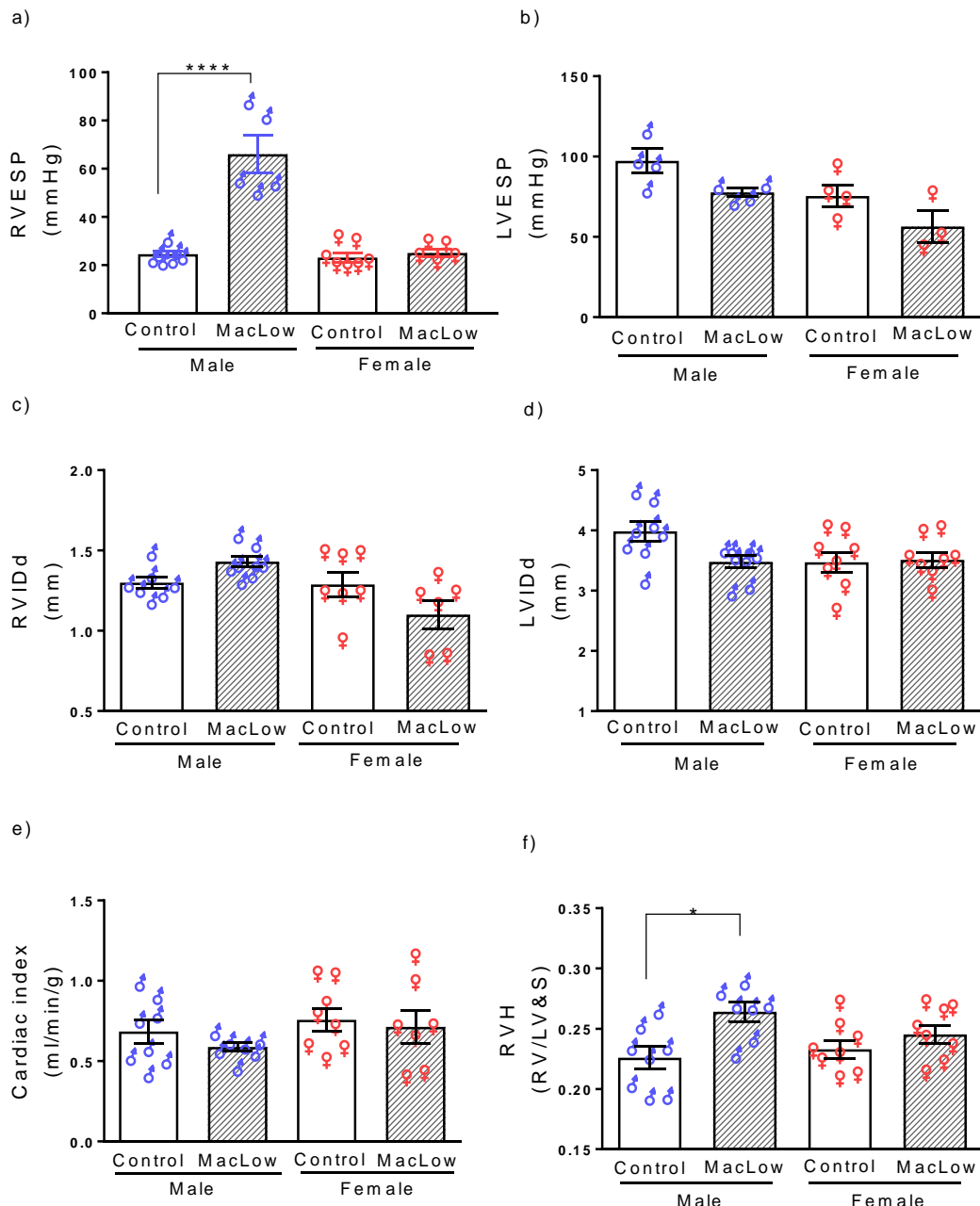
Figure 3.6- Haemodynamic of the PAH phenotype in *MacLow* mice: a) Right ventricle systolic pressure. b) Left ventricle systolic pressure. c) Right ventricle internal diameter in diastoli. d) Left ventricle internal diameter in diastoli. e) Cardiac index (cardiac output/ body weight), f) Right ventricle hypertrophy index. Measurements (a,b) taken using closed chest cardiac pressure volume catheterization. Measurements (c-e) taken using Vevo 770 echocardiography equipment. Data analysed by one- way ANOVA with Bonferroni post hoc test. Error bars represent mean ±SEM, n= 5-8/ group. *P <0.05, ****P< 0.0001. (♂) males, (♀) females.

3.3.2.2.1 Analysis of vessel wall remodelling

The degree of remodelling in the pulmonary arteries was assessed by two measurements; the increase in thickness of different sized pulmonary arteries and by counting the number of muscularised vessels as a proportion of total vessels. The increase in media thickness was calculated by dividing the area of the media by cross-sectional area (CSA) of the whole artery (media /CSA) in sections stained with α- smooth muscle actin staining (figure 3.7). The media /CSA of the small pulmonary arterioles (less than 51 μm) in male *MacLow* group showed a significant increase compared to the male control group as well as both females groups (figure 3.8- a). No significant differences were seen in the medium (51-100 μm) or large (>100 μm) sized vessels between *MacLow* and control male groups, although the difference was significant when male *MacLow* mice were compared to the female groups (figure 3.8- c,e).

Staining with vWF antibody showed the state of the endothelium in pulmonary vessels. A slight increase in thickness of the endothelial layer was seen in *MacLow* male mice compared to control (figure 3.7)

The percentage of muscularised vessels within the lung was calculated in elastin van Gieson stained sections. The results showed a significant increase in the percentage of smaller muscularised vessels sized less than 51μm in the diseased *MacLow* male group when compared to all other groups (figure 3.8-b), other size categories did not show a significant difference between any of the groups (figure 3.8-d,f).
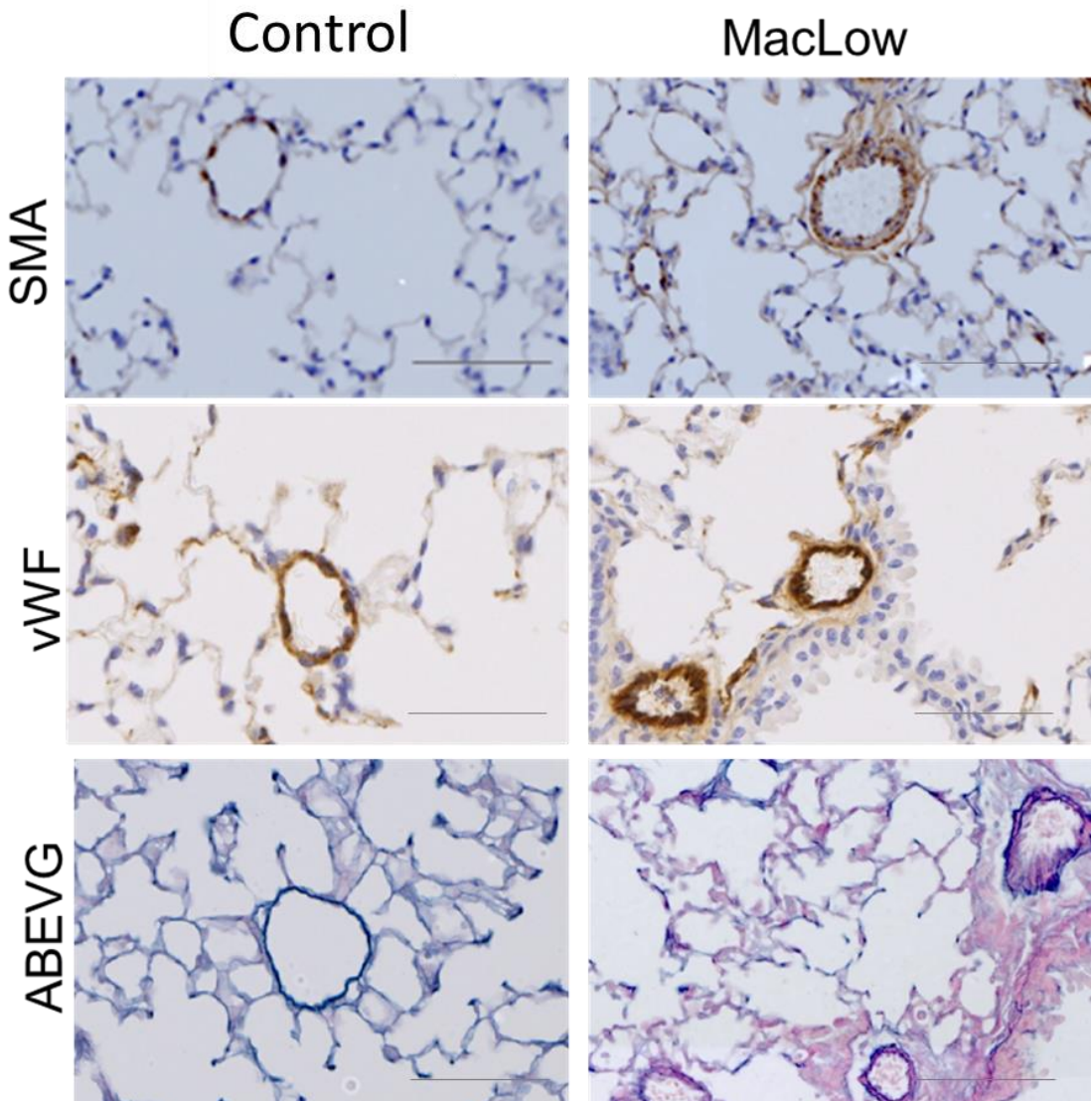
Figure 3.7- Remodelling of pulmonary arteries in *MacLow* male mice compared to controls: Representative histological images of lung sections shows the pulmonary vascular lesion in MacLow male mice compared to male controls. Sections stained with α- smooth muscle actin (SMA) to demonstrate the increase in medial wall thickness (the brown stained layer), or with Alcian blue Elastin van Gieson (ABEVG) to calculate the percentage of muscularised vessels (elastic lamina shown in purple), or with Von Willebrand factor (vWF) to assess the state of endothelial cell layer (stained brown). Images taken and analysed using Zeiss multi-slide scanning microscope at X20 magnification, scale bar= 50 µm.

a) (vessel size: 10-50 µm)

b) (vessel size: 10- 50 µm)

c) (vessel size:51-100 µm)

d) (vessel size:51-100 µm)

e) (vessel size: >100 µm)

f) (vessel size: >100 µm)
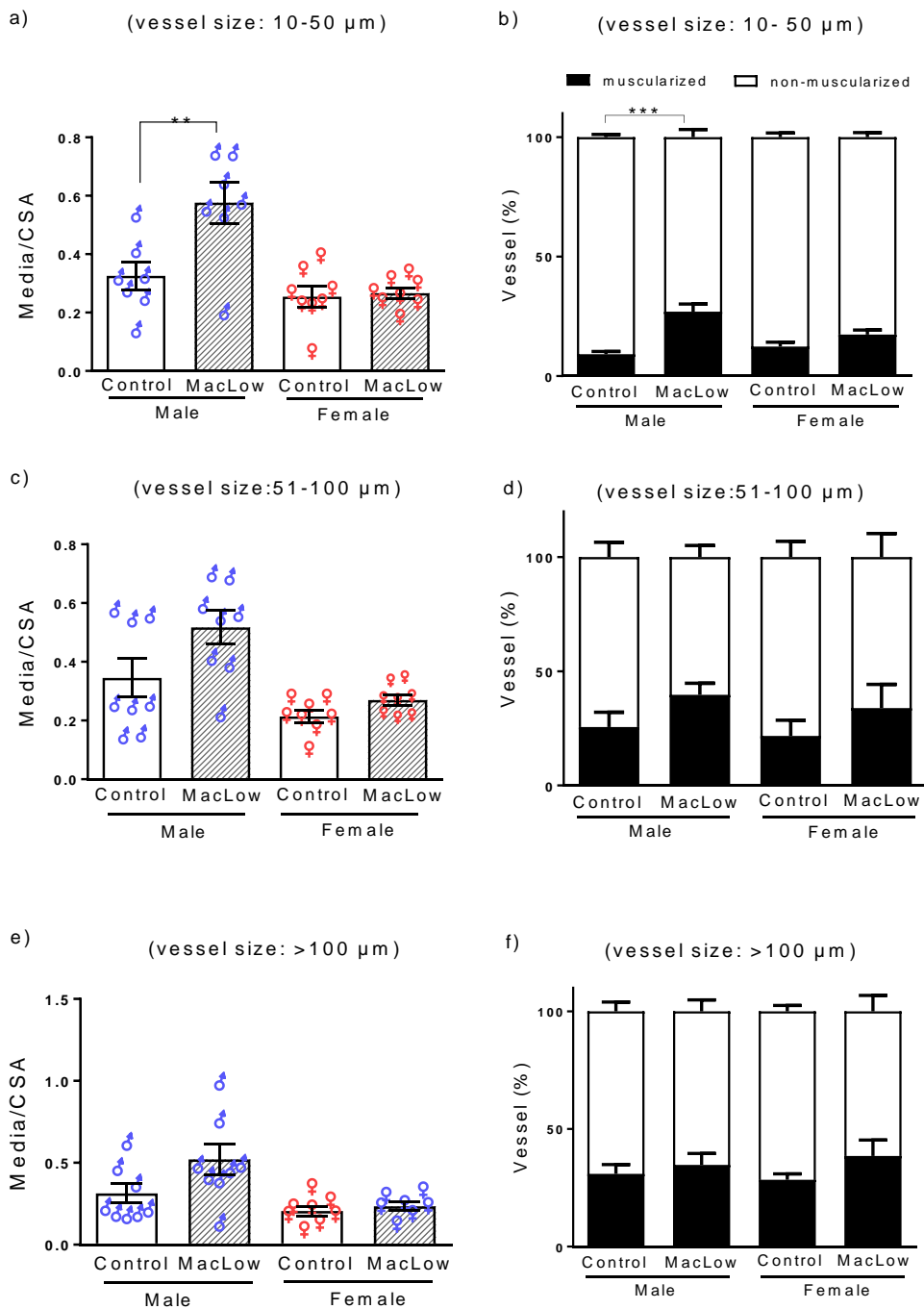
Figure 3.8- Analysis of the degree of remodelling in lung sections: a,c,e) bar graphs represent Media to cross sectional area (CSA) of three different sized groups (10-50 µm, 51-100µm and >100µm respectively), data analysed using a one- way ANOVA with Bonferroni post hoc test.   b,d,f) graphs represent pulmonary vascular remodeling by percentage muscularised vessels of three different sized groups of vessels (10-50 µm, 51-100µm and >100µm respectively) data analysed using two- way ANOVA. In all data n= 8 / group. *P <0.05, **P< 0.01, ***P< 0.001. (♂) males, (♀) females.

3.3.2.3 Analysis of lung macrophages

Analysis of the macrophage population within the lungs was performed using immunohistochemical staining of 5 μm thick paraffin sections. To assess the level of ablation of total macrophage, anti-F4/80 antibody was used (figure 3.9). The results showed a significant 30-40 % reduction in total macrophage number within the lung of *MacLow* mice when compared to controls (figure 3.10-a).

To further analyse the two-macrophage subsets, anti- iNOS and anti- CD206 antibodies were used to label M1 and M2 macrophages respectively (Figure 3.9). As expected, there was a significant reduction in iNOS+ macrophages in male and female *MacLow* mice after the six weeks doxycycline treatment (Figure 3.10-b). However, the reduction in CD206+ macrophages was not significant in male *MacLow* groups, as there was no difference compared to the controls (Figure 3.10-c). Female *MacLow* group showed a trend of reduction in the percentage of CD206+ macrophages, this reduction in M2 population was highly comparable to the reduction in M1 population in *MacLow* female groups. Though, the reduction was significant (P< 0.05) when compared to the female control group using the t-test.
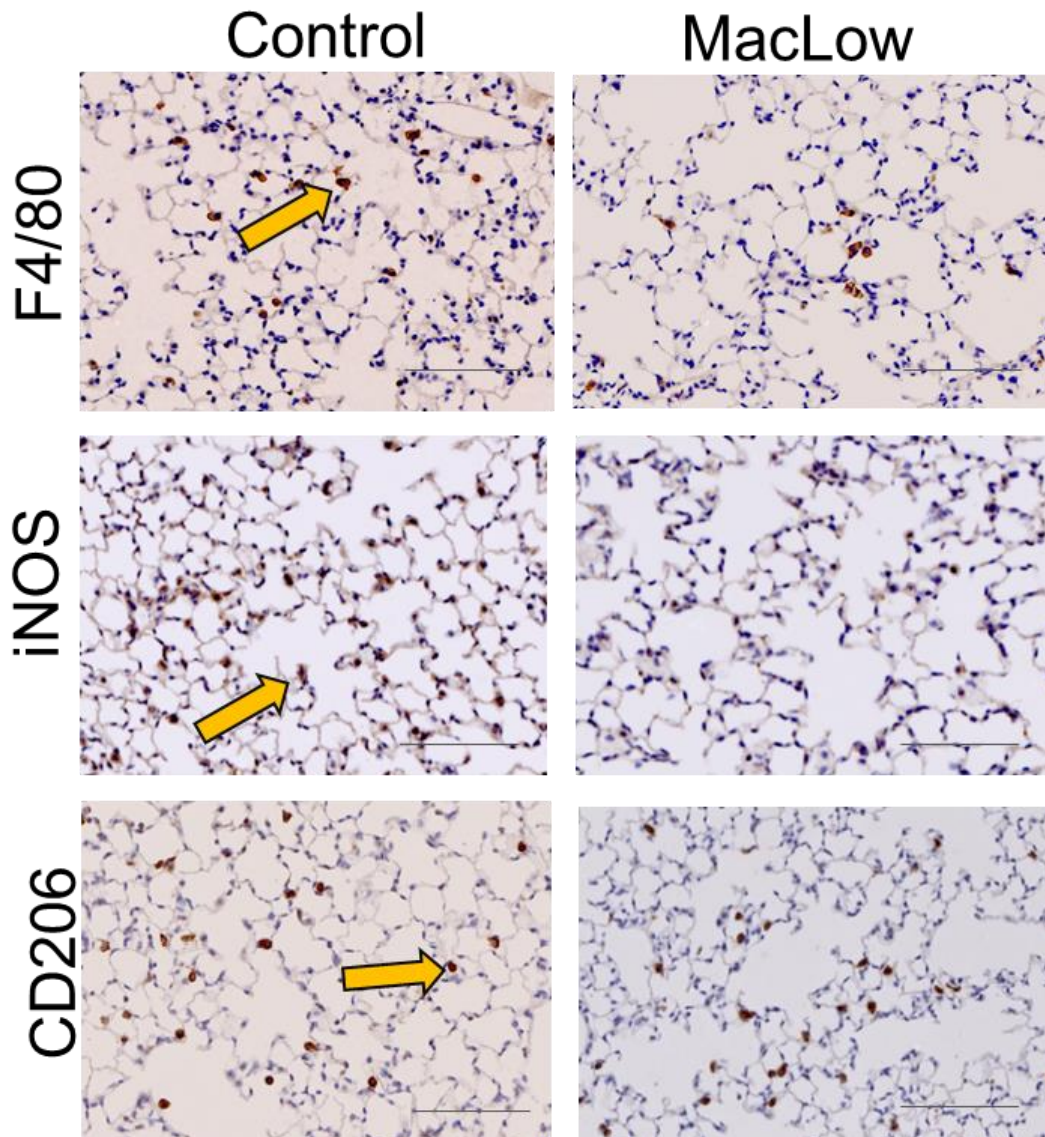
Figure 3.9- Lung macrophages in *MacLow* male mice compared to controls: Representative photomicrographs of lung sections stained with antibodies against F4/80 (total macrophages), iNOS (for M1 macrophages), CD206 (for M2 macrophages) and counterstained with haematoxylin. The images show the difference in macrophage populations (stained brown- arrow-head) that remain within the lung of MacLow male mice compared to control males after six weeks doxycycline treatment. Image taken using Zeiss multi-slide scanning microscope at X20 magnification, scale bar= 50 μm.
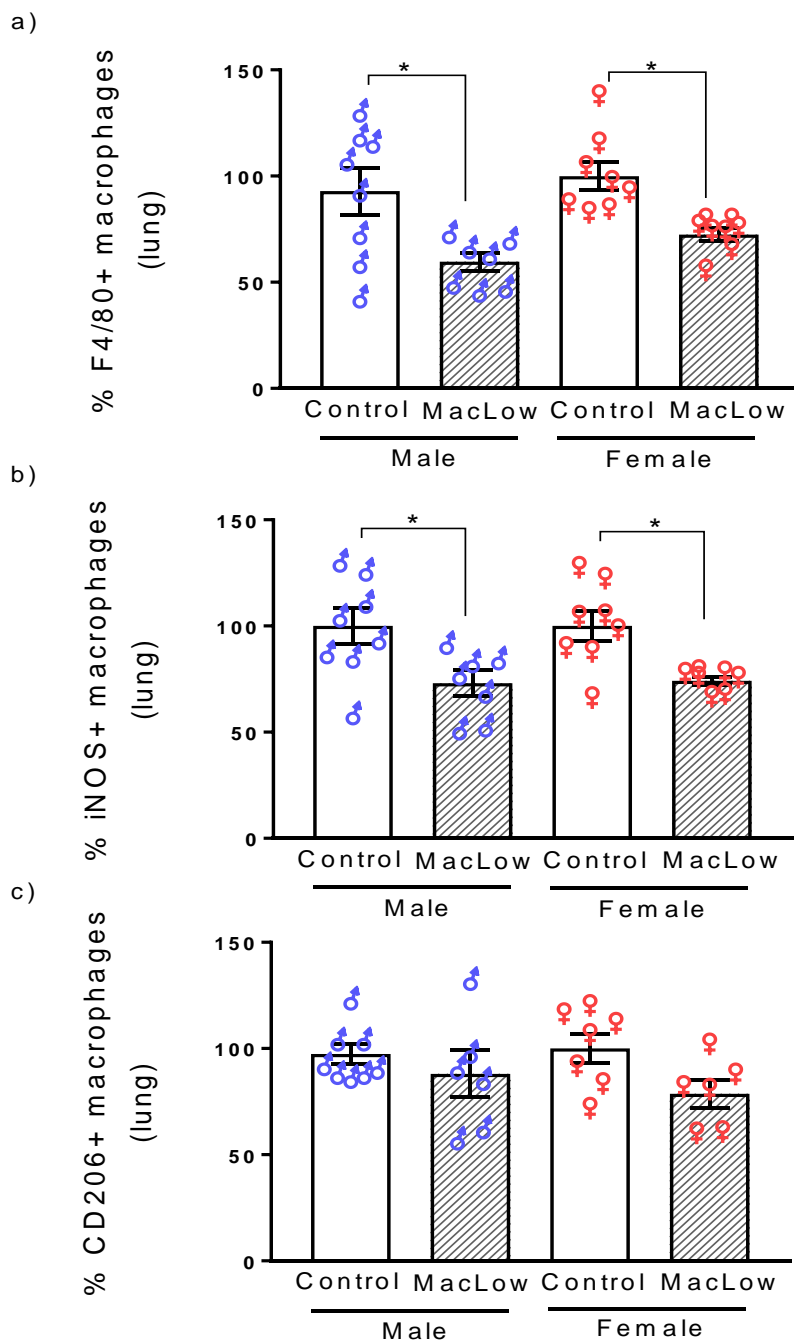
Figure 3.10- Analysis of macrophage subsets in lung sections: Quantification of the number of macrophage remaining within the lung after six weeks treatment of doxycycline. Positively stained cells were counted in 6 field of views / tissue at X20 magnification. a) Quantification of total macrophage using F4/80 antibody. b) Quantification of M1 macrophage subset using iNOS antibody. c) Quantification of M2 macrophage subset using CD206 antibody. Data analysed using a one- way ANOVA with Bonferroni post hoc test. n=7-8 / group. *P <0.05, **P< 0.01. (♂) males, (♀) females.

To examine the co-distribution of macrophages within pulmonary blood vessels of male groups, double immunofluorescent staining with anti-F4/80 and anti-SMA was performed (refer to section 2.2.5 for protocol). Qualitative assessment of the histological images showed the accumulation of F4/80 positive macrophages within the muscularised smooth muscle actin- expressing cells of the small sized vessels in *MacLow* male mice, this accumulation was not seen in the control group (figure 3.11).

Taken together, the *MacLow-* induced PAH phenotype was associated with peri-vascular macrophage accumulation and increasing M2 population (CD206+ macrophages) within the lungs.
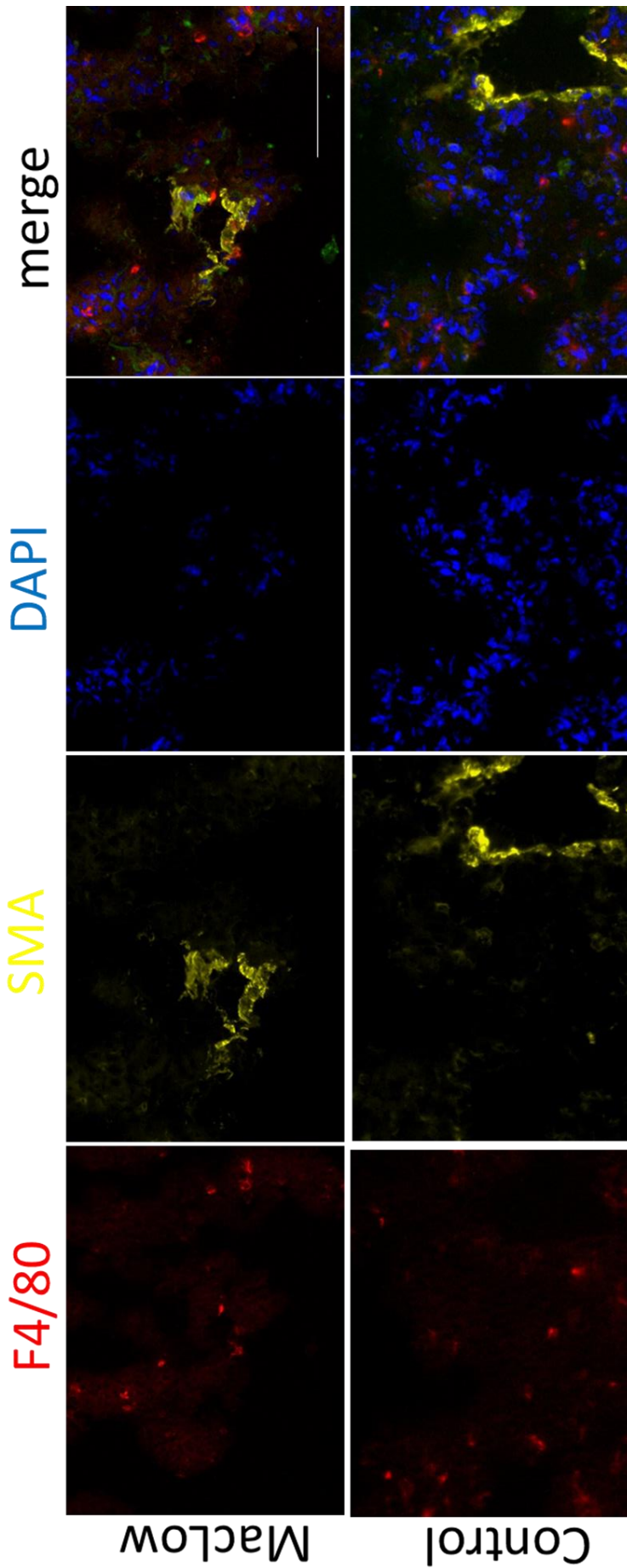
Figure 3.11- Double immunofluorescence staining against the F4/80 and SMA on lung sections: Control and MacLow male mice were treated with doxycycline for six weeks to induce PAH. Representative immunofluorescence image paraffin lung sections stained with anti- F4/80 (red) and SMA (yellow) with cell nuclei labelled with DAPI (blue). Scale bar=50 μm.

3.3.2.4 Analysis of circulating blood monocyte

To relate the changes in haemodynamic and vessel remodelling to the alteration in monocyte/ macrophage cell counts. Blood was collected by cardiac puncture and pooled into a single blood sample for each group (n=5). Following density gradient centrifugation, blood monocytes were isolated and stained with Alexa Fluor ® 488 anti- mouse CD115 (refer to sections 2.1.7 and 2.4). As with the time-point study, the monocyte number was also reduced in *MacLow* mice after doxycycline treatment. Moreover, the reduction was larger in the diseased male *MacLow* group than the females (Figure 3.12), this may suggest that the PAH phenotype in *MacLow* male mice was also associated with a reduction of blood monocyte. However neither of these observations were statistically analysed as there was only one blood sample in each group.
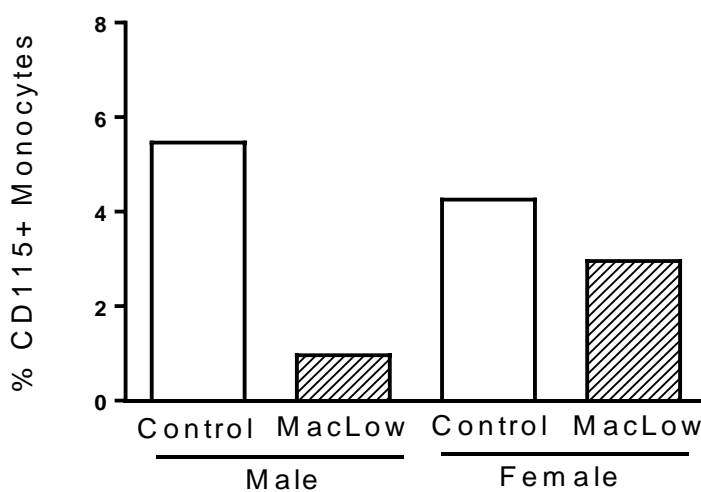
Figure 3.12- Flow cytometric analysis circulating monocyte after six weeks doxycycline treatment: graph represents the number of CD115+ cells obtained from one pooled blood sample for each group (5 mice/ group). Peripheral blood mononuclear cells (PBMC) isolated and stained with Alexa Fluor ® 488 anti- mouse CD115 then analysed by flow cytometry.

3.4 Discussion

Data presented in this chapter further support the modulatory role of macrophages in PAH pathogenicity, and emphasise the notion that the switch in macrophage polarity is important in the disease development. The findings did not support my primary hypothesis, as the specific depletion of macrophages in *MacLow* mice did not protect against induced vascular remodelling. On the contrary, macrophage loss actually led to the development of PAH spontaneously. Additionally, the results showed a unique and interesting sex-specific PAH phenotype induced by the loss of macrophages in male mice suggesting a correlation between sex and macrophages in PAH.

In the *MacLow-* induced PAH study described here, males but not females *MacLow* mice possessed a significant increase in their RVESP, RVH index and vascular remodelling when compared to controls after the loss of CD68+ macrophages. This PAH phenotype correlated mainly to the macrophage depletion in tissues (particularly the lungs) in addition to the male sex susceptibility.

Moreover, all study groups were given doxycycline for the same period of time to preclude the argument that doxycycline itself may cause these changes, especially since tetracyclines have previously been shown to inhibit collagenolytic enzymes (such as matrix metalloproteinases MMPs), which may lead to inhibition of the degradation of connective tissue (Vieillard-Baron et al., 2000).

No previous literature has demonstrated that macrophage depletion leads to the development of PH in animal models. In contrast, previous ablation strategies that aimed to deplete the monocyte/ macrophage cell lineage in rodents such as

liposome containing clodronate (Cl2MBP) or the use of gadolinium chloride (GdCl3), showed that the depletion of the mononuclear cells (referred to as fibrocytes) following the clodronate liposome injection in male rats attenuates the hypoxia- induced pulmonary artery adventitial remodelling (Frid et al., 2006). Importantly, the Cl2MBP liposome when administered as an intravenous injection is unable to cross the barrier of the vascular endothelial, so was not even taken- up by the tissue resident phagocytic cells (Vanrooijen and Sanders, 1994). A similar phenomenon occurs with the GdCl3 injection as the drug aggregates into large particles which are then taken-up by circulating phagocytes only (Singh et al., 2004).

Moreover, therapeutic inhibition of the stromal cell derived factor SDF-1 (important chemokine for the recruitment of inflammatory cells) in the monocrotaline rat model of PH blocks the pulmonary vascular infiltration of CD68+, CD3 and mast cells, this was also associated with reduced pulmonary vascular remodelling (Savai et al., 2012).

Again, another study by Zaloudikova used intra-tracheal chlodronate liposome to investigate whether the ablation of alveolar macrophages can attenuate hypoxia-induced PH in male rats. The findings showed that repeated chlodronate treatment leads to significant reduction in the mean pulmonary artery pressure after hypoxia compared to untreated controls (Zaloudikova et al., 2016).

Interestingly, none of these studies reported any spontaneous increase of the pulmonary pressure or associated remodelling in their normoxic controls after macrophage depletion. As macrophages are extremely versatile, it is likely that each of the macrophage depletions strategies described above targets specific

macrophage populations depending on the drug and the route of the drug delivery.

For instance, within healthy lungs, heterogeneous macrophage populations were detected; lung macrophages were classified as resident alveolar macrophages (AM), and tissue interstitial macrophages (IM). The alveolar macrophages reside within the airways, while the tissue macrophages are located within the lung without contacting the airway sacs. In response to inflammation, additional macrophages are recruited to the lungs (referred to as recruited macrophages) from circulating monocytes (McCubbrey et al., 2016). Each of these population could respond differently to the doxycycline-induced depletion. However, further work will be required to address the speculations. A brief summary of macrophages development and differentiation is shown in Figure 3.13.

Another important observation in the *MacLow-* induced PAH model, was the bias toward the CD206+ population (resembling the alternatively activated M2 subtype) within the lungs of the diseased male mice following six weeks doxycycline treatment. It has been shown previously that in hypoxia- induced PH, hypoxia causes polarization of alveolar macrophages toward M2 phenotype, this was associated with the development of hypoxia- induced PH *in vivo* and proliferation of pulmonary artery smooth muscle cells *in vitro* (Vergadi et al., 2011).

A possible explanation of the accumulation of M2 macrophages within the lung following doxycycline treatment is that the M2 macrophages are resistant to the *MacLow* ablation model, although the female groups showed a trend toward reduction in this population and the M2 population was reduced after a single

doxycycline injection in both sexes of *MacLow* mice. Another possible explanation is that this population developed via differentiation of the surviving macrophages to clear up the dead cells, as one of the M2 macrophages functions is debris scavenging (Weisser et al., 2012). Further studies are required to determine the specific mediators that may be contributing factors in signalling cascade of M2 activation leading to development of PH. Further work will be described in the next chapters to address this observation.

In addition, blood monocyte in *MacLow* mice were also affected by the macrophage depletion. Analysis of blood monocyte by flow cytometry showed a pronounced drop in blood monocyte count following a single doxycycline injection as well as following the six weeks doxycycline treatment. However, the exact mechanism of this reduction is unclear. It could be that monocytes migrate excessively from the peripheral blood to tissues to compensate for the loss of tissue macrophages. Or and most likely, that monocytes are also targeted in *MacLow* depletion model, as all monocyte/ macrophage myeloid lineage shown to express the CD68 antigen (Hume, 2011, Iqbal et al., 2014, McCubbrey et al., 2016).
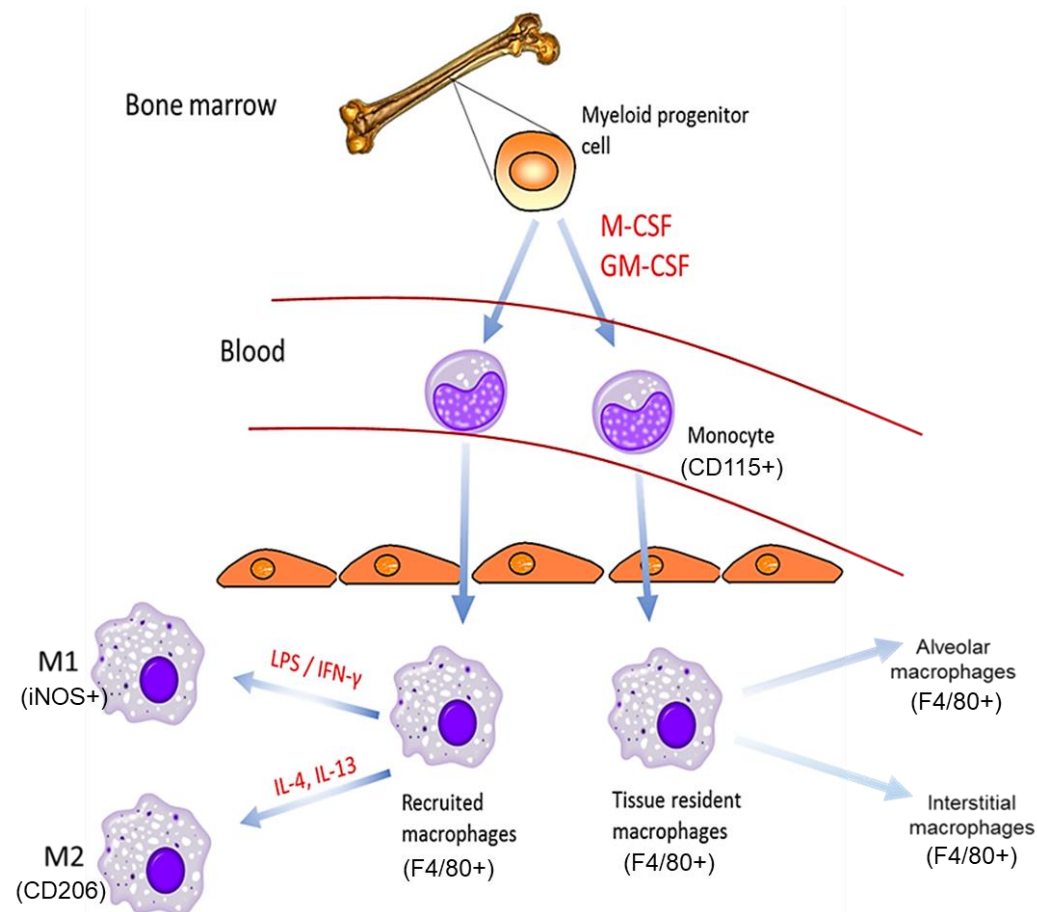
Figure 3.13- Schematic illustration of macrophage development and differentiation: Monocytes are first derived from the differentiation of bone marrow myeloid progenitor cells in presence of the colony stimulation factors (CSF), then circulate in bloodstream for several days before enter the tissues and being differentiated to macrophages. When tissue macrophages depleted for any reason, newly recruited macrophages infiltrate to restore local macrophage population. The acquired differentiated phenotype of macrophages reflects the micro-environmental signals in which macrophages reside: macrophages differentiate to classically activated (M1) macrophages in presence of Lipopolysaccharide (LPS) and interferon gamma (IFN-γ) or to alternatively activated (M2) macrophages in presence of interleukin-4 (IL-4). Within the lungs, the tissue-resident macrophages can be further classified depending on their location within the lung tissue to either alveolar or interstitial macrophage. Markers used to identify monocyte/ macrophage populations shown in brackets.

Finally, the incidence of PAH in female patients is higher than in males, however, men showed the higher mean pressure of the pulmonary artery and higher risk

of death compared to the female (Badesch et al., 2010). It was interesting to see that in the *MacLow* model only the male mice developed the spontaneous PAH phenotype following macrophage depletion. Females in animal models have been shown to be more protected against the induced forms of PH, this is thought to be due to the protective effect of sex hormones such as oestrogen (known as Oestrogen paradox phenomenon). The role of oestrogen in clinical PAH is still not completely known, but in animal models, oestrogen has been shown to be beneficial and has a cardiovascular protective function (Umar et al., 2011). The implication of sex differences in the *MacLow* mouse model will be investigated further in chapter 6.

The following chapter investigates whether bone marrow-derived cells or the tissue resident macrophages are critical for the development of PAH in male *MacLow* mice.

4 The role of circulating versus tissue resident cells in the development of pulmonary arterial hypertension in male *MacLow* mice

4.1 Introduction

In chapter 3, I demonstrated that loss of macrophages in *MacLow* mice can cause a sex- specific spontaneous PAH phenotype, this was associated with increased vascular remodelling and a prevalence of M2 macrophages within the lungs. There is accumulating evidence in the literature showing the ability of circulating progenitor cells to migrate to the lung and to contribute to the pathology of hypoxia- induced PH (Davie et al., 2004, Hayashida et al., 2005, Raoul et al., 2007). The aim of this chapter was to investigate whether bone marrow- derived cells or tissue resident cells were the critical cells for the development of PAH in male *MacLow* mice.

To trace the origin of cells (whether bone marrow or tissue resident), different chimeric mice can be generated by the process of bone marrow transplantation (BMT). The principle of BMT procedure depends on injecting bone marrow hematopoietic stem cells from donor mice (donor inoculum) into the bloodstream of recipient mice with supressed immunity, then the donor cells reconstitute the immune system. The total body irradiation (TBI) is the most commonly used immune-suppression method. TBI suppress the immune system of the recipient mice and prevent graft rejection as it kills the hematopoietic progenitor cells and

the proliferating immune- competent in the recipient (Cui et al., 2002, Duran-Struuck and Dyskoz, 2009).

Leading to the aim of this chapter, the BMT procedure was adopted as a tracing strategy to investigate the contribution of bone marrow- derived cell in PAH development.

Various studies have reported some differences in radio-sensitivity between mice strains, and as there was no previous literature describing a protocol for the generation of *MacLow* chimera, it was essential to perform two pilot studies using a small number of mice before determining the best irradiation regimen for optimization of the BMT protocol. Furthermore, it became apparent using already developed fate-mapping techniques that most tissue-resident macrophages can self- maintain via proliferation without replenishment from blood monocyte (Gundra et al., 2014, Ginhoux and Jung, 2014). It has been also shown that IL-4 can enhance this increase in numbers of tissue macrophages above the homeostatic level, through proliferation rather than infiltration (Jenkins et al., 2013, Jackson-Jones et al., 2016). Thus, the probable proliferation capacity of macrophages in *MacLow-* induced PAH model, and the expression of IL-4 within the diseased lungs was also investigated.

4.2 Methods

4.2.1 Pilot study 1

In this study, four age-matched male mice (9 weeks old) were used as recipients, and two male mice (5 weeks old) were used as cell donors (recipient to donor ratio = 2:1), the chimaeras generated described in the table (4.1).

Table 4.1. *MacLow/* **control chimeras generated from bone marrow transplantation for the pilot studies**

Chimera	Donor	Recipient (n)
1	Control	MacLow (2)
2	MacLow	Control (2)

For the BMT procedure, a standard protocol which has been successfully used in our department was followed (Chamberlain et al., 2006, Evans et al., 2009, West et al., 2014, Hameed et al., 2012). In brief, all mice were kept in individually ventilated caging (IVC) under barrier condition in the biological service unit at the Hallamshire hospital, mice were fed standard chow and started drinking acidified water one day before the transplant to minimized the risk of infection (see appendix II for recipe).

On the day of transplantation, recipient mice were given a fractionated dose of whole body irradiation (5 Gy twice with 4 hours interval) before injecting donor bone marrow. Donor mice were euthanized by cervical dislocation, femurs and tibias removed in sterile PBS on ice. After removing the skin and fur from the bone it was washed with 70% v/v ethanol for 1 minute then the marrow cavity was flushed with 26-27 G syringe containing 2 ml media (RPMI- 1640 media contains 10% v/v FBS) under aseptic condition. Cells were passed through 40 µm cell strainer then centrifuged at 4 ºC 500 *Xg* for 5 minutes before been re-suspended in Hank's buffered salt solution (HBSS).

After the second dose of radiation, recipient mice were left in an incubator at 35ºC for one hour prior to injection. A maximum of 200µl of bone marrow cell suspension containing approximately 2×10^6 cells were injected through the tail

vein. Following BMT mice were monitored daily for any signs of illness, and weighed every two days to monitor changes in body weight.

This strategy was not successful as all mice showed signs of distress and pain within the first two weeks post-transplant, therefore, the procedure was terminated. For qualitative assessment of donor cell re-constitution in the recipients, the legs of culled mice were harvested directly and the bone marrow cells were flushed and prepared as described in section (2.1.9), the DNA was extracted from the bone marrow cells to run a genotyping PCR as described in sections (2.1.1).

4.2.2 Pilot study 2

Based on the fact that different strains of mice have different sensitivities to radiation thus may require different irradiation dose and frequencies (Duran-Struuck and Dyskoz, 2009), a modified irradiation strategy was followed in the second pilot study to enhance the survival. The *MacLow* line was originally derived from an FVB background and it has been reported that the FVB mice were successfully transplanted previously using 10-22 Gy as a single dose (Crawford and Gordon, 2005). Therefore, in the second pilot study the recipient mice were irradiated with a single dose of 10 Gy before receiving the donor inoculum and the same chimeras described in the table (4.1) were generated. Furthermore, aseptic steps were modified when preparing the donor cell suspension, to avoid the excessive use of ethanol on the intact bones, using heat-inactivated FBS and phenol free media for flushing the marrow to minimise negative effects on the reconstitution of the cells after injection.

Finally, for efficient and fluent tail vein injection procedure, recipient mice were sedated with subcutaneous injection of Hypnorm® solution few minutes before receiving the injection. Each mouse received between 5 and 6 x 10^6 cells in 100-200 µl cell suspension then kept warm to recover from sedation for 2-3 hours.

If any mouse showed signs of distress, pain or a loss of weight of greater than 10% of body weight over two consecutive days it was sacrificed. When mice reached the end of the study (70 days post-transplant) or culled on welfare grounds the legs were harvested and bone marrow cells were collected. For qualitative assessment of donor cells re-constitution, the DNA was extracted from the bone marrow cells to run a genotyping PCR. The modified strategy followed for the second pilot study was successful and 3 out of 4 mice survived and reached the endpoint of the study.

4.2.3 Generation of male *MacLow* chimeric mice and induction of pulmonary arterial hypertension

Leading to the main aim of this chapter, male chimeric mice were generated by the process of BMT, the procedure was performed using the optimized protocol from pilot study 2 (the full modified protocol is detailed in section 2.1.3). Age-matched male mice (8-10 weeks) were used as the recipient to generate the chimeras described in the table (4.2). The *MacLow* donor BM cells were transplanted into a genetically different pre-irradiated control recipient (allogenic graft), and the control BM cells were transplanted into pre-irradiated *MacLow* recipient. In addition, two groups received genetically identical graft (syngeneic graft) of *MacLow-* derived BM into *MacLow* mice and control BM into control mice as a positive and negative control groups respectively (figure 4.2-a). Mice were

left to recover for 30 days after the transplant, then the PAH was induced using doxycycline treatment to induce macrophage depletion (doxycycline containing diet) for another six weeks with no other insult. Mice were kept under aseptic condition and given acidified drinking water for the whole period of the study (10 weeks in total).

Table 4.2. ***MacLow*/control chimeras generated from bone marrow transplantation for the PAH study**

Chimera	Donor	Recipient (n)
1	control	MacLow (5)
2	MacLow	Control (5)
3	MacLow	MacLow (8)
4	control	Control (5)

4.2.4 Echocardiography and cardiac catheterization

Following six weeks of doxycycline treatment, non-invasive assessment of the disease was performed using echocardiography under anaesthesia as described in section 2.1.4. Then the closed chest cardiac catheterization was used to take the pressure-volume measurements from both sides of the heart as described in section 2.1.5.

4.2.5 Histological analysis

Tissues were harvested, fixed, processed, and stained according to the standard laboratory procedure described in sections 2.1.6 and 2.2.

4.2.6 Statistical analysis

All statistics were performed using GraphPad Prism version 7.2 (GraphPad software, SanDiego, California USA). Statistical comparison between the different groups was established by the use of one- way analysis of variance (ANOVA) followed by Bonferroni post- hoc analysis. Values are presented as mean ± SEM, and differences of P< 0.05 values were taken as significant.

4.3 Results

4.3.1 Optimal protocol for bone marrow transplant procedure using the *MacLow* mice

To determine the optimal strategy for the generation of *MacLow* chimeric mice, mice were either irradiated twice with 5 Gy in 4 hour interval and engrafted with approximately 2 X10^6 bone marrow cells (pilot study 1), or irradiated once with 10 Gy and engrafted with approximately 5 X10^6 bone marrow cells (pilot study 2). The strategy used for pilot study 1 was severely toxic and all mice had to be culled within 14 days post-irradiation due to severe illness. In contrast, in the second pilot study, three out of four mice survived with little ill effect and reached the end point of the study (70 days post-transplant). As presented in figure 4.1-a, the genotyping PCR for the CD68 gene (should be present in *MacLow* mice and not the controls) in the bone marrow of the recipients showed a failure of reconstitution of the donor bone marrow cells in the first pilot study, as the *MacLow* recipient was still positive for the CD68 and the controls were still negative. While in the second pilot study, the *MacLow* recipients showed less presence of CD68 gene as the bands were dim and the bands were clearer in the controls.

Loss of body mass is an expected adverse effect of irradiation, and regain of any weight loss is a sign of successful engraftment. Figure 4.1-b showed the percentage of weight lost after BMT over time for both pilot studies, the graph represents the pattern of losing and then gaining weight for pilot study 2, whereas in pilot study 1 the weight loss was dropping until the study had to be prematurely terminated. Finally, the percentage survival of the two studies was compared in figure 4.1-c with the clear success of the strategy followed in pilot study 2 (75% survival). In conclusion, based on the outcomes of the two pilot studies and in order to generate the targeted male *MacLow* chimeric mice, the strategy followed on the second pilot study was adopted.

MacLow and control mice underwent BMT to generate the chimeric groups showed in table 4.2, then PAH was induced by depleting macrophages with doxycycline treatment for six weeks. All mice reached the endpoint of the study (100% survival rate) and the pattern of their weight changes is displayed in graph 4.2-b. All mice experienced some weight loss during the first week after the BMT procedure, then they gradually gained this weight back. No significant differences were detected at any point, however, the control recipient transplanted with *MacLow* graft failed to achieve their start weight but they had no sign of illness. To confirm the graft success, random bone marrow samples from the allogenic recipient groups were tested using the genotyping PCR as previously described.
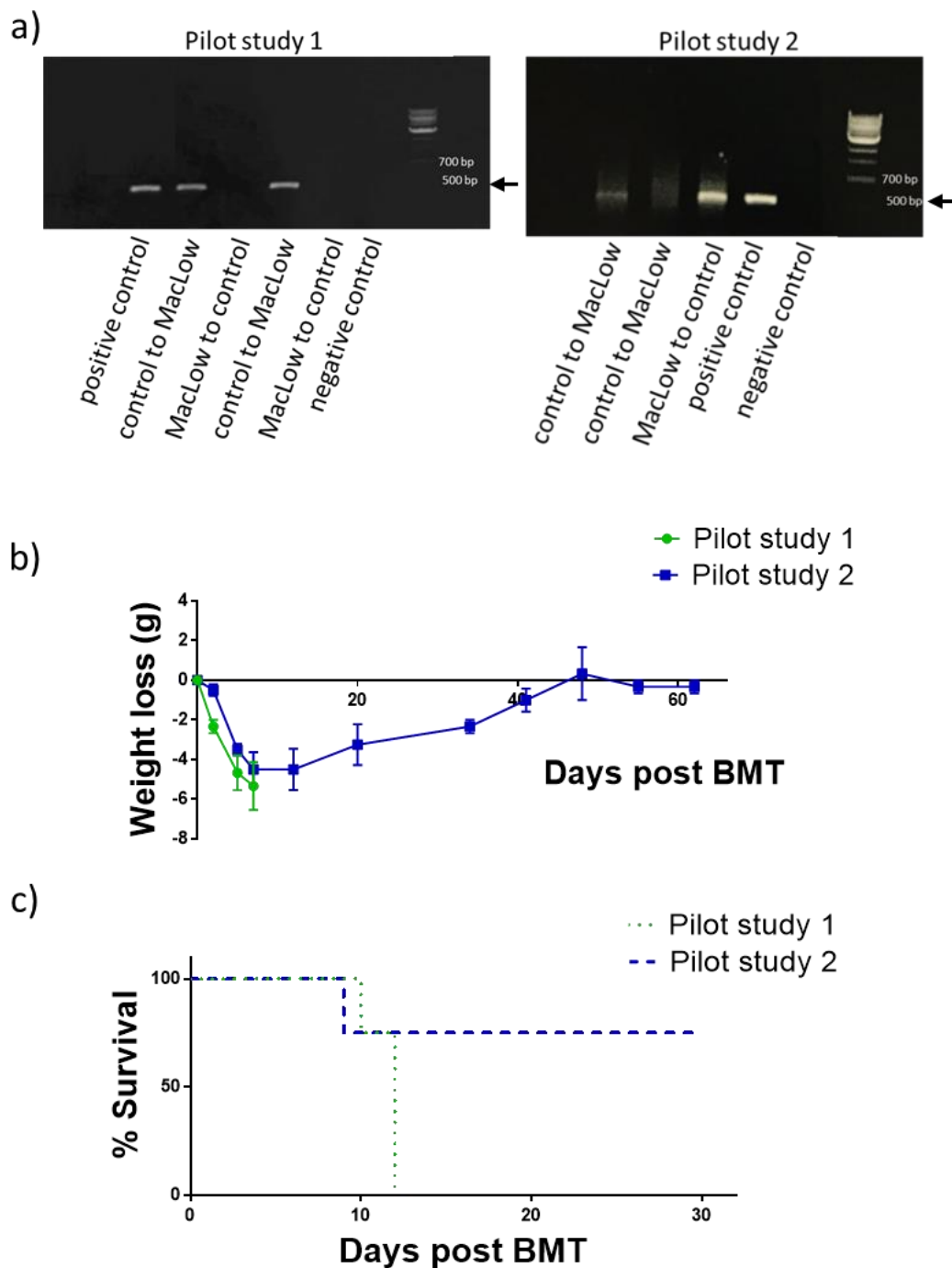
Figure 4.1- Optimizing protocol for total body irradiation and generation of chimeric mice: a) Images of an agarose gel showing PCR amplification of the DNA extracted from the chimeric mice following pilot studies 1 and 2. The DNA extracted from the bone marrow for genotyping, positive samples have the CD68 genes appeared as a 546bp band, known CD68 positive and negative templates were included as the positive and negative controls respectively. b) The graph shows the difference in weight loss of the chimeras from pilot studies 1 and 2 after the bone marrow transplant procedure. c) Comparison of the survival rate of the chimeric mice in pilot studies 1 and 2 at various intervals. n=4.

4.3.2 Confirmation of macrophage depletion in *MacLow* recipient mice

To confirm efficient macrophage depletion, the percentage of macrophages depleted from the liver sections was assessed using immunostaining as previously described (see section 2.2.2). In brief, 5 µm sections of paraffin-embedded liver were stained with anti-F4/80 antibodies, and then macrophages were counted and normalized to the negative control group (control BM into control mice). The results showed a significant reduction in F4/80 positive macrophages (about 35%) in both *MacLow* recipient groups compared to the control recipients (Figure 4.2). In addition, the data showed no difference in macrophage count between the *MacLow* recipients transplanted with either control (allogeneic graft) or *MacLow (*syngeneic graft) derived BM cells after doxycycline treatment. This suggests that doxycycline treatment can induce significant loss of liver macrophages in the *MacLow* chimeras regardless of the genotype of transplanted cells.
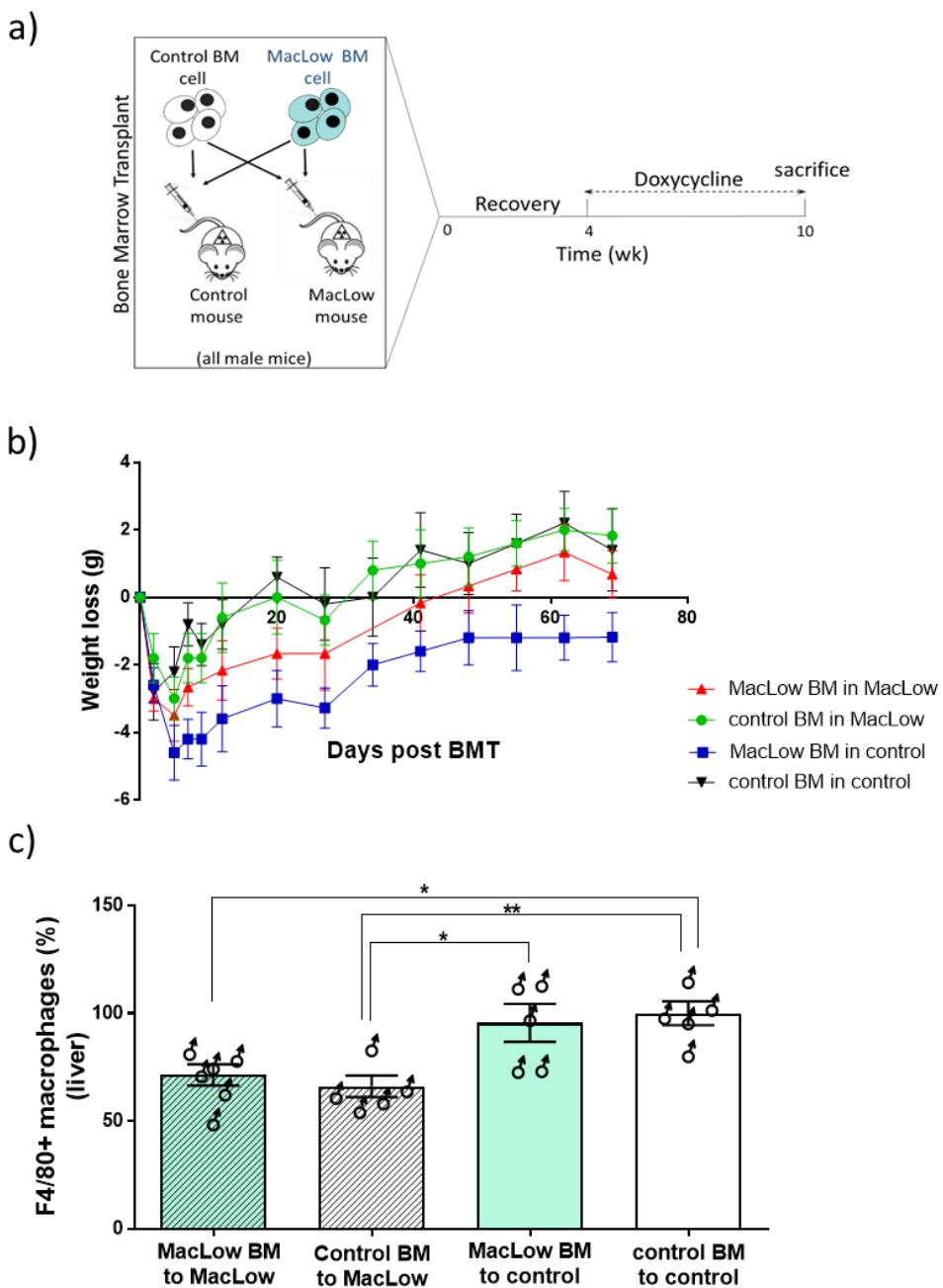
Figure 4.2- Confirming macrophages depletion in the liver after doxycycline treatment: a) Schematic of study design displaying the bone marrow transplant procedure followed by 4 weeks recovery period before starting doxycycline treatment, the disease assessed at the end-point by echocardiography and cardiac catheterization. BM= bone marrow. b) Graph shows the difference in weight loss of the different groups after the bone marrow transplant procedure. BMT= bone marrow transplantation. c) Quantification of the number of F4/80+ macrophages remaining within the liver after six weeks treatment with doxycycline. Positively stained cells were counted in 6 fields of view at X20 magnification. BM= bone marrow. Data analysed using a one- way ANOVA with Bonferroni post hoc test. Error bars represent mean ±SEM, n=5- 8/ group. *P <0.05, **P< 0.01.

4.3.3 Assessment of PAH in male chimeric mice

4.3.3.1 Haemodynamic evaluation

Following macrophage depletion, disease progression was first assessed by measuring different haemodynamic parameters (gathered from the heart catheterization and echocardiography) as well as the right ventricle hypertrophy value. The results showed that transplantation of BM from *MacLow* mice into pre-irradiated control mice was not sufficient to cause a significant increase in their RVESP compared to the positive control group (*MacLow* BM into *MacLow* mice) with 20.58 ±1.566 mmHg vs 28.94 ±2.192 mmHg respectively (figure 4.3-a). It was interesting to see that the control recipients transplanted with *MacLow* BM do not lose their tissue macrophages nor have increased pulmonary pressure following doxycycline treatment, this suggest that *MacLow* BM cells alone are not enough to induce the disease in control mice.

In addition, no conclusion can be made regarding whether the *MacLow* recipients transplanted with control cells were protected or not against the disease development as the pressure readings were not significantly altered (23.26 ± 0.6134 mmHg). However, the average RVESP is trending toward the normal pressure.

This effect was also seen in other haemodynamic parameters measured from the right-side of the heart with no effect on the measurements from the left-side heart (see appendix I). No changes in the cardiac index were detected between the different groups (figure 4.3-b). Furthermore, the increase in RVESP after the loss of macrophages in the *MacLow* syngeneic chimeric group (around 29mmHg) was not as high as the spontaneous increase observed in the normal *MacLow* male

mice (about 66 mmHg) shown in chapter 3 (graph 3.6-a). This could as a result of irradiation that might be affecting the lung resident macrophages (Matute-Bello et al., 2004).

To further investigate whether the increase in pressure has led to right ventricular hypertrophy (RVH), the RVH index was calculated. RVH value was assessed on the basis of the ratio of RV free wall weight to the left ventricle free wall weight plus septum. The results show no significant difference in the RVH value between the groups (figure 4.3-c), which again indicate that the disease phenotype was not aggressive enough to cause any effect on the heart.

Taken together, the PAH phenotype showed only when the donor of the BM cell and the recipient are both *MacLow* mice, this suggests that both bone marrow-derived macrophages and lung resident macrophages need to be depleted in order to develop PAH in male *MacLow* mice.

a)
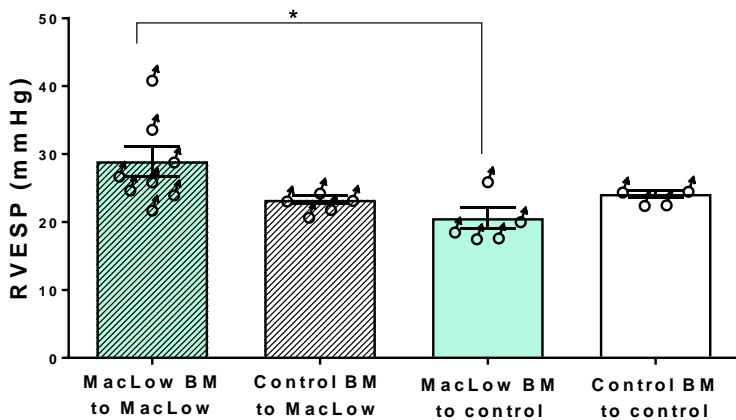
b)
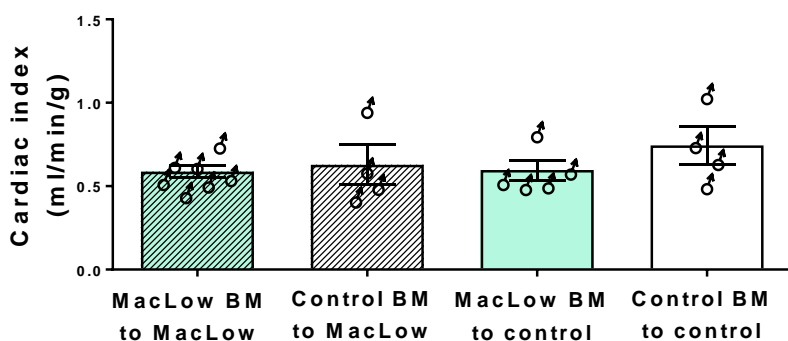
c)
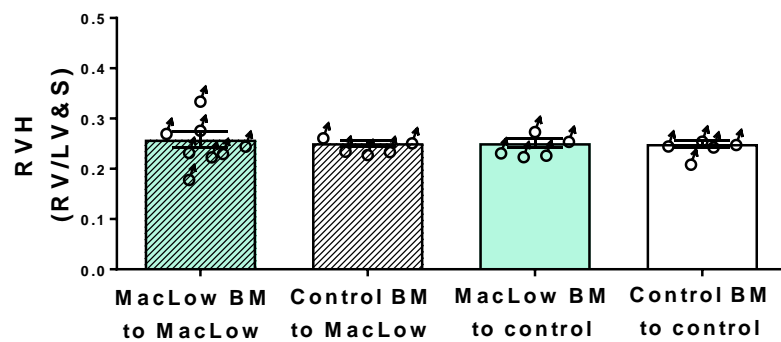
Figure 4.3- Haemodynamic of the PAH phenotype in male chimeric mice: a) Right ventricle systolic pressure (RVESP) taken by closed chest cardiac pressure-volume catheterization b) Cardiac index (cardiac output/ body weight) taken by Vevo 770 echocardiography equipment, c) Right ventricle hypertrophy index (RVH). BM= bone marrow Data analysed by one- way ANOVA with Bonferroni post hoc test. Error bars represent mean ±SEM, n= 5-8/ group. *P <0.05.

4.3.3.2 Analysis of vessel wall remodelling

PAH is usually associated with vascular remodelling, therefore the remodelling was assessed by calculating the increase in media thickness of the pulmonary arteries (by dividing the area of the media by cross-sectional area CSA of the whole artery in sections stained with α-smooth muscle actin staining), and by counting the number of muscularised vessels as a proportion of total vessels. The media /CSA of the small pulmonary arterioles (less than 51 μm) in the allogenic chimeras (control BM in *MacLow* and *MacLow* BM in control) showed no increase as that of the positive control group (figure 4.4-a)

The positive control group (*MacLow* BM in *MacLow*) showed a significant increase in their media thickness compared to all other groups. No significant differences were seen in the medium (51-100 μm) or large (>100 μm) sized vessels between any of the groups.

To calculate the percentage of muscularised vessels within the lung, the number of muscularised vessels (has double elastic lamina) in elastin van Gieson stained sections were divided by the total number of arteries under the same size range multiplied by 100. Although the results here should reflect and emphasise the Media/CSA calculation, no significant differences between the groups under any size category were detected, only a trend toward an increase was observed in the *MacLow* BM to *MacLow* group (figure 4.4-b,d,f).

In summary, the overall remodelling in the chimeric *MacLow* mice was less pronounced than that seen in *MacLow* mice following macrophage ablation, this is consistent with the haemodynamic measurements as the disease phenotype was less severe in the chimeric mice.
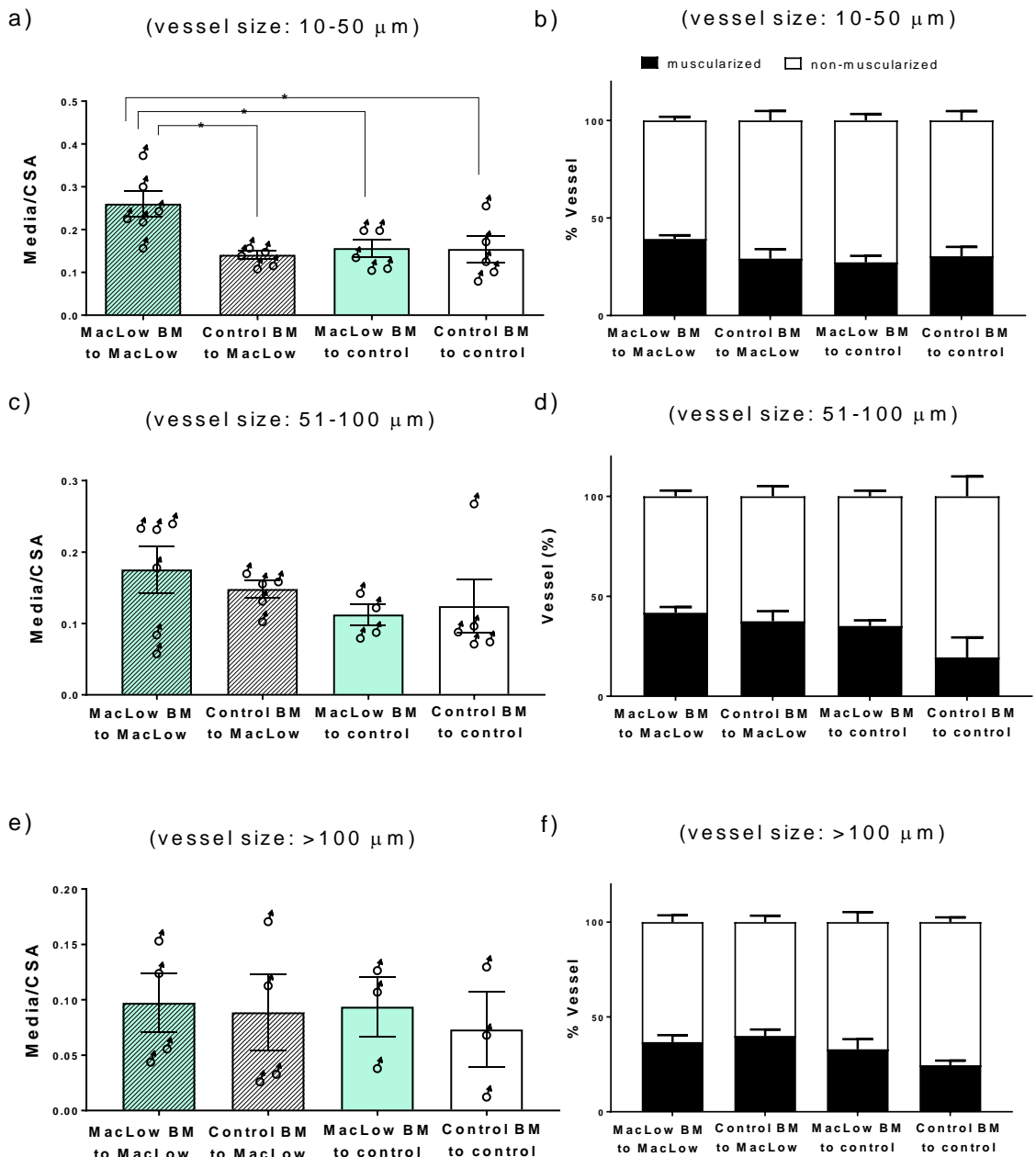
Figure 4.4- Analysis of the degree of remodelling in lung sections: a,c,e) Bar graphs represent Media to the cross-sectional area (CSA) of three different sized groups (10-50 µm, 51-100µm and >100µm respectively), data analysed using a one- way ANOVA with Bonferroni post hoc test. b,d,f) Graphs represent pulmonary vascular remodelling by percentage muscularised vessels of three different sized groups of vessels (10-50 µm, 51-100µm and >100µm respectively) data analysed using two- way ANOVA with Bonferroni post hoc test. BM= bone marrow. In all data n= 3-6 / group. *P <0.05.

4.3.4 Analysis of lung macrophages

Analysis of lung macrophage subsets was performed using immunohistochemical staining of 5 μm thick paraffin sections of lung as previously described. To assess the level of reduction in total macrophages, anti-F4/80 antibody was used (figure 4.5) and then positively stained cells were counted and normalized to the negative control group (control BM into control mice). The results displayed in figure 4.6-a showed non-significant reduction in total macrophage numbers within the lung of both *MacLow* recipient groups when compared to control recipients.

To further analyse macrophage subsets, anti-iNOS and anti-CD206 was used to stain and count M1 and M2 populations respectively (figure 4.6-b,c). The results showed no clear pattern of depletion of either of these populations. The M2 population was still higher in the *MacLow* recipient given *MacLow* BM than control recipients given *MacLow* BM but again the differences were not significant. It was unclear why the depletion of lung macrophage in this study was not significant even though the numbers of liver macrophages were significantly reduced (figure 4.2-c). Possibly, the irradiation is killing some of the resident lung macrophages (particularly the alveolar macrophages), and as they are long-lived, the recovery time was not long enough for the resident population to repopulate following the TBI (Matute-Bello et al., 2004).

MacLow BM to MacLow

Control BM to MacLow

MacLow BM to control

Control BM to Control
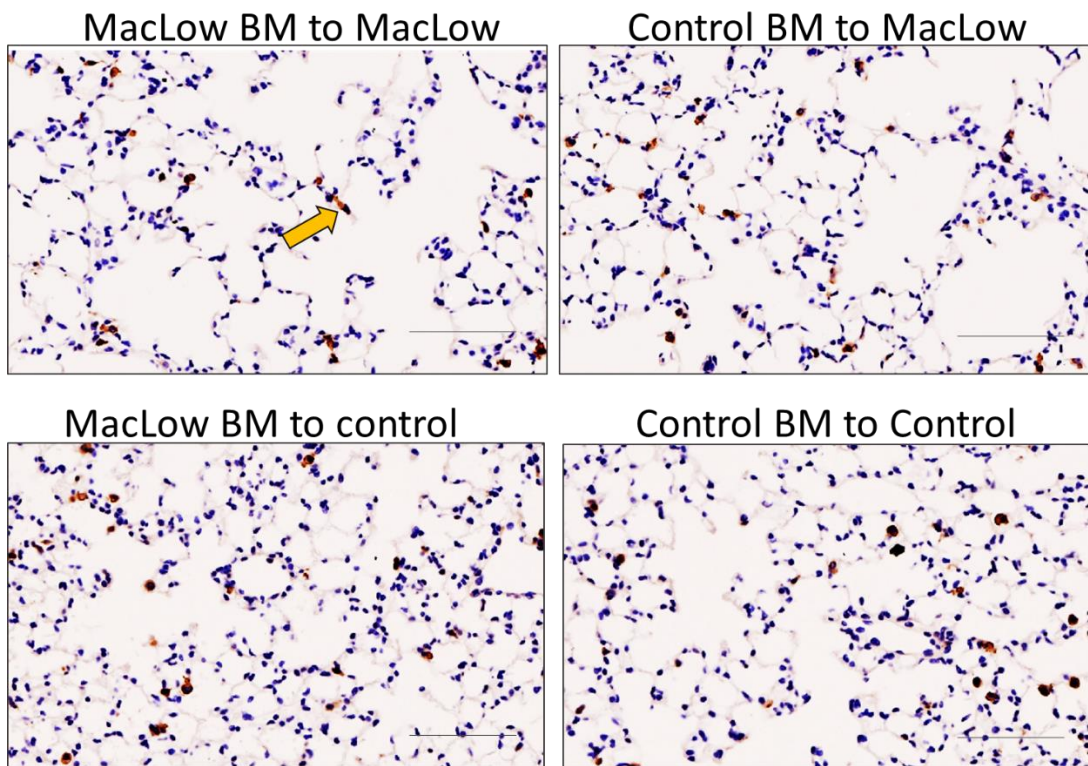
Figure 4.5- Total lung macrophages in male chimeric mice: Representative photomicrographs of   lung sections stained with anti-F4/80 antibody (total macrophages), the images show the different in macrophage (stained brown- arrow head) remained within the lung of each group after six weeks doxycycline treatment. Image taken using Zeiss multi-slide scanning microscope at X20 magnification, scale bar= 50 µm.

a)

b)

c)
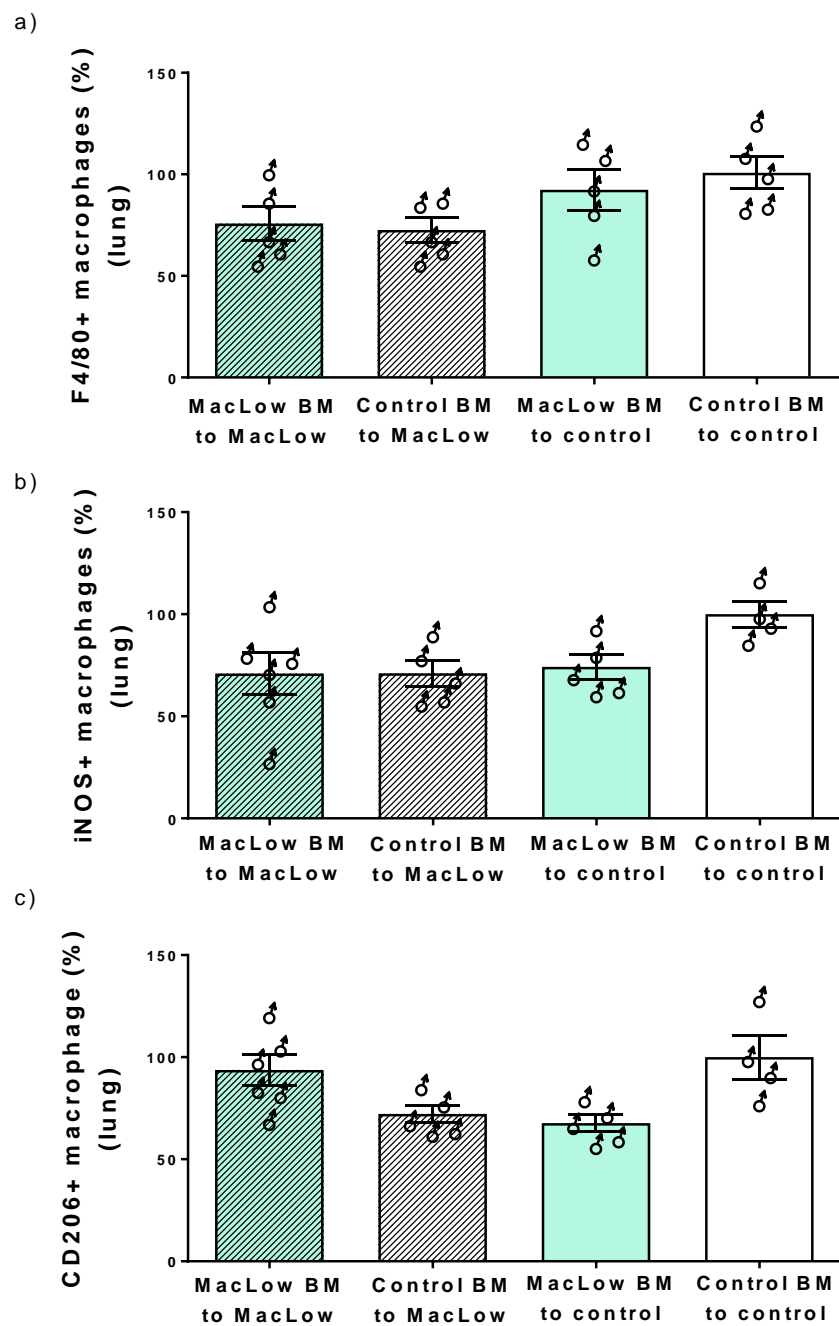
Figure 4.6- Analysis of macrophage subsets in lung sections: Quantification of the number of macrophage remaining within the lung of the chimeric mice following doxycycline treatment. Positively stained cells were counted in 6 fields of views/tissue at X20 magnification, data of each group were normalized to the negative control group (control BM to control recipient) BM= bone marrow. a) Quantification of total macrophage number using F4/80 antibody. b) Quantification of M1 macrophage subset using iNOS antibody. c) Quantification of M2 macrophage subset using CD206 antibody. Data analysed using a one- way ANOVA with Bonferroni post hoc test. Error bars represent mean ±SEM. n= 4-6/ group.

4.3.5 Analysis of circulating blood monocyte

As described in sections 2.1.7 and 2.5, blood was collected by cardiac puncture from each animal and pooled for each of the groups. Following density gradient centrifugation blood monocytes were isolated and stained with Alexa Fluor ® 488 conjugated anti-mouse CD115 antibodies. The number of blood monocyte in the MacLow recipients was about 30-40% less than control recipient group (figure 4.7) which is comparable with the reduction in liver macrophages (figure 4.2).
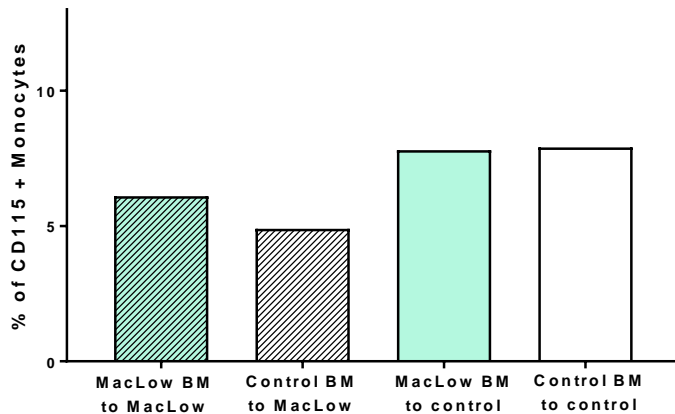
Figure 4.7- Flow cytometric analysis of circulating monocyte: graph represents the number of CD115+ cells obtained from one pooled blood sample for each group (5 mice/ group). Peripheral blood mononuclear cells (PBMC) isolated and stained with Alexa Fluor ® 488 anti-mouse CD115 then analysed by flow cytometry.

4.3.6 Investigating lung macrophage proliferation and IL-4 expression

To investigate whether lung macrophages are capable of self-renewal via proliferation independently of blood monocytes, dual immunofluorescent staining for F4/80 with a cell proliferation marker; proliferating cell nuclear antigen (PCNA)

was performed (refer to the protocol in section 2.2.5). 5µm thick paraffin lung sections from *MacLow* and control mice that have been treated with doxycycline for six weeks was used. Qualitative assessment of the microscopic images (figure 4.8) showed some double positive staining (arrowhead) of F4/80 positive cells (red) and PCNA positive staining (green) in *MacLow* lungs that was not found in the control lung. These positive signals suggest that the macrophages in diseased lung lesions have the capacity for proliferation to self-renew. However, whether this process was a consequence of the depletion and in order to maintain the homeostasis or a result of the disease is still undetermined.

The images also suggest some differences between the *MacLow* and control in term of PCNA co-localization within the cells. In *MacLow* lungs there was an unexpected cytoplasmic expression of PCNA, The PCNA has a well-known function in DNA replication and repair, hence its nuclear localization. However, recent research has also detected PCNA in the cytoplasm which suggests it also has a crosslinking function in term of cell cycle and apoptosis, also it has been shown that mature human neutrophils express PCNA exclusively within the cytosol (Witko-Sarsat et al., 2010, Ohayon et al., 2016)

Furthermore, it has been shown that the proliferation expansion of resident macrophages can be mediated by IL-4 signalling in parasitic infection (Jenkins et al., 2011, Jenkins et al., 2013). To determine whether expression of IL-4 is involved in *MacLow* model of PAH, IL-4 positive cells were counted in paraffin-fixed lung sections from diseased male *MacLow* and from controls. The results presented in the figure 4.9 showed no difference between the diseased and healthy lungs regarding their IL-4 signalling which suggests that the process of macrophage proliferation was unlikely to be mediated by IL-4 signalling.
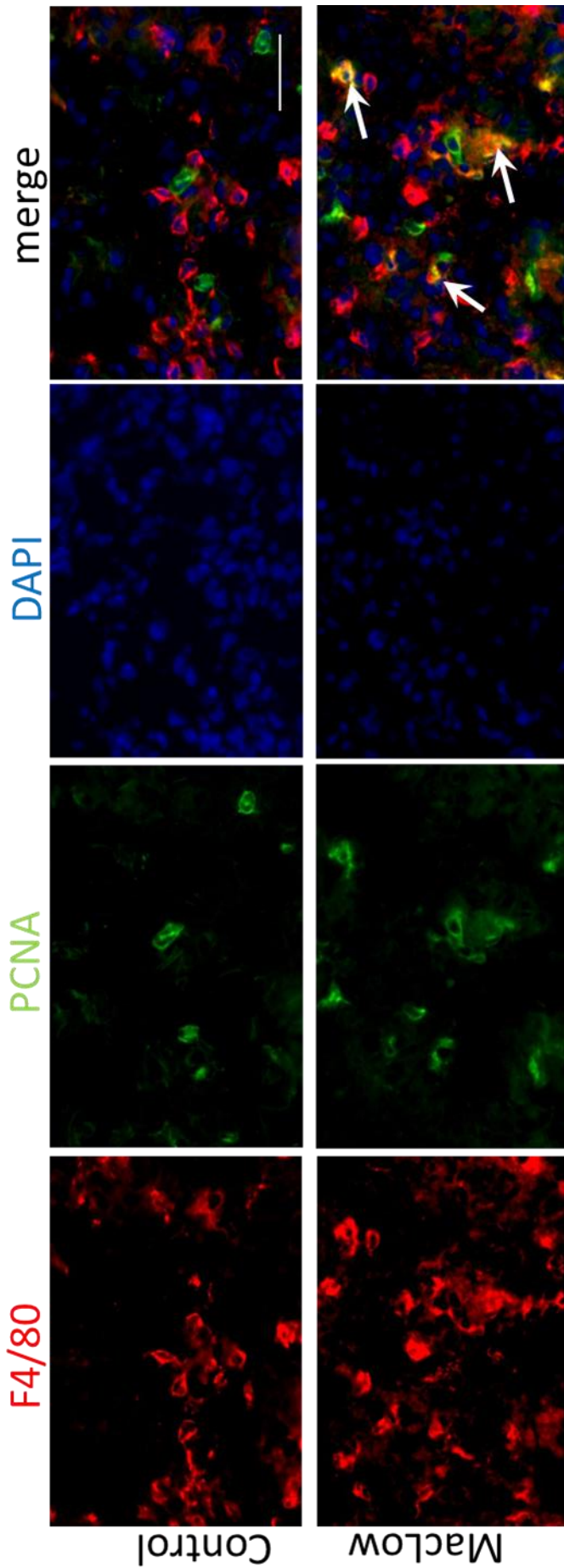
Figure 4.8- Double immunofluorescence staining of F4/80 and PCNA on lung sections: Control and MacLow male mice were treated with doxycycline for six weeks to induce PAH. Representative immunofluorescence image of frozen lung sections stained with anti- F4/80 (red) and PCNA (green) with cell nuclei labelled with DAPI (blue). Double-stained cell shown with the arrow-head. Scale bar=20 µm.

a)

b)
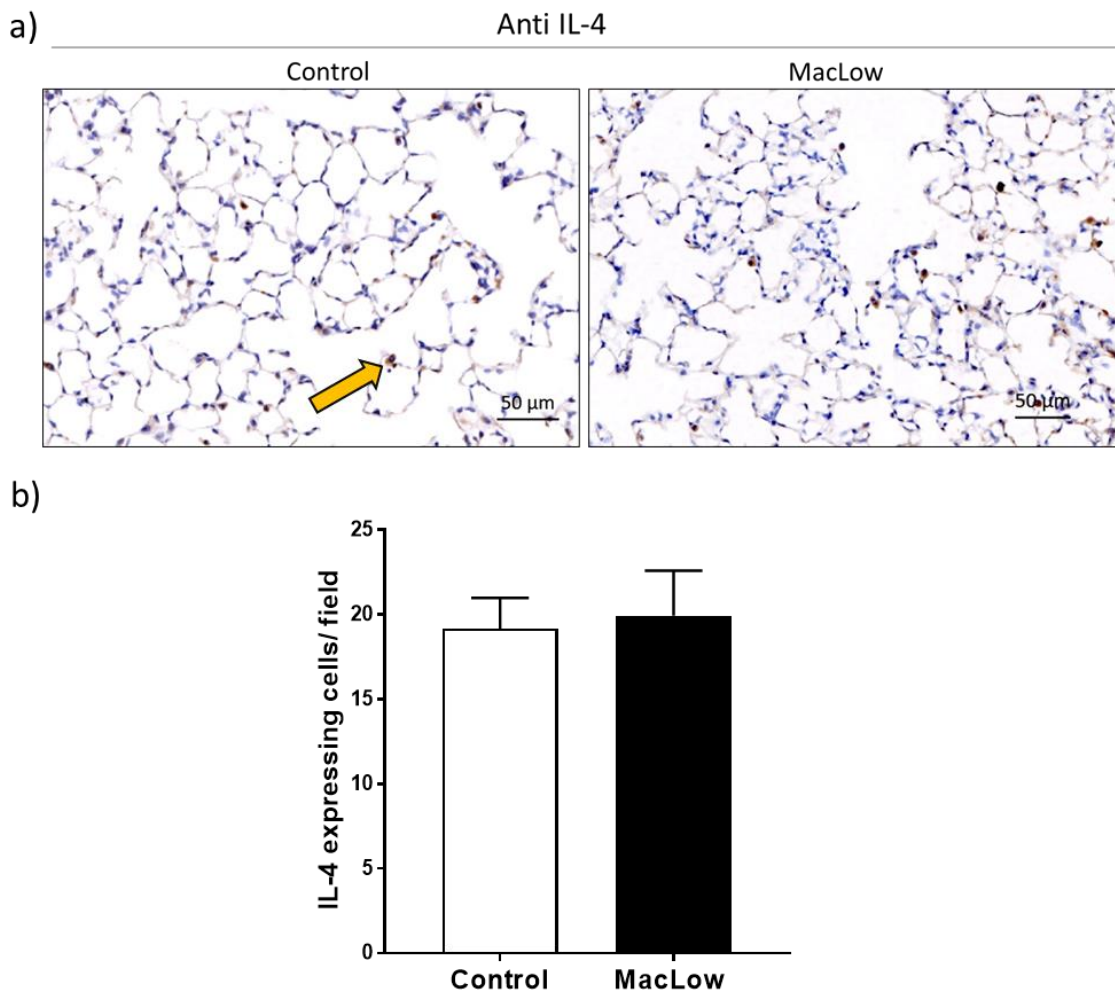
Figure 4.9- Expression of IL-4 within the lung: Control and *MacLow* male mice were treated with doxycycline for six weeks to induce PAH. a) Representative immunohistological staining of paraffin fixed lung sections using anti-IL-4 antibody (cells stained brown, arrow-heads). b) Quantification of IL-4 expressing cells in the lung sections from *MacLow* diseased male mice compared to controls. Sections were stained with anti-IL-4 antibody and the positively stained cells were counted in 8 fields of views/tissue at X20 magnification. n= 8/ group.

4.4 Discussion

In chapter 3, I demonstrated that a loss of macrophages causes a spontaneous PAH phenotype in male *MacLow* mice. However, it was unclear how the disease developed or what was the origin of the responsible cells. The work in this chapter aimed to assess the contribution of bone marrow progenitor cells to the

development of PAH in *MacLow* mice. It has been shown here using bone marrow transplantation that the lung resident macrophages, as well as bone marrow- derived cells, need to be depleted to induce the development of PAH.

Assessing the increase in pressure in the chimeric mice following six weeks of doxycycline treatment showed that transplanting *MacLow-* derived progenitors into control animals was not enough to induce disease development, this emphasised the importance of the resident cells in driving the disease phenotype over the recruited cells. It was also shown that *MacLow* recipient mice were still susceptible to macrophage depletion following doxycycline treatment regardless of the genotype of the donor cells. However, the level of macrophage depletion (particularly within the lungs) in the chimeric animals was not as high as in untransplanted *MacLow* animals in the previous chapter.

The low level of reduction in lung macrophages obtained following the BMT procedure could be due to the effect of irradiation on the lung. It is still not completely known what happens in the lung after irradiation but it has been shown that irradiation can destroy the local stem cells residing in the alveolar spaces thus the total count of alveolar macrophages can fall following irradiation (Tarling et al., 1987). It has been shown that a 30 day recovery period following TBI (using 9 Gy) is enough for the complete reconstitution of peripheral blood cells, however, only 47 % of the resident alveolar macrophages can repopulate in this period (Matute-Bello et al., 2004). However, it is important to also consider that different mouse strains respond differently to irradiation.

Furthermore, it has been observed that the disease phenotype developed by the male chimeric mice was less aggressive than that developed in male *MacLow*

mice as shown by their pressure reading and the unchanged RVH. This suggests a positive correlation between the loss of lung macrophage and the increase in RVESP in *MacLow* mice, but again the reason for this is still not known.

A study by Hayashida and colleagues described the role of BM-derived cells in hypoxia-induced PH using BMT strategy, the diseased chimeric mice showed a significant increase in their RVESP, RVH and vascular remodelling following hypoxia exposure, the histological analysis also reported the ability of BM-derived GFP labelled cells to travel to the pulmonary arteries of the hypoxic mice (Hayashida et al., 2005). As the hypoxia model is mainly an inflammation based model, they expected to see a marked increase in the level of recruited cells from the blood to the vascular lesion. In *MacLow*-induced PAH shown here, the disease developed as a result of the loss of tissue macrophages and it seemed that the factors driving the disease did not originate in the blood.

Another important observation from all of my studies using the *MacLow* mouse model is that the level of depletion observed in the lungs was always less than that seen in other organs (such as liver and spleen). To investigate whether the lung had some compensatory pathways to maintain homeostasis, dual immunofluorescent labelling using both anti-F4/80 antibodies (macrophage marker) along with anti-PCNA anti-bodies (proliferation marker) was performed. Interestingly, these experiments showed some double labelled cells only in *MacLow* lungs following macrophage depletion and not in any of the controls, this suggests that lung macrophages can self- renew via proliferation rather than recruitment from the blood. A study by (Hashimoto et al., 2013) also made it clear that monocytes do not contribute significantly to tissue macrophage repopulation in steady state using either the systemic administration of clodronate liposome or

the CD169-DTR mouse models of macrophage depletion (Hashimoto et al., 2013).

Finally, although IL-4 has been proposed to have a role in promoting mechanisms for local macrophage expansion following parasite infection (Jenkins et al., 2011, Jenkins et al., 2013), there was no increase in expression of IL-4 in *MacLow* lungs following depletion, this was consistent with the finding of (Hashimoto et al., 2013) who also could not detect an increase in expression of this cytokine within the lung after macrophage ablation.

In conclusion, the tracing strategy followed here pointed to the importance of lung resident macrophages in the development of PAH. Lung macrophages can be further divided into two subpopulations according to their localization i.e: alveolar macrophages and interstitial macrophages. The following chapter aims to pinpoint the compartment within the lung by studying these populations separately *in vitro* and investigating some mechanistic pathways that might be involved in the developing the disease using *in vitro* assays.

5   Characterization and polarization of *MacLow*-derived macrophages

5.1   Introduction

Tissue macrophages are a remarkably versatile and heterogeneous population of the immune cells, their heterogeneity and plasticity are important features to fulfil their tissue-specific functions. Within the lungs, at least two macrophage population are found, the alveolar macrophages (AMs) and the interstitial macrophages (IMs). Another population can also be recruited during inflammation referred to as recruited monocyte-derived macrophages (McCubbrey et al., 2016, Byrne et al., 2016).

Following from the previous chapters, this chapter utilized an *in vitro* culture system to understand the underlying mechanisms that might be responsible for the development of *MacLow*-induced PAH *in vivo*. To investigate whether *MacLow-* derived lung macrophages have unique characteristics relevant to their respective roles, a side-by side comparison study of *MacLow-* derived macrophages with macrophages from control mice was performed. For better understand of lung macrophage heterogeneity, cells were cultured either from bone marrow progenitor cells (bone marrow-derived macrophages) or derived from the broncho-alveolar lavage fluid BALF (alveolar macrophages). The comparison study mainly focused on the macrophage's morphology, polarization and differentiation in response to common stimuli, as well as their response to doxycycline.

In addition, leukotriene B4 (LTB4) has been shown as an important inflammatory mediator secreted by macrophages and has been implicated in PH pathogenicity (Wright et al., 1998, Tian et al., 2013, Qian et al., 2015). LTB4 biosynthesis is increased in pulmonary macrophages, the small pulmonary artery endothelial cells (Wright et al., 1998) and in the serum of patients with PAH (Tian et al., 2013). LTB4 is also shown increased in the BALF collected from experimental rats and its inhibition reverse PAH (Tian et al., 2013). Furthermore, it has been reported that LTB4 can induce apoptosis of pulmonary artery endothelial cells and proliferation of human smooth muscle cells (Tian et al., 2013). Thus expression of LTB4 in *MacLow-* derived macrophages was also examined.

5.2 Material and methods

5.2.1 Collection and culturing of mouse primary cells

All of the cells used were murine primary cells obtained from either *MacLow* or control mice. Bone marrow cells were harvested from the tibia and femur as described in section 2.1.9, then cultured for 7 days in M-csf containing media to promote differentiation into mature macrophages (BMDM) as described in 2.3.1.

Alveolar macrophages (AM) were obtained by collecting the broncho-alveolar lavage fluid (BALF) as described in 2.1.10.

BMDMs and the AMs were then stimulated with either LPS/ INFγ, IL-4 or doxycycline.

5.2.2 Detecting surface markers and protein expressions

Following culture and stimulation, cells were phenotyped using flow cytometry (refer to the protocol on section 2.5). Antibodies used were: APC anti-mouse

F4/80, FITC anti-mouse CD68, PE anti-mouse CD206 and Pacific blue anti-mouse CD86. Mature macrophages were defined as F4/80+ CD68+ cells; M1 macrophages as F4/80+ CD86+ cells, whereas M2 macrophages as F4/80+ CD206+ cells.

Expression of LTB4 was determined by detecting the expression of its biosynthesis enzyme the 5-lipoxygenase (5-LO) using IF/ICC (described in 2.6.2.). Cell viability analysis was performed using the ApoTox-Glo ^{TM} Triplex assay kit (Promega, Madison, USA) as previously detailed in section 2.6. Expression of Diphtheria Toxin A (DTA) was detected by using the dot blot technique as detailed in section 2.7.

5.2.3 Statistical analysis

All statistics were performed using GraphPad Prism version 7.2 (GraphPad software, SanDiego, California USA). Statistical comparison between the different groups was established by the use of one-way analysis of variance (ANOVA) followed by Bonferroni post- hoc analysis. Two-way ANOVA was used in the time-point experiments when more than one variable need to be compared. Values are presented as mean ± SEM, and differences of $P < 0.05$ values were taken as significant.

5.3 Results

5.3.1 Characterization of *MacLow* bone marrow derived macrophage (BMDM)

5.3.1.1 Induction of BMDM formation

In presence of M-CSF in the growth media, hematopoietic progenitor cells from the bone marrow were directed into a mature macrophage. Cells from *MacLow* and control mice were cultured in the growth medium for 7 days and the non-adherent cells (dendritic cells) discarded. On day 7, the formation of mature BMDM and analysis of the purity of the population were evaluated using fluorophore-conjugated antibodies to detect cells expressing F4/80 and CD68.

BMDMs were first gated on FSC and SSC to remove debris, then the non-treated macrophages (mature M) were defined as F4/80+ CD68+ subpopulation. The populations that resulted showed approximately 72-88% purity of the gated parent population (figure 5.2). The non-treated mature macrophages also showed some level of expression of CD86 (M1 marker) and CD206 (M2 marker).

Morphological evaluation of the resultant cells showed that the non-treated mature BMDM possessed round with slightly elongated morphology (figure 5.1). No growth, shape or size differences were seen between the *MacLow-* derived cells and the controls.
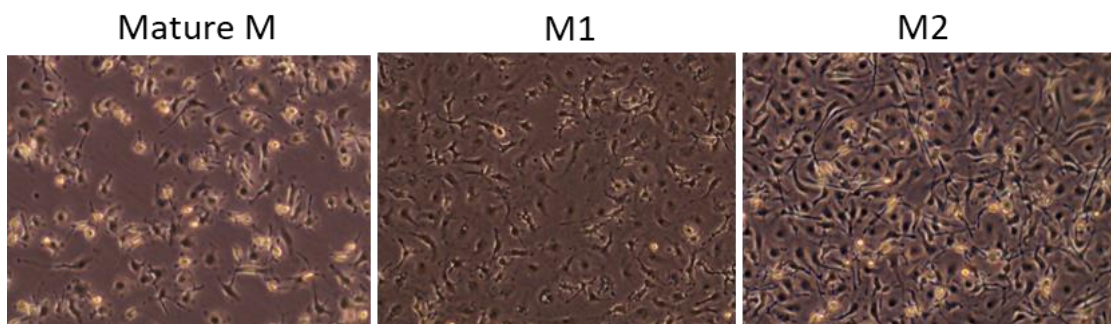
Figure 5.1- Morphological features of macrophage phenotypes: Morphological evaluation of the mature macrophages (Mature M) growing in culture media containing M-CSF at day 7. M1 macrophages resulted following stimulation with LPS/ IFNγ for 48hr and M2 macrophages following stimulation with IL-4 for 48hr. Images were taken at 20X magnification.

5.3.1.2 BMDM polarized activation

Stimulation of M1 macrophages was induced by LPS/ INFγ for 48hr, while activation of M2 macrophages was induced by IL-4 for the same time. The activated macrophages were identified by flow cytometric analysis for expression of surface antigens (M1 as F4/80+ CD86+ cells and M2 as F4/80+ CD206+ cells) as shown in figure 5.3.

The M1 population showed a similar level of co-expression of CD86+F4/80+ in the *MacLow*-derived BMDMs and controls (17.7 ± 5.047% and 16.9 ± 5.077% respectively). Similarly, in M2 population the co-expression of CD206+ F4/80+ was relatively identical and no significant differences detected (68.8 ±1.424% in *MacLow* macrophages vs 69.1 ± 2.073% in control macrophages).

Morphological evaluation of the resulted cells showed that the LPS/IFNγ stimulated cells displayed some rounded shapes as the non-treated. While the IL-4 stimulated cells had more pronounced elongation with the long protrusion (figure 5.1). These morphological features of the resulting cells are consistent with M1 and M2 morphology described in the literature, and again no differences in the size or shape of *MacLow* or control derived cells were detected.

Taken together, no significant differences were noticed between the *MacLow*-derived BMDMs and the controls in term of their polarization toward the M1 and the M2 following activation.
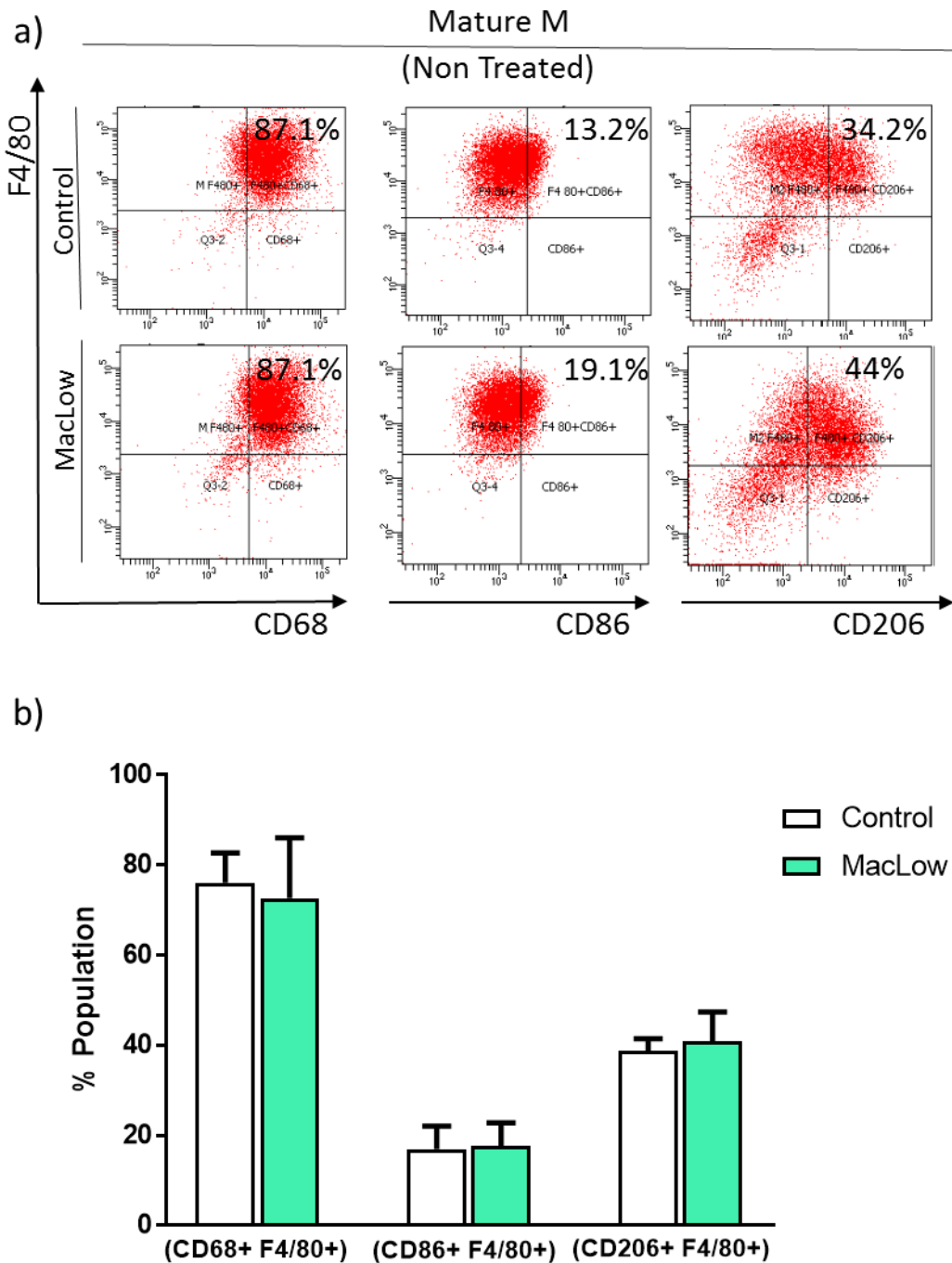
Figure 5.2- Characterization and polarization of mature *MacLow-* derived BMDM: a) Representative flow cytometry scatter plots of bone marrow-derived macrophages (BMDM) from *MacLow* and control following culture using anti- F4/80 versus: anti-CD68, anti-CD86 and anti-CD206. b) Summary data of flow cytometry results shown in (a) in each population before activation. Data analysed using a one-way ANOVA with Bonferroni post hoc test. Error bars represent mean ±SEM from 3 separate experiments.
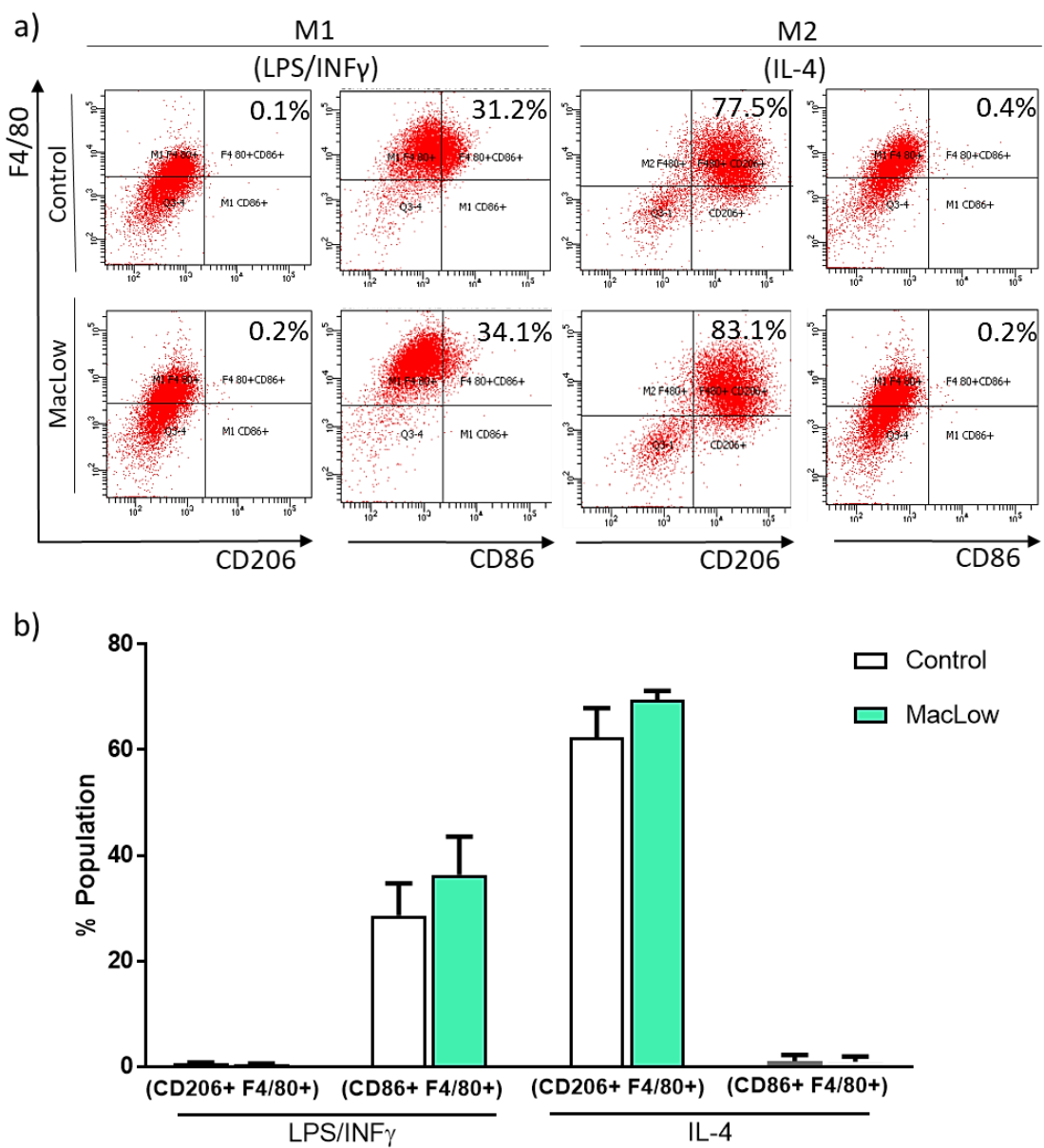
Figure 5.3- Characterization and polarization of activated *MacLow*- derived BMDM: a) Representative flow cytometry scatter plots of bone marrow-derived macrophages (BMDM) from *MacLow* and control following culture and stimulation using anti- F4/80 versus: anti-CD86 and anti-CD206 for both M1 and M2 macrophages. b) Summary data of flow cytometry results shown in (a) in each population upon activation. Data analysed using a one- way ANOVA with Bonferroni post hoc test. Error bars represent mean ±SEM from 3 separate experiments.

5.3.1.3 Characterization and polarization of *MacLow*-derived BMDMs following doxycycline treatment

To examine whether doxycycline can cause any other unique activation or skewing of macrophage phenotype, mature BMDMs were treated with different doses of doxycycline; 1, 5, 10 and 40 µg/ml for 48 hr (the same time required for full differentiation toward M1 and M2) then the expression of surface markers of M1 and M2 were investigated as previously shown.

Interestingly, *MacLow*-derived macrophages stimulated with low doses of doxycycline (1 and 5 µg/ml) seemed to induce the skewing toward the alternatively activated M2 subtype as shown by its relative high frequent expression of CD206+F4/80+ compared to control cells (figure 5.4). However, the difference was not significant between the *MacLow-* derived cells and the controls at any concentration. In the higher doses of doxycycline the expression was also relatively high but with no difference between the *MacLow* and control derived cells, this was probably as a result of the pharmacological/ toxicological effect of doxycycline on macrophages regardless of their phenotype. Thus for all the subsequent experiments, a dose of not more than 5 µg/ml of doxycycline will be used.

To confirm that the observed induction of CD206 level seen in *MacLow-* derived cells was a result of doxycycline, and whether the effect is reversible or not, mature BMDMs were first treated with 5 µg/ml of doxycycline for 48 hour, then the doxycycline removed the culture media and cell's phenotype was tested after 48 hour. The recovery samples showed that the effect was reversible as the expression of CD206 was largely inhibited (figure 5.4)

This suggesting that doxycycline can promote a shift or skew toward an M2-type macrophages cell type in *MacLow-* derived cells. This was also supported by the morphological assessment of doxycycline-treated cell as they were elongated and their morphology is highly resembling the M2 morphology (figure 5.5-a).

Further analysis of the data showed that despite that difference was not statistically significant comparing the stimulated *MacLow* BMDM and the controls at any of the concentrations. However, by comparing the level of expression of CD206 after doxycycline treatment with that caused by IL-4 stimulation, the level was highly comparable and the increase led to a loss the significance seen in the control cell between the doxycycline-treated cell (1µg/ml dose) and IL-4 treated cells. Where in the MacLow cells there was a significant increase in expression of CD206 in the doxycycline-treated cell (5µg/ml dose) compared to untreated cells (figure 5.5).

a)

b)
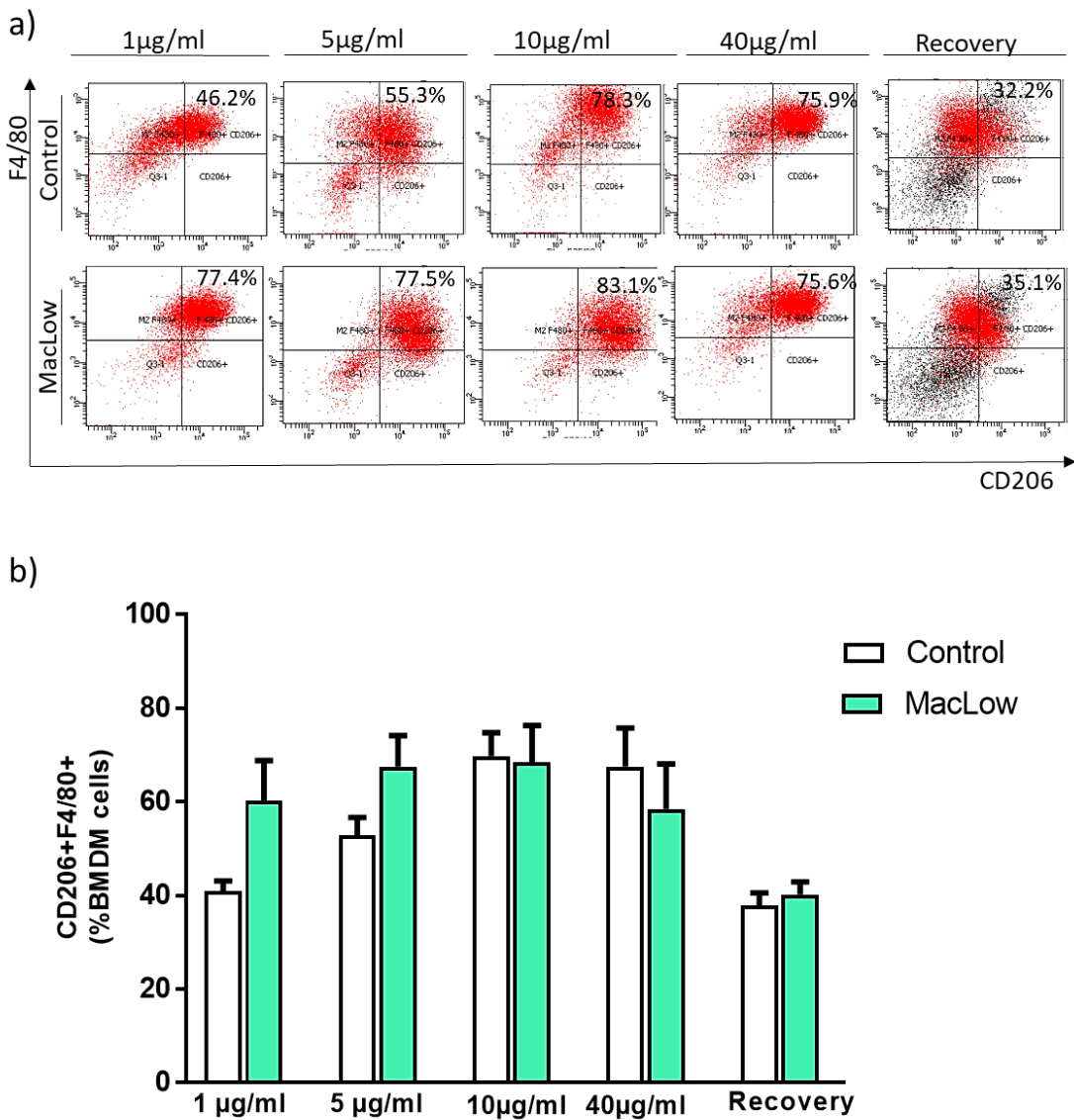
Figure 5.4- Characterization and polarization of *MacLow-* derived BMDM following doxycycline stimulation: a) Representative flow cytometry scatter plots of bone marrow-derived macrophages (BMDM) from *MacLow* and control following stimulation with different concentrations of doxycycline, and after removing doxycycline from the media (recovery), the scatter plot present anti- F4/80 versus anti-CD206 fluorophores. b) Bar graph summarize the flow cytometry results of doxycycline stimulation shown in (a), Data analysed using a one- way ANOVA with Bonferroni post hoc test. Error bars represent mean ±SEM from 3 independent experiments.

a)

Doxycycline treated cells

b)
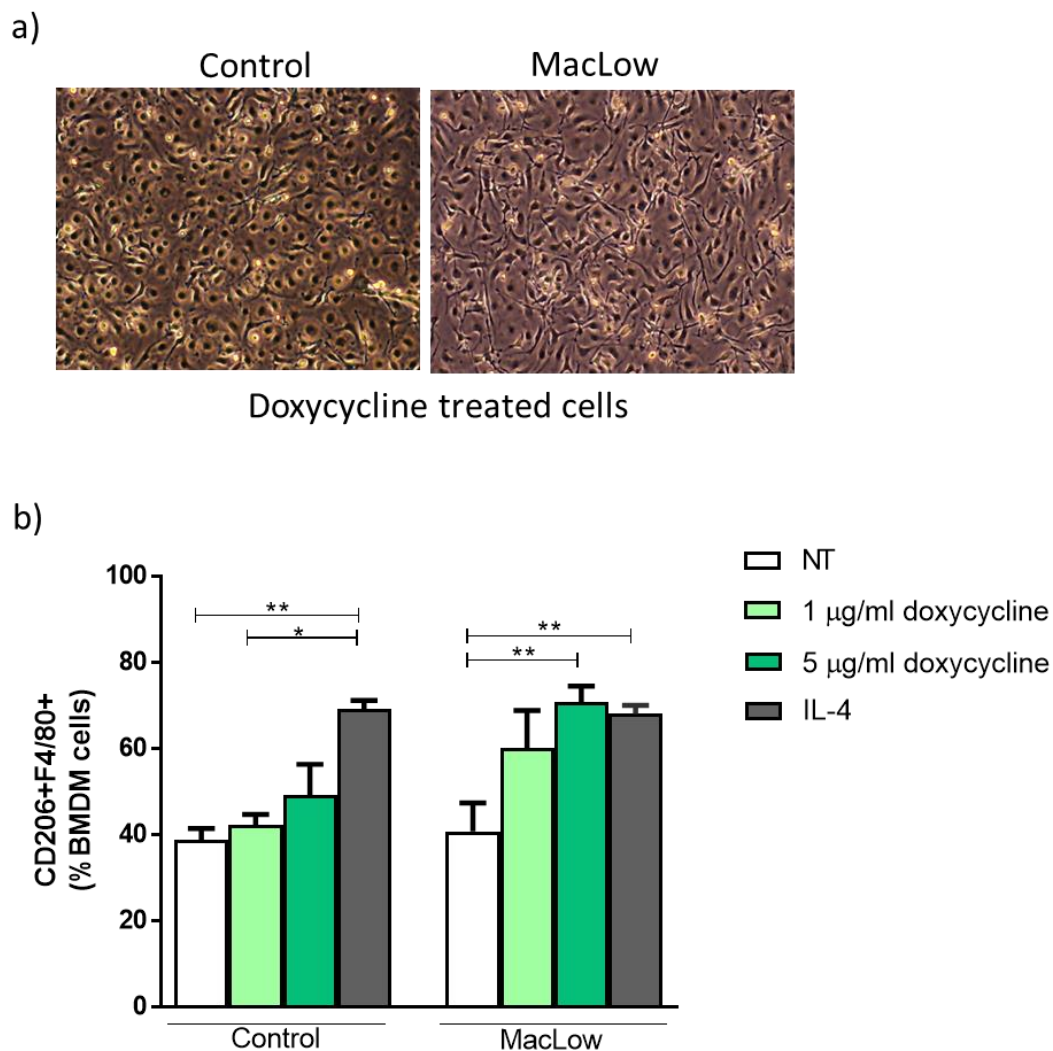
Figure 5.5- Skewing toward alternative activated macrophages: a) morphological feature of control and *MacLow-* derived BMDM following doxycycline treatment. b) Bar graph compare the expression of CD206+ F4/80+ of control and *MacLow-* derived BMDM after doxycycline and IL-4 treatment. Data analysed using a one-way ANOVA with Bonferroni post hoc test. Error bars represent mean ±SEM from 3 separate experiments.

5.3.1.4 Effect of doxycycline on BMDM cell viability

To examine the effect of doxycycline on cell death *in vitro*, cell viability analysis was performed using the ApoTox-Glo TM Triplex assay kit (Promega, Madison, USA) as previously detailed in section 2.6. This assay is a three in one technique that allows assessment of viability, cytotoxicity and caspase activation (a hallmark

of apoptosis) in a single assay. To assess cell viability in doxycycline-treated BMDM at the different time point, the live-cell protease activity was measured. The cell viability dropped significantly following 3 days of doxycycline treatment in *MacLow*-derived cells as well as the control cell. No significant differences were detected in cell viability between the *MacLow* and control derived cells at any of the time-point assessed (figure 5.6-a)

To assess the cytotoxicity of doxycycline, the dead-cell protease activity was measured. Again, the cell toxicity did not significantly change over time although there was a trend of increased cytotoxicity in *MacLow-* derived cells within the first three days after doxycycline treatment compared to control cells (figure 5.6-b). Ideally, viability and cytotoxicity are inversely correlated, however, it could be that the actual changes in cell membrane integrity had not occurred yet and this period will manifest as a decline in viability with no concomitant increase in the cytotoxic biomarker. Finally, to determine whether the cell death occurs via apoptosis, caspase 3/7 activity was measured. The results do not show clear changes in the caspase activity in the *MacLow* and control derived BMDM following doxycycline treatment (figure 5.6-c), this suggests that it is unlikely that the cell died by apoptosis.

a)

b)

c)
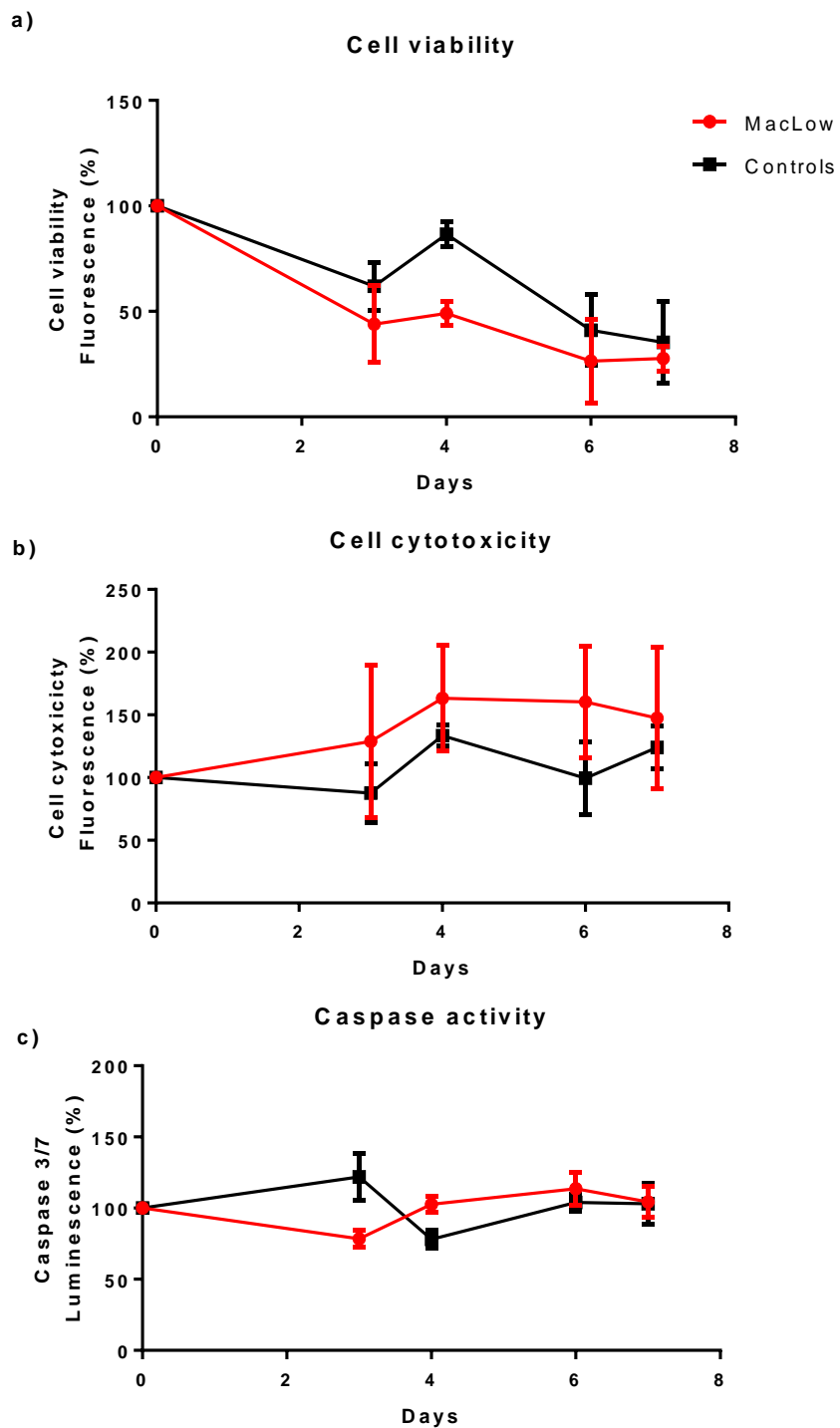
Figure 5.6- Effect of doxycycline on BMDM cell viability: Mature BMDM derived from *MacLow* and control mice were treated with doxycycline (5µg/ml) then cell viability (a), cytotoxicity (b) and caspase activity (c) assessed using the ApoTox-Glo ™ Triplex assay kit. Data presented as mean ± SEM collected from 3 independent experiment. Analysis performed using two-way ANOVA.

Collectively, this experiment showed that doxycycline can induce cell death *in vitro* to some extent and most likely via necrosis, however it was not clear whether this was due to the cytotoxic effect of doxycycline as a substance rather than as a gene inducer as the difference between the *MacLow* and control cells was not as pronounced as *in vivo*.

5.3.2 Characterization of *MacLow*-derived alveolar macrophages (AM)

BALF from *MacLow* and control mice were seeded in 24-well cell culture dishes to enable adherence of macrophages for at least 2 hours. The non-adherent cells were then discarded and the macrophages scraped to be characterized by flow cytometry based on their expression of surface markers.

The resulting preparation showed that over 80% of the cells obtained were F4/80+ thereby identifying them as macrophages (figure 5.7). However, in contrast to the BMDM, the expression of CD68 was not clear and potent using the same protocol and the same antibody. It could be that the auto-fluorescent feature of macrophages interferes with the detection, however, this could give just a sight overestimation or underestimation of the reading.

Although the expression of CD68 was low no difference was detected between the *MacLow* and control derived cells as well as the F4/80 expression. Since the *MacLow* system uses the human CD68 as promoter for the DTA expression, it is possible that the AMs are more resistant to the model if they express less CD68. Because of this, it was essential to investigate the effect of doxycycline on AM *in vitro* and identify whether AM and BMDM respond similarly or to a different extent in term of polarized activation and viability.

5.3.2.1 Characterization and polarization of *MacLow-* derived alveolar macrophages (AM)

To further evaluate the effect of doxycycline on AMs polarization, the adherent AMs were treated with doxycycline (1 and 5 µg/ml) for 48 hours, then the cells scraped to be characterized by flow cytometry based on their expression of surface markers for M1 and M2 polarization.

Following doxycycline treatment, macrophages from either *MacLow* or control exhibited no differences in expression of M1 marker CD86 or the M2 marker CD206, with 4.667 ± 0.938 and 14.03 ± 2.079 respectively in *MacLow-* derived cells, compared with 4.5 ± 0.5 and 15.67 ± 3.49 respectively in the control derived cells (figure 5.7). Also, no difference was detected between the two doses of doxycycline tested (data not shown).

Moreover, to examine the effect of doxycycline on AMs following *in vivo* treatment, age- matched male *MacLow* and control mice were fed with doxycycline containing diet for 2 weeks to induce 50% loss of macrophage (Gheryani et al., 2013), then BALF was collected for cytospin preparation (see section 2.1.10). Liver and lung were also harvested to confirm the loss of macrophage and the expression of DTA within the tissues (will be shown later in this chapter). Qualitative assessment of the cytospin slides showed that the number of AMs (the large mono-nuclear cell) was highly comparable between the *MacLow* and the control mice following doxycycline treatment (figure 5.8), also that the *MacLow* BALF preparation includes other inflammatory cells such as neutrophil (the multi-nucleated cells) and lymphocyte (large dark-staining nucleus) compared to the control preparation. It is appreciated that the

percentage yield of AMs from the BALF is highly dependent on the efficiency of the BALF collection technique, but this was taken into consideration when harvesting the cells and the same number of washes were performed from all mice harvested. These findings strongly suggest that the alveolar macrophages were resistant or affected to lesser degree by the doxycycline- induced depletion than other tissue macrophages.
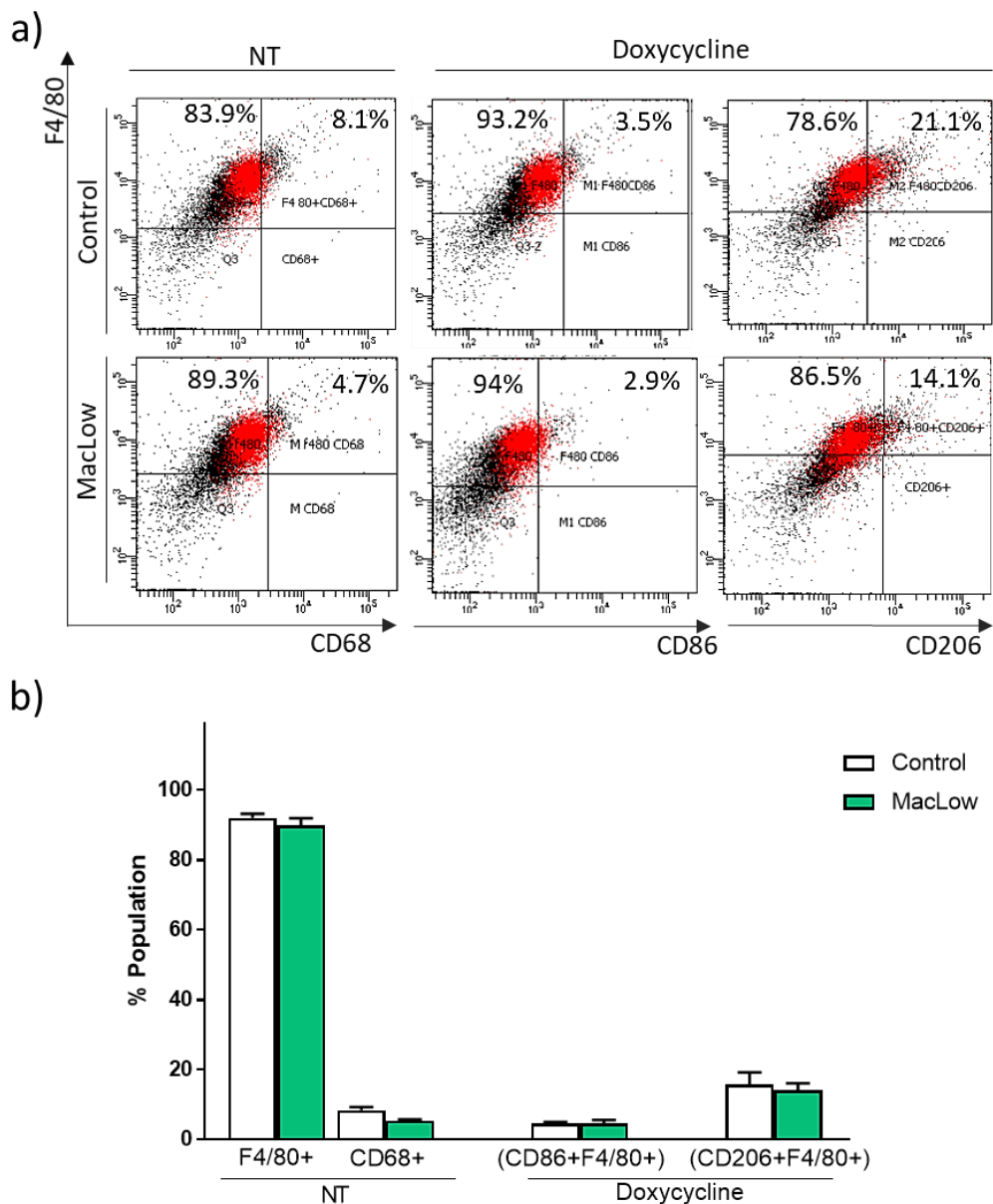
Figure 5.7- Characterization and polarization of *MacLow-* derived AM: Representative flow cytometry scatter plots of alveolar macrophages (AM) following culture and stimulation using anti- F4/80 versus anti-CD68 (for non-treated), and anti-CD206 (for doxycycline-treated). Data analysed using a one- way ANOVA with Bonferroni post hoc test. Error bars represent mean ±SEM.

Control

Macrophages

50 μm

MacLow

Macrophages

Neutrophil

Lymphocyte

50 μm
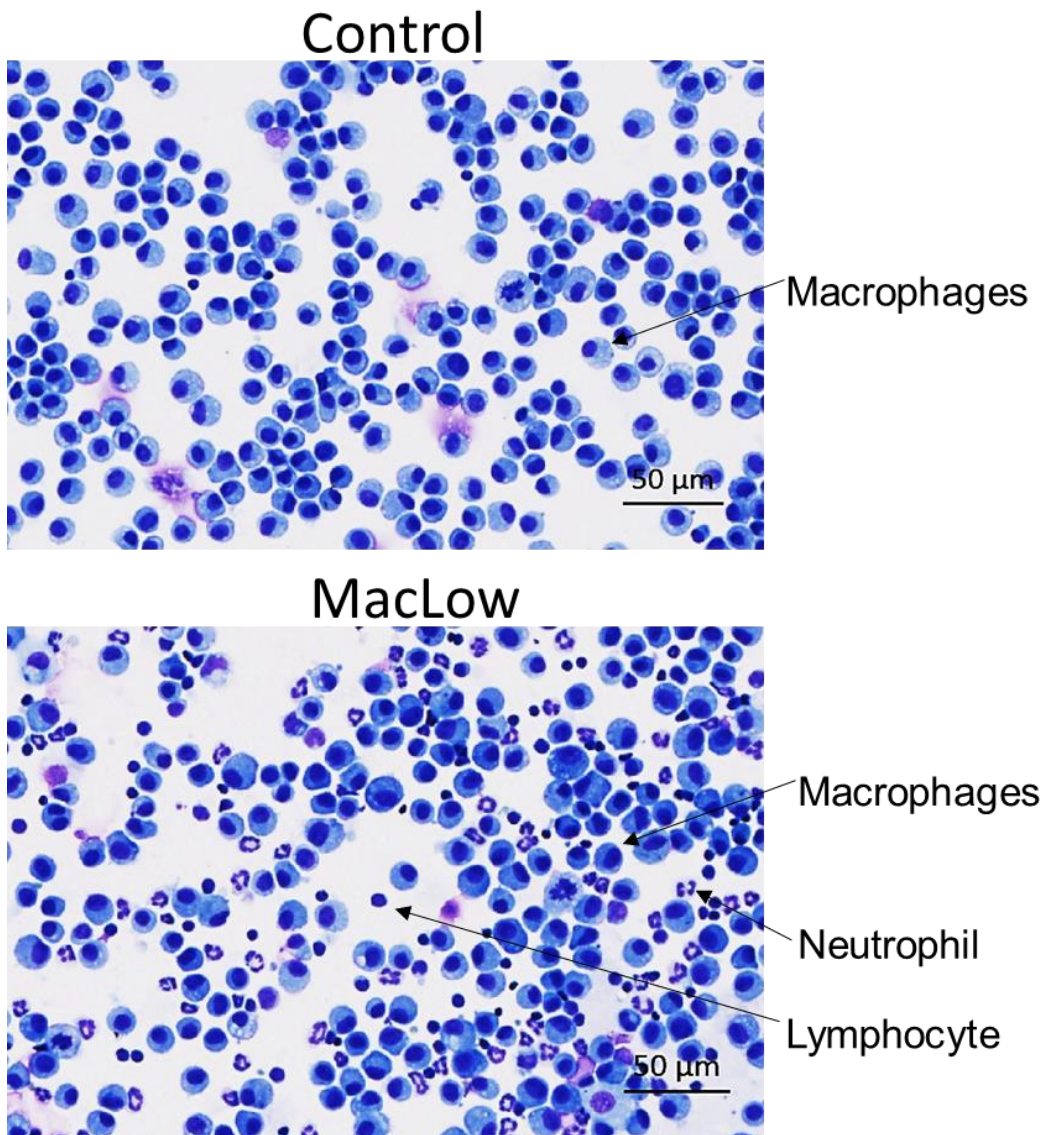
Figure 5.8- BALF cytospin: Cytospin preparation of BALF from control and *MacLow* mice following 2 weeks doxycycline treatment *in vivo*. Magnification X20.

5.3.2.2 Effect of doxycycline on alveolar macrophages viability

To examine the effect of doxycycline on AM cell death *in vitro*, cell viability analysis was performed using the ApoTox-Glo ™ Triplex assay kit as previously detailed. Cultured AM from *MacLow* and control mice were treated with doxycycline *in vitro* and the cell viability, cytotoxicity and caspase activity was

measured. The cell viability of both *MacLow* and control derived AMs dropped following three days of doxycycline treatment. However, the drop was highly comparable for both control and *MacLow* over the whole 7 days of the experiment and no significant differences recorded (figure 5.9). On the other hand, the cytotoxicity profile showed a slight increase within the first three days followed by the steady-state curve for both MacLow and control cells with no statistically significant difference between the *MacLow* and control cells at any time point. Again no clear time-dependent caspase activation detected which suggest that apoptosis not involved in the process of cell death.
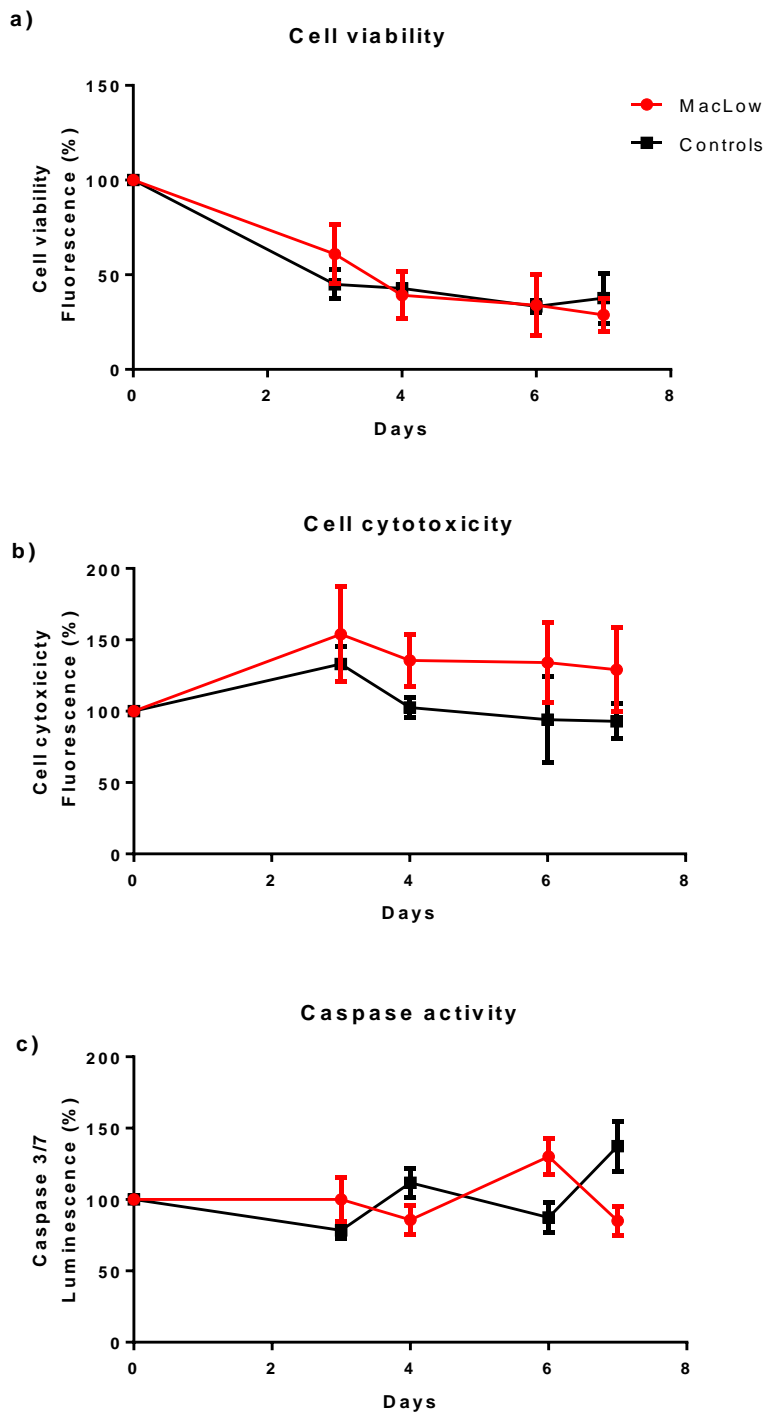
Figure 5.9- Effect of doxycycline on AM cell viability: Cultured AMs derived from *MacLow* and control mice were treated with doxycycline (5µg/ml) then cell viability (a), cytotoxicity (b) and caspase activity (c) were assessed using the ApoTox-Glo ™ Triplex assay kit. Data analysed by two-way ANOVA and presented as mean ± SEM collected from 3 independent experiment.

5.3.3 Expression of Diphtheria toxin A chain (DTA)

The *MacLow* mouse model utilized the Tet-on system for gene expression, whereby doxycycline can switch-on the expression of DTA protein leading to cell death, to determine whether DTA is detectable *in vitro*, dot blot technique was used (see section 2.7). Mature BMDM and cultured AMs from *MacLow* mice were either treated with doxycycline (5 µg/ml) or left with no stimulation for 48 hr. Cells were then processed for protein extraction and transferred onto a nitrocellulose membrane and stained with anti-DTA antibody. Liver tissue harvested from *MacLow* mouse that had been treated with doxycycline for two weeks was used as a positive control. The expression of DTA was confirmed on the liver sample, and by comparing the BMDM and the AMs the blot showed that the expression of DTA in the AMs is less than that of BMDMs following doxycycline treatment *in vitro* (figure 5.10). This finding further suggests that alveolar macrophages have a unique character and respond to the *MacLow* depletion system differently from other tissue macrophages.
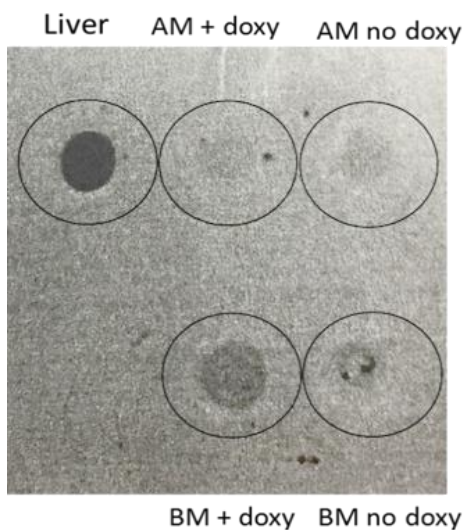
Figure 5.10- expression of diphtheria toxin A in *MacLow*- derived macrophages: Cultured AMs and mature BMDM derived from *MacLow* and mice were treated with doxycycline (5µg/ml) then the expression of DTA was assessed using dot blot technique. Image show nitrocellulose membrane visualized by the LI-COR ® reader using the proper channels.

5.3.4 Investigating 5-LO/ LTB4 signalling

In macrophages, LTB4 is synthesized from arachidonic acid (AA) by the action of 5-Lipoxygenase (5-LO) enzyme. Leukotriene A4 (LTA4) is produced which is then quickly hydrolysed to LTB4 by leukotriene A4 hydrolase (LTA4H) (figure 5.11-a). 5-LO phosphorylation by p38 mitogen-activated protein kinase (MAPK) increases its enzymatic activity *in vitro* (Werz et al., 2000, Werz et al., 2002). LTB4 is shown to be overproduced by macrophages in PH (Tian et al., 2013).

To investigate whether the biosynthesis of LTB4 in either BMDM or AM can be affected following doxycycline treatment i*n vitro*, AM from BALF and BMDM from *MacLow* and control mice were cultured as previously described, then stimulated with 5µg/ml doxycycline for 48 hours. The cells were then fixed and immunofluorescent staining was performed using anti-5LO antibody (section 2.6.2). Immunofluorescence analysis of 5-LO nuclear fluorescent intensity showed a significant increase in nuclear expression in *MacLow*-derived AM compared to control following doxycycline stimulation (figure 5.11). Conversely, 5-LO nuclear fluorescence intensity was significantly lost in BMDM derived from *MacLow* compared to control BMDM following doxycycline treatment.

a)

b)

c)

d)
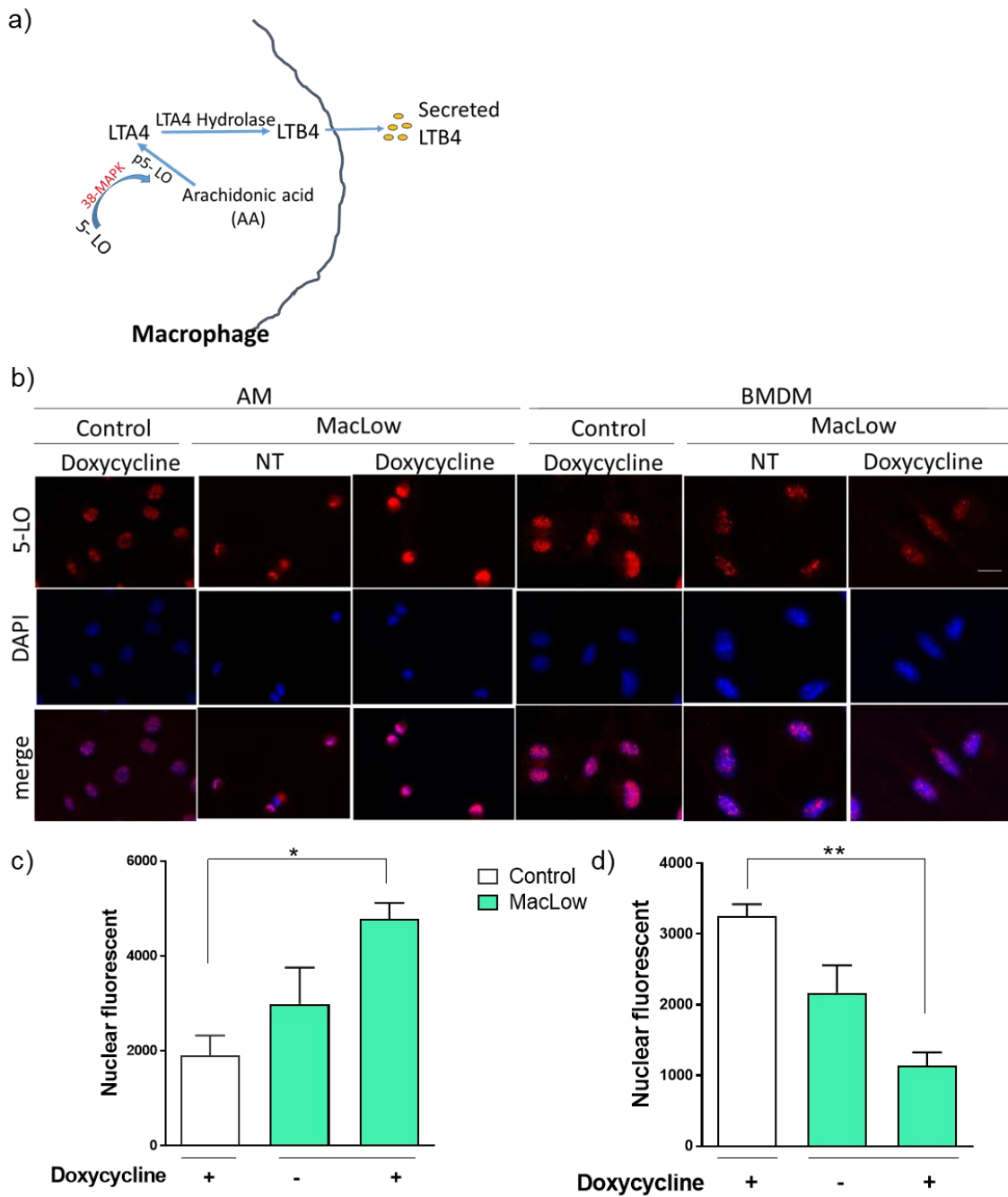
Figure 5.11- 5-Lipoxygenase /Leukotriene B4 signalling: a) Schematic of LTB4 production and secretion by macrophages. b) Representative immunofluorescence images of alveolar macrophages (AM) and bone marrow-derived macrophages (BMDM) stained with 5-LO (red) with nuclei labelled with DAPI (blue), cells derived from either *MacLow* or control mice. c,d) Quantification graphs show the corrected total nuclear fluorescence of AM (c) and BMDM (d) corrected to the background. Images were analysed using FiJi software. Data analysed using a one- way ANOVA with Bonferroni post hoc test. Error bars represent mean ±SEM Bar graph represent mean ±SEM from 3 independent experiment. *P <0.05, **P<0.005.

5.4 Discussion

Data presented in this chapter further highlights the heterogeneity and complexity of the lung macrophage population based on their origin and compartment. I showed here using an *in vitro* culture system that different lung macrophages have unique characteristics in term of cell viability, polarization, expression of DTA and expression of LTB4 following the addition of doxycycline. As the *MacLow*-BMDM showed a change in their phenotype toward the alternative activation state following doxycycline stimulation *in vitro*, while the *MacLow*-derived AMs showed less expression of DTA and therefore may be more resistant to killing following the addition of doxycycline.

Various studies in animal models suggested a key role for lung macrophages in the pathogenesis of PAH, moreover, activation of AMs was highly associated with hypoxia-induced PH (Hayashida et al., 2005, Frid et al., 2006, Vergadi et al., 2011) and depletion of AMs appears to attenuate hypoxic-PH (Zaloudikova et al., 2016). However, the mechanism characterizing the functional phenotype relative to lung localization remains largely unclear.

In hypoxia-induced PH, a recent study has shown that AMs and IMs share a conserved pro-inflammatory programming at 4 days of hypoxic exposure, after which a contrasting phenotype appears by day 14 as the AMs promote their pro-inflammation function, whereas the IMs demonstrated a unique anti-inflammatory programming state (Pugliese et al., 2017).

A study by (McCubbrey et al., 2016) used hCD68rtTA-GFP reporter mouse model for inducible targeting of CD11b^{+} lung macrophages to demonstrated that negligible activation occurs in AMs compared to IMs, they showed that

administration of doxycycline-induced tet-on reporter expression in the recruited and tissue macrophages but not in AMs during inflammation and homeostasis.

The mechanism by which the macrophage inducing system fails to target AMs is not completely clear. However, our data demonstrated an AM phenotype with low expression of CD68 which is the promoter in the tet-on system used in both our *MacLow* model and the model used by McCubbrey et al. Another possibility is that doxycycline cannot access the alveolar spaces, although other studies showed that doxycycline as an antibiotic can be internalised by the AMs (Klimeš et al., 1999). An alternative possibility is that AMs produce yet unknown factor/ factors which are capable of interfering with doxycycline function. Further exploration of this will defiantly be required to fully address the underlying mechanisms.

To isolate distinct lung macrophage population, BALF collection followed by lung digest and cell sorting with flow cytometry is highly recommended, as macrophages and monocyte can be separated into two compartments according to their marker expression: AM (CD64$^+$,CD11c^{hi}, CD11b^{lo}) and IMs (CD64$^+$, CD11c^{lo}, CD11b^{hi}), then further comprehensive analysis of each subset can be performed.

Analysis of BMDM polarization showed an interesting skewing toward the alternatively activated macrophage subtype (M2) following doxycycline stimulation, this was also seen *in vivo* with the *MacLo*w- induced PAH as it was associated with activation of M2 macrophages. Macrophages can sense and respond to the surrounding condition and can alter their phenotype to meet the specific needs of the circumstances, it could be that the induced macrophage

depletion with doxycycline has led to this alternative activation of macrophages, as it has been shown that the presence of cell debris leads to potent polarization of alternatively activated macrophages in the case of pulmonary infection (Mares et al., 2011).

Leukotriene B4 (LTB4) is well recognised for its significant role in clinical PAH, investigating the biosynthesis of LTB4 in *MacLow*-derived macrophages revealed that doxycycline-treated AMs express higher levels compared to control AMs, while the doxycycline treated BMDM express less level than that of control cells following doxycycline treatment. These findings give promising information regarding the importance of LTB4 pathway in the development of the sex-specific *MacLow-* induced PAH, especially since recent data has further demonstrated sex differences in levels of leukotriene (Pace et al., 2017).

Collectively, based on these findings*,* the *MacLow* system can be proposed as a novel powerful tool that can be utilized for lineage tracing and fate mapping to individually target distinct lung macrophage population, the system can be used to sort out the relative contribution of AMs and IMs in PAH associated remodelling, by deleting only one of the subtypes (figure 5.12).

The development of effective therapeutic targets for PAH needs to consider and fully understand the different aspect of macrophage activation as they could have opposing roles during the development of the disease. A better understanding of relative contribution from IMs and AMs in the initiation and maintenance of vascular remodelling may facilitate the reprogramming or the skewing toward the reparative phenotype of macrophage to attenuate the vascular remodelling.
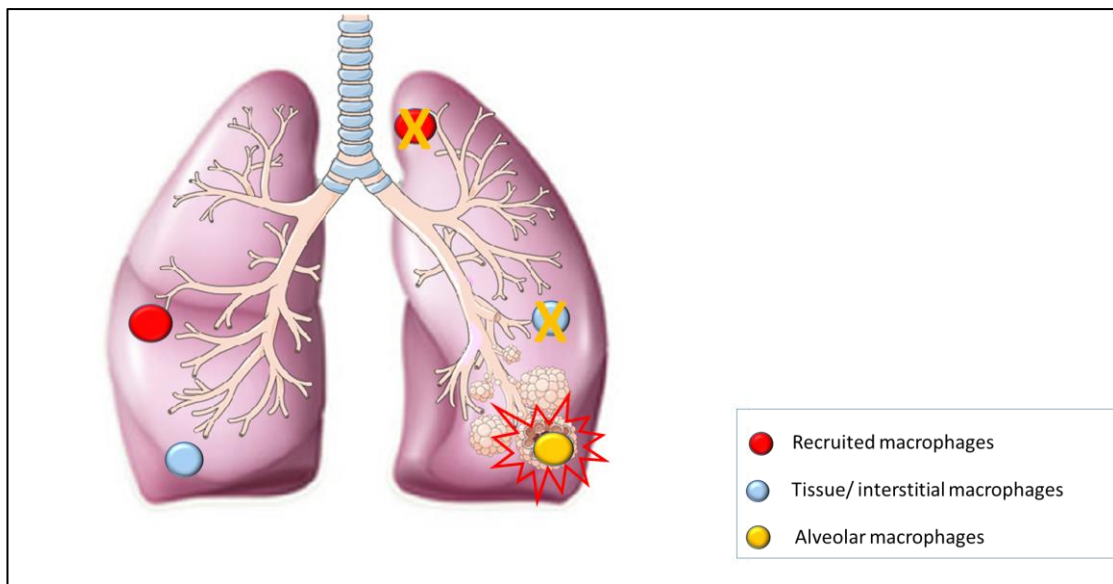
Figure 5.12- proposed model of *MacLow*-induced depletion of lung macrophages: *MacLow* model of induced macrophage depletion targets tissue and the recruited macrophages while leaving the alveolar macrophages less- or un-affected. This could potentially lead to compartment-specific activation of the alveolar macrophages.

6 Sex bias in *MacLow* induced pulmonary arterial hypertension model

6.1 Introduction

As shown in the previous chapters, loss of CD68+ macrophages in *MacLow* mice induced PAH development in male and not female mice (chapter 3), and that the lung resident macrophages, as well as bone marrow- derived cells, need to be depleted to induce the development of PAH (chapter 4), and among the lung resident macrophages each subtype showed unique phenotype when inducing the depletion *in vitro* with doxycycline, this suggested a compartment-specific activation of the alveolar subtype following the loss of the interstitial subtype (chapter 5). This current chapter investigated in depth the implication of sex difference on the development of *MacLow-* induced PAH and how this impacts on disease development.

In patients, PAH develops more predominantly in women than men with a 4.3:1 female to male ratio among the total PAH group (Walker et al., 2006), and 4.1:1 in idiopathic PAH subcategory (Badesch et al., 2010). However, men showed poorer survival and women fare better (Badesch et al., 2010, Shapiro et al., 2012). This is suggested to be in part due to the protective action of sex hormones mainly oestrogen (E2) since ovariectomy exacerbates PH and E2 pre-treatment attenuate its progression in the animal models (Farhat et al., 1993, Tofovic et al., 2006).

The aim of this chapter was to characterize the possible phenotypic differences of macrophages taken from male and female in *MacLow* model *in vivo*, using the bone marrow transplant and generation of mixed-sex chimeras. The main question that will be addressed is whether or not male-derived bone marrow cells can induce disease in female *MacLow* mice.

In addition, an attempt to look at the potential protective effect of oestrogen will be presented at the end of the chapter, however, some problems with the mouse colony occurred that hindered completion of the study.

6.2 Material and method

6.2.1 Generation of mixed-sex *MacLow* chimeric mice and induction of PAH

Mixed-sex chimeric mice were generated by the process of BMT, the procedure was performed using the optimized protocol is detailed in section 2.1.3. In brief, age-matched male and female *MacLow* mice (8-10 weeks) were used as recipients to generate the chimeras described in the table (6.1), recipients were irradiated with 10 Gy in one shot and engrafted with around 5×10^6 bone marrow cells. All the donor cells were taken from *MacLow* male/ female donor. Male donor BM cells were transplanted into the pre-irradiated female recipient and vice versa (female into male). In addition, two groups received a graft from identical sex of male-derived BM into male mice and female BM into female mice as positive and negative control groups respectively (figure 6.1-a). Mice were left to recover for at least 30 days after the transplant then PAH was induced by doxycycline treatment (doxycycline containing diet) to induce macrophage depletion for another six weeks with no other insult.

Table 6.1. Mixed-sex *MacLow* chimeras generated from bone marrow transplantation for the PAH study

Chimera	Donor	Recipient (n)
1 (positive control)	Male	Male (8)
2	Male	Female (5)
3	Female	Male (5)
4 (negative control)	Female	Female (5)

6.2.2 Echocardiography and cardiac catheterization

Following six weeks of doxycycline treatment, non-invasive assessment of the disease was performed using echocardiography under anaesthesia as described in section 2.1.4. Then the closed chest cardiac catheterization was used to take the pressure-volume measurements from both sides of the heart as described in section 2.1.5.

6.2.3 Histological analysis

Tissues were harvested, fixed, processed and stained according to the standard laboratory procedure described in sections 2.1.6 and 2.2.

6.2.4 Statistical analysis

All statistics were performed using GraphPad Prism version 7.2 (GraphPad software, SanDiego, California USA). Statistical comparison between the different groups was established by the use of one- way analysis of variance (ANOVA) followed by Bonferroni post- hoc analysis. Values are presented as mean ± SEM, and differences of $P < 0.05$ values were taken as significant.

6.3 Results

6.3.1 Macrophage depletion in the chimeric mice

It has been confirmed in chapter 4 that *MacLow* chimeric mice were susceptible to macrophage depletion following doxycycline treatment (although higher depletion was detected within the liver than that within the lungs). In the current study, all the recipient mice were *MacLow* mice so they were all expected to get the same level of reduction. To confirm this, 5 µm sections of paraffin-embedded liver were stained with anti-F4/80 antibody as previously shown (see section 2.2.3 and 2.2.3), then the positively stained cells were counted in 6 fields of view and presented as the number of F4/80 positive cells per field. The results showed no statistical difference between male and female groups in term of F4/80+ macrophages remained within the liver following doxycycline treatment (figure 6.1)

In addition, all mice experienced some weight loss during the first week after the BMT procedure, then they regained this weight back gradually. No significant differences were detected at any point, however, the male recipient transplanted with male graft (positive controls) showed slower recovery to retrieve their start weight (figure 6.1-b).
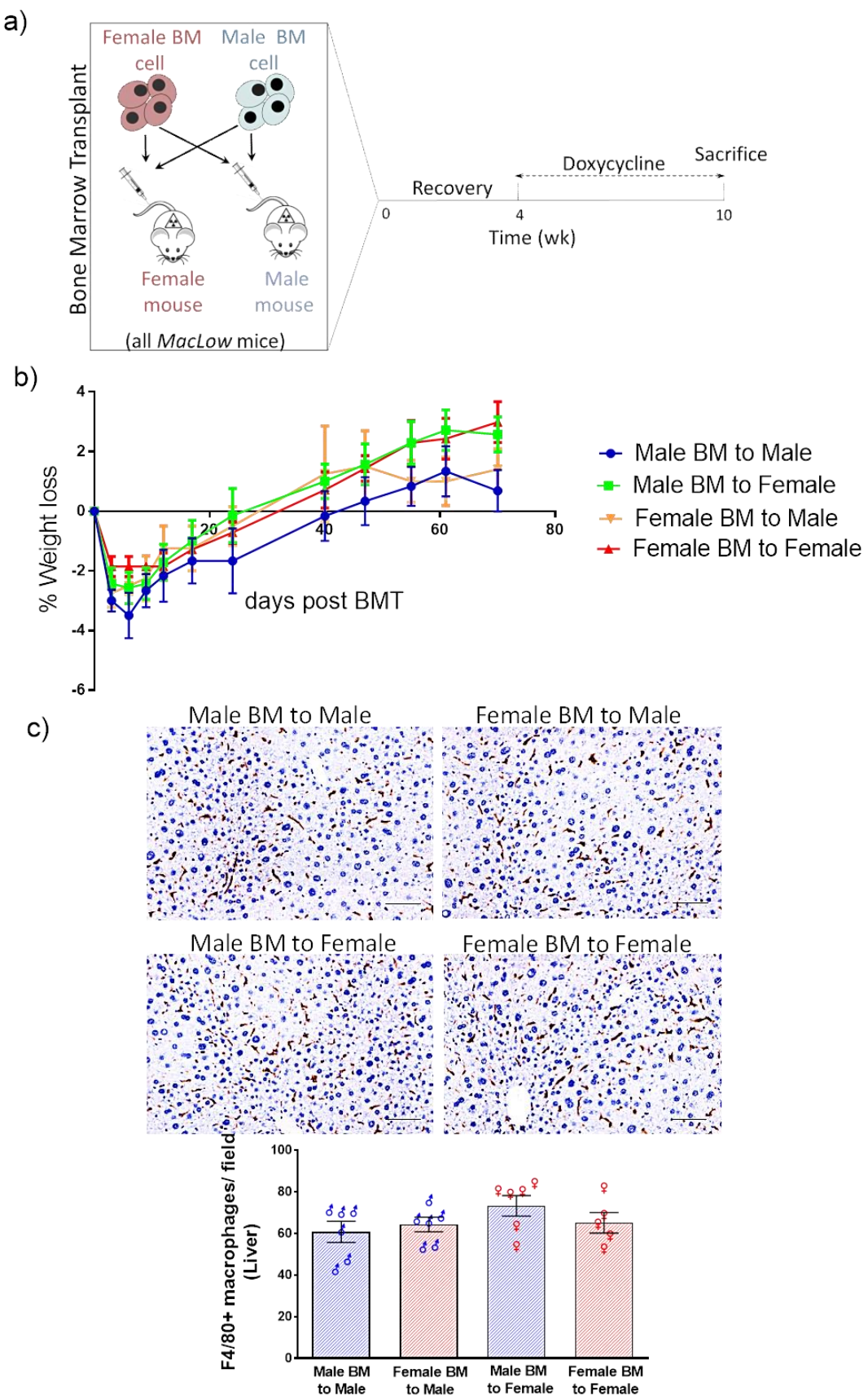
Figure 6.1- macrophages depletion in the liver after doxycycline treatment: a) schematic of study design displaying the bone marrow transplant procedure followed by 4 weeks recovery period before starting doxycycline treatment, the disease assessed at the end-point by echocardiography and cardiac catheterization. BM= bone marrow. b) Graph shows the difference in weight loss of the different groups after the bone marrow transplant procedure (BMT). c) Representative histological images of liver sections stained with anti- F4/80 antibody with the correspondent quantification of the number of F4/80+ macrophages remaining within the liver after treatment with doxycycline. Positively stained cells were counted in 6 fields of view at X20 magnification. BM= bone marrow. Data analysed using a one- way ANOVA with Bonferroni post hoc test. Error bars represent mean ±SEM, n= 5-8/ group. (♂) males, (♀) females.

6.3.2 Assessment of PAH in mixed-sex *MacLow* chimeras

6.3.2.1 Haemodynamic evaluation

Following the six weeks doxycycline treatment, disease progression was assessed by closed chest cardiac catheterization, echocardiography and measuring the hypertrophy of the right ventricle. The readings showed that the RVESP had increased significantly from 21.4 ± 0.339 in the negative control group (female BM to female) to 29.9 ± 2.289 in the positive control group (male BM to male).

The transplantation also showed that injecting BM from male *MacLow* mice into female *MacLow* was not sufficient to cause a significant increase in their RVESP (figure 6.2). In addition, no conclusion can be made regarding whether female BM can protect males from the induced PAH as the RVESP changes was not significant. However, the average pressure suggests that female BM cells may attenuate but not protect males from the induced PAH.

These finding was consistent with other haemodynamic parameters measured from the right-side of the heart with no effect on the measurements from the left-side heart (see appendix I). No changes in the cardiac index were detected between the different groups (figure 6.2-b).

To further investigate whether the increase in pressure has led to right ventricular hypertrophy (RVH), the RVH index was calculated. The results showed no significant difference in the RVH value between the groups (figure 6.2-c), which again indicate that the disease phenotype was not pronounced and it was not enough to cause any effect on the heart.

Taken together, these findings suggest that the recruited cells from the blood are not crucial in the development of *MacLow-* induced PAH as the female mice were still protected following transplantation with male hematopoietic cells.

a)

b)

c)
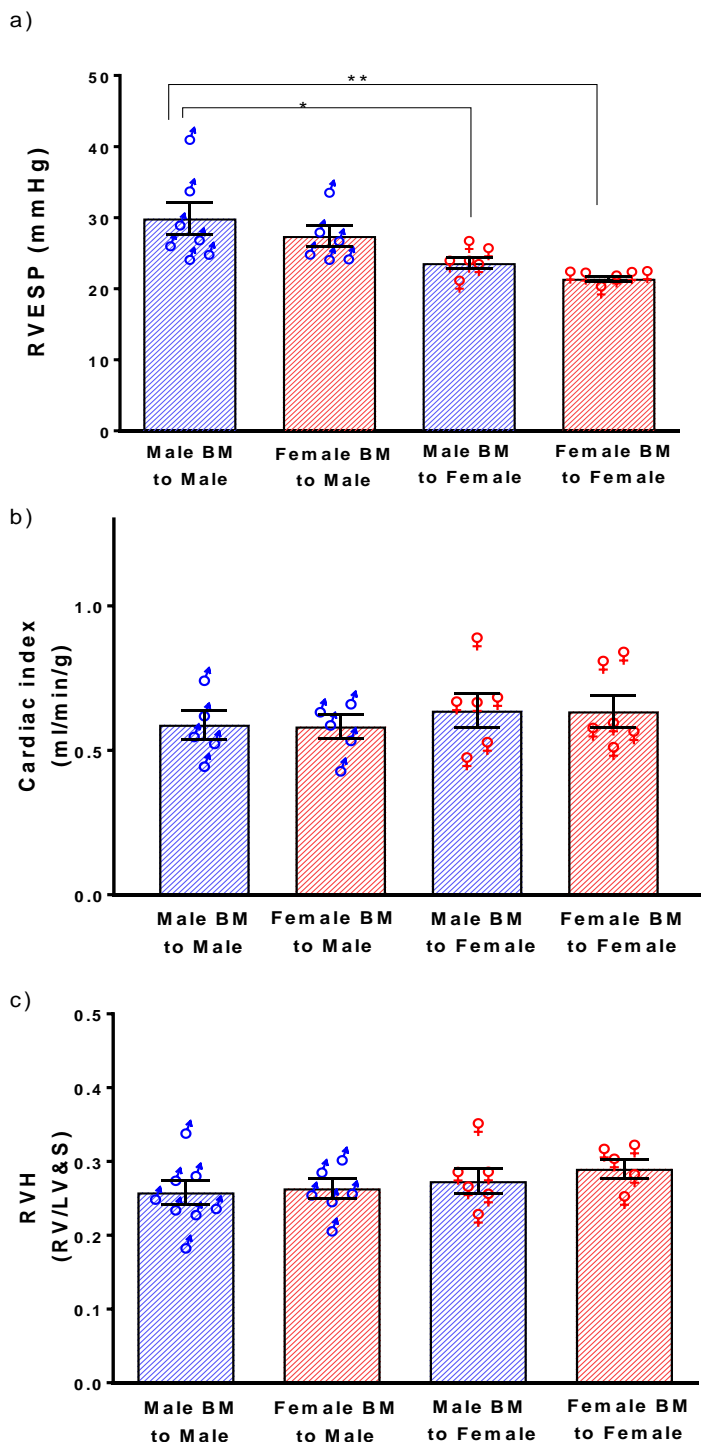
Figure 6.2- Haemodynamic of the PAH phenotype in mixed- sex chimeric mice: a) Right ventricle end-systolic pressure (RVESP) taken using closed chest cardiac pressure volume catheterization b) Cardiac index (cardiac output/ body weight) taken using Vevo 770 echocardiography equipment, c) Right ventricle hypertrophy index (RVH). BM= bone marrow Data analysed by one- way ANOVA with Bonferroni post hoc test. Error bars represent mean ±SEM, n= 5-8/ group. *P <0.05, **P <0.005. (♂) males, (♀) females.

6.3.2.2 Analysis of vessel wall remodelling

PAH is usually associated with vascular remodelling, therefore remodelling was assessed. Histological staining with anti-SMA (figure 6.3) and ABEVG was used to investigate the thickness of pulmonary vessels. In the small sized vessel category (10-50 µm), both the media layer thickness and the number of remodelled vessels were significantly increased in male chimeric group transplanted with male BM cells (the positive control group) following macrophage depletion. No significant increase was observed in both female groups following macrophage loss (figure 6.4)

This further suggest that male *MacLow* haematopoietic cells are not sufficient to induce the PAH in females *MacLow* mice.
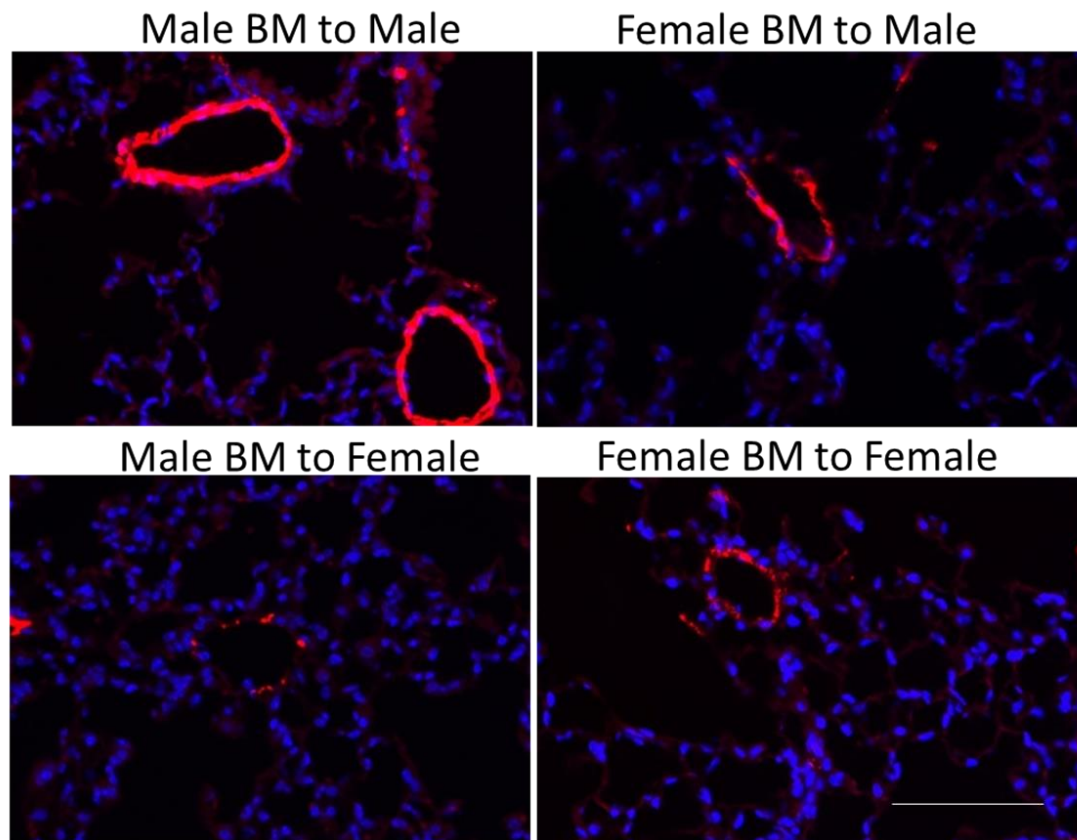
Figure 6.3- Remodelling of pulmonary arteries in mixed-sex *MacLow* chimeras: representative immunofluorescence histological of paraffin fixed lung sections shows the pulmonary vascular lesion in male MacLow chimeric mice compared to other groups. Sections stained with α- smooth muscle actin (SMA) (red) and cell nuclei labelled with DAPI (blue). Sections visualized using Zeiss multi-slide scanning microscope at X20 magnification, scale bar= 50 μm.
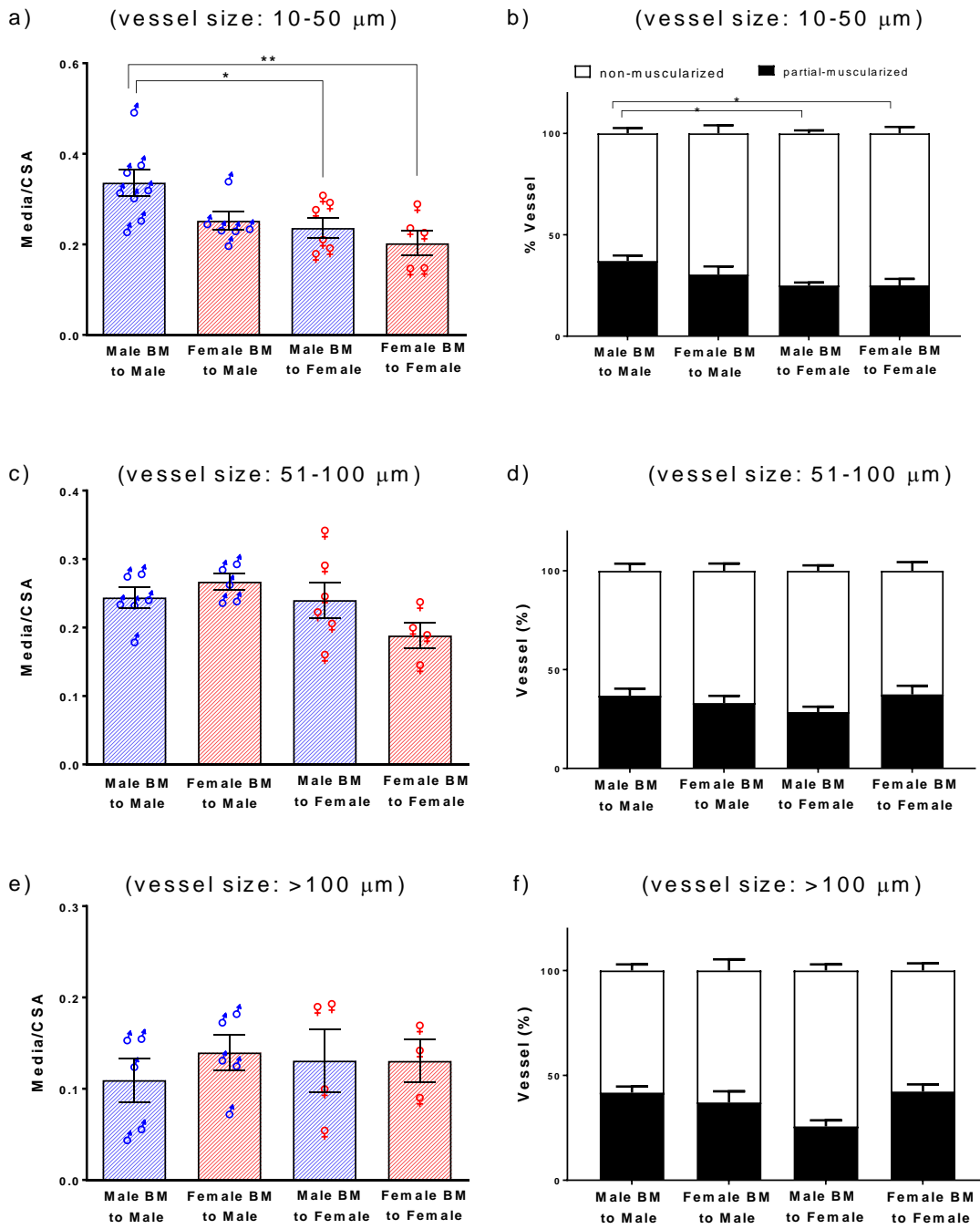
Figure 6.4- Analysis of the degree of remodelling in lung sections: a,c,e) Bar graphs represent Media to cross sectional area (CSA) of three different sized groups (10-50 μm, 51-100μm and >100μm respectively), data analysed using a one- way ANOVA with Bonferroni post hoc test. b,d,f) Graphs represent pulmonary vascular remodelling by percentage muscularised vessels of three different sized groups of vessels (10-50 μm, 51-100μm and >100μm respectively). BM= bone marrow. Data analysed using two- way ANOVA. In all data n= 4-8 / group. *P <0.05, **P <0.005. (♂) males, (♀) females.

6.3.3 Analysis of lung macrophages

Immunohistochemical staining was utilized to assess the level of reduction of total macrophage, M1 and M2, using anti- F4/80, anti- iNOS and anti- CD206 antibodies respectively as previously described. Since all the recipient groups the same level of macrophage reduction following doxycycline treatment was expected. This was confirmed by counting the number of F4/80+ stained cells remaining within the lungs (figure 6.5), the results presented in figure 6.6 showed no significant difference in total macrophage count between any of the groups.

Furthermore, no significant differences detected in either the M1 (iNOS + stained cells) nor the M2 population (CD206 + stained cells) within the lungs following doxycycline treatment (figure 6.6-b,c).

Although the disease phenotype shown previously in chapter 3 was associated with a prevalence of M2 population, but in this BMT study this was not the case. Again, this could be due to that the disease phenotype developed was less pronounced in the chimeric mice that underwent total body irradiation.
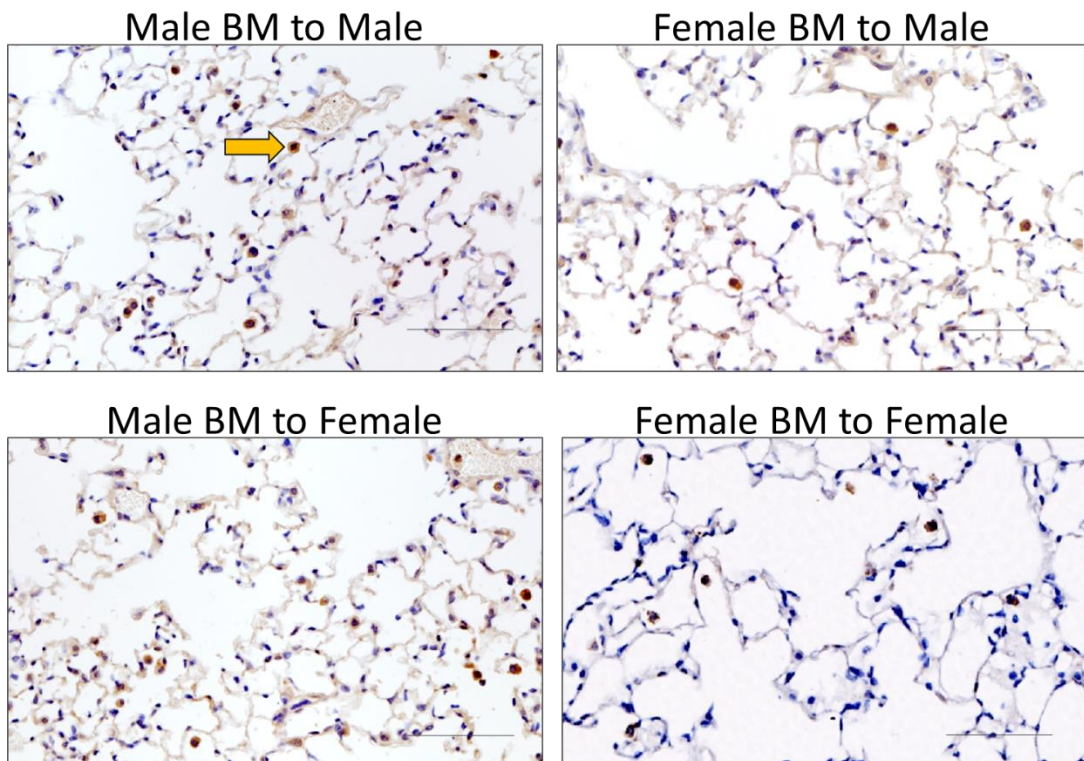
Figure 6.5- Total lung macrophages in mixed-sex *MacLow* chimeric mice: Representative photomicrographs of lung sections stained with anti-F4/80 antibody (total macrophages). The images show the different in macrophage (stained brown- arrow head) remained within the lung of each group after six weeks doxycycline treatment. Image taken using Zeiss multi-slide scanning microscope at X20 magnification, scale bar= 50 µm.

a)

b)

c)
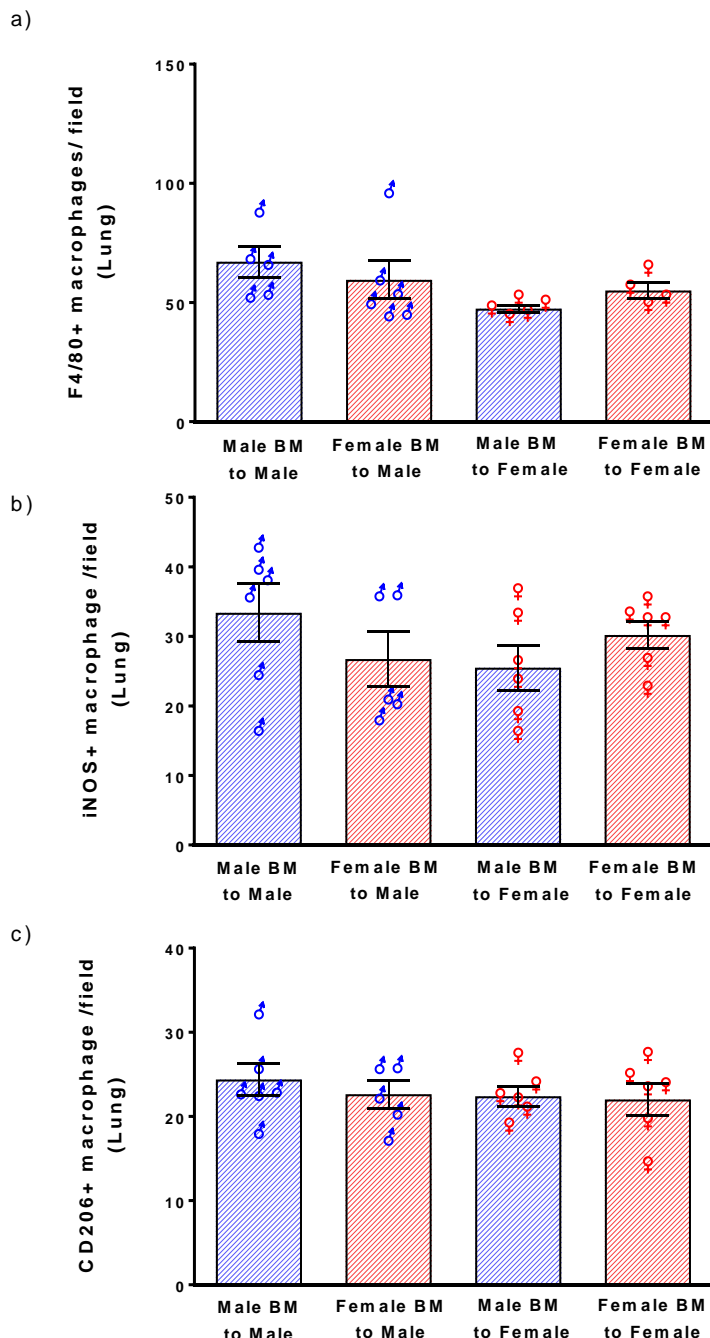
Figure 6.6- Analysis of macrophage subsets in lung sections: Quantification of the number of macrophage remaining within the lung of the chimeric mice following doxycycline treatment. Positively stained cells were counted in 6 field of views / tissue at X20 magnification. a) Quantification of total macrophage using F4/80 antibody. b) Quantification of M1 macrophage subset using iNOS antibody. c) Quantification of M2 macrophage subset using CD206 antibody. BM= bone marrow. Data analysed using a one- way ANOVA with Bonferroni post hoc test. Error bars represent mean ±SEM. n= 5-6/ group. (♂) males, (♀) females.

6.3.4 Oestrogen prophylactic study (preliminary)

To investigate the potential protective effect from oestrogen against the *MacLow-*induced PAH, the disease was induced in male *MacLow* mice using doxycycline treatment and the prophylactic effect of oestrogen was tested. Male *MacLow* mice (12-14 weeks of age) were randomized into 3 groups, the first group was received oestrogen alone as a negative control, the second group was received doxycycline alone as a positive control and the third group received both doxycycline and oestrogen for the same treatment period which was six weeks (figure 6.7-a).

Unexpectedly, none of the groups developed PAH as shown by their normal RVESP, even the positive control group showed normal haemodynamic readings from the right and left ventricles. The study was then repeated and another batch of mice underwent the same procedure for the same period of time using another batch of doxycycline diet, again the same negative results claimed.

To trace this problem, the efficiency of macrophage depletion within different tissues was investigated. The remaining F4/80 + macrophages were counted in the liver and lung sections. There was not any difference in macrophage count between the groups that received doxycycline and the group that did not (figure 6.7), this means that for some unknown reason the macrophage depletion model did not work this time, and subsequently no disease was developed.

It was very unlikely to be because of the doxycycline as the diet was fresh diet from the supplier and the drug should still be effective. Another possibility is that there were some issues with the mouse colony caused by the loss of some of the

genetic features that led to reducing the depletion capability. To address this issue backcrossing of the *MacLow* double transgenic and the tetDTA single transgenic with the FVB mice will be recommended to tackle this issue.
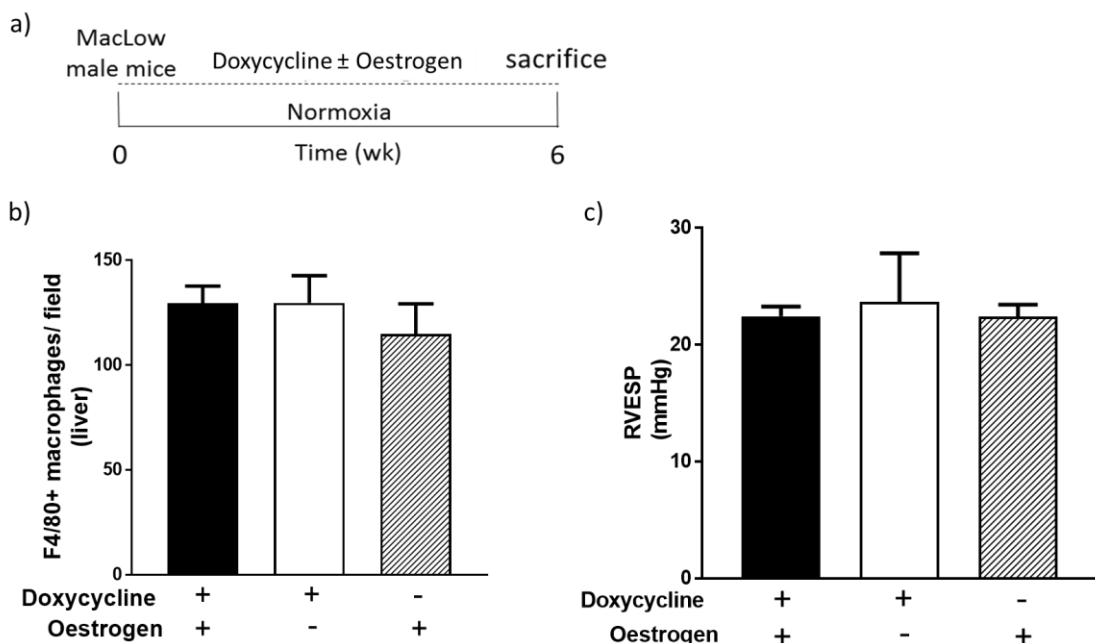
Figure 6.7- Oestrogen prophylactic study: a) Schematic of study design: male *MacLow* mice starting doxycycline treatment with or without oestrogen at day 0 and continued for six weeks, the disease assessed at the end-point by echocardiography and cardiac catheterization. b) Quantification of the number of F4/80+ macrophages remaining within the liver after treatment with doxycycline. Positively stained cells were counted in 6 fields of view at X20 magnification. c) Right ventricle end-systolic pressure taken using closed chest cardiac pressure-volume catheterization. Data analysed using a one- way ANOVA with Bonferroni post hoc test. Error bars represent mean ±SEM, n= 5-8/ group, Doxy= doxycycline.

The negative results from the oestrogen study further suggested a positive correlation between the loss of macrophages and the increase in pressure in male mice. To test whether the reduction in lung F4/80 + macrophages correlates with RVESP increase, measuring of Pearson correlation coefficient was performed using pooled pressure readings from only male *MacLow* mice in the

different set of experiments presented in this thesis. The graph 6.8 did show a positive correlation between the RVESP and the percent reduction of lung macrophages with a significant P value of 0.0431. Thus as the percentage of lung macrophage loss increases, the pulmonary pressure also expected to increase.
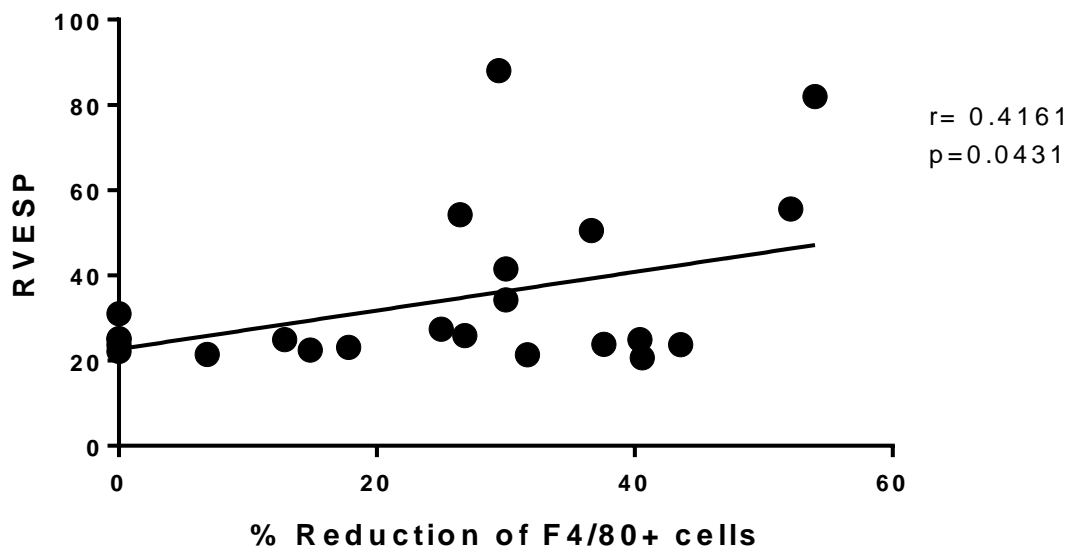
Figure 6.8- Correlation between macrophage depletion and pulmonary pressure: the graph shows the positive correlation between percentage reductions of F4/80 positive macrophage in the lung with the right ventricle end-systolic pressure in male *MacLow* mice following doxycycline treatment. n=24.

6.4 Discussion

Data presented in this chapter demonstrate that lung resident macrophages are the major contributors in the development of *MacLow-* induced PAH in male mice and that male- derived hematopoietic cells alone were not sufficient to induce the disease in females. Although the disease phenotype developed in male *MacLow* chimeras was not severe, it was pronounced enough to conclude that the female

chimera was still protected following transplantation with male inoculum. Again this traced back the origin of the effector cells responsible for the development of PAH in *MacLow* mice to be within the lung itself.

As shown in our previous BMT study in chapter 4, the spontaneous increase in pressure following macrophage ablation was less pronounced in the chimeric mice that underwent total body irradiation compared to non-chimeric mice (figure 4.3). This was probably due to irradiation, as irradiation thought to affects the lung macrophages (Matute-Bello et al., 2004). Taken into account that the alveolar macrophages are long- lived they shown to be resistant to irradiation, and by the time of circulating leukocytes are completely replaced by donor cell, only 47% of the alveolar macrophages repopulate in 30 days following bone marrow transplant (Matute-Bello et al., 2004). This further emphasis the role of AMs in particular in the development and severity of *MacLow-* induced PH phenotype.

Gender/ sex bias does exist in both clinical and experimental forms of PH, as the incident is higher in the female patients. In contrast, in various animal models, females showed less evidence of the disease compared with males. The female rat develops less severe PH, RVH and vascular remodelling following chronic hypoxia compared to males (Rabinovitch et al., 1981, Resta et al., 2001, Umar et al., 2009). These sex differences were mainly attributed to the effect of oestrogen and its metabolites (Umar et al., 2011).

The 'oestrogen paradox' phenomenon arose from the contradictory findings regarding the role of oestrogen in PH. It has been shown that oestrogen and its metabolites can prevent PH in an experimental models of the disease (Farhat et al., 1993, Tofovic et al., 2005), also oestrogen can rescue pre-existing severe PH

in the male rat as it can restore lung and RV function, reduce pulmonary inflammation and limit the monocyte/ macrophage infiltration even after cessation of oestrogen treatment (Umar et al., 2011). On the other hand, unbalanced oestradiol metabolism has been shown to increase the risk of PAH in patients and animal models (Austin et al., 2009). Furthermore, oestrogen level has been shown to be high in male patients with PAH and the level associated with a shorter 6-minute-walk distance (Ventetuolo et al., 2016). Also in experimental PH, treatment with the aromatase inhibitor anastrazole (the aromatase converts androgens to oestrogen and responsible for most of the oestrogen production in men and postmenopausal women) reduced the pulmonary arterial pressure and RV hypertrophy (Mair et al., 2014b, Wright et al., 2015). And importantly, anastrazole significantly reduced oestrogen level in patients with PAH and improved the 6-minute-walk distance (Kawut et al., 2017). Longer and larger phase II clinical trial of anastrazole in this context is now underway (NCT 1545336).

Because of this apparent paradox, the full puzzle of the role of oestrogen in PH is still not completely solved. The *MacLow* model for inducing PAH provides a novel model to study the role of oestrogen in relation to macrophages.

Gender differences have also been reported in a different types of diseases, however, very recently gender differences at the cellular level have been introduced (gender cytology). Cells from males and females can behave differently and display different features, including the mechanisms controlling cell death (Straface et al., 2012). Furthermore, it has been shown that cells have a 'memory' and they can maintain their 'sex' through a number of *in vitro* passages (Straface et al., 2012). There is a growing body of literature that claims

immune cells respond directly to the changes in the concentration of sex hormones via their sex hormone receptor. In term of macrophages, male- derived peritoneal macrophages following LPS stimulation *in vivo* express higher levels of inflammatory cytokine IL-6 and Toll-like receptor 4 (TLR4) protein than female- derived cells in the murine models (Marriott et al., 2006, Rettew et al., 2008).

Despite this evidence that suggested sex-based differences in the biology of immune cells, male- derived bone marrow cells were not enough to induce the disease in female *MacLow* mice, and more likely the female derived cell would not be able to protect males from developing the disease. My results further highlight the sex imbalance in PAH and add the immune cells to this paradigm.

Finally, the work in *MacLow* mouse model further encourages the accurate reporting of the sex of animals in experimental research, which is something considered by many journals recently to improve rigour and reproducibility of biomedical research (Klein and Flanagan, 2016, Florez-Vargas et al., 2016).

7   General discussion and future work

7.1   General discussion

In the work presented in this thesis, I have utilized the *MacLow* mouse model for inducible macrophage depletion to investigate the role of macrophages and macrophage subsets in PAH pathogenicity. The data I collected further support the proposed modulatory role of macrophages in PAH, and emphasise the importance of the switch in macrophage polarity in disease development. The finding did not support my primary hypothesis, as the specific depletion of macrophages in *MacLow* mice did not protect against the induced vascular remodelling. In fact, I showed that macrophage loss actually lead to the development of PAH spontaneously. Additionally, the results showed a unique and interesting sex- specific PAH phenotype induced by loss of macrophages in male mice only. This suggests a correlation between sex and macrophages activation in PAH.

In chapter 3, I showed that loss of CD68+ macrophages in *MacLow* mice induced PAH development in male and not female mice, the disease phenotype was associated with increased RVH and vascular remodelling. By tracing the origin of the effector macrophages responsible for the development of *MacLow-* induced PAH using chimeric mice (presented in chapters 4 and 6), it seems that the major contributor cells originate within the lung tissue. Furthermore, the *in vitro* characterization of lung macrophage subsets presented in chapter 5 suggested that the alveolar macrophage possess weak response to the doxycycline-

induced macrophage depletion *in vitro,* this may led to a compartment- specific activation of the alveolar subtype following the loss of the interstitial subtype.

An additional important observation in the *MacLow-* induced PAH model was the skewing toward the CD206+ population (resembling the alternatively activated M2 subtype), this was seen *in vivo* within the lungs of the diseased male mice following six weeks doxycycline treatment, as well as *in vitro* using *MacLow-* derived BMDMs following doxycycline stimulation. Consistent with this finding, it has been shown previously that in hypoxia- induced PH, the hypoxia causes polarization of alveolar macrophages toward M2 phenotype and that was associated with the development of hypoxia- induced PH *in vivo* (Vergadi et al., 2011, Hashimoto-Kataoka et al., 2015). It is possible that in *MacLow* mice following macrophage depletion, the surviving macrophages switch their phenotype to the alternative activation state to clear up the dead cells and cell debris (Weisser et al., 2012). It is also possible, however, that the skewing toward the M2 macrophage in *MacLow-* induced PAH is associated with the disease pathogenicity, this is shown by the female *MacLow* mice displaying less pronounced M2 population within the lungs. Again this further highlights the sex imbalance in PAH development and may add the immune cell to this paradigm.

It became well evidenced that the inflammation associated with PH is characterized by influx of leukocytes particularly macrophages into the perivascular/ adventitial compartment of the pulmonary vessels (Stenmark et al., 2011, Savai et al., 2012, Stenmark et al., 2012, Stenmark et al., 2013). However, less is known about the mechanism nor the stimuli that induce recruitment and activation of macrophages. The adventitial fibroblast has been shown to possess hyper-proliferative and pro-inflammatory phenotype that is involved in the

recruitment and activation of macrophages in patients and animal model of PH (Li et al., 2011, Wang et al., 2014). This though to be, or at least in part, due to the activation of STAT3 and HIF1 signalling alongside with expression of pro-remodelling genes such as *Arg-1* (El Kasmi et al., 2014). Moreover, T cells were also shown to have a role in regulating the recruitment and activation of inflammatory cells (such as monocyte, macrophages and dendritic cells) (Tamosiuniene et al., 2011). Maladaptation of the immune response has been also an area of interest in PH research as this may explain the accumulation of vascular inflammatory cells and the increased cytokine levels in patients. The T cells (particularly T reg cells) has a well-known role in controlling self- tolerance and a disturbed T reg function has been detected in PAH patients (Tamosiuniene et al., 2011). In athymic rat model (congenital absence of T cells) a vascular injury by VEGF inhibitor lead to development of PH in association with activation and recruitment of macrophages which is reversed by T cell reconstitution (Tamosiuniene et al., 2011). A convincing explanation of this is that the normal T regs functions lead to activation of macrophages to promote injury repair while in absence of T regs the activated macrophages participates in injury evolution (Rabinovitch et al., 2014). In *MacLow*-induced PH, the signalling pathways that might be involved in macrophages polarized activation and whether the *MacLow* mice have impaired T cells function will require further investigation to define.

In addition, by studying the role of the circulating progenitor cells versus the lung resident macrophages using the BMT procedure, I found that the lung resident macrophages are the major contributors to the development of *MacLow-* induced PAH in male mice, and that male- derived hematopoietic cells alone were not sufficient to induce the disease in females. Interestingly, in this study, the

depletion of lung macrophages was less pronounced in the chimeric mice that underwent total body irradiation compared to the non- irradiated mice, this suggested to be most likely due to irradiation effect.

Irradiation impact on the lung is not completely known, but it has been shown that irradiation can affects not only the circulating leukocytes but also can influence the lung macrophages especially the alveolar subtype (Tarling et al., 1987, Matute-Bello et al., 2004). Whilst circulating leukocytes are completely replaced by donor cells in 30 days following bone marrow transplant, only 47% of the alveolar macrophages repopulate in the same period (Matute-Bello et al., 2004). This suggests that the baseline count of the alveolar macrophages in the BMT studies was already below the normal before inducing the depletion even in the controls, this could affect the severity of disease phenotype developed, especially as I showed a positive correlation between the percent reduction in lung macrophages and the increase in RVESP in male *MacLow* mice (figure 6.8).

Additionally, the circulating monocytes also seem to be affected by the *MacLow* depletion strategy. This can be seen as the blood monocyte count was notably reduced following doxycycline treatment in all of the studies conducted. This data suggests that all the monocyte/ macrophages lineage is affected in *MacLow* mouse model.

I also showed using an *in vitro* culture system that different lung macrophages have unique characteristics in terms of their cell viability, polarization, expression of DTA and expression of LTB4 following the addition of doxycycline. *MacLow-*BMDM showed a change in their phenotype toward the alternative activation state following doxycycline stimulation *in vitro*, while the *MacLow-* derived AMs showed

less expression of CD68 and DTA and therefore may be more resistant to killing following the addition of doxycycline. In consistent with this phenotypic differences between the AMs and the IMs, a recent study by (Pugliese et al., 2017) showed a significant difference in overall gene expression of the AMs and IMs following hypoxia exposure, as the IMs switch phenotype to anti-inflammatory phenotype later in course of the disease while the AMs conserve their pro-inflammatory phenotype.

Taken together, I proposed that the *MacLow* induced depletion targets the tissue and the recruited macrophages while leaving the alveolar macrophages affected to a lesser degree (or unaffected). This could potentially lead to compartment-specific activation (alternative activation) of the alveolar macrophages and dominancy of the pro-inflammatory phenotype. However, male sex susceptibility is still questionable.

Gender/ sex bias does exist in both clinical and experimental forms of PH. In patients, PAH develops more predominantly in women than men with a 4.1:1 female to male ratio in idiopathic PAH subcategory (Badesch et al., 2010). However, men showed more severe disease phenotype, worse RV function and poorer survival, while women showed better pulmonary hemodynamic and improvement of the RV function after treatment (Badesch et al., 2010, Shapiro et al., 2012, Jacobs et al., 2014). In contrast, in various animal models, female sex shown to be protective and females showed less evidence of the disease compared with males. Female rat develops less severe PH, RVH and vascular remodelling following chronic hypoxia compared to males (Rabinovitch et al., 1981, Resta et al., 2001, Umar et al., 2009).

There are different contradictory literature about the cause of sex- difference in PAH prevalence and survival. Also the complex role played by the sex hormones (such as oestrogen) in the pulmonary circulation and the RV was not fully explained. In some reports, oestrogen shown to have protective effect against the induced PH in animal model (monocrotaline and hypoxia models) since ovariectomy exacerbates PH and E2 pre-treatment attenuate its progression in the animal models (Farhat et al., 1993, Tofovic et al., 2006, Umar et al., 2011). On the other hand, other reports correlates female sex, oestrogen and oestrogen metabolites to the development of PAH (Austin et al., 2009, White et al., 2012, Mair et al., 2014a). Also other transgenic mouse models demonstrated the increased susceptibility of female sex in the development of PAH, such as the transgenic mouse overexpressing human serotonin transporter SERT+ mice (White et al., 2011) and mice overexpressing calcium- binding protein S100A4/ Mits1 (Dempsie et al., 2011). Moreover, others argued that sex hormones alone may not be sufficient to clarify the gender imbalance in PAH, recent work by (Umar et al., 2017) showed that the Y chromosome have protective role against hypoxia- induced PH. In this work they studied the role of sex hormones independently of gonadal hormones using the Four Core Genotypes mouse (FCG mouse model), in this model male mice can have XX and XY and the female mice can carry XX and XY. They showed that hypoxic XY male developed less severe PH regardless of gonadal sex compared to XX mice (Umar et al., 2017). Collectively, the data collected from the *MacLow-* induced PAH model provides additional argument into the influence of sex in the development of PH. Increased susceptibility of male sex to the development of PAH following macrophage depletion can be correlated to the protective role of oestrogen in females, but also

can be correlated to the severe phenotype and worse RV function seen in male patients. Furthermore, this could also provide a new insight into the protective role of pulmonary macrophages in male mice as their depletion increase the susceptibility to pulmonary vascular diseases.

The development of effective therapeutic targets for PAH needs to consider and fully understand the different aspects of macrophage activation as they could have opposing roles during the development of the disease. A better understanding of relative contribution from IMs and AMs in the initiation and maintenance of vascular remodelling may facilitate the reprogramming or the skewing toward the reparative phenotype of macrophage to attenuate the vascular remodelling. The *MacLow* system can be proposed as a novel and powerful tool that can also be utilised for lineage tracing to target distinct lung macrophage populations. The system can be used to sort out the relative contribution of AMs and IMs in PAH associated remodelling, by depleting only one of the subtypes.

7.2 Future work

I believe that, in the future, there is huge amount of work that can be done to follow up from my research. For example, it would be very tempting to investigate the potential protective effect of oestrogen in the *MacLow-* induced PAH model, this can be done either by treating male *MacLow* mice with an oestrogen analogue alongside with doxycycline treatment to see whether oestrogen treatment can protect male *MacLow* from developing PAH, or by conducting an ovariectomy procedure to the female *MacLow* mice before being treated with doxycycline and investigate whether ovariectomy can induce PAH in females. The potential therapeutic effect of oestrogen can also be investigated by treating

the male mice with oestrogen analogue after establishing the PAH and determine whether the oestrogen treatment can reverse the established PAH. Alternatively, treatment of established PH in *MacLow* mice with the aromatase inhibitor anastrazole to evaluate its therapeutic efficacy is also very interesting future recommendation.

My data also hint for a role of LTB4 released from macrophages in the development of *MacLow-* induced PAH. To investigate this further LTB4/ 5LO inhibitor (such as Bestatin) can be utilized to determine whether blocking LTB4 formation will have an effect on the development of PAH in *MacLow* mice.

In addition, the chimeric *MacLow* mice developed less severe phenotype compared to the non- irradiated mice, this has been speculated to be due to the irradiation effect and the short recovery period. To address this limitation I propose to assess the severity of PAH phenotype in *MacLow* chimeric mice following a longer recovery time after the irradiation (60 days instead of 30 days). As it has been shown that the alveolar macrophages need about 60 days to repopulate following TBI (Matute-Bello et al., 2004). Moreover, to further address the key role of AMs in *MacLow-* induced PAH, I propose the use of chlodronate liposome depletion model in association with the induced depletion of macrophages with doxycycline in *MacLow* male mice. Repeated intratracheal chlodronate liposome injections can be used to locally deplete alveolar macrophages (Zaloudikova et al., 2016), in combination with doxycycline treatment for six weeks. This experiment will give supportive evidence regarding the relative contribution of lung macrophage subsets by depleting both the tissue resident and the alveolar macrophages and then assessing the spontaneous development of PAH.

The role of AMs versus IMs in *MacLow* mice following macrophage depletion can be further addressed using fluorescence- activated cell sorting technique of lung digest preparations. Behavioural and genetic features of each population can be then studied separately following treatment with different stimulus including doxycycline and oestrogen.

I also propose to investigate the sex- dependent role of macrophages in *MacLow* mice using other models of PH (other than the hypoxia model), the hypoxia model is inflammatory- based model and may not be comprehensive as hypoxia alone not able to recapitulate the full vascular pathological features seen in patients. Instead, the VEGF inhibitor SUGEN in combination with chronic hypoxia can be used as more pronounced model of PAH. this model provides human- like spectrum of PAH with endothelial proliferation, precapillary occlusion and formation of plexiform lesion (Taraseviciene-Stewart et al., 2001). Similarly, other models of PH such as the bleomycin model (Harrison and Lazo, 1987), high fat diet- fed ApoE knock out mouse model (Weng et al., 2011) and vasoactive intestinal peptide VIP knock out model (Said et al., 2007) can also be used in conjugation with *MacLow* induced macrophage depletion to further confirm the role of macrophage in relation to sex in the development of different forms of PH.

Importantly, although animal models have significantly enriched our understanding of the pathological processes involved in the development of the disease, the conclusions drawn may not be fully translatable into human diseases. Thus my research should be further expanded to determine whether the sex- dependent macrophage phenotype observed in *MacLow* mice is also observed in human PAH. One way this could be established is by culturing human blood- derived macrophages from PAH patients of both genders and studying

their differentiation and polarization characteristics, also the changes in transcriptomic and metabolic profiles can be studied in isolated RNA samples to determine any conserved features between the *MacLow* model and human PAH.

Finally, the work in *MacLow* mouse model further encourage the accurate reporting of the sex of animals in experimental research, which is something considered by many journals recently to improve rigour and reproducibility of the biomedical research (Klein and Flanagan, 2016, Florez-Vargas et al., 2016).

8 Bibliography

ARNOLD, L., HENRY, A., PORON, F., BABA-AMER, Y., VAN ROOIJEN, N., PLONQUET, A., GHERARDI, R. K. & CHAZAUD, B. 2007. Inflammatory monocytes recruited after skeletal muscle injury switch into antiinflammatory macrophages to support myogenesis. *Journal of Experimental Medicine,* 204**,** 1057-1069.

ATKINSON, C., STEWART, S., UPTON, P. D., MACHADO, R., THOMSON, J. R., TREMBATH, R. C. & MORRELL, N. W. 2002. Primary pulmonary hypertension is associated with reduced pulmonary vascular expression of type II bone morphogenetic protein receptor. *Circulation,* 105**,** 1672-8.

AUSTIN, E. D., COGAN, J. D., WEST, J. D., HEDGES, L. K., HAMID, R., DAWSON, E. P., WHEELER, L. A., PARL, F. F., LOYD, J. E. & PHILLIPS, J. A., 3RD 2009. Alterations in oestrogen metabolism: implications for higher penetrance of familial pulmonary arterial hypertension in females. *Eur Respir J,* 34**,** 1093-9.

AUSTIN, E. D. & LOYD, J. E. 2014. The Genetics of Pulmonary Arterial Hypertension. *Circulation research,* 115**,** 189-202.

BADESCH, D. B., RASKOB, G. E., ELLIOTT, C. G., KRICHMAN, A. M., FARBER, H. W., FROST, A. E., BARST, R. J., BENZA, R. L., LIOU, T. G., TURNER, M., GILES, S., FELDKIRCHER, K., MILLER, D. P. & MCGOON, M. D. 2010. Pulmonary Arterial Hypertension Baseline Characteristics From the REVEAL Registry. *Chest,* 137**,** 376-387.

BISWAS, S. K. & MANTOVANI, A. 2010. Macrophage plasticity and interaction with lymphocyte subsets: cancer as a paradigm. *Nature Immunology,* 11**,** 889-896.

BOUCHER, P., GOTTHARDT, M., LI, W. P., ANDERSON, R. G. & HERZ, J. 2003. LRP: role in vascular wall integrity and protection from atherosclerosis. *Science,* 300**,** 329-32.

BURNETT, S. H., KERSHEN, E. J., ZHANG, J. Y., ZENG, L., STRALEY, S. C., KAPLAN, A. M. & COHEN, D. A. 2004. Conditional macrophage ablation in transgenic mice expressing a Fas-based suicide gene. *Journal of Leukocyte Biology,* 75**,** 612-623.

BYRNE, A. J., MAHER, T. M. & LLOYD, C. M. 2016. Pulmonary Macrophages: A New Therapeutic Pathway in Fibrosing Lung Disease? *Trends in Molecular Medicine,* 22**,** 303-316.

CACOUB, P., DORENT, R., NATAF, P., CARAYON, A., RIQUET, M., NOE, E., PIETTE, J. C., GODEAU, P. & GANDJBAKHCH, I. 1997. Endothelin-1 in the lungs of patients with pulmonary hypertension. *Cardiovasc Res,* 33**,** 196-200.

CAGLAYAN, E., VANTLER, M., LEPPANEN, O., GERHARDT, F., MUSTAFOV, L., TEN FREYHAUS, H., KAPPERT, K., ODENTHAL, M., ZIMMERMANN, W. H., TALLQUIST, M. D. & ROSENKRANZ, S. 2011. Disruption of platelet-derived growth factor-dependent phosphatidylinositol 3-kinase and phospholipase Cgamma 1 activity abolishes vascular smooth muscle cell proliferation and migration and attenuates neointima formation in vivo. *J Am Coll Cardiol,* 57**,** 2527-38.

CHAMBERLAIN, J., EVANS, D., KING, A., DEWBERRY, R., DOWER, S., CROSSMAN, D. & FRANCIS, S. 2006. Interleukin-1β and Signaling of Interleukin-1 in Vascular Wall and Circulating Cells Modulates the Extent of Neointima Formation in Mice. *The American Journal of Pathology,* 168**,** 1396-1403.

CHRISTMAN, B. W., MCPHERSON, C. D., NEWMAN, J. H., KING, G. A., BERNARD, G. R., GROVES, B. M. & LOYD, J. E. 1992. An imbalance between the excretion of thromboxane and prostacyclin metabolites in pulmonary hypertension. *N Engl J Med,* 327**,** 70-5.

COHEN, M. H., JOHNSON, J. R., CHEN, Y. F., SRIDHARA, R. & PAZDUR, R. 2005. FDA drug approval summary: erlotinib (Tarceva) tablets. *Oncologist,* 10**,** 461-6.

COHEN, M. H., WILLIAMS, G. A., SRIDHARA, R., CHEN, G. & PAZDUR, R. 2003. FDA drug approval summary: gefitinib (ZD1839) (Iressa) tablets. *Oncologist,* 8**,** 303-6.

COHEN-KAMINSKY, S., HAUTEFORT, A., PRICE, L., HUMBERT, M. & PERROS, F. 2014. Inflammation in pulmonary hypertension: what we know and what we could logically and safely target first. *Drug Discovery Today.*

CONDLIFFE, R., PICKWORTH, J. A., HOPKINSON, K., WALKER, S. J., HAMEED, A. G., SUNTHARALIGAM, J., SOON, E., TREACY, C., PEPKE-ZABA, J., FRANCIS, S. E., CROSSMAN, D. C., NEWMAN, C. M. H., ELLIOT, C. A., MORTON, A. C., MORRELL, N. W., KIELY, D. G. & LAWRIE, A. 2012. Serum osteoprotegerin is increased and predicts survival in idiopathic pulmonary arterial hypertension. *Pulmonary circulation,* 2**,** 21-7.

CORBIN, J. D., BEASLEY, A., BLOUNT, M. A. & FRANCIS, S. H. 2005. High lung PDE5: a strong basis for treating pulmonary hypertension with PDE5 inhibitors. *Biochem Biophys Res Commun,* 334**,** 930-8.

CRAWFORD, P. A. & GORDON, J. I. 2005. Microbial regulation of intestinal radiosensitivity. *Proceedings of the National Academy of Sciences of the United States of America,* 102**,** 13254-13259.

CUI, Y. Z., HISHA, H., YANG, G. X., FAN, T. X., JIN, T., LI, Q., LIAN, Z. & IKEHARA, S. 2002. Optimal protocol for total body irradiation for allogeneic bone marrow transplantation in mice. *Bone Marrow Transplantation,* 30**,** 843-849.

DAHAL, B. K., CORNITESCU, T., TRETYN, A., PULLAMSETTI, S. S., KOSANOVIC, D., DUMITRASCU, R., GHOFRANI, H. A., WEISSMANN, N., VOSWINCKEL, R., BANAT, G. A., SEEGER, W., GRIMMINGER, F. & SCHERMULY, R. T. 2010. Role of epidermal growth factor inhibition in experimental pulmonary hypertension. *Am J Respir Crit Care Med,* 181**,** 158-67.

DAVIE, N. J., CROSSNO, J. T., FRID, M. G., HOFMEISTER, S. E., REEVES, J. T., HYDE, D. M., CARPENTER, T. C., BRUNETTI, J. A., MCNIECE, I. K. & STENMARK, K. R. 2004. Hypoxia-induced pulmonary artery adventitial remodeling and neovascularization: contribution of progenitor cells. *American Journal of Physiology-Lung Cellular and Molecular Physiology,* 286**,** L668-L678.

DEMPSIE, Y., NILSEN, M., WHITE, K., MAIR, K. M., LOUGHLIN, L., AMBARTSUMIAN, N., RABINOVITCH, M. & MACLEAN, M. R. 2011.

Development of pulmonary arterial hypertension in mice over-expressing S100A4/Mts1 is specific to females. *Respiratory Research,* 12.

DENG, Z., HAGHIGHI, F., HELLEBY, L., VANTERPOOL, K., HORN, E. M., BARST, R. J., HODGE, S. E., MORSE, J. H. & KNOWLES, J. A. 2000. Fine mapping of PPH1, a gene for familial primary pulmonary hypertension, to a 3-cM region on chromosome 2q33. *Am J Respir Crit Care Med,* 161**,** 1055-9.

DUFFIELD, J. S., FORBES, S. J., CONSTANDINOU, C. M., CLAY, S., PARTOLINA, M., VUTHOORI, S., WU, S. J., LANG, R. & IREDALE, J. P. 2005. Selective depletion of macrophages reveals distinct, opposing roles during liver injury and repair. *Journal of Clinical Investigation,* 115**,** 56-65.

DURAN-STRUUCK, R. & DYSKOZ, R. C. 2009. Principles of Bone Marrow Transplantation (BMT): Providing Optimal Veterinary and Husbandry Care to Irradiated Mice in BMT Studies. *Journal of the American Association for Laboratory Animal Science,* 48**,** 11-22.

EDDAHIBI, S., GUIGNABERT, C., BARLIER-MUR, A. M., DEWACHTER, L., FADEL, E., DARTEVELLE, P., HUMBERT, M., SIMONNEAU, G., HANOUN, N., SAURINI, F., HAMON, M. & ADNOT, S. 2006. Cross talk between endothelial and smooth muscle cells in pulmonary hypertension: critical role for serotonin-induced smooth muscle hyperplasia. *Circulation,* 113**,** 1857-64.

EDDAHIBI, S., HUMBERT, M., FADEL, E., RAFFESTIN, B., DARMON, M., CAPRON, F., SIMONNEAU, G., DARTEVELLE, P., HAMON, M. & ADNOT, S. 2001. Serotonin transporter overexpression is responsible for pulmonary artery smooth muscle hyperplasia in primary pulmonary hypertension. *Journal of Clinical Investigation,* 108**,** 1141-1150.

EDDAHIBI, S., HUMBERT, M., SEDIAME, S., CHOUAID, C., PARTOVIAN, C., MAITRE, B., TEIGER, E., RIDEAU, D., SIMONNEAU, G., SITBON, O. & ADNOT, S. 2000. Imbalance between platelet vascular endothelial growth factor and platelet-derived growth factor in pulmonary hypertension. Effect of prostacyclin therapy. *Am J Respir Crit Care Med,* 162**,** 1493-9.

EL KASMI, K. C., PUGLIESE, S. C., RIDDLE, S. R., POTH, J. M., ANDERSON, A. L., FRID, M. G., LI, M., PULLAMSETTI, S. S., SAVAI, R., NAGEL, M. A., FINI, M. A., GRAHAM, B. B., TUDER, R. M., FRIEDMAN, J. E., ELTZSCHIG, H. K., SOKOL, R. J. & STENMARK, K. R. 2014. Adventitial Fibroblasts Induce a Distinct Proinflammatory/Profibrotic Macrophage Phenotype in Pulmonary Hypertension. *Journal of Immunology,* 193**,** 597-609.

EMERY, J. G., MCDONNELL, P., BURKE, M. B., DEEN, K. C., LYN, S., SILVERMAN, C., DUL, E., APPELBAUM, E. R., EICHMAN, C., DIPRINZIO, R., DODDS, R. A., JAMES, I. E., ROSENBERG, M., LEE, J. C. & YOUNG, P. R. 1998. Osteoprotegerin is a receptor for the cytotoxic ligand TRAIL. *J Biol Chem,* 273**,** 14363-7.

EPELMAN, S., LAVINE, KORY J. & RANDOLPH, GWENDALYN J. 2014. Origin and Functions of Tissue Macrophages. *Immunity,* 41**,** 21-35.

EVANS, D. J. W., JACKMAN, L. E., CHAMBERLAIN, J., CROSDALE, D. J., JUDGE, H. M., JETHA, K., NORMAN, K. E., FRANCIS, S. E. & STOREY, R. F. 2009. Platelet P2Y(12) Receptor Influences the Vessel

Wall Response to Arterial Injury and Thrombosis. *Circulation,* 119**,** 116-U236.

FANG, F. C. 2004. Antimicrobial reactive oxygen and nitrogen species: concepts and controversies. *Nature Reviews Microbiology,* 2**,** 820.

FARHAT, M. Y., CHEN, M. F., BHATTI, T., IQBAL, A., CATHAPERMAL, S. & RAMWELL, P. W. 1993. Protection by oestradiol against the development of cardiovascular changes associated with monocrotaline pulmonary hypertension in rats. *Br J Pharmacol,* 110**,** 719-23.

FERRARA, N., GERBER, H.-P. & LECOUTER, J. 2003. The biology of VEGF and its receptors. *Nature Medicine,* 9**,** 669.

FERRERO-MILIANI, L., NIELSEN, O. H., ANDERSEN, P. S. & GIRARDIN, S. E. 2007. Chronic inflammation: importance of NOD2 and NALP3 in interleukin-1β generation. *Clinical and Experimental Immunology,* 147**,** 227-235.

FLOREZ-VARGAS, O., BRASS, A., KARYSTIANIS, G., BRAMHALL, M., STEVENS, R., CRUICKSHANK, S. & NENADIC, G. 2016. Bias in the reporting of sex and age in biomedical research on mouse models. *Elife,* 5.

FRID, M. G., BRUNETTI, J. A., BURKE, D. L., CARPENTER, T. C., DAVIE, N. J., REEVES, J. T., ROEDERSHEIMER, M. T., VAN ROOIJEN, N. & STENMARK, K. R. 2006. Hypoxia-induced pulmonary vascular remodeling requires recruitment of circulating mesenchymal precursors of a monocyte/macrophage lineage. *American Journal of Pathology,* 168**,** 659-669.

GALIE, N., PALAZZINI, M. & MANES, A. 2010. Pulmonary arterial hypertension: from the kingdom of the near-dead to multiple clinical trial meta-analyses. *European Heart Journal,* 31**,** 2080-2086.

GALIÈ, N., HOEPER, M. M., HUMBERT, M., TORBICKI, A., VACHIERY, J.-L., BARBERA, J. A., BEGHETTI, M., CORRIS, P., GAINE, S., GIBBS, J. S., GOMEZ-SANCHEZ, M. A., JONDEAU, G., KLEPETKO, W., OPITZ, C., PEACOCK, A., RUBIN, L., ZELLWEGER, M., SIMONNEAU, G., VAHANIAN, A., AURICCHIO, A., BAX, J., CECONI, C., DEAN, V., FILIPPATOS, G., FUNCK-BRENTANO, C., HOBBS, R., KEARNEY, P., MCDONAGH, T., MCGREGOR, K., POPESCU, B. A., REINER, Z., SECHTEM, U., SIRNES, P. A., TENDERA, M., VARDAS, P., WIDIMSKY, P., AL ATTAR, N., ANDREOTTI, F., ASCHERMANN, M., ASTEGGIANO, R., BENZA, R., BERGER, R., BONNET, D., DELCROIX, M., HOWARD, L., KITSIOU, A. N., LANG, I., MAGGIONI, A., NIELSEN-KUDSK, J. E., PARK, M., PERRONE-FILARDI, P., PRICE, S., DOMENECH, M. T. S., VONK-NOORDEGRAAF, A. & ZAMORANO, J. L. 2009. Guidelines for the diagnosis and treatment of pulmonary hypertensionThe Task Force for the Diagnosis and Treatment of Pulmonary Hypertension of the European Society of Cardiology (ESC) and the European Respiratory Society (ERS), endorsed by the International Society of Heart and Lung Transplantation (ISHLT). *European Heart Journal,* 30**,** 2493-2537.

GEISSMANN, F., AUFFRAY, C., PALFRAMAN, R., WIRRIG, C., CIOCCA, A., CAMPISI, L., NARNI-MANCINELLI, E. & LAUVAU, G. 2008. Blood monocytes: distinct subsets, how they relate to dendritic cells, and their

possible roles in the regulation of T-cell responses. *Immunology And Cell Biology,* 86**,** 398.

GEISSMANN, F., MANZ, M. G., JUNG, S., SIEWEKE, M. H., MERAD, M. & LEY, K. 2010. Development of monocytes, macrophages, and dendritic cells. *Science,* 327**,** 656-61.

GERACI, M. W., GAO, B., SHEPHERD, D. C., MOORE, M. D., WESTCOTT, J. Y., FAGAN, K. A., ALGER, L. A., TUDER, R. M. & VOELKEL, N. F. 1999. Pulmonary prostacyclin synthase overexpression in transgenic mice protects against development of hypoxic pulmonary hypertension. *J Clin Invest,* 103**,** 1509-15.

GHERYANI, N., COFFELT, S. B., GARTLAND, A., RUMNEY, R. M. H., KISS-TOTH, E., LEWIS, C. E., TOZER, G. M., GREAVES, D. R., DEAR, T. N. & MILLER, G. 2013. Generation of a novel mouse model for the inducible depletion of macrophages in vivo. *Genesis,* 51**,** 41-49.

GHOFRANI, H. A., MORRELL, N. W., HOEPER, M. M., OLSCHEWSKI, H., PEACOCK, A. J., BARST, R. J., SHAPIRO, S., GOLPON, H., TOSHNER, M., GRIMMINGER, F. & PASCOE, S. 2010. Imatinib in pulmonary arterial hypertension patients with inadequate response to established therapy. *Am J Respir Crit Care Med,* 182**,** 1171-7.

GHOFRANI, H. A., SEEGER, W. & GRIMMINGER, F. 2005. Imatinib for the Treatment of Pulmonary Arterial Hypertension. *New England Journal of Medicine,* 353**,** 1412-1413.

GIAID, A., YANAGISAWA, M., LANGLEBEN, D., MICHEL, R. P., LEVY, R., SHENNIB, H., KIMURA, S., MASAKI, T., DUGUID, W. P. & STEWART, D. J. 1993. Expression of endothelin-1 in the lungs of patients with pulmonary hypertension. *N Engl J Med,* 328**,** 1732-9.

GILL, R. G. 2010. NK Cells: Elusive Participants in Transplantation Immunity and Tolerance. *Current opinion in immunology,* 22**,** 649-654.

GINHOUX, F. & JUNG, S. 2014. Monocytes and macrophages: developmental pathways and tissue homeostasis. *Nature Reviews Immunology,* 14**,** 392-404.

GOLEMBESKI, S. A., WEST, J., TADA, Y. & FAGAN, K. A. 2005. Interleukin-6 causes mild pulmonary hypertension and augments hypoxia-induced pulmonary hypertension in mice. *Chest,* 128**,** 572S-573S.

GUNDRA, U. M., GIRGIS, N. M., RUCKERL, D., JENKINS, S., WARD, L. N., KURTZ, Z. D., WIENS, K. E., TANG, M. S., BASU-ROY, U., MANSUKHANI, A., ALLEN, J. E. & LOKE, P. N. 2014. Alternatively activated macrophages derived from monocytes and tissue macrophages are phenotypically and functionally distinct. *Blood,* 123**,** e110-e122.

HAMEED, A. G., ARNOLD, N. D., CHAMBERLAIN, J., PICKWORTH, J. A., PAIVA, C., DAWSON, S., CROSS, S., LONG, L., ZHAO, L., MORRELL, N. W., CROSSMAN, D. C., NEWMAN, C. M. H., KIELY, D. G., FRANCIS, S. E. & LAWRIE, A. 2012. Inhibition of tumor necrosis factor-related apoptosis-inducing ligand (TRAIL) reverses experimental pulmonary hypertension. *Journal of Experimental Medicine,* 209**,** 1919-1935.

HARRISON, J. H., JR. & LAZO, J. S. 1987. High dose continuous infusion of bleomycin in mice: a new model for drug-induced pulmonary fibrosis. *J Pharmacol Exp Ther,* 243**,** 1185-94.

HASHIMOTO, D., CHOW, A., NOIZAT, C., TEO, P., BEASLEY, M. B., LEBOEUF, M., BECKER, C. D., SEE, P., PRICE, J., LUCAS, D., GRETER, M., MORTHA, A., BOYER, S. W., FORSBERG, E. C., TANAKA, M., VAN ROOIJEN, N., GARCIA-SASTRE, A., STANLEY, E. R., GINHOUX, F., FRENETTE, P. S. & MERAD, M. 2013. Tissue-Resident Macrophages Self-Maintain Locally throughout Adult Life with Minimal Contribution from Circulating Monocytes. *Immunity,* 38**,** 792-804.

HASHIMOTO-KATAOKA, T., HOSEN, N., SONOBE, T., ARITA, Y., YASUI, T., MASAKI, T., MINAMI, M., INAGAKI, T., MIYAGAWA, S., SAWA, Y., MURAKAMI, M., KUMANOGOH, A., YAMAUCHI-TAKIHARA, K., OKUMURA, M., KISHIMOTO, T., KOMURO, I., SHIRAI, M., SAKATA, Y. & NAKAOKA, Y. 2015. Interleukin-6/interleukin-21 signaling axis is critical in the pathogenesis of pulmonary arterial hypertension. *Proceedings of the National Academy of Sciences,* 112, E2677.

HAYASHIDA, K., FUJITA, J., MIYAKE, Y., KAWADA, H., ANDO, K., OGAWA, S. & FUKUDA, K. 2005. Bone marrow-derived cells contribute to pulmonary vascular remodeling in hypoxia-induced pulmonary hypertension. *Chest,* 127**,** 1793-1798.

HERVE, P., LAUNAY, J. M., SCROBOHACI, M. L., BRENOT, F., SIMONNEAU, G., PETITPRETZ, P., POUBEAU, P., CERRINA, J., DUROUX, P. & DROUET, L. 1995. Increased plasma serotonin in primary pulmonary hypertension. *Am J Med,* 99**,** 249-54.

HETTINGER, J., RICHARDS, D. M., HANSSON, J., BARRA, M. M., JOSCHKO, A.-C., KRIJGSVELD, J. & FEUERER, M. 2013. Origin of monocytes and macrophages in a committed progenitor. *Nature Immunology,* 14**,** 821-+.

HIGASHI-KUWATA, N., JINNIN, M., MAKINO, T., FUKUSHIMA, S., INOUE, Y., MUCHEMWA, F. C., YONEMURA, Y., KOMOHARA, Y., TAKEYA, M., MITSUYA, H. & IHN, H. 2010. Characterization of monocyte/macrophage subsets in the skin and peripheral blood derived from patients with systemic sclerosis. *Arthritis Research & Therapy,* 12.

HOEPER, M. M., BARST, R. J., BOURGE, R. C., FELDMAN, J., FROST, A. E., GALIE, N., GOMEZ-SANCHEZ, M. A., GRIMMINGER, F., GRUNIG, E., HASSOUN, P. M., MORRELL, N. W., PEACOCK, A. J., SATOH, T., SIMONNEAU, G., TAPSON, V. F., TORRES, F., LAWRENCE, D., QUINN, D. A. & GHOFRANI, H. A. 2013a. Imatinib mesylate as add-on therapy for pulmonary arterial hypertension: results of the randomized IMPRES study. *Circulation,* 127**,** 1128-38.

HOEPER, M. M., BOGAARD, H. J., CONDLIFFE, R., FRANTZ, R., KHANNA, D., KURZYNA, M., LANGLEBEN, D., MANES, A., SATOH, T., TORRES, F., WILKINS, M. R. & BADESCH, D. B. 2013b. Definitions and Diagnosis of Pulmonary Hypertension. *Journal of the American College of Cardiology,* 62**,** D42-D50.

HONG, K. H., LEE, Y. J., LEE, E., PARK, S. O., HAN, C., BEPPU, H., LI, E., RAIZADA, M. K., BLOCH, K. D. & OH, S. P. 2008. Genetic ablation of the BMPR2 gene in pulmonary endothelium is sufficient to predispose to pulmonary arterial hypertension. *Circulation,* 118**,** 722-30.

HOSHIKAWA, Y., VOELKEL, N. F., GESELL, T. L., MOORE, M. D., MORRIS, K. G., ALGER, L. A., NARUMIYA, S. & GERACI, M. W. 2001. Prostacyclin receptor-dependent modulation of pulmonary vascular remodeling. *Am J Respir Crit Care Med,* 164**,** 314-8.

HUERTAS, A., TU, L., GAMBARYAN, N., GIRERD, B., PERROS, F., MONTANI, D., FABRE, D., FADEL, E., EDDAHIBI, S., COHEN-KAMINSKY, S., GUIGNABERT, C. & HUMBERT, M. 2012. Leptin and regulatory T-lymphocytes in idiopathic pulmonary arterial hypertension. *European Respiratory Journal,* 40**,** 895-904.

HUMBERT, M., MONTANI, D., PERROS, F., DORFMULLER, P., ADNOT, S. & EDDAHIBI, S. 2008. Endothelial cell dysfunction and cross talk between endothelium and smooth muscle cells in pulmonary arterial hypertension. *Vascul Pharmacol,* 49**,** 113-8.

HUMBERT, M., MONTI, G., BRENOT, F., SITBON, O., PORTIER, A., GRANGEOT-KEROS, L., DUROUX, P., GALANAUD, P., SIMONNEAU, G. & EMILIE, D. 1995. Increased interleukin-1 and interleukin-6 serum concentrations in severe primary pulmonary hypertension. *Am J Respir Crit Care Med,* 151**,** 1628-31.

HUMBERT, M., MONTI, G., FARTOUKH, M., MAGNAN, A., BRENOT, F., RAIN, B., CAPRON, F., GALANAUD, P., DUROUX, P., SIMONNEAU, G. & EMILIE, D. 1998. Platelet-derived growth factor expression in primary pulmonary hypertension: comparison of HIV seropositive and HIV seronegative patients. *European Respiratory Journal,* 11**,** 554-559.

HUME, D. A. 2011. Applications of myeloid-specific promoters in transgenic mice support in vivo imaging and functional genomics but do not support the concept of distinct macrophage and dendritic cell lineages or roles in immunity. *Journal of Leukocyte Biology,* 89**,** 525-538.

IQBAL, A. J., MCNEILL, E., KAPELLOS, T. S., REGAN-KOMITO, D., NORMAN, S., BURD, S., SMART, N., MACHEMER, D. E. W., STYLIANOU, E., MCSHANE, H., CHANNON, K. M., CHAWLA, A. & GREAVES, D. R. 2014. Human CD68 promoter GFP transgenic mice allow analysis of monocyte to macrophage differentiation in vivo. *Blood,* 124**,** e33.

JACKSON-JONES, L. H., RUCKERL, D., SVEDBERG, F., DUNCAN, S., MAIZELS, R. M., SUTHERLAND, T. E., JENKINS, S. J., MCSORLEY, H. J., BENEZECH, C., MACDONALD, A. S. & ALLEN, J. E. 2016. IL-33 delivery induces serous cavity macrophage proliferation independent of interleukin-4 receptor alpha. *European Journal of Immunology,* 46**,** 2311-2321.

JACOBS, W., VAN DE VEERDONK, M. C., TRIP, P., DE MAN, F., HEYMANS, M. W., MARCUS, J. T., KAWUT, S. M., BOGAARD, H.-J., BOONSTRA, A. & VONK NOORDEGRAAF, A. 2014. The Right Ventricle Explains Sex Differences in Survival in Idiopathic Pulmonary Arterial Hypertension. *Chest,* 145, 1230-1236.

JENKINS, S. J., RUCKERL, D., COOK, P. C., JONES, L. H., FINKELMAN, F. D., VAN ROOIJEN, N., MACDONALD, A. S. & ALLEN, J. E. 2011. Local Macrophage Proliferation, Rather than Recruitment from the Blood, Is a Signature of T(H)2 Inflammation. *Science,* 332**,** 1284-1288.

JENKINS, S. J., RUCKERL, D., THOMAS, G. D., HEWITSON, J. P., DUNCAN, S., BROMBACHER, F., MAIZELS, R. M., HUME, D. A. & ALLEN, J. E. 2013. IL-4 directly signals tissue-resident macrophages to proliferate beyond homeostatic levels controlled by CSF-1. *Journal of Experimental Medicine,* 210**,** 2477-2491.

JENSEN, T. O., SCHMIDT, H., MOLLER, H. J., HOYER, M., MANIECKI, M. B., SJOEGREN, P., CHRISTENSEN, I. J. & STEINICHE, T. 2009. Macrophage Markers in Serum and Tumor Have Prognostic Impact in American Joint Committee on Cancer Stage I/II Melanoma. *Journal of Clinical Oncology,* 27**,** 3330-3337.

JONIGK, D., GOLPON, H., BOCKMEYER, C. L., MAEGEL, L., HOEPER, M. M., GOTTLIEB, J., NICKEL, N., HUSSEIN, K., MAUS, U., LEHMANN, U., JANCIAUSKIENE, S., WELTE, T., HAVERICH, A., RISCHE, J., KREIPE, H. & LAENGER, F. 2011. Plexiform Lesions in Pulmonary Arterial Hypertension: Composition, Architecture, and Microenvironment. *The American Journal of Pathology,* 179**,** 167-179.

KAGAN, E. & HARTMANN, D. P. 1984. ELIMINATION OF MACROPHAGES WITH SILICA AND ASBESTOS. *Methods in Enzymology,* 108**,** 325-335.

KAWUT, S. M., ARCHER-CHICKO, C. L., DEMICHELE, A., FRITZ, J. S., KLINGER, J. R., KY, B., PALEVSKY, H. I., PALMISCIANO, A. J., PATEL, M., PINDER, D., PROPERT, K. J., SMITH, K. A., STANCZYK, F., TRACY, R., VAIDYA, A., WHITTENHALL, M. E. & VENTETUOLO, C. E. 2017. Anastrozole in Pulmonary Arterial Hypertension. A Randomized, Double-Blind, Placebo-controlled Trial. *Am J Respir Crit Care Med,* 195**,** 360-368.

KEEGAN, A., MORECROFT, I., SMILLIE, D., HICKS, M. N. & MACLEAN, M. R. 2001. Contribution of the 5-HT(1B) receptor to hypoxia-induced pulmonary hypertension: converging evidence using 5-HT(1B)-receptor knockout mice and the 5-HT(1B/1D)-receptor antagonist GR127935. *Circ Res,* 89**,** 1231-9.

KIELY, D. G., ELLIOT, C. A., SABROE, I. & CONDLIFFE, R. 2013. Pulmonary hypertension: diagnosis and management. *Bmj-British Medical Journal,* 346.

KLEIN, S. L. & FLANAGAN, K. L. 2016. Sex differences in immune responses. *Nat Rev Immunol,* 16**,** 626-638.

KLIMEŠ, J., DOHNALOVÁ, M. & SEDLÁČEK, J. 1999. Microcolumn high-performance liquid chromatographic assay for doxycycline in isolated alveolar macrophages. *Journal of Chromatography A,* 846**,** 181-184.

LANNER, M. C., RAPER, M., PRATT, W. M. & RHOADES, R. A. 2005. Heterotrimeric G proteins and the platelet-derived growth factor receptor-beta contribute to hypoxic proliferation of smooth muscle cells. *Am J Respir Cell Mol Biol,* 33**,** 412-9.

LAWRIE, A., HAMEED, A. G., CHAMBERLAIN, J., ARNOLD, N., KENNERLEY, A., HOPKINSON, K., PICKWORTH, J., KIELY, D. G., CROSSMAN, D. C. & FRANCIS, S. E. 2011. Paigen Diet-Fed Apolipoprotein E Knockout Mice Develop Severe Pulmonary Hypertension in an Interleukin-1-Dependent Manner. *American Journal of Pathology,* 179**,** 1693-1705.

LAWRIE, A., WATERMAN, E., SOUTHWOOD, M., EVANS, D., SUNTHARALINGAM, J., FRANCIS, S., CROSSMAN, D., CROUCHER, P., MORRELL, N. & NEWMAN, C. 2008. Evidence of a role for osteoprotegerin in the pathogenesis of pulmonary arterial hypertension. *American Journal of Pathology,* 172**,** 256-264.

LEE, P., MORLEY, G., HUANG, Q., FISCHER, A., SEILER, S., HORNER, J. W., FACTOR, S., VAIDYA, D., JALIFE, J. & FISHMAN, G. I. 1998. Conditional lineage ablation to model human diseases. *Proceedings of*

the National Academy of Sciences of the United States of America, 95**,** 11371-11376.

LEWIS, C. & MURDOCH, C. 2005. Macrophage Responses to Hypoxia: Implications for Tumor Progression and Anti-Cancer Therapies. *The American Journal of Pathology,* 167**,** 627-635.

LI, M., RIDDLE, S. R., FRID, M. G., EL KASMI, K. C., MCKINSEY, T. A., SOKOL, R. J., STRASSHEIM, D., MEYRICK, B., YEAGER, M. E., FLOCKTON, A. R., MCKEON, B. A., LEMON, D. D., HORN, T. R., ANWAR, A., BARAJAS, C. & STENMARK, K. R. 2011. Emergence of Fibroblasts with a Proinflammatory Epigenetically Altered Phenotype in Severe Hypoxic Pulmonary Hypertension. *Journal of Immunology,* 187**,** 2711-2722.

LONG, L., MACLEAN, M. R., JEFFERY, T. K., MORECROFT, I., YANG, X., RUDARAKANCHANA, N., SOUTHWOOD, M., JAMES, V., TREMBATH, R. C. & MORRELL, N. W. 2006. Serotonin increases susceptibility to pulmonary hypertension in BMPR2-deficient mice. *Circ Res,* 98**,** 818-27.

LONG, L., ORMISTON, M. L., YANG, X., SOUTHWOOD, M., GRÄF, S., MACHADO, R. D., MUELLER, M., KINZEL, B., YUNG, L. M., WILKINSON, J. M., MOORE, S. D., DRAKE, K. M., ALDRED, M. A., YU, P. B., UPTON, P. D. & MORRELL, N. W. 2015. Selective enhancement of endothelial BMPR-II with BMP9 reverses pulmonary arterial hypertension. *Nature Medicine,* 21**,** 777.

MACHADO, R. D., EICKELBERG, O., ELLIOTT, C. G., GERACI, M. W., HANAOKA, M., LOYD, J. E., NEWMAN, J. H., PHILLIPS, J. A., 3RD, SOUBRIER, F., TREMBATH, R. C. & CHUNG, W. K. 2009. Genetics and genomics of pulmonary arterial hypertension. *J Am Coll Cardiol,* 54**,** S32-42.

MACINTYRE, P. D., BHARGAVA, B., HOGG, K. J., GEMMILL, J. D. & HILLIS, W. S. 1992. The effect of i.v. sumatriptan, a selective 5-HT1-receptor agonist on central haemodynamics and the coronary circulation. *Br J Clin Pharmacol,* 34**,** 541-6.

MACLEAN, M. R., CLAYTON, R. A., TEMPLETON, A. G. & MORECROFT, I. 1996a. Evidence for 5-HT1-like receptor-mediated vasoconstriction in human pulmonary artery. *Br J Pharmacol,* 119**,** 277-82.

MACLEAN, M. R., DEUCHAR, G. A., HICKS, M. N., MORECROFT, I., SHEN, S. B., SHEWARD, J., COLSTON, J., LOUGHLIN, L., NILSEN, M., DEMPSIE, Y. & HARMAR, A. 2004. Overexpression of the 5-hydroxytryptamine transporter gene - Effect on pulmonary hemodynamics and hypoxia-induced pulmonary hypertension. *Circulation,* 109**,** 2150-2155.

MACLEAN, M. R., HERVE, P., EDDAHIBI, S. & ADNOT, S. 2000. 5-hydroxytryptamine and the pulmonary circulation: receptors, transporters and relevance to pulmonary arterial hypertension. *British Journal of Pharmacology,* 131**,** 161-168.

MACLEAN, M. R., SWEENEY, G., BAIRD, M., MCCULLOCH, K. M., HOUSLAY, M. & MORECROFT, I. 1996b. 5-Hydroxytryptamine receptors mediating vasoconstriction in pulmonary arteries from control and pulmonary hypertensive rats. *Br J Pharmacol,* 119**,** 917-30.

MAIR, K. M., WRIGHT, A. F., DUGGAN, N., ROWLANDS, D. J., HUSSEY, M. J., ROBERTS, S., FULLERTON, J., NILSEN, M., LOUGHLIN, L.,

THOMAS, M. & MACLEAN, M. R. 2014a. Sex-Dependent Influence of Endogenous Estrogen in Pulmonary Hypertension. *American Journal of Respiratory and Critical Care Medicine,* 190**,** 456-467.

MAIR, K. M., WRIGHT, A. F., DUGGAN, N., ROWLANDS, D. J., HUSSEY, M. J., ROBERTS, S., FULLERTON, J., NILSEN, M., LOUGHLIN, L., THOMAS, M. & MACLEAN, M. R. 2014b. Sex-dependent influence of endogenous estrogen in pulmonary hypertension. *Am J Respir Crit Care Med,* 190**,** 456-67.

MARES, C. A., SHARMA, J., LI, Q., RANGEL, E. L., MORRIS, E. G., ENRIQUEZ, M. I. & TEALE, J. M. 2011. Defect in efferocytosis leads to alternative activation of macrophages in Francisella infections. *Immunol Cell Biol,* 89**,** 167-72.

MARRIOTT, I., BOST, K. L. & HUET-HUDSON, Y. M. 2006. Sexual dimorphism in expression of receptors for bacterial lipopolysaccharides in murine macrophages: A possible mechanism for gender-based differences in endotoxic shock susceptibility. *Journal of Reproductive Immunology,* 71**,** 12-27.

MARTINET, W., VERHEYE, S. & DE MEYER, G. R. Y. 2007. Selective depletion of macrophages in atherosclerotic plaques via macrophage-specific initiation of cell death. *Trends in Cardiovascular Medicine,* 17**,** 69-75.

MATUTE-BELLO, G., LEE, J. S., FREVERT, C. W., LILES, W. C., SUTLIEF, S., BALLMAN, K., WONG, V., SELK, A. & MARTIN, T. R. 2004. Optimal timing to repopulation of resident alveolar macrophages with donor cells following total body irradiation and bone marrow transplantation in mice. *J Immunol Methods,* 292**,** 25-34.

MCCUBBREY, A. L., BARTHEL, L., MOULD, K. J., MOHNING, M. P., REDENTE, E. F. & JANSSEN, W. J. 2016. Selective and inducible targeting of CD11b(+) mononuclear phagocytes in the murine lung with hCD68-rtTA transgenic systems. *American Journal of Physiology-Lung Cellular and Molecular Physiology,* 311**,** L87-L100.

MELOCHE, J., RENARD, S., PROVENCHER, S. & BONNET, S. 2013. Anti-inflammatory and Immunosuppressive Agents in PAH. *Pharmacotherapy of Pulmonary Hypertension,* 218**,** 437-476.

MERKLINGER, S. L., JONES, P. L., MARTINEZ, E. C. & RABINOVITCH, M. 2005. Epidermal growth factor receptor blockade mediates smooth muscle cell apoptosis and improves survival in rats with pulmonary hypertension. *Circulation,* 112**,** 423-31.

METCHNIKOFF, E. 1893. *Lectures on the comparative pathology of inflammation delivered at the Pasteur Institute in 1891,* London, Kegan Paul.

MITCHELL, J. A., AHMETAJ-SHALA, B., KIRKBY, N. S., WRIGHT, W. R., MACKENZIE, L. S., REED, D. M. & MOHAMED, N. 2014. Role of prostacyclin in pulmonary hypertension. *Global Cardiology Science & Practice,* 2014**,** 382-393.

MONTANI, D., CHAUMAIS, M. C., SAVALE, L., NATALI, D., PRICE, L. C., JAIS, X., HUMBERT, M., SIMONNEAU, G. & SITBON, O. 2009. Phosphodiesterase type 5 inhibitors in pulmonary arterial hypertension. *Adv Ther,* 26**,** 813-25.

MORENO, M., BANNERMAN, P., MA, J., GUO, F., MIERS, L., SOULIKA, A. M. & PLEASURE, D. 2014. Conditional Ablation of Astroglial CCL2 Suppresses CNS Accumulation of M1 Macrophages and Preserves Axons in Mice with MOG Peptide EAE. *The Journal of neuroscience : the official journal of the Society for Neuroscience,* 34**,** 8175-85.

MORRELL, N. W., ADNOT, S., ARCHER, S. L., DUPUIS, J., JONES, P. L., MACLEAN, M. R., MCMURTRY, I. F., STENMARK, K. R., THISTLETHWAITE, P. A., WEISSMANN, N., YUAN, J. X. J. & WEIR, E. K. 2009. Cellular and Molecular Basis of Pulmonary Arterial Hypertension. *Journal of the American College of Cardiology,* 54**,** S20-S31.

MOSSER, D. M. & EDWARDS, J. P. 2008. Exploring the full spectrum of macrophage activation. *Nat Rev Immunol,* 8**,** 958-69.

MURRAY, P. J. & WYNN, T. A. 2011. Protective and pathogenic functions of macrophage subsets. *Nature Reviews Immunology,* 11**,** 723-737.

NAGENDRAN, J., ARCHER, S. L., SOLIMAN, D., GURTU, V., MOUDGIL, R., HAROMY, A., ST AUBIN, C., WEBSTER, L., REBEYKA, I. M., ROSS, D. B., LIGHT, P. E., DYCK, J. R. & MICHELAKIS, E. D. 2007. Phosphodiesterase type 5 is highly expressed in the hypertrophied human right ventricle, and acute inhibition of phosphodiesterase type 5 improves contractility. *Circulation,* 116**,** 238-48.

NICHOLS, W. C., KOLLER, D. L., SLOVIS, B., FOROUD, T., TERRY, V. H., ARNOLD, N. D., SIEMIENIAK, D. R., WHEELER, L., PHILLIPS, J. A., 3RD, NEWMAN, J. H., CONNEALLY, P. M., GINSBURG, D. & LOYD, J. E. 1997. Localization of the gene for familial primary pulmonary hypertension to chromosome 2q31-32. *Nat Genet,* 15**,** 277-80.

OHAYON, D., DE CHIARA, A., CHAPUIS, N., CANDALH, C., MOCEK, J., RIBEIL, J.-A., HADDAOUI, L., IFRAH, N., HERMINE, O., BOUILLAUD, F., FRACHET, P., BOUSCARY, D. & WITKO-SARSAT, V. 2016. Cytoplasmic proliferating cell nuclear antigen connects glycolysis and cell survival in acute myeloid leukemia. *Scientific Reports,* 6.

PACE, S., ROSSI, A., KRAUTH, V., DEHM, F., TROISI, F., BILANCIA, R., WEINIGEL, C., RUMMLER, S., WERZ, O. & SAUTEBIN, L. 2017. Sex differences in prostaglandin biosynthesis in neutrophils during acute inflammation. *Sci Rep,* 7**,** 3759.

PASSLICK, B., FLIEGER, D. & ZIEGLER-HEITBROCK, H. W. 1989. Identification and characterization of a novel monocyte subpopulation in human peripheral blood. *Blood,* 74**,** 2527-34.

PERROS, F., MONTANI, D., DORFMUELLER, P., DURAND-GASSELIN, I., TCHERAKIAN, C., LE PAVEC, J., MAZMANIAN, M., FADEL, E., MUSSOT, S., MERCIER, O., HERVE, P., EMILIE, D., EDDAHIBI, S., SIMONNEAU, G., SOUZA, R. & HUMBERT, M. 2008. Platelet-derived growth factor expression and function in idiopathic pulmonary arterial hypertension. *American Journal of Respiratory and Critical Care Medicine,* 178**,** 81-88.

PFARR, N., FISCHER, C., EHLKEN, N., BECKER-GRUNIG, T., LOPEZ-GONZALEZ, V., GORENFLO, M., HAGER, A., HINDERHOFER, K., MIERA, O., NAGEL, C., SCHRANZ, D. & GRUNIG, E. 2013. Hemodynamic and genetic analysis in children with idiopathic, heritable,

and congenital heart disease associated pulmonary arterial hypertension. *Respir Res,* 14**,** 3.

PLUCHART, H., KHOURI, C., BLAISE, S., ROUSTIT, M. & CRACOWSKI, J.-L. 2017. Targeting the Prostacyclin Pathway: Beyond Pulmonary Arterial Hypertension. *Trends in Pharmacological Sciences,* 38**,** 512-523.

POUSADA, G., BALOIRA, A., VILARINO, C., CIFRIAN, J. M. & VALVERDE, D. 2014. Novel mutations in BMPR2, ACVRL1 and KCNA5 genes and hemodynamic parameters in patients with pulmonary arterial hypertension. *PLoS One,* 9**,** e100261.

PUGLIESE, S. C., KUMAR, S., JANSSEN, W. J., GRAHAM, B. B., FRID, M. G., RIDDLE, S. R., EL KASMI, K. C. & STENMARK, K. R. 2017. A Time- and Compartment-Specific Activation of Lung Macrophages in Hypoxic Pulmonary Hypertension. *J Immunol,* 198**,** 4802-4812.

PULLAMSETTI, S., KISS, L., GHOFRANI, H. A., VOSWINCKEL, R., HAREDZA, P., KLEPETKO, W., AIGNER, C., FINK, L., MUYAL, J. P., WEISSMANN, N., GRIMMINGER, F., SEEGER, W. & SCHERMULY, R. T. 2005. Increased levels and reduced catabolism of asymmetric and symmetric dimethylarginines in pulmonary hypertension. *Faseb Journal,* 19**,** 1175-+.

PULLAMSETTI, S. S., SAVAI, R., JANSSEN, W., DAHAL, B. K., SEEGER, W., GRIMMINGER, F., GHOFRANI, H. A., WEISSMANN, N. & SCHERMULY, R. T. 2011. Inflammation, immunological reaction and role of infection in pulmonary hypertension. *Clinical Microbiology and Infection,* 17**,** 7-14.

QIAN, J., TIAN, W., JIANG, X., TAMOSIUNIENE, R., SUNG, Y. K., SHUFFLE, E. M., TU, A. B., VALENZUELA, A., JIANG, S., ZAMANIAN, R. T., FIORENTINO, D. F., VOELKEL, N. F., PETERS-GOLDEN, M., STENMARK, K. R., CHUNG, L., RABINOVITCH, M. & NICOLLS, M. R. 2015. Leukotriene B-4 Activates Pulmonary Artery Adventitial Fibroblasts in Pulmonary Hypertension. *Hypertension,* 66**,** 1227-1239.

RABINOVITCH, M. 2008. Molecular pathogenesis of pulmonary arterial hypertension. *Journal of Clinical Investigation,* 118**,** 2372-2379.

RABINOVITCH, M., GAMBLE, W. J., MIETTINEN, O. S. & REID, L. 1981. Age and sex influence on pulmonary hypertension of chronic hypoxia and on recovery. *American Journal of Physiology - Heart and Circulatory Physiology,* 240**,** H62.

RABINOVITCH, M., GUIGNABERT, C., HUMBERT, M. & NICOLLS, M. R. 2014. Inflammation and Immunity in the Pathogenesis of Pulmonary Arterial Hypertension. *Circulation Research,* 115**,** 165-175.

RAOUL, W., WAGNER-BALLON, O., SABER, G., HULIN, A., MARCOS, E., GIRAUDIER, S., VAINCHENKER, W., ADNOT, S., EDDAHIBI, S. & MAITRE, B. 2007. Effects of bone marrow-derived cells on monocrotaline- and hypoxia-induced pulmonary hypertension in mice. *Respiratory Research,* 8**,** 8.

RENSHALL, L., ARNOLD, N., WEST, L., BRAITHWAITE, A., PICKWORTH, J., WALKER, R., ALFAIDI, M., CHAMBERLAIN, J., CASBOLT, H., THOMPSON, A. A. R., HOLT, C., IGLARZ, M., FRANCIS, S. & LAWRIE, A. 2018. Selective improvement of pulmonary arterial hypertension with a dual ETA/ETB receptors antagonist in the apolipoprotein E(-/-) model of PAH and atherosclerosis. *Pulm Circ,* 8**,** 2045893217752328.

RESTA, T. C., KANAGY, N. L. & WALKER, B. R. 2001. Estradiol-induced attenuation of pulmonary hypertension is not associated with altered eNOS expression. *Am J Physiol Lung Cell Mol Physiol,* 280**,** L88-97.

RETTEW, J. A., HUET-HUDSON, Y. M. & MARRIOTT, I. 2008. Testosterone Reduces Macrophage Expression in the Mouse of Toll-Like Receptor 4, a Trigger for Inflammation and Innate Immunity. *Biology of Reproduction,* 78**,** 432-437.

ROGERS, N. M., FERENBACH, D. A., ISENBERG, J. S., THOMSON, A. W. & HUGHES, J. 2014. Dendritic cells and macrophages in the kidney: a spectrum of good and evil. *Nature Reviews Nephrology,* 10**,** 625-643.

ROMBERG, E. 1891. Ueber sklerose der lungen arterie. *Dtsch Arch Klin Med,* 48**,** 197-206.

RONDELET, B., VAN BENEDEN, R., KERBAUL, F., MOTTE, S., FESLER, P., MCENTEE, K., BRIMIOULLE, S., KETELSLEGERS, J. M. & NAEIJE, R. 2003. Expression of the serotonin 1b receptor in experimental pulmonary hypertension. *European Respiratory Journal,* 22**,** 408.

RUAN, C.-H., DIXON, R. A. F., WILLERSON, J. T. & RUAN, K.-H. 2010. Prostacyclin Therapy for Pulmonary Arterial Hypertension. *Texas Heart Institute Journal,* 37**,** 391-399.

RUBIN, L. J., BADESCH, D. B., BARST, R. J., GALIÈ, N., BLACK, C. M., KEOGH, A., PULIDO, T., FROST, A., ROUX, S., LECONTE, I., LANDZBERG, M. & SIMONNEAU, G. 2002. Bosentan Therapy for Pulmonary Arterial Hypertension. *New England Journal of Medicine,* 346**,** 896-903.

RUMNEY, R. M. H., COFFELT, S. B., NEALE, T. A., DHAYADE, S., TOZER, G. M. & MILLER, G. 2017. PyMT-Maclow: A novel, inducible, murine model for determining the role of CD68 positive cells in breast tumor development. *PLoS One,* 12**,** e0188591.

SAFDAR, Z. 2011. Treatment of pulmonary arterial hypertension: The role of prostacyclin and prostaglandin analogs. *Respiratory Medicine,* 105**,** 818-827.

SAID, S. I., HAMIDI, S. A., DICKMAN, K. G., SZEMA, A. M., LYUBSKY, S., LIN, R. Z., JIANG, Y. P., CHEN, J. J., WASCHEK, J. A. & KORT, S. 2007. Moderate pulmonary arterial hypertension in male mice lacking the vasoactive intestinal peptide gene. *Circulation,* 115**,** 1260-8.

SAKAO, S., TATSUMI, K. & VOELKEL, N. F. 2009. Endothelial cells and pulmonary arterial hypertension: apoptosis, proliferation, interaction and transdifferentiation. *Respiratory Research,* 10**,** 95-95.

SAVAI, R., PULLAMSETTI, S. S., KOLBE, J., BIENIEK, E., VOSWINCKEL, R., FINK, L., SCHEED, A., RITTER, C., DAHAL, B. K., VATER, A., KLUSSMANN, S., GHOFRANI, H. A., WEISSMANN, N., KLEPETKO, W., BANAT, G. A., SEEGER, W., GRIMMINGER, F. & SCHERMULY, R. T. 2012. Immune and Inflammatory Cell Involvement in the Pathology of Idiopathic Pulmonary Arterial Hypertension. *American Journal of Respiratory and Critical Care Medicine,* 186**,** 897-908.

SCHERMULY, R. T., DONY, E., GHOFRANI, H. A., PULLAMSETTI, S., SAVAI, R., ROTH, M., SYDYKOV, A., LAI, Y. J., WEISSMANN, N., SEEGER, W. & GRIMMINGER, F. 2005. Reversal of experimental pulmonary hypertension by PDGF inhibition. *J Clin Invest,* 115**,** 2811-21.

SEO, B., OEMAR, B. S., SIEBENMANN, R., VON SEGESSER, L. & LUSCHER, T. F. 1994. Both ETA and ETB receptors mediate contraction to endothelin-1 in human blood vessels. *Circulation,* 89**,** 1203-8.

SHAPIRO, S., TRAIGER, G. L., TURNER, M., MCGOON, M. D., WASON, P. & BARST, R. J. 2012. Sex differences in the diagnosis, treatment, and outcome of patients with pulmonary arterial hypertension enrolled in the registry to evaluate early and long-term pulmonary arterial hypertension disease management. *Chest,* 141**,** 363-373.

SICA, A. & MANTOVANI, A. 2012. Macrophage plasticity and polarization: in vivo veritas. *Journal of Clinical Investigation,* 122**,** 787-795.

SIMONNEAU, G., GATZOULIS, M. A., ADATIA, I., CELERMAJER, D., DENTON, C., GHOFRANI, A., GOMEZ SANCHEZ, M. A., KUMAR, R. K., LANDZBERG, M., MACHADO, R. F., OLSCHEWSKI, H., ROBBINS, I. M. & SOUZA, R. 2013. Updated Clinical Classification of Pulmonary Hypertension. *Journal of the American College of Cardiology,* 62**,** D34-D41.

SINGH, B., PEARCE, J. W., GAMAGE, L. N., JANARDHAN, K. & CALDWELL, S. 2004. Depletion of pulmonary intravascular macrophages inhibits acute lung inflammation. *American Journal of Physiology-Lung Cellular and Molecular Physiology,* 286**,** L363-L372.

SINGH, S. & GOYAL, A. 2007. The Origin of Echocardiography: A Tribute to Inge Edler. *Texas Heart Institute Journal,* 34**,** 431-438.

SITBON, O., BADESCH, D. B., CHANNICK, R. N., FROST, A., ROBBINS, I. M., SIMONNEAU, G., TAPSON, V. F. & RUBIN, L. J. 2003. Effects of the dual endothelin receptor antagonist bosentan in patients with pulmonary arterial hypertension: a 1-year follow-up study. *Chest,* 124**,** 247-54.

SONG, Y., JONES, J. E., BEPPU, H., KEANEY, J. F., JR., LOSCALZO, J. & ZHANG, Y. Y. 2005. Increased susceptibility to pulmonary hypertension in heterozygous BMPR2-mutant mice. *Circulation,* 112**,** 553-62.

STACHER, E., GRAHAM, B. B., HUNT, J. M., GANDJEVA, A., GROSHONG, S. D., MCLAUGHLIN, V. V., JESSUP, M., GRIZZLE, W. E., ALDRED, M. A., COOL, C. D. & TUDER, R. M. 2012. Modern Age Pathology of Pulmonary Arterial Hypertension. *American Journal of Respiratory and Critical Care Medicine,* 186**,** 261-272.

STANLEY, E. R., BERG, K. L., EINSTEIN, D. B., LEE, P. S., PIXLEY, F. J., WANG, Y. & YEUNG, Y. G. 1997. Biology and action of colony--stimulating factor-1. *Mol Reprod Dev,* 46**,** 4-10.

STEIN, M., KESHAV, S., HARRIS, N. & GORDON, S. 1992. Interleukin 4 potently enhances murine macrophage mannose receptor activity: a marker of alternative immunologic macrophage activation. *J Exp Med,* 176**,** 287-92.

STEINER, M. K., SYRKINA, O. L., KOLLIPUTI, N., MARK, E. J., HALES, C. A. & WAXMAN, A. B. 2009. Interleukin-6 Overexpression Induces Pulmonary Hypertension. *Circulation Research,* 104**,** 236-U208.

STENMARK, K. R., DAVIE, N. J., REEVES, J. T. & FRID, M. G. 2005. Hypoxia, leukocytes, and the pulmonary circulation. *Journal of Applied Physiology,* 98**,** 715-721.

STENMARK, K. R., FRID, M. G., YEAGER, M., LI, M., RIDDLE, S., MCKINSEY, T. & EL KASMI, K. C. 2012. Targeting the adventitial

microenvironment in pulmonary hypertension: A potential approach to therapy that considers epigenetic change. *Pulm Circ,* 2**,** 3-14.

STENMARK, K. R., NOZIK-GRAYCK, E., GERASIMOVSKAYA, E., ANWAR, A., LI, M., RIDDLE, S. & FRID, M. 2011. The Adventitia: Essential Role in Pulmonary Vascular Remodeling. *Comprehensive Physiology,* 1**,** 141-161.

STENMARK, K. R., YEAGER, M. E., EL KASMI, K. C., NOZIK-GRAYCK, E., GERASIMOVSKAYA, E. V., LI, M., RIDDLE, S. R. & FRID, M. G. 2013. The Adventitia: Essential Regulator of Vascular Wall Structure and Function. *Annual Review of Physiology,* 75**,** 23-47.

STRAFACE, E., GAMBARDELLA, L., BRANDANI, M. & MALORNI, W. 2012. Sex differences at cellular level: "cells have a sex". *Handb Exp Pharmacol***,** 49-65.

TAKEMOTO, M., SUN, J., HIROKI, J., SHIMOKAWA, H. & LIAO, J. K. 2002. Rho-kinase mediates hypoxia-induced downregulation of endothelial nitric oxide synthase. *Circulation,* 106**,** 57-62.

TALATI, M., WEST, J., ZAYNAGETDINOV, R., HONG, C. C., HAN, W., BLACKWELL, T., ROBINSON, L., BLACKWELL, T. S. & LANE, K. 2014. BMP Pathway Regulation of and by Macrophages. *Plos One,* 9.

TAMOSIUNIENE, R., TIAN, W., DHILLON, G., WANG, L., SUNG, Y. K., GERA, L., PATTERSON, A. J., AGRAWAL, R., RABINOVITCH, M., AMBLER, K., LONG, C. S., VOELKEL, N. F. & NICOLLS, M. R. 2011. Regulatory T cells limit vascular endothelial injury and prevent pulmonary hypertension. *Circ Res,* 109**,** 867-79.

TARASEVICIENE-STEWART, L., KASAHARA, Y., ALGER, L., HIRTH, P., MCMAHON, G., WALTENBERGER, J., VOELKEL, N. F. & TUDER, R. M. 2001. Inhibition of the VEGF receptor 2 combined with chronic hypoxia causes cell death-dependent pulmonary endothelial cell proliferation and severe pulmonary hypertension. *Faseb Journal,* 15**,** 427-438.

TARLING, J. D., LIN, H. & HSU, S. 1987. SELF-RENEWAL OF PULMONARY ALVEOLAR MACROPHAGES - EVIDENCE FROM RADIATION CHIMERA STUDIES. *Journal of Leukocyte Biology,* 42**,** 443-446.

TIAN, W., JIANG, X., TAMOSIUNIENE, R., SUNG, Y. K., QIAN, J., DHILLON, G., GERA, L., FARKAS, L., RABINOVITCH, M., ZAMANIAN, R. T., INAYATHULLAH, M., FRIDLIB, M., RAJADAS, J., PETERS-GOLDEN, M., VOELKEL, N. F. & NICOLLS, M. R. 2013. Blocking macrophage leukotriene b4 prevents endothelial injury and reverses pulmonary hypertension. *Sci Transl Med,* 5**,** 200ra117.

TOFOVIC, S. P., SALAH, E. M., MADY, H. H., JACKSON, E. K. & MELHEM, M. F. 2005. Estradiol metabolites attenuate monocrotaline-induced pulmonary hypertension in rats. *J Cardiovasc Pharmacol,* 46**,** 430-7.

TOFOVIC, S. P., ZHANG, X., JACKSON, E. K., DACIC, S. & PETRUSEVSKA, G. 2006. 2-Methoxyestradiol mediates the protective effects of estradiol in monocrotaline-induced pulmonary hypertension. *Vascul Pharmacol,* 45**,** 358-67.

TUDER, R. M., ARCHER, S. L., DORFMUELLER, P., ERZURUM, S. C., GUIGNABERT, C., MICHELAKIS, E., RABINOVITCH, M., SCHERMULY, R., STENMARK, K. R. & MORRELL, N. W. 2013. Relevant Issues in the Pathology and Pathobiology of Pulmonary

Hypertension. *Journal of the American College of Cardiology,* 62**,** D4-D12.

UMAR, S., CUNNINGHAM, C. M., ITOH, Y., MOAZENI, S., VAILLANCOURT, M., SARJI, S., CENTALA, A., ARNOLD, A. P. & EGHBALI, M. 2017. The Y Chromosome Plays a Protective Role in Experimental Hypoxic Pulmonary Hypertension. *American Journal of Respiratory and Critical Care Medicine.*

UMAR, S., DE VISSER, Y. P., STEENDIJK, P., SCHUTTE, C. I., LAGHMANI, E. H., WAGENAAR, G. T. M., BAX, W. H., MANTIKOU, E., PIJNAPPELS, D. A., ATSMA, D. E., SCHALIJ, M. J., VAN DER WALL, E. E. & VAN DER LAARSE, A. 2009. Allogenic stem cell therapy improves right ventricular function by improving lung pathology in rats with pulmonary hypertension. *American Journal of Physiology - Heart and Circulatory Physiology,* 297**,** H1606.

UMAR, S., IORGA, A., MATORI, H., NADADUR, R. D., LI, J., MALTESE, F., VAN DER LAARSE, A. & EGHBALI, M. 2011. Estrogen Rescues Preexisting Severe Pulmonary Hypertension in Rats. *American Journal of Respiratory and Critical Care Medicine,* 184**,** 715-723.

VAN DEN BERG, L., IMHOLZ, S., VERSTEEG, S. A., LEEGWATER, P. A., ZIJLSTRA, C., BOSMA, A. A. & VAN OOST, B. A. 2004. Isolation and characterization of the canine serotonin receptor 1B gene (htr1B). *Gene,* 326**,** 131-9.

VANROOIJEN, N. & SANDERS, A. 1994. LIPOSOME-MEDIATED DEPLETION OF MACROPHAGES - MECHANISM OF ACTION, PREPARATION OF LIPOSOMES AND APPLICATIONS. *Journal of Immunological Methods,* 174**,** 83-93.

VENTETUOLO, C. E., BAIRD, G. L., BARR, R. G., BLUEMKE, D. A., FRITZ, J. S., HILL, N. S., KLINGER, J. R., LIMA, J. A., OUYANG, P., PALEVSKY, H. I., PALMISCIANO, A. J., KRISHNAN, I., PINDER, D., PRESTON, I. R., ROBERTS, K. E. & KAWUT, S. M. 2016. Higher Estradiol and Lower Dehydroepiandrosterone-Sulfate Levels Are Associated with Pulmonary Arterial Hypertension in Men. *Am J Respir Crit Care Med,* 193**,** 1168-75.

VERGADI, E., CHANG, M. S., LEE, C., LIANG, O. D., LIU, X., FERNANDEZ-GONZALEZ, A., MITSIALIS, S. A. & KOUREMBANAS, S. 2011. Early Macrophage Recruitment and Alternative Activation Are Critical for the Later Development of Hypoxia-Induced Pulmonary Hypertension. *Circulation,* 123**,** 1986-U299.

VIEILLARD-BARON, A., FRISDAL, E., EDDAHIBI, S., DEPREZ, I., BAKER, A. H., NEWBY, A. C., BERGER, P., LEVAME, M., RAFFESTIN, B., ADNOT, S. & D'ORTHO, M. P. 2000. Inhibition of matrix metalloproteinases by lung TIMP-1 gene transfer or doxycycline aggravates pulmonary hypertension in rats. *Circulation Research,* 87**,** 418-425.

WALKER, A. M., LANGLEBEN, D., KORELITZ, J. J., RICH, S., RUBIN, L. J., STROM, B. L., GONIN, R., KEAST, S., BADESCH, D., BARST, R. J., BOURGE, R. C., CHANNICK, R., FROST, A., GAINE, S., MCGOON, M., MCLAUGHLIN, V., MURALI, S., OUDIZ, R. J., ROBBINS, I. M., TAPSON, V., ABENHAIM, L. & CONSTANTINE, G. 2006. Temporal trends and drug exposures in pulmonary hypertension: an American experience. *Am Heart J,* 152**,** 521-6.

WANG, D., ZHANG, H., LI, M., FRID, M. G., FLOCKTON, A. R., MCKEON, B. A., YEAGER, M. E., FINI, M. A., MORRELL, N. W., PULLAMSETTI, S. S., VELEGALA, S., SEEGER, W., MCKINSEY, T. A., SUCHAROV, C. C. & STENMARK, K. R. 2014. MicroRNA-124 Controls the Proliferative, Migratory, and Inflammatory Phenotype of Pulmonary Vascular Fibroblasts. *Circulation Research,* 114**,** 67-78.

WEISSER, S. B., VAN ROOIJEN, N. & SLY, L. M. 2012. Depletion and reconstitution of macrophages in mice. *Journal of visualized experiments : JoVE,* 4105-4105.

WENG, M., RAHER, M. J., LEYTON, P., COMBS, T. P., SCHERER, P. E., BLOCH, K. D. & MEDOFF, B. D. 2011. Adiponectin Decreases Pulmonary Arterial Remodeling in Murine Models of Pulmonary Hypertension. *American Journal of Respiratory Cell and Molecular Biology,* 45**,** 340-347.

WERZ, O., KLEMM, J., SAMUELSSON, B. & RADMARK, O. 2000. 5-lipoxygenase is phosphorylated by p38 kinase-dependent MAPKAP kinases. *Proceedings of the National Academy of Sciences of the United States of America,* 97**,** 5261-5266.

WERZ, O., SZELLAS, D., STEINHILBER, D. & RADMARK, O. 2002. Arachidonic acid promotes phosphorylation of 5-lipoxygenase at Ser-271 by MAPK-activated protein kinase 2 (MK2). *Journal of Biological Chemistry,* 277**,** 14793-14800.

WEST, J., TADA, Y., FAGAN, K. A., STEUDEL, W., FOUTY, B. W., HARRAL, J. W., MILLER, M., OZIMEK, J., TUDER, R. M. & RODMAN, D. M. 2005. Suppression of type II bone morphogenic protein receptor in vascular smooth muscle induces pulmonary arterial hypertension in transgenic mice. *Chest,* 128**,** 553s.

WEST, L. E., STEINER, T., JUDGE, H. M., FRANCIS, S. E. & STOREY, R. F. 2014. Vessel wall, not platelet, P2Y12 potentiates early atherogenesis. *Cardiovascular Research,* 102**,** 429-435.

WHITE, K., DEMPSIE, Y., NILSEN, M., WRIGHT, A. F., LOUGHLIN, L. & MACLEAN, M. R. 2011. The serotonin transporter, gender, and 17 beta oestradiol in the development of pulmonary arterial hypertension. *Cardiovascular Research,* 90**,** 373-382.

WHITE, K., JOHANSEN, A. K., NILSEN, M., CIUCLAN, L., WALLACE, E., PATON, L., CAMPBELL, A., MORECROFT, I., LOUGHLIN, L., MCCLURE, J. D., THOMAS, M., MAIR, K. M. & MACLEAN, M. R. 2012. Activity of the Estrogen-Metabolizing Enzyme Cytochrome P450 1B1 Influences the Development of Pulmonary Arterial Hypertension. *Circulation,* 126**,** 1087-U202.

WITKO-SARSAT, V., MOCEK, J., BOUAYAD, D., TAMASSIA, N., RIBEIL, J.-A., CANDALH, C., DAVEZAC, N., REUTER, N., MOUTHON, L., HERMINE, O., PEDERZOLI-RIBEIL, M. & CASSATELLA, M. A. 2010. Proliferating cell nuclear antigen acts as a cytoplasmic platform controlling human neutrophil survival. *Journal of Experimental Medicine,* 207**,** 2631-2645.

WONG, K. L., YEAP, W. H., TAI, J. J. Y., ONG, S. M., TRUONG MINH, D. & WONG, S. C. 2012. The three human monocyte subsets: implications for health and disease. *Immunologic Research,* 53**,** 41-57.

WRIGHT, A. F., EWART, M.-A., MAIR, K., NILSEN, M., DEMPSIE, Y., LOUGHLIN, L. & MACLEAN, M. R. 2015. Oestrogen receptor alpha in pulmonary hypertension. *Cardiovascular Research,* 106**,** 206-216.

WRIGHT, L., TUDER, R. M., WANG, J., COOL, C. D., LEPLEY, R. A. & VOELKEL, N. F. 1998. 5-lipoxygenase and 5-lipoxygenase activating protein (FLAP) immunoreactivity in lungs from patients with primary pulmonary hypertension. *American Journal of Respiratory and Critical Care Medicine,* 157**,** 219-229.

XU, W., KANEKO, F. T., ZHENG, S., COMHAIR, S. A., JANOCHA, A. J., GOGGANS, T., THUNNISSEN, F. B., FARVER, C., HAZEN, S. L., JENNINGS, C., DWEIK, R. A., ARROLIGA, A. C. & ERZURUM, S. C. 2004. Increased arginase II and decreased NO synthesis in endothelial cells of patients with pulmonary arterial hypertension. *Faseb j,* 18**,** 1746-8.

YOSHIDA, H., HAYASHI, S. I., KUNISADA, T., OGAWA, M., NISHIKAWA, S., OKAMURA, H., SUDO, T., SHULTZ, L. D. & NISHIKAWA, S. I. 1990. THE MURINE MUTATION OSTEOPETROSIS IS IN THE CODING REGION OF THE MACROPHAGE COLONY STIMULATING FACTOR GENE. *Nature,* 345**,** 442-444.

ZALOUDIKOVA, M., VYTASEK, R., VAJNEROVA, O., HNILICKOVA, O., VIZEK, M., HAMPL, V. & HERGET, J. 2016. Depletion of Alveolar Macrophages Attenuates Hypoxic Pulmonary Hypertension but not Hypoxia-Induced Increase in Serum Concentration of MCP-1. *Physiological Research,* 65**,** 763-768.

ZAWIA. 2011. *investigating the effect of macrophage ablation using a novel transgenic mouse on hypoxia- induced pulmonary arterial hypertension.* MSc, University of Sheffield.

ZIEGLER-HEITBROCK, L., ANCUTA, P., CROWE, S., DALOD, M., GRAU, V., HART, D. N., LEENEN, P. J., LIU, Y. J., MACPHERSON, G., RANDOLPH, G. J., SCHERBERICH, J., SCHMITZ, J., SHORTMAN, K., SOZZANI, S., STROBL, H., ZEMBALA, M., AUSTYN, J. M. & LUTZ, M. B. 2010a. Nomenclature of monocytes and dendritic cells in blood. *Blood,* 116**,** e74-80.

ZIEGLER-HEITBROCK, L., ANCUTA, P., CROWE, S., DALOD, M., GRAU, V., HART, D. N., LEENEN, P. J. M., LIU, Y.-J., MACPHERSON, G., RANDOLPH, G. J., SCHERBERICH, J., SCHMITZ, J., SHORTMAN, K., SOZZANI, S., STROBL, H., ZEMBALA, M., AUSTYN, J. M. & LUTZ, M. B. 2010b. Nomenclature of monocytes and dendritic cells in blood. *Blood,* 116**,** E74-E80.

9   Appendices

9.1   Appendix I - Haemodynamic measurements

Haemodynamic parameters collected in the *MacLow*- induced PAH study:

Table of the haemodynamic parameter collected by echocardiography

Parameter	control male			MacLow male			control female			MacLow female		
	Mean	SEM	n	Mean	SEM	n	Mean	SEM	n	Mean	SEM	n
weight (g)	29.48	1.08	8	29.58	0.95	8	24.61	0.74	8	23.96	0.78	7
LVIDd(mm)	3.98	0.17	8	3.48	0.10	8	3.47	0.17	8	3.51	0.12	8
LVIDs(mm)	2.81	0.18	8	2.11	0.15	8	1.85	0.18	8	2.11	0.18	8
LVEF%	56.33	4.78	8	69.76	3.91	8	77.87	4.01	8	70.73	5.08	8
LVFS%	29.69	3.19	8	39.47	3.65	8	47.15	4.16	8	40.39	3.74	8
LV mass (corr) mg	123.73	8.57	8	143.28	3.77	8	118.19	6.45	8	114.26	14.14	8
LVSV(MM)	39.25	4.72	8	35.00	2.58	8	39.46	4.27	8	36.07	3.48	8
LVCO(MM)	20.11	2.32	8	15.58	2.44	8	18.67	1.87	8	17.05	2.02	8
Ao VTI (cm)	3.23	0.33	8	3.03	0.24	8	3.40	0.13	8	3.37	0.18	8
AoV-Mean Vel (mm/s)	529.30	60.79	8	494.43	36.34	8	537.45	28.45	8	503.82	20.49	8
Ao SV(ul)	44.81	4.77	8	35.73	3.71	8	44.97	2.12	8	39.98	2.41	8
Ao CO (ml/min)	23.30	2.73	8	17.24	1.63	8	21.89	1.74	8	18.46	1.19	8
Ao SVi (m/g)	1.52	0.15	8	1.22	0.13	8	1.84	0.11	8	1.66	0.09	7
Ao CI (m/min/g)	792.43	88.03	8	586.78	57.09	8	899.78	85.26	8	758.96	52.71	7
PAAT (ms)	17.10	1.02	8	16.77	0.48	8	19.15	0.63	8	18.15	0.65	8
PAET (mc)	58.48	1.61	8	61.25	0.92	8	63.85	2.08	8	60.81	2.49	8
PA AT/ET ratio	0.29	0.02	8	0.27	0.01	8	0.30	0.01	8	0.30	0.00	8
RVIDd	1.32	0.04	8	1.43	0.03	8	1.30	0.07	8	1.10	0.09	6
RVIDs	0.68	0.04	8	0.69	0.07	8	0.57	0.06	8	0.49	0.04	6
RVWTs	0.60	0.04	8	0.65	0.05	8	0.64	0.04	8	0.58	0.03	6
RVFS% (M-Mode)	48.44	3.64	8	51.97	4.49	8	56.45	3.22	8	54.63	4.04	6
PA VTI	2.78	0.14	8	2.72	0.21	8	3.07	0.18	8	2.64	0.10	8
CI (from LV)	0.68	0.07	8	0.51	0.08	8	0.76	0.07	8	0.71	0.10	7

Table of the haemodynamic parameter collected by cardiac catheterization of the right ventricle

	control male			MacLow male			control female			MacLow female		
Parameter	Mean	SEM	n	Mean	SEM	n	Mean	SEM	n	Mean	SEM	n
Heart rate (bpm)	460.57	16.94	7	515	15.99	6	390.43	46.97	7	439.8	39.53	5
Maximum Volume (RVU)	21.98	1.5	7	20.44	2.22	6	20.87	1.96	7	18.61	1.5	5
Minimum Volume (RVU)	19.62	1.09	7	18.66	2	6	18.62	1.73	7	17.47	1.5	5
End-systolic Volume (RVU)	20.17	1.19	7	19.22	2.05	6	19.01	1.71	7	17.81	1.49	5
End-diastolic Volume (RVU)	21.47	1.33	7	19.76	2.25	6	20.53	2	7	18.11	1.37	5
Maximum Pressure (mmHg)	24.88	1.2	7	59.04	9.85	6	23.22	1.95	7	25.09	1.64	5
Minimum Pressure (mmHg)	0.27	0.04	7	0.47	0.13	6	0.28	0.06	7	0.76	0.47	5
End-systolic Pressure (mmHg)	24.51	1.23	7	58.74	9.72	6	23.11	1.95	7	25.07	1.63	5
End-diastolic Pressure (mmHg)	2.37	0.26	7	2.85	0.81	6	1.94	0.38	7	2.38	0.83	5
Stroke Volume (RVU)	2.36	0.62	7	1.78	0.34	6	2.25	0.66	7	1.13	0.21	5
Ejection Fraction (%)	10.25	2.14	7	8.59	1.26	6	10.6	2.42	7	6.21	1.28	5
Cardiac Output (RVU/min)	1100.77	309.56	7	921.1	181.07	6	809.2	225.5	7	500.94	99.9	5
Stroke Work (mmHg*RVU)	34.71	12.08	7	48.67	36.49	6	33.86	15.68	7	-0.6	9.09	5
Arterial Elastance (Ea) (mmHg/RVU)	15.81	3.77	7	44.16	16.95	6	18.68	6.2	7	25.03	3.96	5
dPdt max (mmHg/sec)	2213.29	194.12	7	5421.67	1237.39	6	2183.43	745.95	7	2013	333.29	5
dPdt min (mmHg/sec)	-1676.57	180.48	7	-4712.67	1473.49	6	-1545.57	360.34	7	-1492.2	171.2	5
dVdt max (RVU/sec)	110.43	32.75	7	94.5	13.67	6	83.14	19.64	7	57.8	18.65	5

Parameter	Mean	SEM	n	Mean	SEM	n	Mean	SEM	n	Mean	SEM	n
dVdt min (RVU/sec)	-68.29	13.38	7	-88	17.58	6	-59.57	12.99	7	-35.6	6.49	5
P@dVdt max (mmHg)	1.12	0.53	7	8.64	2.5	6	3.56	1.54	7	11.91	4.15	5
P@dPdt max (mmHg)	12.14	1.69	7	26.95	7.24	6	9.94	2	7	10.49	1.55	5
V@dPdt max (RVU)	21.31	1.36	7	19.69	2.3	6	20.45	1.94	7	18	1.36	5
V@dPdt min (RVU)	19.72	1.11	7	19.26	1.92	6	18.85	1.77	7	17.87	1.55	5
Tau_w (msec)	8.18	0.74	7	6.72	1.68	6	10.06	1.87	7	10.12	1.58	5
Tau_g (msec)	16.15	2.87	7	12.63	3.54	6	32.98	15.48	7	13.13	1.1	5
Tau_l (msec)	0	0	7	0	0	6	0	0	7	0	0	5
Maximal Power (mWatts)	0.18	0.04	7	0.57	0.27	6	0.13	0.04	7	0.06	0.02	5
Preload adjusted maximal power (mWatts/µL^2)	3.87	0.75	7	11.57	2.92	6	3.03	0.62	7	1.83	0.53	5

Table of the haemodynamic parameter collected by cardiac catheterization of the left ventricle

	control male			MacLow male			control female			MacLow female		
Parameter	Mean	SEM	n	Mean	SEM	n	Mean	SEM	n	Mean	SEM	n
Heart rate (bpm)	465.67	39.56	3	501.25	20.62	4	477.25	51.10	4	367.00	51.79	3
Maximum Volume (RVU)	24.68	0.50	3	24.06	1.94	4	24.52	1.47	4	17.86	0.70	3
Minimum Volume (RVU)	20.99	0.76	3	19.46	1.09	4	20.28	0.72	4	15.64	0.70	3
End-systolic Volume (RVU)	21.62	0.92	3	20.20	1.01	4	21.70	0.86	4	16.42	0.82	3
End-diastolic Volume (RVU)	23.67	0.39	3	23.60	1.91	4	24.09	1.53	4	17.34	0.91	3
Maximum Pressure (mmHg)	98.85	9.81	3	79.34	2.16	4	82.67	8.99	4	72.56	16.03	3
Minimum Pressure (mmHg)	0.40	0.08	3	1.60	1.21	4	0.42	0.08	4	0.27	0.02	3
End-systolic Pressure (mmHg)	97.14	10.59	3	77.64	2.68	4	81.50	9.51	4	72.26	15.99	3

End-diastolic Pressure (mmHg)	3.56	0.42	3	3.99	1.15	4	3.18	0.56	4	2.53	0.30	3
Stroke Volume (RVU)	3.68	0.90	3	4.61	1.31	4	4.25	0.92	4	2.22	0.75	3
Ejection Fraction (%)	14.86	3.55	3	18.35	4.54	4	16.82	2.85	4	12.30	3.81	3
Cardiac Output (RVU/min)	1772.00	511.96	3	2287.17	609.54	4	2163.43	657.07	4	811.32	254.93	3
Stroke Work (mmHg*RVU)	252.33	51.41	3	265.00	89.57	4	210.00	44.58	4	52.00	86.40	3
Arterial Elastance (Ea) (mmHg/RVU)	33.28	14.13	3	28.59	14.66	4	24.09	7.55	4	36.97	8.13	3
dPdt max (mmHg/sec)	9639.33	1525.18	3	6153.00	381.82	4	6168.50	558.61	4	4297.33	1372.77	3
dPdt min (mmHg/sec)	-9986.67	2141.45	3	-6328.25	1276.52	4	-5406.75	515.50	4	-4095.33	1797.90	3
dVdt max (RVU/sec)	127.33	37.67	3	156.25	44.47	4	163.50	44.44	4	98.00	25.12	3
dVdt min (RVU/sec)	-139.67	44.35	3	-152.50	40.34	4	-186.25	57.66	4	-70.00	18.50	3
P@dVdt max (mmHg)	34.32	4.10	3	8.89	4.19	4	10.58	0.71	4	6.35	4.66	3
P@dPdt max (mmHg)	65.71	8.32	3	41.36	2.59	4	41.81	9.56	4	34.07	6.91	3
V@dPdt max (RVU)	24.43	0.32	3	23.40	2.06	4	23.96	1.53	4	17.03	1.19	3
V@dPdt min (RVU)	21.38	0.74	3	19.70	1.18	4	21.00	0.81	4	16.14	0.78	3
Tau_w (msec)	5.67	0.13	3	7.06	1.09	4	6.74	1.41	4	11.44	2.32	3
Tau_g (msec)	9.37	0.74	3	11.28	2.50	4	12.76	3.63	4	19.60	4.11	3
Tau_l (msec)	0.00	0.00	3	0.00	0.00	4	0.00	0.00	4	0.00	0.00	3
Maximal Power (mWatts)	1.70	0.49	3	1.48	0.42	4	1.65	0.52	4	0.36	0.17	3
Preload adjusted maximal power (mWatts/µL^2)	30.03	8.23	3	24.40	4.41	4	25.87	5.86	4	11.50	4.50	3

Haemodynamic parameters collected in the bone marrow transplant study presented in chapter 3

Table of the main haemodynamic parameter collected by echocardiography

	MacLow BM to MacLow			control BM to MacLow			MacLow BM to control			control BM to control		
Parameter	Mean	SEM	n	Mean	SEM	n	Mean	SEM	n	Mean	SEM	n
Weight (g)	32.51	1.15	8	31.82	0.72	5	31.22	0.53	5	31.20	0.92	5
AoET (ms)	58.50	1.82	7	57.10	0.89	5	55.00	1.52	5	56.25	1.64	4
RVWTd (mm)	0.49	0.04	7	0.47	0.01	4	0.51	0.01	5	0.51	0.02	4
RVIDd	1.37	0.05	7	1.36	0.22	4	1.57	0.09	5	1.47	0.07	4
RVWTs	0.68	0.09	7	0.75	0.14	4	0.65	0.02	5	0.78	0.07	4
RVIDs	0.71	0.09	7	0.65	0.17	4	0.69	0.06	5	0.81	0.05	4
PAAT (ms)	16.60	1.14	7	18.37	0.21	5	17.93	0.87	5	16.00	0.78	4
PAET (ms)	62.07	2.33	7	63.23	2.00	5	59.97	1.46	5	58.92	3.73	4
PAAT/ET	0.27	0.01	7	0.29	0.01	5	0.30	0.02	5	0.27	0.00	4
CI (m/min/g)	0.59	0.04	7	0.63	0.12	4	0.60	0.06	5	0.82	0.12	3

Table of the haemodynamic parameter collected by cardiac catheterization of the right ventricle

	MacLow BM to MacLow			control BM to MacLow			MacLow BM to control			control BM to Control		
	Mean	SEM	n	Mean	SEM	n	Mean	SEM	n	Mean	SEM	n
Heart rate (bpm)	530.38	17.52	8	501.20	13.02	5	449.40	15.34	5	501.75	32.61	4
Maximum Volume (RVU)	26.81	0.89	8	28.01	1.80	5	26.81	1.95	5	26.21	1.03	4
Minimum Volume (RVU)	24.74	0.96	8	25.89	1.27	5	24.72	1.71	5	23.82	0.45	4
End-systolic Volume (RVU)	25.30	0.88	8	26.66	1.41	5	25.12	1.63	5	24.59	0.48	4
End-diastolic Volume (RVU)	26.09	0.89	8	27.41	1.75	5	26.01	1.91	5	25.61	1.14	4
Maximum Pressure (mmHg)	29.01	2.17	8	23.30	0.60	5	20.60	1.56	5	24.19	0.62	4
Minimum Pressure (mmHg)	0.28	0.04	8	0.26	0.03	5	0.29	0.11	5	0.20	0.02	4
End-systolic Pressure (mmHg)	28.94	2.19	8	23.26	0.61	5	20.58	1.57	5	24.11	0.57	4

End-diastolic Pressure (mmHg)	1.35	0.20	8	1.60	0.18	5	2.20	0.53	5	1.95	0.23	4
Stroke Volume (RVU)	2.07	0.34	8	2.12	0.56	5	2.09	0.85	5	2.40	0.71	4
Ejection Fraction (%)	7.76	1.31	8	7.16	1.65	5	7.47	2.84	5	8.88	2.37	4
Cardiac Output (RVU/min)	1078.79	172.34	8	1074.54	292.50	5	921.40	365.37	5	1153.92	293.03	4
Stroke Work (mmHg*RVU)	23.63	11.03	8	22.20	12.25	5	12.40	10.27	5	15.25	22.05	4
Arterial Elastance (Ea) (mmHg/RVU)	17.60	3.27	8	17.64	6.22	5	16.66	4.92	5	13.61	4.17	4
dPdt max (mmHg/sec)	2486.13	289.42	8	2344.00	133.89	5	1826.20	314.07	5	2302.50	281.36	4
dPdt min (mmHg/sec)	-2339.88	310.67	8	-1619.60	42.33	5	-1680.00	400.74	5	-1835.50	200.10	4
dVdt max (RVU/sec)	114.75	14.59	8	122.80	35.42	5	90.80	36.89	5	112.00	26.56	4
dVdt min (RVU/sec)	-87.38	11.45	8	-78.60	22.69	5	-72.00	11.97	5	-94.25	23.94	4
P@dVdt max (mmHg)	4.24	1.97	8	5.26	4.76	5	4.45	2.89	5	11.93	6.68	4
P@dPdt max (mmHg)	10.98	0.92	8	9.39	0.98	5	8.54	1.40	5	11.23	0.87	4
V@dPdt max (RVU)	26.17	0.89	8	27.31	1.72	5	25.84	1.92	5	25.16	1.06	4
V@dPdt min (RVU)	25.02	1.00	8	26.18	1.30	5	24.98	1.62	5	24.42	0.55	4
Tau_w (msec)	7.94	0.50	8	8.24	1.00	5	6.58	2.33	5	7.12	0.68	4
Tau_g (msec)	61.43	43.17	8	128.86	111.66	5	102.43	70.15	5	10.08	1.18	4
Tau_l (msec)	0.00	0.00	8	0.00	0.00	5	0.00	0.00	5	0.00	0.00	4
Maximal Power (mWatts)	0.22	0.04	8	0.13	0.03	5	0.12	0.02	5	0.16	0.08	4
Preload adjusted maximal power (mWatts/µL^2)	3.09	0.51	8	1.61	0.31	5	1.78	0.33	5	2.17	1.03	4

Haemodynamic parameters from the bone marrow transplant study presented in chapter 6

Table of the main haemodynamic parameter collected by echocardiography

	Male BM to Male			Female BM to Male			Male BM to Female			Female BM to Female		
	Mean	SEM	n	Mean	SEM	n	Mean	SEM	n	Mean	SEM	n
Weight (g)	32.51	1.15	8	31.23	0.65	6	28.87	0.31	6	28.98	1.21	6
LVCO (MM)	18.88	1.41	7	18.31	1.21	5	18.36	1.61	6	18.11	1.03	6
AoET (ms)	58.50	1.82	7	56.30	1.91	5	53.83	0.71	6	54.00	1.37	6
RVWTd ((mm)	0.49	0.04	7	0.54	0.02	6	0.46	0.03	6	0.45	0.01	6
RVIDd (mm)	1.37	0.05	7	1.49	0.06	6	1.30	0.08	6	1.41	0.09	6
RVWTs	0.68	0.09	7	0.79	0.06	6	0.69	0.03	6	0.89	0.05	6
RVIDs	0.71	0.09	7	0.67	0.03	6	0.52	0.06	6	0.53	0.07	6
PAAT (ms)	16.60	1.14	7	16.58	0.45	6	16.25	0.50	6	15.67	0.66	6
PAET (ms)	62.07	2.33	7	58.89	0.67	6	55.89	0.72	6	55.72	1.54	6
PAAT/ET	0.27	0.01	7	0.28	0.01	6	0.29	0.01	6	0.28	0.01	6
CI (m/min/g)	0.59	0.04	7	0.58	0.04	5	0.64	0.06	6	0.63	0.06	6

Table of the haemodynamic parameter collected by cardiac catheterization of the right ventricle

Parameter	Male BM to Male			Female BM to Male			Male BM to Female			Female BM to Female		
	Mean	SEM	n	Mean	SEM	n	Mean	SEM	n	Mean	SEM	n
Heart rate (bpm)	530.38	17.52	8	483.00	34.69	6	454.33	33.93	6	423.67	42.56	6
Minimum Volume (RVU)	24.74	0.96	8	26.42	2.02	6	26.12	2.34	6	21.86	1.65	6
End-systolic Volume (RVU)	25.30	0.88	8	27.22	2.05	6	26.57	2.34	6	22.04	1.66	6
End-diastolic Volume (RVU)	26.09	0.89	8	27.72	2.09	6	28.04	2.76	6	22.99	1.71	6
Maximum Pressure (mmHg)	29.01	2.17	8	27.29	1.52	6	21.97	0.56	6	23.61	0.79	6
Minimum Pressure (mmHg)	0.28	0.04	8	0.40	0.12	6	0.21	0.02	6	0.23	0.02	6
End-systolic Pressure (mmHg)	28.94	2.19	8	27.41	1.47	6	21.40	0.34	6	23.60	0.79	6
End-diastolic Pressure (mmHg)	1.35	0.20	8	1.96	0.22	6	2.17	0.47	6	2.24	0.26	6

Stroke Volume (RVU)	2.07	0.34	8	1.80	0.36	6	2.51	0.54	6	1.44	0.26	6
Ejection Fraction (%)	7.76	1.31	8	6.32	1.10	6	8.14	1.30	6	6.14	0.93	6
Cardiac Output (RVU/min)	1078.79	172.34	8	1225.21	158.36	6	1220.16	315.33	6	595.62	133.14	6
Stroke Work (mmHg*RVU)	23.63	11.03	8	32.33	6.26	6	31.67	8.88	6	17.83	4.02	6
Arterial Elastance (Ea) (mmHg/RVU)	17.60	3.27	8	10.74	1.53	6	13.82	5.36	6	21.70	6.69	6
dPdt max (mmHg/sec)	2486.13	289.42	8	2369.33	293.59	6	1627.17	161.26	6	1503.17	167.87	6
dPdt min (mmHg/sec)	-2339.88	310.67	8	-1589.17	216.81	6	-1324.67	123.72	6	-1281.50	177.17	6
dVdt max (RVU/sec)	114.75	14.59	8	82.67	14.97	6	103.67	21.85	6	72.00	10.48	6
dVdt min (RVU/sec)	-87.38	11.45	8	-71.67	15.18	6	-85.33	22.41	6	-44.00	8.09	6
P@dVdt max (mmHg)	4.24	1.97	8	10.90	5.10	6	1.38	0.68	6	2.29	0.85	6
P@dPdt max (mmHg)	10.98	0.92	8	12.32	1.63	6	7.82	0.92	6	10.01	0.76	6
V@dPdt max (RVU)	26.17	0.89	8	27.62	2.07	6	27.93	2.75	6	22.90	1.66	6
V@dPdt min (RVU)	25.02	1.00	8	26.83	2.13	6	26.24	2.34	6	21.95	1.67	6
Tau_w (msec)	7.94	0.50	8	9.76	2.51	6	10.10	1.54	6	12.50	2.46	6
Tau_g (msec)	61.43	43.17	8	26.94	2.55	6	50.28	32.75	6	41.93	15.72	6
Tau_l (msec)	0.00	0.00	8	0.00	0.00	6	0.00	0.00	6	0.00	0.00	6
Maximal Power (mWatts)	0.22	0.04	8	0.17	0.04	6	0.21	0.06	6	0.11	0.02	6
Preload adjusted maximal power (mWatts/µL^2)	3.09	0.51	8	2.05	0.41	6	2.27	0.46	6	2.12	0.37	6

9.2 Appendix II – Animal work reagent

Genotyping reagents and buffers

Tail Lysis Buffer (TLB)

- 10ml of 1M Tris-Hcl pH 8.5

- 0.4ml of 0.5M EDTA PH8

- 10ml of 10% v/v Tween 20

- Make up to 200ml with dH2o

Filtered, aliquoted and stored at -20ºC

0.5 M EDTA (pH8)

- 186.1g of disodium ethylene-diamine tetra-acetic acid.dihydrate (EDTA)

- 800ml dH20

- Stir thoroughly in magnetic stirrer

- Adjust pH to 8 with ~20g NaOH pellets

Sterilized with autoclave and stored at room temperature away from direct sun light.

10 mg/ml Proteinase K stock solution

- 100mg Proteinase K (Proteinase K from Tritirachium album supplied by SIGMA- P2308)

- 10 ml storage buffer

Aliquoted and stored at -20ºC

Storage buffer:

- 50ml Glycerol

- 1ml of 1M Tris-Hcl pH7.5

- Make up to 100 ml with Deionized dH2O

Autoclaved and stored at room temperature

10X TBE buffer

- 108g Tris base

- 55g Boric acid

- 800ml dH2O

- Stir in magnetic stirrer

- 40ml of 0.5M EDTA (pH8)

- Make up to 1000ml with dH2O

Stored at room temperature away from light. For X1 working solution dilute with

deionized dH2O.

Other reagents:

X100 Acidified water used in BMT studies

- 10ml sterile filter conc HCl .12M (37%)

- 840ml dH2O

Autoclaved and stored at room temperature away from direct sunlight. For X1

working solution dilute 10.1ml of the X100 stock in 1000m dH2O.

Sodium citrate

- 4g Sodium citrate dihydrate

- Make up to 100ml with H2O

Sterile filtered and stored at 2-8ºC.

10% formalin

- 4g sodium phosphate (NaH2PO4)

- 7.1g Di-sodium hydrogen orthophosphate (Na2HPO4)

- 100ml formaldehyde

- 900ml dH2O

Stored at room temperature away from direct sunlight.

9.3 Appendix III - Immunohistochemistry buffers and reagents

Primary antibodies used in immune-histological staining of tissue sections:

antibody	clone	Catalogue number and supplier	reactivity	Dilution used	storage
Anti-F4/80 antibody	Cl: A3-1	Ab6640 abcam Cambridge, UK	mouse	1:100	-20ºC
Anti-iNOS antibody	polyclonal	Ab15323 abcam Cambridge, UK	Mouse, rat	1:100	-20ºC
MMR/CD206 antibody	polyclonal	AF2535 R&D systems Minnesota, US	mouse	1:100	-20ºC
Anti-SMA antibody	Cl:1A4	M0851 Dako, Agilent Santa Clara, US	Human, mouse	1:150	2-8 ºC
Anti-vWF antibody	polyclonal	A0082 Dako, Agilent Santa Clara, US	Human, cow, horse,	1:300	2-8 ºC

			mouse, swine		
Anti-PCNA antibody	PC10	M0876 Dako, Agilent Santa Clara, US	Mouse, rat, zebrafish	1:125	2-8 ºC
Anti-IL-4 antibody	polyclonal	Orb360766 Biorbyt California, US	Human, mouse, rat	1:150	-20ºC

Secondary antibodies used in immune-histological staining of tissue sections:

All secondary antibodies used at 1:200 dilution and stored at 2-8 ºC

Antibody	**Catalogue number and supplier**
Biotinylated goat anti-rat IgG	BA9400 Vector Laboratories, Peterborough, UK
Biotinylated goat anti-mouse IgG	BA9200 Vector Laboratories, Peterborough, UK
Biotinylated goat anti-rabbit IgG	BA1000 Vector Laboratories, Peterborough, UK
Alexa Fluor® 488 goat anti-rat IgG (H+L)	A11006 Invitrogen by ThermoFisher MA, US
Alexa Fuor™ 555 goat anti-mouse IgG (H+L)	A21422 Invitrogen by ThermoFisher MA, US

Acid alcohol

- 5 ml of 1% v/v Hcl

- 495 ml of 70% v/v IMS

Stored at room temperature away from direct sunlight.

10mM Citrate Buffer

- 2.1g citric acid monohydrate
- 900 ml dH2O
- Adjusted to PH6 with ~ 13ml of 2M NaOH
- Fill with dH2O to 1000ml

Stored at room temperature away from direct sunlight.

Curtis' Modified Van Gieson

- 10 ml of 1% w/v Ponceau S [aq]

- 90 ml of saturated aq. Picric acid

- 1 ml of glacial acetic

Stored at room temperature away from direct sunlight.

Alcian blue

- 5g Alcian blue

- 485 ml H2O

- 15ml acetic acid

Stored at room temperature away from direct sunlight.

3% Hydrogen peroxide solution

- 1 ml of 30% stock solution

- 9 ml of PBS

Stock solution was stored at 4°C.

1% Milk blocking buffer

- 4g of Marvel dried milk (from local supermarket)

- 400 ml of PBS

Marvel dried milk powder was stored at room temperature.

Tris buffered saline (TBS)

- 1 foil pouches of TBS powder (T-6664-10PAK, SIGMA)

- 1000ml dH2O

The buffered saline (0.05M TBS, pH8) stored at room temperature away from direct sunlight.

SIGMAFAST™ 3,3'-Diaminobenzidine tablets (D4418,Sigma Aldrich, Dorset, UK)

- 1 Urea Hydrogen Peroxide tablet

- 1 3,3'-Diaminobenzidine (DAB) tablet

- added to 15 ml of water

The DAB kit was stored at -20°C.

VECTASTAIN Elite ABC Kit (Standard*) (PK-6100, Vector Laboratories, Peterborough, UK)

- 1 drop of Reagent A

- 1 drop of Reagent B

- 2.5 ml of PBS

The kit was stored at 4°C.

9.4 Appendix IV – Flow cytometry reagents

Antibodies used in flow cytometry analysis of mouse derived monocyte/ macrophage cells: all antibodies stored in dark at 2-8 ºC

Antibody	Clone	Catalogue number and the supplier	reactivity	Dilution used
Alexa Fluor® 488 anti-mouse CD115 (CSF-1R)	AFS98	135511 BioLegend California, US	mouse	1µg/ 100µl (2 µl/ million cell)
FITC anti-mouse CD68	FA-11	137005 BioLegend California, US	mouse	0.2µg/ 100µl (1 µl/ million cell)
PE anti-mouse CD206 (MMR)	C068C2	141705 BioLegend California, US	mouse	0.2µg/ 100µl (1 µl/ million cell)
Pacific blue™ anti-mouse CD86	GL-1	105021 BioLegend California, US	mouse	0.5µg/ 100µl (1 µl/ million cell)
APC anti-mouse F4/80	BM8	123115 BioLegend California, US	mouse	0.2µg/ 100µl (1 µl/ million cell)

9.5   Appendix V- *In vitro* work reagents

Freezing media for BMDM

- 90ml FBS

- 10ml di-methyl sulfoxide DMSO(D-5879, Sigma)

Stored at 2-8 ºC.

RIPA buffer (radio- immunoprecipitation assay buffer)

- 150 mM NaCl

- 20 mM Tris

- 1% Triton X-100

- 0.1% sodium dodecyl sulfate (SDS)

Stored at 2-8ºC.

20 mM Tris- HCl (pH8) for M-CSF reconstitution

- 31.52g Tris- HCl

- 10ml sterile H2O

- Adjust pH with NaOH

Stored at 2-8 ºC.

Antibodies used in immunocytochemistry

Primary antibody: rabbit polyclonal Anti-5 Lipoxygenase antibody, from abcam (ab39347). Used at 1:100 dilution.

Secondary antibody: Alexa Fluor® 555 goat anti-rabbit IgG H&L, from abcam (ab150078). Used at 1:200 diluion.

Antibodies used in dot blot assay

Primary antibody: mouse anti-Diphtheria toxin A subunit [8A4], from abcam (ab8308). Used at 1:2000 dilution

Secondary antibody: goat anti-mouse IgG (H&L) from Dyssey. Used at 1:10000 dilution.